Harnessing endothelial lipid signaling for ischemic stroke protection

Ammar Benarab

Université de Paris

École doctorale Bio Sorbonne Paris Cité (BioSPC - ED562)

Biologie Cellulaire et Moléculaire, Physiologie et Physiopathologie

INSERM U970, Centre de recherche cardiovasculaire de Paris

Harnessing endothelial lipid signaling for ischemic stroke protection

Par **Ammar BENARAB**

Thèse de doctorat de Biologie Cellulaire et Moléculaire

Dirigée par le **Dr. Eric CAMERER**

Présentée et soutenue publiquement le 15 décembre 2021

Devant un jury composé de :

Dr. Christian WAEBER, Professeur, Université Collège de Cork	Rapporteur
Dr. Robert BRUNKHORST, Assistant Professeur, Université de Aachen	Rapporteur
Dr. Isabelle MARGAILL, Professeur (PU), Université de Paris	Examinatrice
Dr. Eric CAMERER, DR, HDR, Université de Paris	Directeur de thèse

To my family

Table of Contents

ACKNOWLEDGEMENTS **5**

ABSTRACT **7**

RESUME **8**

PREFACE **10**

LIST OF ABBREVIATIONS **11**

CHAPTER 1. SPHINGOSINE 1-PHOSPHATE **13**

S1P METABOLISM **14**
S1P EXPORT **15**
S1P CHAPERONES **16**
S1P SPATIAL GRADIENTS **16**
S1P SIGNALING MECHANISMS **17**
INTRACELLULAR SIGNALING 17
S1P RECEPTORS 18
S1P SIGNALING IN EMBRYONIC DEVELOPMENT **19**
S1P SIGNALING IN ANGIOGENESIS **20**
S1P SIGNALING IN THE REGULATION OF VASCULAR INTEGRITY **21**
S1P SIGNALING IN THE REGULATION OF VASCULAR TONE AND BLOOD PRESSURE **23**
S1P SIGNALING IN INFLAMMATION **24**
S1PR MODULATORS **25**
FINGOLIMOD 25
S1PR SELECTIVE MODULATORS 25
ENGINEERED S1P CHAPERONES 27

CHAPTER 2. THE NEUROVASCULAR UNIT **28**

THE BLOOD-BRAIN BARRIER **28**
THE ENDOTHELIUM **29**
BARRIER FUNCTIONS OF THE ENDOTHELIUM 29
THE VASOACTIVE ROLE OF THE ENDOTHELIUM 30
REGULATION OF COAGULATION AND THROMBOSIS AND INFLAMMATION BY THE ENDOTHELIUM 31
NEURONS **31**
ASTROCYTES **31**
PERICYTES **32**
CEREBROVASCULAR ANATOMY IN MOUSE AND MAN **33**
REGULATION OF CEREBRAL PERFUSION **35**
S1P SIGNALING AT THE NVU **38**

CHAPTER 3. STROKE **40**

EPIDEMIOLOGY **40**
PATHOPHYSIOLOGY OF ISCHEMIC STROKE **41**
OVERVIEW 41
THROMBOTIC OCCLUSION OF LARGE CEREBRAL ARTERIES 42
ENGAGEMENT OF CEREBRAL COLLATERALS 43
BLOOD FLOW DISTURBANCE, ENDOTHELIAL ACTIVATION, AND LOSS OF MICROVASCULAR PATENCY 44
ENDOTHELIAL DYSFUNCTION 44
PLATELETS AND THE INTRINSIC COAGULATION CASCADE 45
T CELLS AND THROMBO-INFLAMMATION 46
MICROGLIA AND MONOCYTE-DERIVED MACROPHAGES 49
NEUTROPHILS IN ISCHEMIC STROKE 49
SEQUENTIAL BBB BREAKDOWN 50
ISCHEMIC STROKE MODELING IN RODENTS **52**
STROKE THERAPY ACADEMIC INDUSTRY ROUNDTABLE RECOMMENDATIONS FOR STROKE RESEARCH 52

CHAPTER 4. MODULATING SPHINGOSINE 1-PHOSPHATE SIGNALING IN STROKE **59**

EFFICACY AND SAFETY OF FINGOLIMOD TREATMENT IN ISCHEMIC STROKE **59**
MECHANISM OF ACTION OF FINGOLIMOD PROTECTION IN ISCHEMIC STROKE **62**
INTRACEREBRAL AND SUBARACHNOID HEMORRHAGE **66**
$S1P_2$ SIGNALING IN STROKE **67**
S1PR MODULATION IN CLINICAL STROKE TRIALS **68**
ISCHEMIC STROKE 68
INTRACEREBRAL HEMORRHAGE 69
CURRENT STATUS OF S1PR MODULATION FOR STROKE TREATMENT **70**

CONTEXT AND OBJECTIVES OF THE THESIS PROJECT **73**

CHAPTER 5. EXTENDED METHODS **74**

EXPERIMENTAL ISCHEMIC STROKE MODELING IN MICE **74**
FILAMENT-INDUCED DISTAL TMCAO 76

CHAPTER 6. DISCUSSION **86**

BIBLIOGRAPHY **90**

APPENDIX. PAPER 1 ..... **1**

APPENDIX. PAPER 2 ..... **1**

Acknowledgements

I would like to express my deep gratitude to my supervisor Dr. Eric Camerer for welcoming me to his laboratory and giving me the opportunity to work in his team since January 2017, first for my master internship and then for my PhD project. I will always be grateful for his guidance and mentorship; my vision and conception of science have completely changed during these years. Moving from a medical and clinical background to a basic science research environment was a fantastic experience. From when I was in medical school, I have always been fascinated by the molecular and cellular mechanisms of diseases and the insight it gives into the genesis of pathology, the presentation of clinical signs, and the origin for targeted treatment strategies. I therefore very much enjoyed my PhD project, which involved the modeling of experiment ischemic stroke and the characterization of a cellular therapeutic target that could potentially serve in adjunct therapies for stroke patients.

I will always be grateful for Dr. Camerer's guidance and mentorship and for his help with my thesis writing. I am also thankful for the immersion in the English environment of his laboratory, which has greatly improved my English skills. I am also grateful to Dr. Camerer for his help in obtaining funding for my thesis and for involving me in the Leducq Sphingonet Network, which allowed me to interact with world class scientists in vascular biology and neuroscience and to participate in scientific conferences in Europe and the United States.

I would also like to express my gratitude to Véronique Baudrie, Marine Poittevin, Gabrielle Mangin, Rajkumar Vutukuri, Teresa Sanchez and Rhita Lamthari, as they helped me troubleshoot and master the two experimental stroke models that I used during my thesis, and to all the members of the Leducq Sphinonet Network for discussions and valuable advice during this period.

I am very grateful to all the respected jury members for accepting the request for reviewing and evaluating my thesis. I would also like to thank the members of my CSI committee, Bertrand Tavitian and Benoit Ho Tin Noé, who provided me comments and helpful advice on my thesis progress.

I would like to thank all those who directly contributed to this large collaborative project, including Anja Nitzsche, Marine Poittevin, Philippe Bonnin, Giuseppe Faraco, Lidia Garcia-Bonilla, Hiroki Uchida, Julie Favre, Mari Kono, Manuela Garcia, Pierre-Louis Léger, Christiane Charriaut-Marlangue, Veronique Baudrie, Hira Niazi, Ludovic Couty, Aline Chevallier, Thomas Mathivet and Gwennhael Autret, and to express my gratitude towards our collaborators without whose help the project would not have been realized, including Nathalie Kubis, Daniel Henrion, Timothy Hla, Richard Proia, Teresa Sanchez, Costantino Iadecola, Patrice Thérond, Anne Eichmann, Bertrand Tavitian, Pierre-Louis Tharaux, Jerold Chun and Susan Schwab.

This work would also never have been accomplished without all the help of the technical staff at PARCCs core facilities. I am especially thankful to those running the animal facility, including Corina, Gwendoline, Nicolas, Guillaume, and Francoise, to Stéphanie Lamoureux, and to the administrative staff at the PARCC, including Karima, Catherine, Murielle, Laurie, Dominique, Annette, Bruno, Cyrille, Julian and Dominic, as well as to Chantal Boulanger for her support as Director of the center.

Finally, I would like to thank the French foundation for medical research (FRM; Fondation pour la Recherche Médicale), INSERM (Institut national de la santé et de la recherche médicale), and the Leducq Foundation for supporting me financially during my graduate studies.

Abstract

Rationale: Cerebrovascular function is critical for brain health, and endogenous vascular protective pathways may provide therapeutic targets for neurological disorders. S1P (Sphingosine 1-phosphate) signaling coordinates vascular functions in other organs, and $S1P_1$ (S1P receptor-1) modulators including fingolimod show promise for the treatment of ischemic and hemorrhagic stroke. However, $S1P_1$ also coordinates lymphocyte trafficking, and lymphocytes are currently viewed as the principal therapeutic target for $S1P_1$ modulation in stroke.

Objective: To address roles and mechanisms of engagement of endothelial cell $S1P_1$ in the naive and ischemic brain and its potential as a target for cerebrovascular therapy.

Methods and results: Using spatial modulation of S1P provision and signaling, we demonstrate a critical vascular protective role for endothelial $S1P_1$ in the mouse brain. With an $S1P_1$ signaling reporter, we reveal that abluminal polarization shields $S1P_1$ from circulating endogenous and synthetic ligands after maturation of the blood-neural barrier, restricting homeostatic signaling to a subset of arteriolar endothelial cells. $S1P_1$ signaling sustains hallmark endothelial functions in the naive brain and expands during ischemia by engagement of cell-autonomous S1P provision. Disrupting this pathway by endothelial cell-selective deficiency in S1P production, export, or the $S1P_1$ receptor substantially exacerbates brain injury in permanent and transient models of ischemic stroke. By contrast, profound lymphopenia induced by loss of lymphocyte $S1P_1$ provides modest protection only in the context of reperfusion. In the ischemic brain, endothelial cell $S1P_1$ supports blood-brain barrier function, microvascular patency, and the rerouting of blood to hypoperfused brain tissue through collateral anastomoses. Boosting these functions by supplemental pharmacological engagement of the endothelial receptor pool with a blood-brain barrier penetrating $S1P_1$-selective agonist can further reduce cortical infarct expansion in a therapeutically relevant time frame and independent of reperfusion.

Conclusions: This study provides genetic evidence to support a pivotal role for the endothelium in maintaining perfusion and microvascular patency in the ischemic penumbra that is coordinated by S1P signaling and can be harnessed for neuroprotection with blood-brain barrier-penetrating $S1P_1$ agonists.

Résumé

Abstract : La fonction cérébrovasculaire est essentielle au maintien de l'intégrité cérébrale, et la signalisation vasculaire endogène représente une cible thérapeutique potentiel lors des pathologies cérébrales. La signalisation S1P (sphingosine 1-phosphate) régule les fonctions vasculaires cérébrale et aussi dans d'autres organes, en plus les modulateurs $S1P_1$ (récepteur S1P-1), y compris le fingolimod, ont démontré des bénéfices prometteurs pour le traitement de l'AVC ischémique et hémorragique. Le récepteur $S1P_1$ est impliqué également dans la coordination de la migration des cellules lymphocytaires, et actuellement il est suggéré que les lymphocytes sont la principale cible thérapeutique lors de la modulation du récepteur $S1P_1$ dans le contexte des accidents vasculaires cérébraux.

Objectif : Déterminer le rôle et les mécanismes d'activation du récepteur $S1P_1$ au niveau des cellules endothéliales cérébrale a l'état physiologique et dans le contexte de l'ischémie cérébrale et son potentiel modulation thérapeutique.

Méthodes et résultats : En utilisant la modulation spatiale de la production et de la signalisation S1P, nous avons démontré un rôle protecteur vasculaire critique du récepteur $S1P_1$ endothélial dans le cerveau de la souris. Avec l'utilisation d'une souris reportrice de la signalisation $S1P_1$, nous avons révélé qu' après maturation de la barrière hémato-neurale, $S1P_1$ présente une polarisation abluminale ce qui le rend insensible aux ligands endogènes produit par les cellules hématopoïétiques, et limitant la signalisation homéostatique uniquement à un sous-ensemble de cellules endothéliales artériolaires. La signalisation $S1P_1$ maintient les fonctions endothéliales caractéristiques dans le cerveau naïf et pendant l'ischémie y a promotion de ces fonctions par l'engagement de la production autonome de S1P des cellules endothéliales. La perturbation de cette voie par une déficience sélective des cellules endothéliales soit dans la production, l'exportation ou le récepteur $S1P_1$ aggrave considérablement les lésions cérébrales dans les modèles permanents et transitoires d'AVC ischémique. En revanche, la lymphopénie profonde induite par la perte du $S1P_1$ au niveau des lymphocytes résulte uniquement en une modeste protection observée uniquement lors du model d'ischémie reperfusion. Lors de l'ischémie cérébrale, le récepteur $S1P_1$ exprimé au niveau des cellules endothéliales est impliqué dans le maintien de la fonction de la barrière hémato-encéphalique, de la perméabilité microvasculaire et de la redirection du flux sanguin vers le tissu cérébral hypoperfusé via les anastomoses collatérales. L'activation de ces fonctions par une stimulation pharmacologique supplémentaire des récepteurs endothéliaux avec un agoniste sélectif de $S1P_1$ ayant la propriété de diffusé via la barrière hémato-encéphalique peut être efficace pour réduire l'expansion de l'infarctus cortical dans un délai thérapeutiquement pertinent et indépendamment de la reperfusion.

Conclusions : Notre étude établie des évidences génétiques qui suggèrent un rôle central de l'endothélium cérébral dans le maintien de la perfusion et de la perméabilité microvasculaire

dans la zone de pénombre ischémique cérébrale, et ce rôle majeur est régulé par la signalisation S1P, en plus d'un potentiel thérapeutique de neuro-protection lors de l'ischémie cérébrale par l'utilisation d' agonistes $S1P_1$ traversant la barrière hémato-encéphalique.

Preface

This PhD thesis entitled “Harnessing endothelial lipid signaling for ischemic stroke protection” comprises research work conducted in the laboratory of Dr. Eric CAMERER at the Paris Cardiovascular Research Center (PARCC)/INSERM U970 between October 2018 and September 2021. The work presented in the thesis is for partial fulfillment of the requirement of doctoral school ED562 BCMPP, University of Paris under the specialization “Cellular and molecular biology”. The other requirements fulfilled are: >100h of training across 3 training axes (scientific, transdisciplinary, and professional insertion), 1 scientific article published as a co-first author, 1 poster presentation at an international conference.

The work resulted in one scientific paper, which is included in the appendix of my thesis:

Endothelial $S1P_1$ signaling counteracts infarct expansion in ischemic stroke. Nitzsche A*, Poittevin M*, **Benarab A***, Bonnin P*, Faraco G, Uchida H, Favre J, Garcia-Bonilla L, Leger P-L, Therond P, Mathivet T, Autret G, Couty L, Kono M, Chevallier A, Niazi H, Tharaux P-L, Chun J, Schwab SR, Eichmann A, Tavitian B, Proia RL, Charriaut- Marlangue C, Henrion D, Sanchez T, Kubis N, Iadecola C, Hla T, and Camerer E. In revision. *equal contribution. Circ Res. 2021 Feb 5;128(3):363-382. doi: 10.1161/CIRCRESAHA.120.316711.

During this period, I also contributed to a brief synopsis of the above paper and one additional study. As the synopsis was in French and the other paper not directly related to the main focus of my research, these are listed below but not included in the thesis:

Endothelial sphingosine 1-phosphate signaling maintains perfusion of the cerebral cortex in ischemic stroke. Nitzsche A, Poittevin M, **Benarab A,** Bonnin P, Camerer E. Med Sci (Paris). 2021 Aug-Sep;37(8-9):709-711. doi: 10.1051/medsci/2021103. Epub 2021 Sep 7.

Murine platelet production is suppressed by S1P release in the hematopoietic niche, not facilitated by blood S1P sensing. Niazi H*, Zoghdani N*, Couty L, Leuci A, Nitzsche A, Allende ML, Mariko B, Ishaq R, Aslan Y, Becker PH, Gazit SL, Poirault-Chassac S, Decouture B, Baudrie V, De Candia E, Kono M, **Benarab A**, Gaussem P, Tharaux PL, Chun J, Provot S, Debili N, Therond P, Proia RL, Bachelot- Loza C, Camerer E. Blood Adv. 2019 Jun 11;3(11):1702-1713. *equal contribution

The French foundation for medical research (FRM; Fondation pour la Recherche Médicale), INSERM (Institut national de la santé et de la recherche médicale), and the Leducq Foundation supported me financially during my graduate studies.

_____

Ammar Benarab
Doctoral candidate. Paris, October 2021.

List of Abbreviations

ACA	Anterior Cerebral Artery
ApoB	Apolipoprotein B
ApoM	Apolipoprotein M
BA	Basilar Artery
BBB	Blood-Brain Barrier
CBF	Cerebral Blood Flow
CCA	Common Carotid Artery
CNS	Central Nervous System
COX-2	Cyclooxygenase-2
EC	Endothelial Cell
ECA	External Carotid Artery
eNOS	endothelial Nitric Oxide Synthase
ET-1	Endothelin-1
FXII	Coagulation Factor XII
GP	Glycoprotein
GPCR	G Protein-Coupled Receptor
HDL	High Density Lipoproteins
HPC	Hypoxic Preconditioning
i.p.	intraperitoneal
ICA	Internal Carotid Artery
ICAM-1	Inter-Cellular Adhesion Molecule-1
ICH	Intra-Cerebral Hemorrhage
LDF	Laser Doppler Flowmetry
LDL	Low Density Lipoproteins
LSF	Laser Speckle flowmetry
MCA	Middle Cerebral Artery
Mfsd2b	Major facilitator superfamily transporter 2b
MHC	Major Histocompatibility Complex
MMP	Matrix Metalloproteinase
MRI	Magnetic Resonance Imaging
mTOR	mammalian Target of Rapamycin
NET	Neutrophil Extracellular Traps
NF-kappa B	Nuclear Factor Kappa-light-chain-enhancer of Activated B cells
NO	Nitric Oxide
NVU	Neurovascular Unit
pMCAO	permanent Middle Cerebral Artery Occlusion
PPA	Pterygopalatine Artery
ROS	Reactive Oxygen Species
S1P	Sphingosine 1-Phosphate
$S1P_1$	S1P Receptor-1
$S1P_2$	S1P Receptor-2
$S1P_3$	S1P Receptor-3
$S1P_4$	S1P Receptor-4
$S1P_5$	S1P Receptor-5
S1PR	S1P Receptor
SAH	Subarachnoid Hemorrhage
Sphk	Sphingosine kinase
Spns2	Spinster homolog 2
STAIR	Stroke Therapy Academic Industry Roundtable
TIA	Transient Ischemic Attack
TJ	Tight Junction
tMCAO	transient Middle Cerebral Artery Occlusion
TNF	Tumor Necrosis Factor
TRAF2	TNF Receptor-Associated Factor 2

Treg	Regulatory T cells
TTT	Triphenyltetrazolium Chloride
VCAM-1	Vascular Cell Adhesion Molecule-1
VEGF	Vascular Endothelial Growth Factor
VLDL	Very Low-Density Lipoprotein
VWF	Von Willebrand Factor
ZO	Zonula Occludens

Chapter 1. Sphingosine 1-Phosphate

In this chapter, I will introduce sphingosine-1-phosphate (S1P), its metabolism, and its bioactive properties, highlighting its importance during vascular development. I will then discuss the capacity of S1P to regulate vascular functions via the activation of its cognate G protein-coupled receptors (GPCRs). I will round up the chapter by discussing how S1P signaling can be modulated pharmacologically.

Sphingosine 1-phosphate (S1P) is a lysophospholipid discovered as a terminal product of membrane sphingolipid metabolism in the 1960s (Stoffel, Sticht, and LeKim 1968). Studies in cultured cells later suggested that S1P had potent bioactive functions (H. Zhang et al. 1991). It was originally thought that S1P functioned as a second messenger akin to Ca^{2+} and diacylglycerol (Olivera and Spiegel 1993). However, the identification of S1P as a ligand for the orphan G protein-coupled receptor (GPCR) EDG1 (M. J. Lee et al. 1998), subsequently named S1P receptor-1 ($S1P_1$), revealed that S1P can also act extracellularly like a hormone. $S1P_1$ turned out to be the prototype of a family of 5 dedicated S1PRs (Cartier and Hla 2019). S1PR activation results in the activation of diverse intracellular signaling pathways, thereby modulating cell behavior and organ function (Figure 1) (Cartier and Hla 2019). Genetic and pharmacological studies have revealed that S1P signaling plays critical roles during embryonic development and under homeostasis and that its deregulation can contribute to pathophysiology in multiple organ systems (Proia and Hla 2015). Fingolimod (also known as FTY720), an immunotherapeutic drug that mimics sphingosine, the precursor of S1P, was shown to mediate its immunosuppressive effects through S1P receptors (S1PRs) (Mandala et al. 2002). After successful clinical trials, FTY720 was approved for the treatment of Multiple sclerosis by the United States Food and Drug Administration in 2010 (Brinkmann et al. 2010).

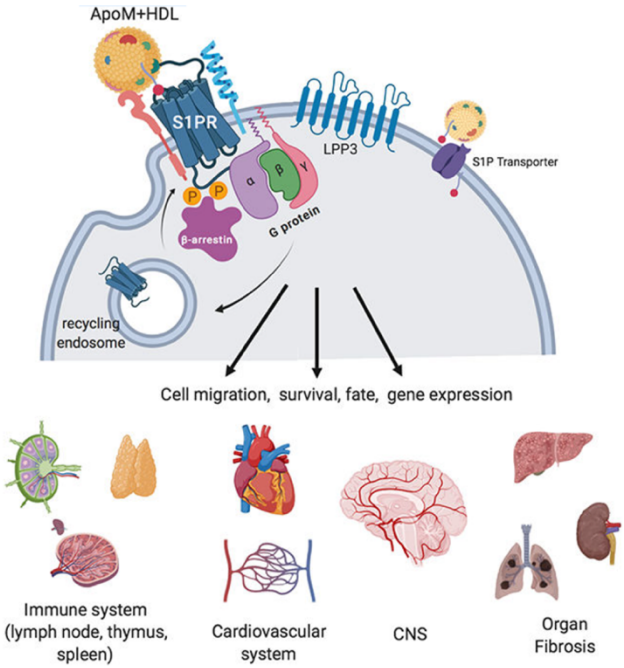

Figure 1. S1PR signaling regulatesmultiorgan physiological processes. Extracellular S1P gradients created by transporters, chaperones (ApoM + HDL), and metabolic enzymes (LPP3) interact with S1PRs on the cell surface. Receptor activity, transmitted by means of G proteins, is regulated by multiple mechanisms, including ß-arrestin coupling, endocytosis, and receptor modulators. the resultant cellular changes influence multiple organ systems in physiology and disease. Reproduced with permission from (Cartier and Hla, 2019).

As a consequence, a substantial growth in research and drug development efforts have been initiated in order to target this pathway for other autoimmune indications as well as for cardiovascular diseases (Cartier and Hla 2019).

S1P metabolism

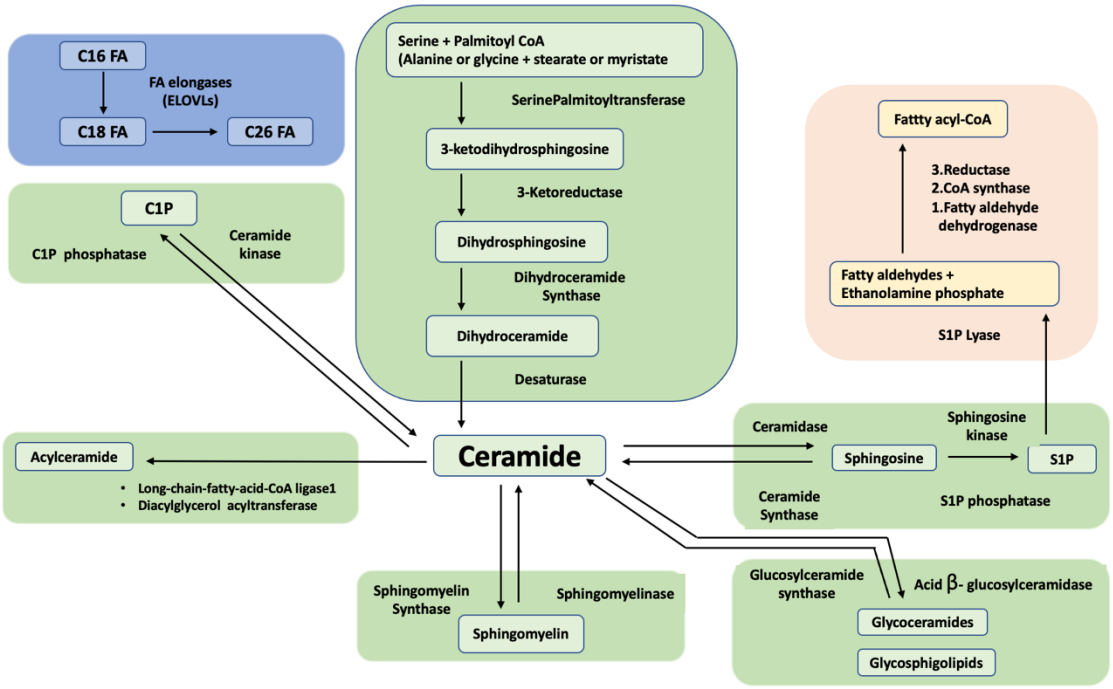

Figure 2. Overview of sphingolipid metabolism. The *de novo* biosynthetic pathway is initiated in the endoplasmic reticulum by the action of serine palmitoyltransferase (SPT). Sequential reactions lead to the generation of ceramides. Preferential substrates include serine and palmitoyl-CoA, but alanine or glycine and stearate or myristate can also be used. Ceramides are then incorporated into various complex sphingolipids (predominantly in the Golgi) through modifications at the 1-hydroxyl position to generate ceramide-1-phosphate (C1P), sphingomyelin or glycoceramides, which in turn serve as the precursors for the various glycosphingolipids. Ceramides can be acylated to form 1-O-acyl-ceramides. In sphingolipid catabolic pathways, sphingomyelin, C1P and glycosphingolipids are hydrolysed, resulting in the formation of ceramide. Constitutive catabolism occurs in the lysosome. Ceramide can then be deacylated to generate sphingosine, which in turn is phosphorylated to sphingosine-1-phosphate (S1P). Exit from sphingolipids is initiated by the action of S1P lyase, which cleaves S1P (or dihydroS1P) to a fatty aldehyde and ethanolamine phosphate. The fatty aldehyde undergoes further metabolism, resulting in the formation of palmitoyl-CoA. The fatty acid elongation module is an important adjunct component of the sphingolipid pathway, as sphingolipids are the primary lipids with very-long (C22–26) and ultra-long (longer than C26) fatty acyl chains. Reproduced with permission from (Hannun and Obeid 2018).

S1P is generated by two enzymes, namely sphingosine kinases (Sphks) 1 and 2, by reversible phosphorylation of sphingosine, which is in turn a product of ceramide metabolism as shown in Figure 2. While early studies demonstrated that Sphk1&2 are both widely expressed (H. Liu et al. 2000), it has become clear later that they play non-redundant roles in S1P production in some cell types (e.g. Sphk1 in red cells and Sphk2 in platelets) (Gazit et al. 2016). These enzymes differ in their intracellular localization, regulation, level of tissue expression and

therefore their functions (Alemany et al. 2007). Sphk1 is largely cytoplasmic and can acutely associate with the plasma membrane (Pitson et al. 2003), phagosomes (Thompson et al. 2005), and endosomal vesicles (Shen et al. 2014). While Sphk2 is also present in cytoplasm it is predominantly localized in the nucleus (N. Igarashi et al. 2003)(Proia and Hla 2015), the inner mitochondrial membrane and the endoplasmic reticulum. This could argue that Sphk1 is more important for S1P production for cellular export, although Sphk1 knockout (KO) mice are viable and show only a 50% reduction in plasma S1P (Allende et al. 2004). In contrast, Sphk2 KO mice have high plasma S1P levels due to deficient S1P clearance (Kharel et al. 2020). Sphingosine is produced from ceramide under the action of ceramidases. Ceramide generation is the pivotal step of the sphingolipid metabolic pathway. It can be produced in the smooth endoplasmic reticulum by *de novo* synthesis of sphingolipids, initiated by the condensation of acid serine and palmitoyl-CoA resulting in 3-keto-dihudrosphingosine under the action of serine palmitoyl transferase. Alternatively, it can be generated by sphingomyelin hydrolysis and/or the recycling of complex sphingolipids (Maceyka and Spiegel 2014) (Hakomori 2000). In addition to S1P, ceramide metabolism also generates complex sphingolipids such as sphingomyelin by sphingomyelin synthase and glucosylceramide by glucosylceramide synthases, both crucial components of cellular membranes. S1P can be exported from the cell in which it is produced, dephosphorylated intracellularly by S1P phosphatases or extracellularly by lipid phosphate phosphatases, or irreversibly degraded by S1P lyase into phospho-ethanolamine and hexadecenal. The ORMDL and NOGO families of sphingolipid biosynthesis regulators control *de novo* sphingolipid synthesis by inhibiting serine palmitoyl transferase (Cantalupo et al. 2015) (Y. Zhang et al. 2016).

S1P export

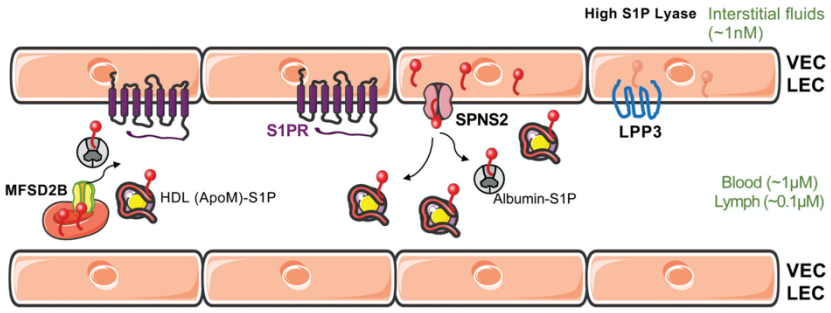

Figure 3. Establishing and maintaining S1P gradients in vessels. S1P is transported by chaperones ApoM HDL and albumin in the circulation and presented to S1PRs. S1P export by vascular ECs (VECs) and lymphatic ECs (LECs) (by Spns2) and by RBCs (by MFS2B) as well as degradation of S1P by the phosphatase LPP3 modify the extracellular S1P gradient. Low interstitial tissue S1P is achieved by the S1P lyase. Tissue concentrations of S1P are indicated in parentheses. S1PR, sphingosine 1-phosphate receptor; Spns2, sphingolipid transporter 2; MFSD2B, major facilitator superfamily domain containing 2B; LPP3, lipid phosphate phosphatase 3. Reproduced with permission from (Cartier and Hla 2019).

S1P is exported from cells by dedicated transporters and is attributed to spinster homolog 2 (Spns2) in endothelial cells (ECs) and major facilitator superfamily domain containing 2b (Mfsd2b) in erythrocytes and platelets (Figure 3). Major sources of circulating S1P are erythrocytes and ECs; erythrocytes are particularly efficient at S1P production as they express

Mfsd2b but not S1P degrading enzymes. Mice lacking Sphk1 or Mfsd2b in erythrocytes both show a 50% decrease in plasma S1P (Ito et al. 2007)(Xiong et al. 2014). Endothelial cells express Spns2 and also contribute S1P to plasma (Venkataraman et al. 2008)(Kawahara et al. 2009). Endothelial cell secretion of S1P is controlled by fluid shear stress (Venkataraman et al. 2008). Platelets also lack S1P degrading enzymes and express Mfsd2b (Vu et al. 2017). However, plasma S1P concentrations are normal in mice lacking platelets or with platelet-selective deletion of *Sphk1&2* or *Mfsd2b* (Venkataraman et al. 2008)(Pappu et al. 2007)(Gazit et al. 2016)(Chandrakanthan et al. 2021). Platelets do release S1P upon activation, and S1P concentrations in serum are twice those of plasma, suggesting that platelet activation will increase local S1P concentrations (Y. Igarashi and Yatomi 1998) (Gazit et al. 2016). Although ECs are a minor source of plasma S1P, Spns2-mediated export of S1P from lymphatic ECs is critical for S1P contribution to lymph and for the egress of lymphocytes from lymph nodes into circulation (Fukuhara et al. 2012)(Mendoza et al. 2012)(Cartier and Hla 2019).

S1P chaperones

Once exported, S1P can activate S1PRs in the same cell in an autocrine manner. S1P is poorly water soluble because of its hydrophobic nature, and carrier proteins are required for efficient transport and circulation, enhancing S1P diffusion in the extracellular environment. This allows for the generation of a spatial gradient and the activation of S1PRs in a paracrine and/or endocrine manner (Figure 3). In plasma, several chaperones carry S1P including high density lipoproteins (HDL; ~60 %), albumin (~30%), low density lipoproteins (~8%) and very low density lipoprotein (2-3%) (N. Murata et al. 2000). S1P associates with HDL with high affinity through apolipoprotein M (ApoM) (Obinata et al. 2019) (Christoffersen et al. 2011). In contrast, albumin has a relatively low affinity for S1P (~40 uM) (Fleming et al. 2016). Through additional interactions between other lipoproteins and endothelial receptors (e.g. SR-B1), HDL-bound ApoM appears to be more important than albumin S1P for activation of $S1P_1$ on ECs, where it plays important roles in suppressing inflammation and promoting barrier function and nitric oxide (NO) release (Galvani et al. 2015). It is noteworthy that in mice deficient in both ApoM and albumin, S1P still associates with HDL via ApoA4 (Obinata et al. 2019).

S1P spatial gradients

While S1P levels in blood and lymph are high due to continuous export from erythrocytes and (ECs), S1P levels in tissue are maintained very low through the activity of the S1P degradation mechanisms. The spatial gradient formed between high S1P concentrations in blood and lymph to low concentrations in interstitial fluids is critical for lymphocyte egress into circulation (Figure 3) (Schwab et al. 2005)(Cartier and Hla 2019). Loss of S1P export and

disturbances in the local S1P gradient is also implicated in vascular defects inducing early hearing loss (J. Chen et al. 2014) and defective retinal angiogenesis (Fang et al. 2018).

S1P signaling mechanisms

Intracellular signaling

S1P has been implicated in three main intracellular functions, which include the epigenetic regulation of gene expression, the regulation of mitochondrial function, and the regulation of inflammation and cell survival. Sphk2, which is mainly found in the nucleolus, was shown to associate with histone H3 and produce S1P to regulate histone acetylation (Hait et al. 2009). S1P bound to histone deacetylases 1&2 and inhibited their enzymatic activity. Histone deacetylases have thus been suggested to be direct intracellular targets of S1P and link S1P to epigenetic regulation of gene expression. S1P produced in the mitochondria predominantly by sphingosine kinase 2 (Sphk2), has also been shown to bind with high affinity and specificity to prohibitin 2, a highly conserved protein that regulates mitochondrial assembly and function (Strub et al. 2011). Tumor-necrosis factor (TNF) receptor-associated factor 2 (TRAF2) has been proposed as an intracellular target of S1P, suggesting a key role of Sphk1/S1P in TNF-alpha signaling and Nuclear Factor Kappa-light-chain-enhancer of Activated B cells (NF-kappa B) pathway activation thus directly contributing to inflammatory and cell survival pathways (Alvarez et al. 2010). TRAF2 represent a key component in NF-kappa B signaling triggered by TNF-alpha. Sphk1 and the production of S1P were shown to be necessary for lysine-63-linked polyubiquitination of RIP1, leading to NF-kappa B activation. Importantly, some of these intracellular functions attributed to S1P have later been contested (Cartier and Hla 2019)(Etemadi et al. 2015)(Xiong et al. 2016).

S1P receptors

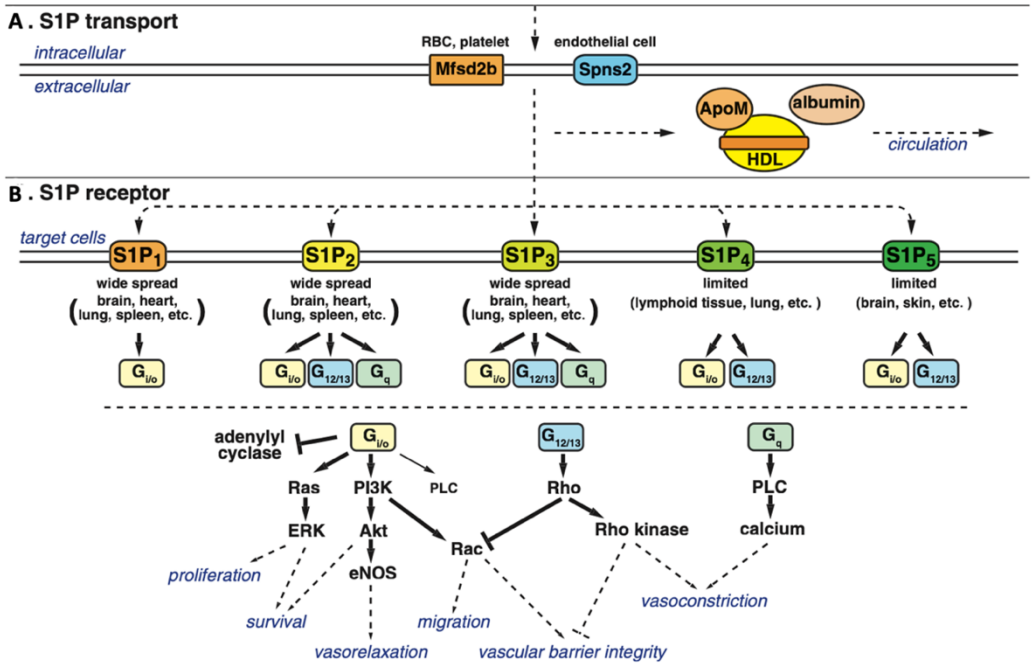

Figure 4. Overview of the S1P-S1P receptor signaling system. **A.** S1P produced intracellularly is transported by specific transporters such as Mfsd2b [red blood cell (RBC) and platelet] and Spns2 (endothelial cells) and carried by albumin and HDL-associated specific S1P chaperone protein, ApoM. **B.** S1P activates S1P receptors, $S1P_{1\text{-}5}$, which transmit diverse intracellular signals depending on the coupled Gα subunits of heterotrimeric G protein and the expression pattern of each receptor in a given cell type. Modified with permission from (Obinata and Hla 2019).

Genetic and pharmacological studies in mice have attributed many of the key developmental and physiological roles of S1P to its extracellular, receptor-mediated actions (Figure 4). The interaction between S1P and its receptors can induce a wide range of physiological responses such as proliferation, migration, inhibition of apoptosis, formation of actin stress fibers, stimulation of adherent junctions, and enhanced extracellular matrix assembly (Park and Im 2017). Downstream intracellular signaling pathways controlled by heterotrimeric G proteins include Rho family small guanosine triphosphatases and the protein kinase AKT, which coordinate changes to the cytoskeleton, cell adhesion, and cell survival (X. E. Zhang, Adderley, and Breslin 2016). S1PRs couple to heterotrimeric G proteins, consisting of one variable subunit (Gα) of several subclasses including $G\alpha_i$, $G\alpha_q$, and $G\alpha_{12/13}$, and two constant subunits (Gβ and Gγ) (Reinhard et al. 2017). Once S1P binds, S1PRs act as guanine nucleotide exchange factors, exchanging guanosine diphosphate on the G protein α subunit for guanosine 5'-triphosphate. This results in the dissociation of the heterotrimer, releasing Gα-GTP from the Gβ-Gγ dimer and inducing the activation of downstream effectors. S1PR expression is heterogenous: $S1P_1$ is expressed primarily in the vascular endothelium and in hematopoietic cells; $S1P_3$ is expressed on smooth muscle cells, cardiomyocytes, fibroblasts, and dendritic cells; $S1P_2$ can be expressed on most of the above cell types but its expression is low under homeostasis; $S1P_4$ is predominantly expressed in innate immune cells; and $S1P_5$ is expressed

in lymphocytes, natural killer cells and in the central nervous system (Kleuser 2018). S1P receptor activation relies on specific G protein coupling in different cell types. $S1P_1$ couples exclusively with $G\alpha_i$; $S1P_4$ and $S1P_5$ also couple to $G\alpha i$ but also to $G\alpha_{12/13}$, whereas $S1P_2$ and $S1P_3$ are more promiscuous and couple to $G\alpha_i$, $G\alpha_{q/11}$ and $G\alpha_{12/13}$ (Cannavo et al. 2017).

S1P signaling in embryonic development

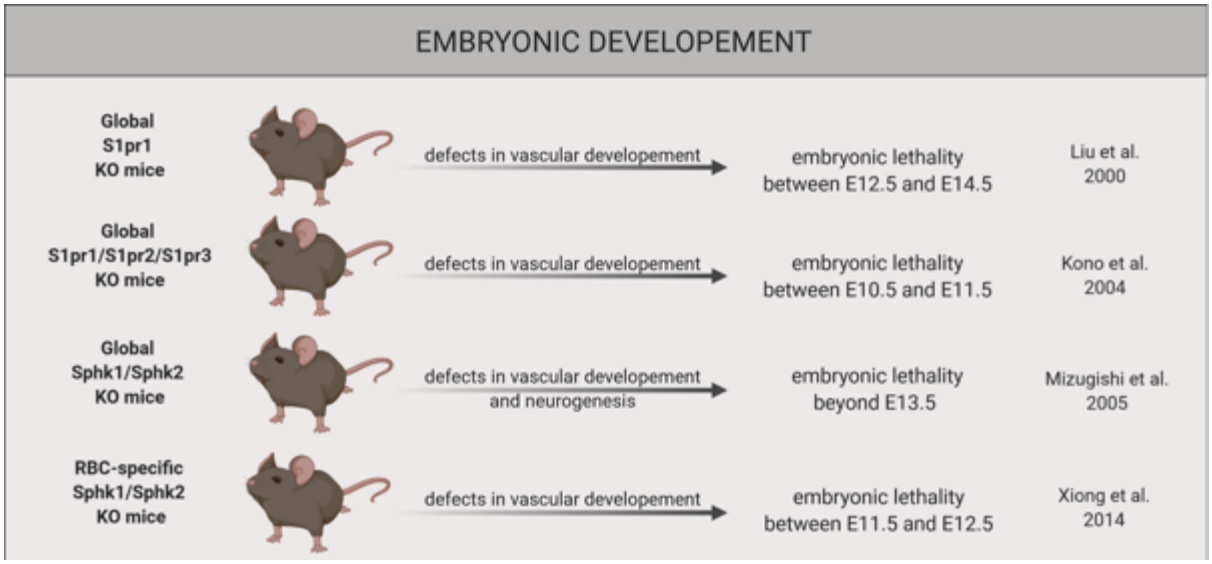

Figure 5. Deficient S1P production and signaling impairs mouse embryonic development. Complete deficiency in S1P production or signaling and isolated global or endothelial-selective deficiency in $S1P_1$ signaling all impair embryonic development. In contrast, mice with isolated global deficiency in Sphk1, Sphk2, and all S1PRs except $S1P_1$ are all viable. S1PR - sphingosine-1-phosphate receptor, Sphk – sphingosine kinase, RBC – red blood cell, KO – knockout mice. Reproduced with permission from (Jozefczuk, Guzik, and Siedlinski 2020).

S1P signaling contributes to proper development of the circulatory system during murine and zebrafish embryogenesis (Jozefczuk, Guzik, and Siedlinski 2020) (Figure 5). The primitive embryonic vasculature forms by vasculogenesis, which is driven by aggregation of endothelial progenitor cells to form a primitive vascular network. Several mechanisms are later involved in the expansion of this network, including its remodeling, stabilization and maturation to make a complex, fully functional network of vessels (Moccia et al. 2019). Global or endothelial-selective $S1P_1$ deficiency in mice results in death in utero between embryonic days 12 and 14 with failed vascular maturation and severe bleeding (Y. Liu et al. 2000) (Gaengel et al. 2012)(Allende, Yamashita, and Proia 2003). With compound deficiency of $S1P_{1,2\&3}$, mice die between embryonic days 10 and 12, also with bleeding (Kono et al. 2004). Compound deletion of *SphK1&SphK2* also resulted in death before E13.5 with bleeding and failed neurogenesis (Mizugishi et al. 2005). These observations highlight the vital importance of S1P production and S1PR activation for vascular maturation.

S1P signaling in Angiogenesis

Angiogenesis represents the sprouting of new blood vessels from existing blood vessels (Chung and Ferrara 2011). Physiological angiogenesis occurs mainly during organ development; in adults it is restricted to processes such as wound healing, skeletal growth, pregnancy, and the menstrual cycle. Excessive angiogenesis is a hallmark of cancer and other pathologies. In a tissue deprived of oxygen, angiogenesis is initiated by the activation of hypoxia-inducible factor and vascular endothelial growth factor (VEGF). This, in turn, is followed by induction of neovascularization via increased vascular permeability, induction of endothelial cell proliferation, migration and tube formation (Krock, Skuli, and Simon 2011). Vessel maturation and stabilization are achieved by the recruitment of mural cells and deposition of basement membrane (Potente, Gerhardt, and Carmeliet 2011). When vascular sprouts fuse from primary networks, the formation of a vascular lumen allows plasma S1P to access ECs (Gaengel et al. 2009) (Jung et al. 2012). These fusion events coincide with the induction of $S1P_1$ expression in the endothelium, and consequently, the formation of adherens junctions and cell-extracellular matrix adhesions that enable the vascular barrier to form as shown in Figure 6 (M. J. Lee et al. 1999)(Paik et al. 2004). Activation of endothelial NO synthase (eNOS) dilates vessels and promotes blood flow. $S1P_1$ counteracts VEGF function to prevent excessive vessel sprouting once vessels form lumens, by regulating junctional proteins and the mechanosensing machinery (Jung et al. 2012). $S1P_1$ signaling downregulates VEGF-induced phosphorylation of VEGF receptor 2 (VEGFR2), ERK1/2 and Akt and prevents vascular endothelial cadherin internalization and thus stabilizes endothelial cell adherens junctions (Gaengel et al. 2012). $S1P_1$ deletion is associated with hyper sprouting of the developing aorta, suggesting a similar role in the developing vasculature. Contrasting the role of $S1P_1$, $S1P_2$ deficiency reduces pathological neovascularization (Skoura et al. 2007). Multiple redundant sources of circulating S1P form RBCs, ECs, and platelets maintain circulating S1P levels during vascular development (Xiong et al. 2014) (Swendeman et al. 2017)(Swendeman et al. 2017) (Gazit et al. 2016).

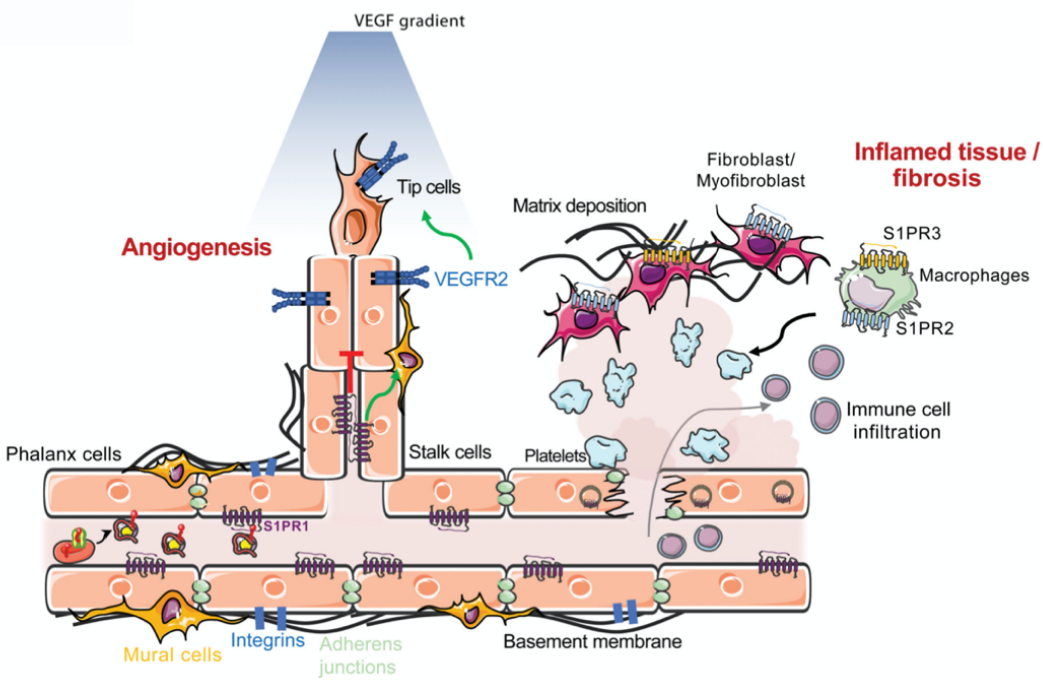

Figure 6. S1P function in vascular development, homeostasis, and pathology Vascular network development, maturation, and stabilization are regulated by endothelial $S1P_1$. Activation of $S1P_1$ inhibits sprouting angiogenesis and vascular endothelial growth factor receptor 2 (VEGRF2) and promotes vascular stability through adherens junctions and cell–extracellular matrix adhesion (integrins). Loss of cell-surface $S1P_1$ and destabilization of the endothelium causes the leakage of plasma and immune cells into the tissue, leading to inflammation. Vascular damage also leads to thrombosis (platelet aggregation) and fibrin deposition in the interstitial space, which activates fibroblasts and macrophages. Loss of S1PR1 signaling on endothelial cells and activated S1PR2 and S1PR3 signaling on macrophages and fibroblasts ultimately leads to tissue fibrosis, with extracellular matrix deposition, and organ dysfunction. Reproduced with permission from (Cartier and Hla 2019).

S1P signaling in the regulation of vascular integrity

The endothelial barrier maintains transport selectivity of fluids and solutes between blood and surrounding tissues (Nagy et al. 2008). Contractile forces are provided by actin-myosin crosslinking in addition to cell-cell and cell matrix interactions, which ultimately contribute to the maintenance of vessel wall integrity. The presence of a glycocalyx on the luminal surface of blood vessels is another component of the blood to tissue barrier (Bermejo-Martin et al. 2018). Endothelial barrier disruption results in vascular leakage (Xiong and Hla 2014), is a hallmark of acute inflammatory diseases such as sepsis and acute lung injury (Opal and van der Poll 2015) and promotes tumor cell invasion and metastasis spread (Reymond, d'Água, and Ridley 2013). $S1P_1$ signaling has been shown to play a critical role in promoting endothelial barrier function to limit plasma and leukocyte extravasation (Figures 6&7) (Swendeman et al. 2017)(Burg et al. 2018). In vitro, EC $S1P_1$ activation promotes adherence junction formation, increases electrical impedance in monolayers of ECs and promotes tight junction (TJ) assembly (M. J. Lee et al. 1999) (Garcia et al. 2001).

In mice, genetic deficiency in S1P provision to plasma increased vascular leak under homeostasis and mortality after inflammatory challenges (Camerer et al. 2009). Increased basal leak could be reversed by transfusion with wild-type erythrocytes or treatment with an

$S1P_1$ agonist, and replicated with endothelial-selective deletion of *S1pr1* (Camerer et al. 2009) (Gazit et al. 2016). Plasma albumin stabilizes the endothelial glycocalyx and its depletion result in glycocalyx shedding from endothelial surface and disruption of barrier integrity *in vitro* (Zeng et al. 2014) (Lum et al. 1991). *In vitro* studies have suggested that S1P action through $S1P_1$ suppresses the activity of metalloproteinases MMPs that mediate endothelial glycocalyx shedding (Zeng et al. 2014). However, the role for S1P in stabilizing the endothelial glycocalyx has so far not been confirmed *in vivo.* The control of local S1P signaling may be vascular bed and possibly organ-specific to enable precise control of the vascular system in response to organ specific metabolic and physiological challenges (Cartier and Hla 2019). Cellular response to S1P may also depend on plasma S1P concentrations and chaperone partitioning. Deficient S1P signaling may thus contribute to endothelial barrier dysfunction in disease conditions, and potentially be overcome by replenishment of plasma S1P or $S1P_1$ agonists. For example, administration of S1P during resuscitation in the context of hemorrhagic shock improved endothelial barrier function and protected against microvascular leakage in rats (Alves et al. 2019).

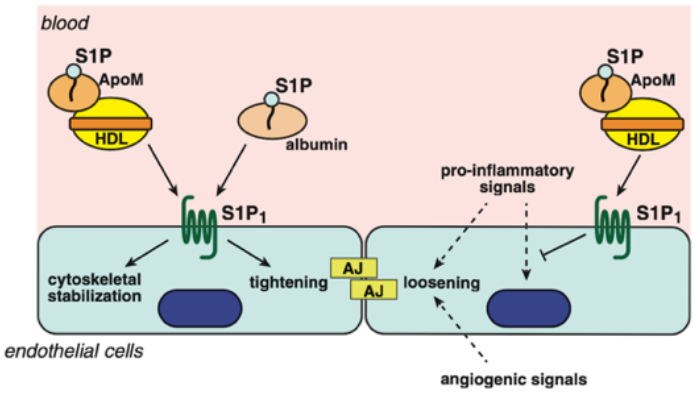

Figure 7. S1P and vascular integrity. S1P, either carried by albumin or HDL-ApoM, acts on $S1P_1$ and induces cytoskeletal stabilization and tightening of adherens junctions (AJs) in endothelial cells, while angiogenic signals such as vascular endothelial growth factor from hypoxic tissues or pro-inflammatory signals such as histamine and leukotrienes induce loosening of AJs. S1P carried by HDL-ApoM also suppresses pro-inflammatory endothelial responses induced by cytokines. These anti-angiogenic and anti-inflammatory actions by the S1P-S1P receptor signaling system contribute to the maintenance of vascular integrity. Reproduced with permission from (Obinata and Hla 2019).

S1P has also been suggested to be the main contributor to the vascular protective effect of plasma administration in patients after trauma associated hemorrhagic shock (Halbgebauer et al. 2018). However, while S1P plays a role as a barrier protective agent under physiological conditions, it may disrupt endothelial barrier function at higher concentrations or when endothelial $S1P_2$ expression is induced by inflammatory mediators (Xiong and Hla 2014)(Komarova, Mehta, and Malik 2007)(Shikata, Birukov, and Garcia 2003). In contrast to $S1P_1$, $S1P_2$, $S1P_3$ and downstream Rho activation has been associated with increased vascular permeability both *in vitro* and *in vivo* (Singleton et al. 2006)(G. Zhang et al. 2013)(Sanchez et al. 2007).

S1P signaling in the regulation of vascular tone and blood pressure

$S1P_1$ and $S1P_3$ are highly expressed in ECs, while $S1P_2$ and $S1P_3$ are both present in vascular smooth muscle cells, and the capacity of S1P signaling to regulate vascular tone is well recognized (Kerage, Brindley, and Hemmings 2014) (Kluk and Hla 2002) (Skoura and Hla 2009). Activation of S1P signaling through endothelial receptors $S1P_1$ and $S1P_3$ induces production of the potent vasodilator NO, in opposition to vasoconstrictive effects of S1P that are mediated by smooth muscle $S1P_2$ and $S1P_3$ via Rho kinase (Schuchardt et al. 2011)(Junsuke Igarashi and Michel 2009). These effects are species and vessel specific (Intapad 2019). For instance, in rats and mice S1P induces eNOS dependent vasorelaxation in epinephrine pre-constricted mesenteric arterioles. In contrast, S1P induced vasoconstriction in canine basilar arteries, rodent cerebral arteries, as well as in mesenteric resistance arteries from aged rats (Hemmings 2006) (Salomone et al. 2003). This suggests that depending on the vessel type, dilatory or contractile effects of S1P may dominate. This may reflect S1P receptor expression and could involve the induction of $S1P_2$ expression in ECs during ageing and inflammation (Scherer et al. 2010), as $S1P_2$ has been shown to counteract $S1P_1$-mediated eNOS activation in ECs (Cui et al. 2013). Effects of exogenous S1P may also depend on the level of EC autonomous S1P production. In ECs S1P production is sensitive to shear stress, suggesting that S1P-$S1P_1$ is engaged to regulate vascular tone in response to mechanotransduction (Cantalupo et al. 2015) (Jung et al. 2012). While intravenous administration of S1P induces a transient decrease in mean arterial pressure, continuous infusion of S1P increases blood pressure in both mice and rats (Forrest et al. 2004). It is likely that these effects are mediated by activation of $S1P_1$ and $S1P_3$, respectively. Indeed, SEW2871, a specific $S1P_1$ agonist, has been shown to provide an antihypertensive effect by a marked reduction in systolic blood pressure (around 25 mmHg decrease) in mice with angiotensin II-induced hypertension (Cantalupo et al. 2015). Although reportedly expressed on both ECs and smooth muscle cells, $S1P_3$ accounts for S1P-mediated vasoconstriction but plays a limited role in S1P-mediated vasodilation in isolated mesenteric arteries (Cantalupo et al. 2017). $S1P_2$ is also implicated in S1P-mediated vasoconstriction in other vascular beds, notably after inflammatory challenge, and mice lacking $S1P_2$ exhibit impaired vasoconstriction and display reduced peripheral vascular resistance (Lorenz et al. 2007). In experimental hypertension models induced by Ang II-infusion, plasma S1P levels are significantly elevated, and mice with a global deletion of Sphk1 or Sphk2 develop less severe Ang II-dependent hypertension (Wilson et al. 2015) (Siedlinski et al. 2017) (Meissner et al. 2017). Although $S1P_1$, $S1P_2$, $S1P_3$ and Sphks are expressed in the kidneys, the contribution of renal S1P signaling to the regulation of blood pressure has not yet been investigated (Intapad 2019)(Q. Zhu et al. 2011).

S1P signaling in inflammation

Vascular dysfunction, characterized by impaired endothelial vasodilatation, increased vascular permeability, oxidative stress and inflammation, constitutes an early hallmark of cardiovascular disease and an initiating factor for the development and the progression of atherosclerosis (Gimbrone and García-Cardeña 2016). In atherosclerosis there is a significant decrease in anti-atherogenic HDL and an increase in plasma levels of triglycerides and apolipoprotein B (ApoB)-containing lipoproteins such as LDL, intermediate-density lipoprotein and VLDL (Bobryshev et al. 2017) (Mineo 2020). HDL has anti-inflammatory, anti-oxidative, anti-thrombotic, pro-angiogenic and vasorelaxant actions on the vessel wall (Nicholls and Nelson 2019). Some of these are mediated by ApoM/S1P-dependent activation of $S1P_{1\&3}$, which not only enhance endothelial barrier function and promote vasorelaxation through eNOS activation (J. Igarashi, Bernier, and Michel 2001), but also prevent the activation of NFkB and nuclear glucocorticoid receptor pathways and thus endothelial inflammation (Engelbrecht et al. 2020). The capacity of HDL to suppress NFkB depends in part on S1PR activation and can be mimicked by $S1P_1$ agonists (Galvani et al. 2015). Moreover, $S1P_1$ deficient mice show increased expression of EC adhesion molecules and chemokine release both under homeostasis and after exposure to an atherogenic diet and are resistant to the development of atherosclerosis (Galvani et al. 2015)(Engelbrecht et al. 2020). The vasodilatory effect of HDL was reduced in mice lacking $S1P_3$, arguing a role also for this receptor (Nofer et al. 2004). HDL-induced EC S1PR signaling supports coronary circulation through eNOS dependent vasodilatation and protection from myocardial ischemia-reperfusion injury (Levkau et al. 2004). HDL-associated S1P can also prevent EC apoptosis (Kimura et al. 2003)(Nofer et al. 2004), and $S1P_1$ signaling promotes EC survival and proliferation after severe lung injury (Akhter et al. 2021). Endothelial activation in response to inflammatory mediators may also increase EC S1P release secondary to the induction of *Sphk1* expression and alter responses to S1P secondary to the induction of $S1P_2$ expression (Meissner et al. 2012) (G. Zhang et al. 2013). This in turn can reverse the impact of S1P signaling on the endothelium, increasing vasoconstriction after heart failure (Kroetsch and Bolz 2013) and aggravating endothelial dysfunction and organ damage during endotoxemia and after ischemic stroke (G. Zhang et al. 2013) (Kim et al. 2015). It is not known if this switch is sensitive to different sources of S1P or chaperone distribution.

S1PR modulators

Fingolimod

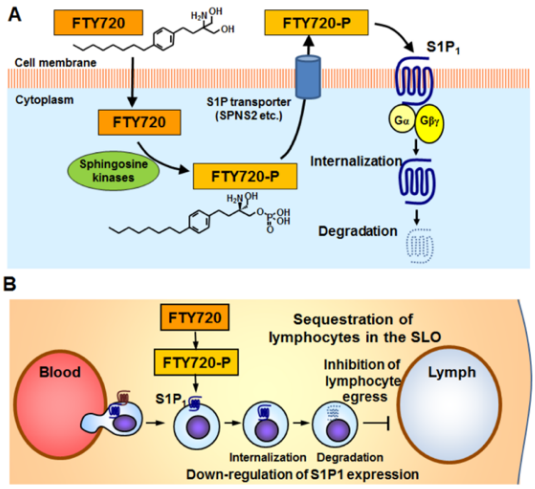

Figure 8. FTY720-P converted from FTY720 acts as a functional antagonist at lymphocytic $S1P_1$. (A) FTY720-P is converted from FTY720 by sphingosine kinases, binds $S1P_1$ receptor, and induces internalization and degradation of $S1P_1$. (B) FTY720-P inhibits $S1P_1$-dependent lymphocyte egress from the SLO. SLO= Secondary lymphoid organs. Reproduced with permission from (Chiba et al. 2014).

In 1992, Fingolimod (FTY720) was discovered by Yoshitomi Pharmaceuticals. It was synthesized from the fungal metabolite myriocin (ISP-1), which was isolated from Isaria Siclairii, known to be used for eternal youth in Chinese medicine (Adachi and Chiba 2007). FTY720 is a strong immunosuppressive drug that was approved for the treatment of multiple sclerosis by the United States Food and Drug Administration in 2010 (Singer 2013). FTY720 is phosphorylated intracellularly by Sphk2 to its physiologically active form FTY720-P (Paugh et al. 2003), which is then transported to the extracellular space by S1P transporters including Spns2 (Hisano et al. 2011). FTY720 acts as an agonist with high affinity on four of the five known G protein coupled S1P receptors (S1P1, S1P2, S1P3, S1P5) (Brinkmann and Lynch 2002) (Mandala et al. 2002). It also acts as a functional antagonist on $S1P_1$ by transient downregulation (endocytosis) and degradation of the receptor. FTY720 thereby prevents lymphocyte egress from secondary lymphoid organs to lymph and blood, resulting in strong lymphopenia and alleviation of detrimental lymphocytic inflammation (Figure 8). In humans, FTY720 shows high plasma protein binding with more than 99% and bioavailability around 93%. Oral application takes 12-16 hours to reach maximal plasma concentrations. The half-life of FTY720 is 6-9 days (David, Kovarik, and Schmouder 2012). Side effects reported with clinical use of FTY720 include bradycardia, macular edema, hypertension, and pulmonary complications and have been attributed to positive and negative modulation of cardiac and vascular S1PRs (Behjati, Etemadifar, and Abdar Esfahani 2014). To gain benefit from S1PR modulation and avoid the described side effects, more specific S1PR agonists have been developed.

S1PR selective modulators

The success of FTY720 in the treatment of multiple sclerosis has led to the development of several novel S1PRs modulators to allow more selective S1PR targeting and eliminate side effects. These have been explored in cell culture models and in experimental studies, and several have also been pursued in clinical trials and reached approval for clinical use. The primary focus of the pharmaceutical industry has been to retain the lymphocyte depleting

effects of FTY720 as well as its positive effects on remyelination while eliminating cardiovascular side effects. Pharmacological and genetic studies have attributed side effects to activation (bradycardia and hypertension) or desensitization (macular edema, pulmonary complications and potentially hypertension) of vascular receptors, notably $S1P_1$ (bradycardia, macular edema, pulmonary complications and potentially hypertension) and $S1P_3$ (bradycardia in mice, and hypertension) (Fryer et al. 2012). While receptor selectivity may be useful for eliminating the component of hypertension driven by $S1P_3$ activation (another component may be explained by $S1P_1$ desensitization), drug dosing has been more important for overcoming bradycardia and loss of vascular integrity, which, like lymphocyte depletion, both depend on $S1P_1$. Experience with selective modulators suggest that lymphocyte depletion and remyelination depend on $S1P_1$ and $S1P_5$, respectively, and that functional $S1P_1$ antagonism is safer than pure antagonism for the inhibition of lymphocyte egress. Siponimod (BAF312) and Ozanimod, functional antagonists of $S1P_1$ that also target $S1P_5$, and Ponesimod, an $S1P_1$-selective modulator, were all recently FDA approved for the treatment of multiple sclerosis (Kappos et al. 2018) (Roy, Alotaibi, and Freedman 2021).

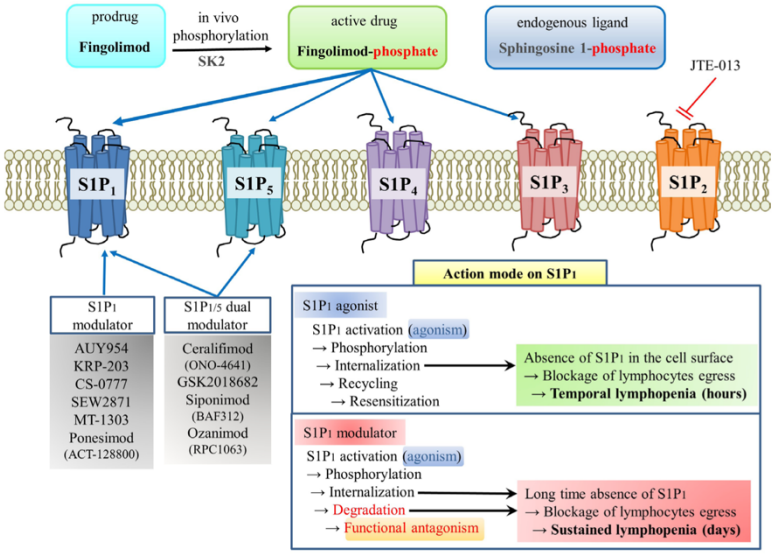

Figure 9. Action mechanism of FTY720 and other S1P receptor modulators. FTY720 is transformed to FTY720-phosphate *in vivo* by sphingosine kinases. FTY720-phosphate can activate $S1P_1$, $S1P_3$, $S1P_4$, and $S1P_5$, which recruits b-arrestin and induces $S1P_1$ internalization, blocks lymphocyte egression from secondary lymphoid organs and reduces T and B cell counts in the blood. Lymphopenia is presumed to be the main mechanism whereby FTY720 causes immune suppression in autoimmune diseases, modified with permission (Park and Im 2017).

It is important to note that because these drugs were all developed with the aim of obtaining lymphopenia, they are all desensitizing on $S1P_1$ (Poirier et al. 2020). In addition to these three clinically approved agonists, several selective S1PR modulators have been developed that have been useful for exploring the functions of S1P receptors in experimental models and for testing the potential benefit of positive modulation of $S1P_1$ in the cardiovascular system (Figure 9). SEW2871 was one of the first highly selective $S1P_1$ agonist to be developed, which has been extensively used in cell culture studies and experimental models (Sanna et al. 2004)(Hale et al. 2004). This include studies to demonstrate that $S1P_1$ activation can provide benefit in the context of LPS-induced acute lung injury, diabetes, Alzheimer's disease, liver fibrosis, acute kidney injury and ischemic stroke (Sammani et al. 2010) (Lien et al. 2006)(Park and Im 2017). CYM 5442, an $S1P_1$ selective agonist which was used in a mouse model of

multiple sclerosis, rapidly distributes to the brain, triggers only transient immune-suppression, and is mostly washed out from plasma and brain 24 hour after administration (Gonzalez-Cabrera et al. 2008). KRP-203 has been explored in experimental autoimmune myocarditis (Shimizu et al. 2005) and inflammatory bowel disease such as Crohn's disease. AUY954, another potent and selective $S1P_1$ agonist had beneficial effects in rat heart transplantation (Pan et al. 2006) and in experimental autoimmune neuritis and lung inflammation (Z.-Y. Zhang et al. 2009). SAR247799, an $S1P_1$ agonist recently developed by Sanofi, may allow positive targeting of endothelial $S1P_1$ without induction of lymphopenia by virtue of biased agonism on this receptor (Grailhe et al. 2020). Selective negative modulation of S1PR1 can be achieved with W146 (Gonzalez-Cabrera et al. 2008) or NIBR-0213 (Quancard et al. 2012). While multiple selective modulators exist for $S1P_1$, the tools developed for other S1PRs are more limited. JTE-013 is a potent $S1P_2$ antagonist shown to inhibited brain endothelium microvascular permeability intracerebral hemorrhage end neurovascular injury in experimental model of stroke (Kim et al. 2015). However, although JTE-013 is reported not to target the other four S1P receptors (Osada et al. 2002), it has non-specific effects on other GPCRs (S. Salomone et al. 2008). Selective modulators have been developed for $S1P_3$ (Jo et al. 2012), and the role of $S1P_5$ is often defined by comparing effects of $S1P_1$ modulators with bi-selective $S1P_{1/5}$ modulators (Chun, Giovannoni, and Hunter 2021).

Engineered S1P chaperones

S1P chaperones provide an additional opportunity for S1P receptor modulation. Although S1P infusion has been shown to provide benefit in some studies, this is not a viable approach because of the extremely short half-life of S1P. ApoM protects S1P from degradation, and lipoprotein-associated S1P is thought to have a considerably longer half-life than albumin-associated S1P. HDL-S1P has also been shown to promote more sustained $S1P_1$ signaling on ECs than albumin-S1P (Galvani et al. 2015)(Argraves et al. 2008). These properties of ApoM prompted the development of recombinant, stabilized, ApoM for therapeutic targeting of endothelial S1P receptors (Swendeman et al. 2017). Infusion of an engineered, S1P loaded ApoM (ApoM-Fc), was shown to suppress the induction of endothelial inflammation *in vitro* (Kurano et al. 2018)(Cartier and Hla 2019) and to improve outcome in experimental models of hypertension, stroke and myocardial infarction (Swendeman et al. 2017)(Cartier and Hla 2019). Similar to SAR247799, ApoM-S1P did not induce lymphopenia, indicating that chaperones-bound S1P also sustained activation of $S1P_1$ in the endothelium without inducing receptor downregulation in secondary lymph organs. This highlights the utility of biased agonists of $S1P_1$ that do not induce receptor endocytosis and degradation for sustained endothelial protective effects through NO synthesis, increased barrier function and endothelial cell survival (Cartier and Hla 2019). On the other hand, ApoM-S1P is not receptor selective and could therefore potentially lead to undesirable side effect by activating pro-inflammatory $S1P_2$ and $S1P_3$ (Cartier and Hla 2019).

Chapter 2. The neurovascular unit

In this chapter I will address the physiology of the neurovascular unit and the components of the blood brain barrier BBB. I will also introduce the anatomy of the brain vasculature in mice and humans, brain arterial perfusion, and currently known roles of S1P singling in the neurovascular unit.

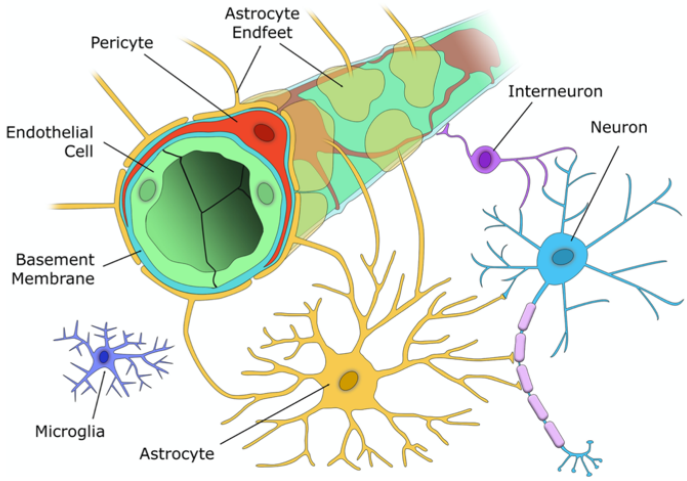

Figure 10. The cellular components of the NVU. The capillary wall contains a single EC layer (green) connected by tight junctions that form the blood-brain barrier along with pericytes (red), that are embedded within the capillary basement membrane (light blue), and nearby astrocyte endfeet (yellow). Excitatory neurons (blue) synapse with both vasoactive interneurons (purple), and astrocytes (yellow), who in turn signal to the capillary to alter blood flow according to the metabolic demands of that brain region. Microglia (indigo) are located in the brain parenchyma and respond to any aversive stimuli to protect the brain. Reproduced with permission from (Brown et al. 2019).

The blood-brain barrier

The term blood-brain barrier (BBB) is used to describe the ability of cerebral blood vessels to prevent hydrophilic and large molecules from entering the brain and thus preserving brain homeostasis (Figure 10). This property of cerebral vessels was first described by Paul Ehrlich in 1885. In 1900, Max Lewandowski drew the conclusion that the morphological correlate of this barrier function can be attributed to the capillary wall. In 1967 Reese and Karnovsky, supported this conclusion in a study in which the barrier role of endothelial cell TJ of cerebral capillaries was suggested (Reese and Karnovsky,1967). Three major transmembrane protein families play crucial roles in brain endothelial barrier function: occludins, claudins and junction associated proteins (JAMs). Additional cytoplasmic proteins including the zonula occludens (ZO) protein family (ZO-1, ZO-2 and ZO-3) provide a link between TJ and the actin cytoskeleton (Wolburg and Lippoldt 2002) (Zlokovic 2008). Although peripheral organs also express endothelial TJ, some proteins were found to be brain specific such as cingulin, claudin-3 and-5 (S. Liebner et al. 2000) (Hawkins and Davis 2005). Under physiological conditions, the ability of cerebral ECs to maintain barrier function is supported by interactions with pericytes, astrocytes, neurons and the extracellular matrix, together forming the neurovascular unit (NVU) (Zlokovic 2008). In this context, astrocytes and pericytes are thought to confer BBB characteristics to adjacent cerebral ECs (Stewart and Wiley 1981) (Bell et al. 2012)(Dente et al. 2001) (Winkler, Bell, and Zlokovic 2011). During early development and throughout aging

the establishment and maintenance of the BBB represents a continuously regulated process (Armulik et al. 2010) (Daneman et al. 2010). Experimental disruption of endothelial TJ results in failure of NVU homeostasis and the generation of epileptiform activity, highlighting the impact of endothelial function for brain homeostasis (Seiffert et al. 2004).

The Endothelium

Barrier functions of the endothelium

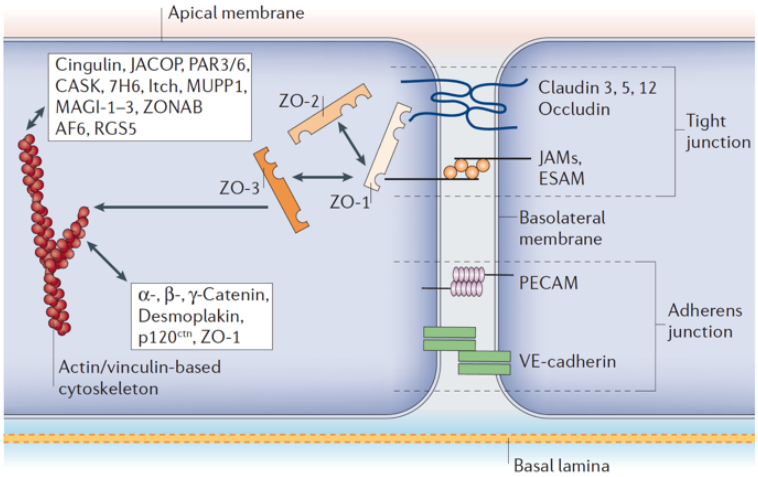

Figure 11: Molecular composition of endothelial tight junctions. Occludin and the claudins — proteins with four transmembrane domains and two extracellular loops — are the most important membranous components. The junctional adhesion molecules (JAMs) and the endothelial selective adhesion molecule (ESAM) are members of the immunoglobulin superfamily. Within the cytoplasm are many first-order adaptor proteins, including zonula occludens 1, 2 and 3 (ZO-1–3) and Ca2+-dependent serine protein kinase (CASK), that bind to the intramembrane proteins. Reproduced with permission from (Abbott, Rönnbäck, and Hansson 2006).

The endothelium is sometimes viewed as an independent organ that plays a critical role in maintaining vascular health (Figure 11). Positioned between extravascular and intravascular compartments, it acts as a selectively permeable barrier to maintain homeostasis (Claesson-Welsh, Dejana, and McDonald 2021). Another important function of ECs is the maintenance of a non-thrombogenic surface within blood vessels and thus the prevention of blood clot formation (Cahill and Redmond 2016). ECs respond to shear stress and take on a long and flat form with an orientation along the direction of flow in the long axis of the blood vessel. An average endothelial cell is 20-40 µM long, 10-15 µM wide and only 0.1-0.5 µM thick (Vion et al. 2020). Endothelial cell TJ located on the lateral borders give the endothelium a continuous form and restrict the movement of macromolecules (Komarova et al. 2017). Macromolecules cross the endothelial barrier by the involvement of multiples mechanisms, including a passage through the ECs via transcytosis, via lateral diffusion between endothelial cell membrane, through cell-to cell junctions or transcytosis (Daneman and Prat 2015).

The vasoactive role of the endothelium

In 1980 Furchgott and Zawadski discovered endothelial-derived relaxing factor as chemically identical to NO (Ignarro et al. 1987). Consequently, ECs were recognized as a key player in the local regulation of vascular tone. Endothelial NO is synthesized by eNOS from L-arginine (Furchgott and Vanhoutte 1989)(Moncada and Higgs 1991). A free radical, NO diffuses easily across biological membranes to induce the relaxation of adjacent smooth muscle cells and, consequently, vasodilatation (Moncada and Higgs 1991). NO is implicated in several key actions that maintain vascular homeostasis including vasodilatation, anti-proliferative, antioxidant and anti-inflammatory functions (Gkaliagkousi and Ferro 2011). Endothelial NOS is stimulated by shear stress as well as by soluble mediators (Govers and Rabelink 2001). Reduced NO in the arterial wall has been correlated with several cardiovascular diseases risk factors including hypertension, smoking, hypercholesterolemia and diabetes mellitus (Yetik-Anacak and Catravas 2006). The term endothelial dysfunction is often used to describe a reduction in the biological activity of NO (Versari et al. 2009). In current clinical practice NO donors such as nitroglycerin are used in the context of angina treatment and NO release is also enhanced by antioxidants and L-arginine, the natural substrate for eNOS (Yetik-Anacak and Catravas 2006) as intravenous L-arginine enhances endothelial function, promoting vasodilatation and reducing monocyte adhesion (de Nigris et al. 2003).

Prostacyclin, also known as prostaglandin I2 or PGI2, is another important endothelial-derived vasodilator that is synthesized by cyclooxygenase-2 (COX-2) from arachidonic acid (Fukai and Ushio-Fukai 2011). A member of the eicosanoid family of lipid mediators, prostacyclin exerts its actions through the prostacyclin receptor (or PGI2/IP receptor), a GPCR that triggers an increase in the second messenger cyclic adenosine monophosphate in smooth muscle cells (Narumiya, Sugimoto, and Ushikubi 1999)(Smyth et al. 2009). Prostacyclin does not appear to maintain basal vascular tone of large arteries, but in patients with decreased NO bioavailability, it provides a compensatory vasodilator effect (Szerafin et al. 2006). Prostacyclin also facilitates the release of NO by ECs (Shimokawa et al. 1988). Its effects counteract that of thromboxane A2, which is synthesized through COX-1 and causes platelet aggregation, vasoconstriction, and vascular proliferation. This balance is important in cardiovascular homeostasis (Smyth et al. 2009).

On the other hand, endothelin-1 (ET-1) is a potent vasoconstrictor peptide generated by endothelin-converting enzyme-mediated cleavage of the precursor big endothelin-1 (Yanagisawa, Inoue, et al. 1988)(Thorin and Webb 2010). ET-1 is mainly produced by ECs, but can also be produced by vascular smooth muscle cells, leukocytes and macrophages (Thorin and Webb 2010). NO inhibits the release of ET-1 from the endothelium and ET-1 inhibits NO-mediated vasodilatation (Thorin and Webb 2010)(Gilbert, Tremblay, and Thorin 2001) and contributes to the maintenance of vascular tone (Callera et al. 2007)

Regulation of coagulation and thrombosis and inflammation by the endothelium

Another important function of the endothelium is the maintenance of vascular patency by counteracting intravascular coagulation and thrombosis (Jackson 2011). In endothelial dysfunction the hemostatic balance is also disturbed, leading to reduced blood fluidity and possible pathologic hemorrhage or clot formation at sites of vascular injury (Cahill and Redmond 2016). The endothelium maintains an anti-thrombotic role through several factors including the production and release of NO and prostacyclin, which are potent inhibitors of platelet aggregation, heparin-like molecules, thrombomodulin, the endothelial protein C receptor, Ecto-ADPase, tissue plasminogen activator and urokinase (R. C. Jin, Voetsch, and Loscalzo 2005). Upon activation and in the context of endothelial dysfunction, the endothelium can switch its phenotype towards pro-thrombotic behavior by synthesizing thromboxane A2 (TxA2), which enhances platelet aggregation, as well as several adhesive co factors for platelets such as Willebrand factor, fibronectin, thrombospondin and procoagulant factors such as factor V (Tanaka, Key, and Levy 2009). By expression of chemokines and adhesion molecules, it can also recruit monocytes, neutrophils, and platelets, which in turn can trigger coagulation activation and platelet aggregation. The activated endothelium may also in exceptional cases express tissue factor, a trigger for the coagulation cascade (Giesen et al. 2000)-(Mackman 2009). Activated ECs also secrete plasminogen activator inhibitor-1, an inhibitor of the fibrinolytic pathway that can reduce the rate of fibrin breakdown (T. Murata et al. 1991). Thus, while the normal endothelium actively supports the fluid state of flowing blood and prevents activation of circulating cells, endothelial dysfunction favors blood arrest and vessel wall repair, platelet aggregation and activation, encouraging leukocyte adhesion as well as the release of platelet-derived growth factors (Schäfer and Bauersachs 2008)-(Ruggeri 2002).

Neurons

Neurons play a fundamental function in the NVU and have been attributed the role of brain “pacemakers” due to their physiological role in fine tuning cerebral blood flow (CBF) according to local metabolic needs (Muoio, Persson, and Sendeski 2014) (Petzold and Murthy 2011). Neurons are extremely sensitive to perturbation of oxygen and nutrients delivered by the blood, in the case of ischemia signals are generated to alert nearby astrocytes, either directly or via interneurons, driving the activation of alternative pathways in ECs (Figley and Stroman 2011) (Muoio, Persson, and Sendeski 2014).

Astrocytes

Astrocytes are located between neurons and ECs within the NVU (Zonta et al. 2003). NVU astrocyte “end-feet” surround almost the entire surface of the arterioles and capillaries and cover the entire cerebral vasculature (Mathiisen et al. 2010), allowing astrocyte/EC

communication (Gordon, Howarth, and MacVicar 2011). They play an important role in BBB formation and maintenance (Arthur, Shivers, and Bowman 1987) (Sofroniew and Vinters 2010). Astrocytes also express aquaporin 4 and K+ transporters which are directly involved in the regulation of removal and excretion of water, ions, and neurotransmitters from the brain (Abbott, Rönnbäck, and Hansson 2006). Recently, astrocytes have also been attributed a role in regulating CBF (Metea and Newman 2006). Neurotransmitters, mainly glutamate, released at synapses of adjacent neurons regulate astrocyte activity (Petzold and Murthy 2011). Increased intracellular free Ca2+ in astrocytes in turn results in the release of a vasoactive arachidonic acid metabolite from astrocyte end-feet, which then modulates vascular function (Mulligan and MacVicar 2004).

Pericytes

Pericytes have been attributed a supportive role in the neurovascular unit. In the brain, pericytes are found along the microvascular capillaries, in direct contact with the endothelium and the vascular BM. Pericytes contribute to several important processes in the development, maturation, and functionality of the BBB and other microvascular beds (Balabanov and Dore-Duffy 1998) (Sá-Pereira, Brites, and Brito 2012). At the BBB, pericytes indirectly regulate the expression of EC proteins important for BBB function and mediate the polarization and attachment of astrocyte end-feet to blood vessels (Armulik et al. 2010). Pericytes have also been proposed to have the capacity to modulate vascular diameter, and consequently local CBF (McConnell et al. 2017).

Cerebrovascular anatomy in mouse and man

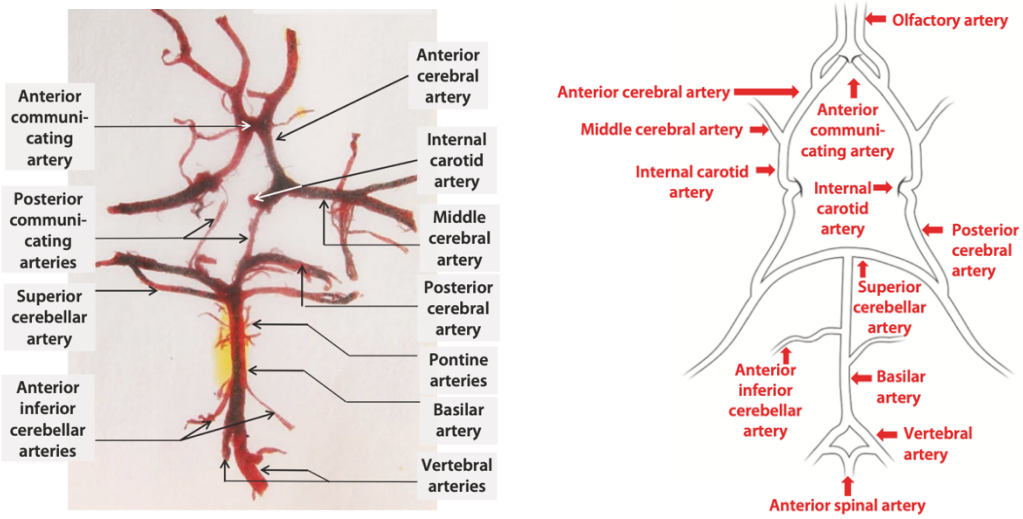

Figure 12. Differences in the circle of Willis in mouse and man. Left: The human circle of Willis. The internal carotid artery continues directly into the middle cerebral artery and gives rise to the anterior cerebral artery, which is connected with that of the contralateral side via the anterior communicating artery. The vertebral arteries fuse to form the basilar artery which at its rostral end gives rise to the posterior cerebral arteries. The latter are connected with the internal carotid artery via the posterior communicating arteries closing the arterial circle (Schröder, Moser, and Huggenberger 2020). **Right: The murine circle of Willis**. In mouse, the posterior cerebral artery is thought to be the caudal branch of the internal carotid artery, the superior cerebellar artery to arise from the rostral bifurcation of the basilar artery. The rostral branching pattern of the internal carotid artery is grossly comparable with that of humans. Reproduced with permission from (Starosolski et al. 2015).

Cerebrovascular anatomy is characterized by vascular redundancy at the circle of Willis and between arterial and venous trees and branches (collateral anastomosis) that serves to safeguard brain perfusion and drainage in the event of vascular occlusion or insufficiency (Figure 12). The use of mice in cerebrovascular research has become more prevalent during the past two decades due to their amenability to genetic manipulation, more recently coupled with the adaptation of a variety of experimental disease models to mice. Especially for stroke research, which involves the use of surgical occlusion of arteries, photothrombotic and other procedures, and intravital imaging, it is essential to have a good understanding of cerebrovascular anatomy and the major differences between mouse and human and within mouse strains both to implement experimental models and to allow for translation of preclinical observations to clinical practice.

Ward et al. (1990) described cerebral vessels and the circle of Willis in the C57BL/6J strain, which is widely used in biomedical research (Ward et al. 1990). Starosolski et al. (2015) later used ultrahigh-resolution computed tomography and a contrast agent to explore the C57BL/6J cerebrovascular anatomy in further detail (Starosolski et al. 2015). They concluded that the internal carotid artery (ICA) extends rostrally to the bifurcation into the middle cerebral artery (MCA) and the anterior cerebral artery (ACA). The bilateral terminal branches of the ACAs are the olfactory arteries and the anterior communicating arteries connecting either side of the circle. The caudal main branch of the ICA is the posterior cerebral artery

(PCA). The vertebral arteries fuse to form the unpaired basilar artery (BA). The rostral most branches of the BA are the superior cerebellar arteries which run laterally to fuse with the PCAs. In addition, a 3D reconstruction displays a posterior communicating artery which appears to cross the PCA. In conclusion, although this illustrates similarities between the mouse and the human circle of Willis, there are also major differences including the fact that the posterior cerebral artery does not originate from the BA in mice.

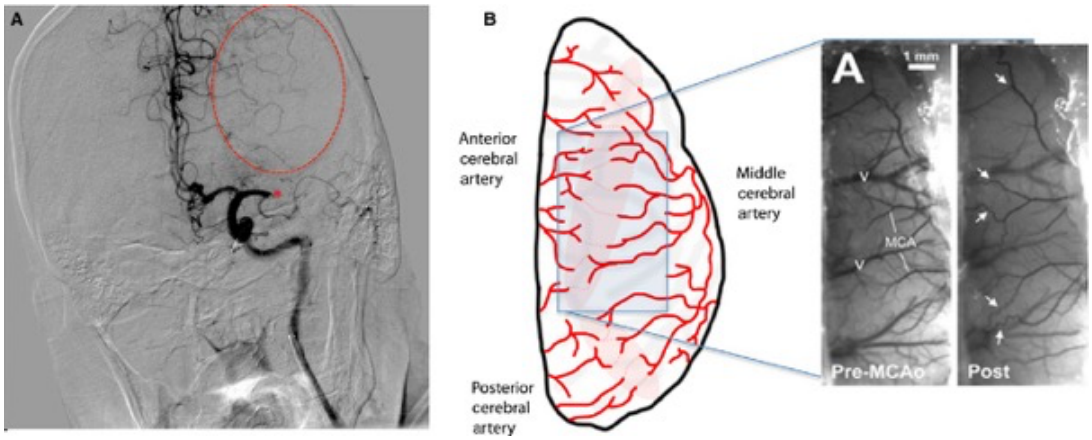

Figure 13. Pial collateral blood flow imaging in humans and rodents. A. Digital subtraction angiogram showing retrograde filling of the territory of the MCA (see region demarcated by dashed red line) via collateral connections with the ACA after MCA occlusion (red asterisk). **B**. LSCI maps of CBF in rats after thromboembolic occlusion of the MCA. Maps of blood flow can be acquired over the distal regions of the ACA and MCA territories through a thin skull preparation(Winship 2014). Baseline images show branches of the MCA, but no anastomoses with the ACA. After MCA occlusion, numerous anastomoses are apparent (white arrows), and flow through these pial collaterals maintains perfusion in distal branches of the MCA. Reproduced with permission from (Armitage et al. 2010) and (Winship et al.

In adult man, the olfactory arteries are lacking, and the mouse internal carotid artery lacks a siphon. Collateral anastomosis are highly conserved, exist to variable extent in all mammals and are particularly abundant in the cerebral cortex (Brozici, van der Zwan, and Hillen 2003). They can be engaged for partial maintenance of blood flow when primary conduits are blocked or insufficient. As they are mainly engaged in the context of obstructive vascular disease, the role and dynamics of collateral blood flow has been explored mostly in the context of ischemic stroke. The brain collateral circulation is represented by venous collaterals as well as primary and secondary arterial collaterals. Venous collaterals are engaged during venous occlusion to enhance drainage of cerebral blood. Primary arterial collaterals refer to short arterial segments in the circle of Willis that allow blood flow between territories of the internal carotid arteries and vertebrobasilar system or between cerebral hemispheres (Hendrikse et al. 2005). The pial or leptomeningeal collaterals represent the secondary collaterals and connect the distal segments of the middle cerebral artery (MCA) with distal branches of the anterior cerebral artery (ACA) and posterior cerebral artery (PCA). While these are characterized by low and alternating flow under homeostasis, they are immediately engaged if a cerebral artery upstream of one of the vascular territories they connect to is occluded, allowing blood flow to be redirected from the unobstructed to the

obstructed territories (Armitage et al. 2010) (Shuaib et al. 2011). This allows for the formation of the ischemic penumbra in the affected territory, an area where partial maintenance of blood flow through collateral anastomoses can delay or prevent cell death (Lipton 1999) (Fisher 2004). If a proportion of the ischemic penumbra maintains viability in the absence of recanalization of the blocked artery, the collateral connections may undergo outward remodeling to allow sustained augmentation of blood supply to the region (Figure 13). The pre-existing collateral extent is a significant predictor of stroke severity and recanalization rate in both humans and experimental animals. Collateral therapies attempt to take advantage of these vascular redundancies by enhancing blood flow through pial collaterals to reduce ischemia and brain damage after cerebral arterial occlusion (Winship 2015).

Regulation of Cerebral Perfusion

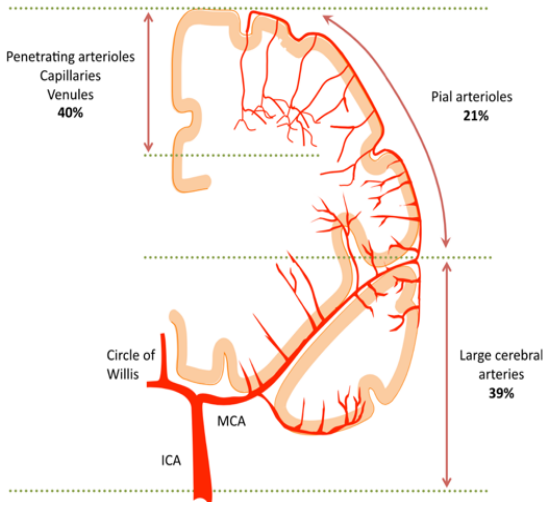

Figure 14. Anatomy of the Cerebrovascular Tree and Segmental Vascular Resistance. The internal carotid artery (ICA) enters the skull and merges with branches of the vertebral arteries to form the circle of Willis at the base of the brain. The middle cerebral artery (MCA) takes off from the circle of Willis and supplies a large territory of the cerebral cortex. The MCA gives rise to pial arteries and arterioles that run on the surface of the brain, forming a heavily interconnected network from which arterioles penetrating the substance of the brain originate (penetrating arterioles). Penetrating arterioles give rise to the capillary network, which feeds into the venous system returning the blood to the heart. The component (percentage) of the total vascular resistance each cerebrovascular segment offers to blood flow, which reflects their potential for flow control. Reproduced with permission from (De Silva and Faraci 2016).

The brain represents only 2 % of the weight but accounts for 20 % of the energy consumption of the human body (Siegel 1999). As the brain does not have the capacity to store energy, it requires constant supply of glucose and oxygen from the arterial circulation to sustain normal function. Brain perfusion is secured by delivery through the circle of Willis (Figure 14) and takes advantage of the active regulation of the diameter of pial and penetrating arteries to adapt local perfusion to the demand of energy though a mechanism known as neurovascular coupling (Schaeffer and Iadecola 2021). Neuronal activity controls neurovascular coupling through several mediators in synchronization with the other cells of the neurovascular unit. Glutamate receptor activation in neurons leads to increased cytosolic Ca^{2+} and activation of NOS and COX-2, which ultimately will lead to production of vasodilators such as NO and prostanoids (Lecrux and Hamel 2016). Interneurons can also release NO and contribute to vasodilatation as well as constriction through the secretion of neuropeptide Y (Duchemin et al. 2012).

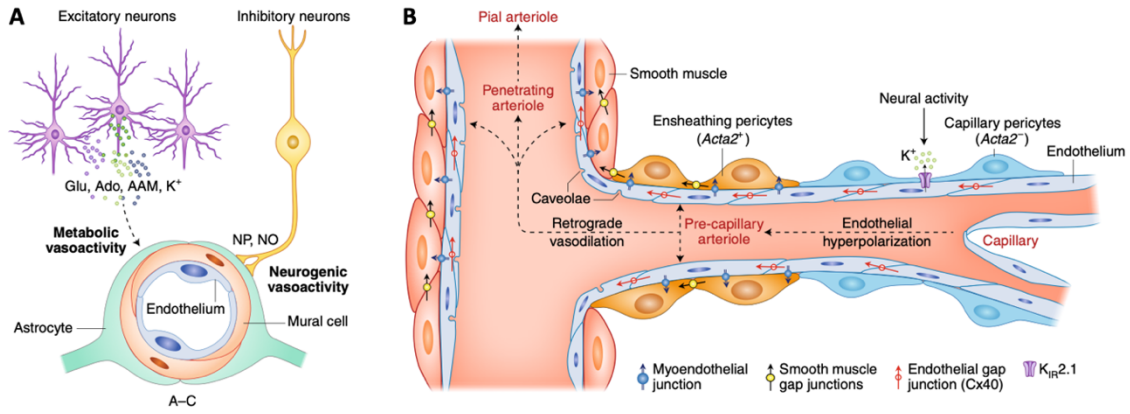

Figure 15. Neurovascular coupling. A, excitatory neurons have a powerful effect on local neural activity and energy metabolism, and may drive local vascular changes through neurotransmitters, vasoactive ions, as well as by-products of neural activity such as adenosine (Ado) and arachidonic acid metabolites (AAMs). Astrocytes may also participate in this process. Interneurons, which have little impact on local neural activity, may signal blood vessels through direct neurovascular connections releasing neuropeptides (Nps) and NO. Glu, glutamate. **B**, the local vascular response elicited by overall neural activity leads to hyperpolarization of ECsthrough $K_{IR}2.1$ channels. Whether mesh and thin-strand (capillary) pericytes (ACtA2-negative) participate in this process remains unclear. Hyperpolarization is propagated retrogradely through inter-endothelial gap junctions and is transmitted to contractile mural cells, ACtA2-containing ensheathing pericytes and SMCs, likely via myoendothelial junctions and K_{IR} channels. In turn, mural cell hyperpolarization suppresses voltage-gated Ca^{2+} channel activity, resulting in intracellular Ca^{2+} depletion, relaxation of the contractile apparatus and vasodilatation. the relaxation is then transmitted to adjacent mural cells through intercellular gap junctions, leading to retrograde vasodilation, which eventually reaches pial arterioles at the brain surface Reproduced with permission from (Schaeffer and Iadecola 2021).

In astrocytes, glutamate induced Ca^{2+} release leads to the activation of phospholipase A2 and release of arachnoid acid, resulting in the production of PGE2 and epoxyeicosatrienoic acids (MacVicar and Newman 2015). Additionally, Ca^{2+} signaling in astrocytes may mediate potassium release that induces VSMC relaxation and an increase in blood vessel diameter, and ATP may also be generated inducing either direct vasoconstriction or indirect vasodilatation (Filosa and Iddings 2013). Neurovascular coupling can also take place at the level of capillary ECs, which can propagate signals retrograde to pial arterioles via gap junctions (Schaeffer and Iadecola 2021). At the arteriolar level, ECs then secrete several vasodilators including NO, prostanoids and endothelin, which in turn regulate VSMC contractility and vessel diameter (Figure 15) (Nava and Llorens 2019). Pericytes have also been attributed contractile function and implicated in the regulation of capillary diameter, but this may be a feature that is specific to cells in the peripheral zone between capillaries and arterioles, or at precapillary sphincters, where a population of cells exists that share features of pericytes and VSMC (Eltanahy, Koluib, and Gonzales 2021).

Hemodynamic forces also regulate EC function, smooth muscle cell behavior, and the interaction of EC with VSMC (Figure 16) (Cullen et al. 2004), leukocytes and other blood constituents (Pradhan and Sumpio 2004). ECs are exposed to pulsatile blood flow and are therefore subjected to hemodynamic forces including shear stress and cyclic strain (Cahill and Redmond 2016). Shear stress is the tangential frictional force acting primarily at the EC surface, while cyclic strain/ stretch acts perpendicular to the vessel wall and affects both

endothelial and smooth muscle cells together with underlying matrix (Cahill and Redmond 2016). ECs express several mechanotransducers that modulate response to mechanical forces, including ion channels, tyrosine kinase receptors, GPCRs (including $S1P_1$), cell adhesion molecules, the glycocalyx and primary cilia (Ando and Yamamoto 2011)(Hsieh et al. 2014) (Jung et al. 2012). Increased shear stress causes vasodilatation mainly by increased eNOS activity and NO production, but other vasoactive substance such as prostacyclin may also play a role (Bagher and Segal 2011). Prolonged changes in shear stress triggers changes to endothelial cell transcription (J. Zhang and Friedman 2012). This can contribute to inward or outward vascular remodeling to adapt to changes in blood flow (Chatzizisis et al. 2007). Shear stress also regulates the expression of thrombomodulin, heparin sulfate proteoglycans and tissue plasminogen activator tPA, and is thus important for maintaining a non-thrombogenic endothelium as discussed above (Helenius et al. 2008). Hemodynamic forces also regulate the endothelial production of growth factors and cytokines, including platelet derived growth factor basic fibroblast growth factor, transforming growth factor beta and interleukin-1 and 6 (Riha et al. 2005). These factors affect behavior of the underlying VSMC and are implicated in the pathogenesis of vascular disease (Lacolley et al. 2012). Thus, through its mechanosensing machinery, ECs regulate both acute and long-term adaptation of vascular diameter to blood flow, and the absence of laminar shear stress can induce vascular dysfunction, vaso-occlusion and capillary rarefaction (Hoefer, den Adel, and Daemen 2013).

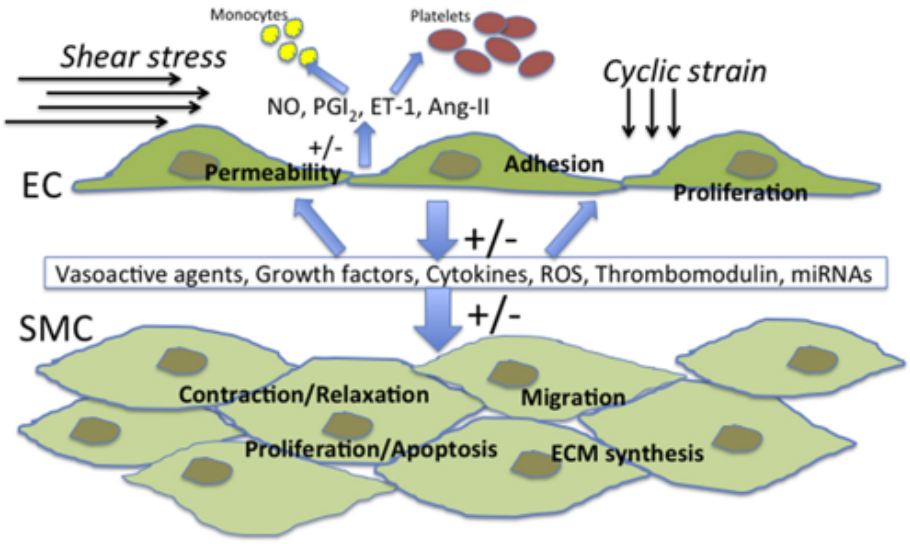

Figure 16. Shear stress and cyclic strain are important stimuli for ECs (EC). These hemodynamic forces are sensed by mechanoreceptors that include ion channels, G protein-coupled receptors, integrins, cytoskeletal components and receptor tyrosine kinases. Hemodynamic forces modulate endothelial release and expression of a myriad of substances including vasoactive agents, growth factors, cytokines, microRNAs (miRNAs), thrombomodulin and reactive oxygen species (ROS) that may affect the aggregation and adhesion of cells circulating in the blood (i.e., platelets and monocytes), the permeability, adhesivity and angiogenic potential of EC themselves, as well as the growth, migration, vasoreactivity and extracellular matrix (ECM) synthesis of the underlying vascular smooth muscle (SMC). Reproduced with permission from (Cahill and Redmond 2016).

S1P signaling at the NVU

S1P signaling is well known to regulate vascular development and homeostasis through $S1P_1$ signaling. However, only a few studies have addressed the role of endothelial $S1P_1$ signaling in the brain. In one recent study, it was shown that mice lacking $S1P_1$ specifically in ECs ($S1pr1^{ECKO}$ mice) exhibit leak of low molecular weight tracers (<10 kDa) without major signs of CNS inflammation or injury (Yanagida et al. 2017). Accordingly, pharmacological blockage of $S1P_1$ with high dose FTY720 (5 mg/kg for 3 days) also resulted in size-selective opening the BBB (Yanagida et al. 2017). Size-selective BBB disruption has been attributed to changes in the actin cytoskeleton (Shi et al. 2016). $S1P_1$ is known to promote cortical actin formation and the stability of adherens junctions in cultured ECs by stabilizing VE–cadherin (Oo et al. 2011). However, no changes were observed in the subcellular distribution VE–cadherin in $S1pr1^{ECKO}$ brains (Yanagida et al. 2017). Deficiency of the TJ proteins claudin-5, either alone or in combination with occludin, is known to result in enhanced paracellular permeability, suggesting that small-molecule transport through the BBB may occur via the paracellular route (Keaney and Campbell 2015). Interestingly, the molecular size threshold for increased permeability observed in $S1pr1^{ECKO}$ mice (3–10 kDa) is comparable to that observed with claudin-5/occludin double knockdown (Keaney and Campbell 2015). Although only subtle changes in the subcellular localization of TJ proteins could be observed in $S1P_1$ deficient ECs, this suggested that size-selective BBB opening in $S1pr1^{ECKO}$ mice may be attributed to reduced TJ stability.

In a second recent study it was shown that ApoM-/- mice display increased permeability in cerebral arterioles that can be reversed with a specific $S1P_1$ agonist (Mathiesen Janiurek et al. 2019). Intriguingly, $S1P_1$ activation by ApoM/S1P counteracted both transcellular and paracellular permeability in cerebral arteries. Again, the lack of ApoM was associated with an increase in BBB permeability without any detectable change in the size, structure, magnitude, or subcellular localization of TJ complexes. Accordingly, an up 10-fold increase in transcytosis was observed in the ECs of both pial and penetrating arterioles, with no significant increase in venules or capillaries. ApoM/S1P thus regulates the flux of small and large molecules in several functional and anatomical areas of the microvascular tree. The capacity of SEW2871 to reduce BBB increased permeability suggested that the observed effects were primarily mediated via $S1P_1$.

In humans, plasma HDL concentrations correlate inversely with the susceptibility to cerebro-and cardiovascular diseases (Rader and Tall 2012) (Hovingh, Rader, and Hegele 2015) (Fellows et al. 2015), and approximately 5% of HDL contains apoM (Christoffersen et al. 2006). Lower plasma concentrations of HDL were also associated with dementia (Vitali, Wellington, and Calabresi 2014). The beneficial effects of HDL could potentially be mediated by $S1P_1$ signaling. Size-selective leakage of the BBB observed in $S1pr1^{ECKO}$ mice may thus impact the initiation or progression of CNS diseases. $S1P_1$ agonists may be protective in ischemic stroke (Swendeman et al. 2017), and the anticoagulant protein S displayed a protective role in hypoxic/ischemic BBB disruption in an $S1P_1$- dependent manner (D. Zhu et al. 2010). Together

with the studies discussed above, these observations raise the possibility that EC $S1P_1$ is not only a homeostatic regulator of BBB function, but that is also engaged to protect the BBB during ischemic brain injury and dementia.

Chapter 3. Stroke

In this chapter I will address the epidemiology of stroke and models explaining the pathophysiology of stroke, the kinetics of BBB breakdown in during ischemic stroke, and frequently employed experimental models of ischemic stroke in mice.

Epidemiology

Stroke is the second cause of death worldwide. Ischemic stroke and hemorrhagic stroke are the two most common subtypes of stroke. In 2019, 101.5 million individuals suffered stroke world-wide. Ischemic stroke represented 77.2 million cases, while 20.7 million patients were affected by intracerebral and 8.4 million subarachnoid hemorrhages. In 2019, 6.6 million deaths were caused by cerebrovascular disease. Globally, ischemic stroke resulted in the death of 3.3 million individuals, intracerebral hemorrhage 2.9 million individuals and subarachnoid hemorrhage 0.4 million individuals (Virani et al. 2021). The global incidence, mortality and disability-adjusted life years for ischemic stroke decreased over the 1990-2013 period (Saver et al. 2016). Although ischemic stroke prevalence also increased from 1990 to 2005, it decreased again from 2005 to 2013 (Feigin et al. 2015). This may be explained by improved detection and secondary prevention, and reduced stroke mortality. The level of a country's income correlates directly with the trend in the epidemiology of ischemic stroke: the incidence, mortality, disability-adjusted life years and mortality to incidence ratio decreased in high income countries, while no significant difference were observed in low-income and middle-income countries over the same time frame (Krishnamurthi et al. 2013). Several factors contribute to this difference including population age, demographics, life expectancy, health status and standards of health care provision (Campbell et al. 2019).

Stroke is the major cause of serious disability affecting older people, who also suffer the highest incidence of stroke (Katan and Luft 2018). Of 79500 individuals suffering from a stroke, 26 % remain disabled in basic activities of daily living and 50 % have reduced mobility due to hemiparesis, aphasia and depression (Kelly-Hayes et al. 2003). Stroke burden is a function of socioeconomic status with greater odds of disability in patients with lower education and income (Bettger et al. 2014). Evidence to demonstrate that specialized stroke rehabilitation reduces long term disability and stroke related costs exists for different countries and health care systems including Switzerland (Mahler et al. 2008), the UK (O'Connor et al. 2011) (Turner-Stokes et al. 2016) and Japan (K. Murata et al. 2017). Extended life expectancy of the world's population can explain the increase in the global burden of ischemic stroke in the last decades (GBD 2015 Mortality and Causes of Death Collaborators 2016). Currently, in Western countries around 3-4% of total health care expenditures are stroke related (Struijs et al. 2006). The mean lifetime cost of ischemic stroke per person, including inpatient care, rehabilitation, and follow-up care, is estimated at 140,048 $ in the US (Johnson, Bonafede, and Watson 2016). The total annual direct costs in the United States are estimated to 20-30 billion and indirect costs to 15-25 billion USD (Ma, Chan, and

Carruthers 2014). For the EU plus Iceland, Norway, and Switzerland, the total annual direct costs were estimated at 26.6 billion euros in 2010 (Gustavsson et al. 2011). Inpatient hospital costs for acute stroke accounts for 70 % of first-year post-stroke costs. Comorbidities such as ischemic heart disease and atrial fibrillation predict higher costs (Go et al. 2014). A study performed in 8 different European countries found that the risk of stroke increased by 9% per year in men and 10 % per year in women (Asplund et al. 2009). High incidence of stroke in women can be in part explained by longer life span and increased prevalence of hypertension and atrial fibrillation, key risk factors for stroke (Cordonnier et al. 2017). Differences in vascular function, immunity, hormonal profiles, lifestyle factors and societal roles, as well as risks related to pregnancy and the postpartum state may also contribute (Cordonnier et al. 2017). Non-modifiable risk factors for ischemic stroke include age, sex and genetic factors and longer life expectancy. Several modifiable risk factors for ischemic stroke have been identified in the INTERSTROKE study, with 10 factors accounting for 91.5% of the population-attributed risk for ischemic stroke worldwide and consistently associated with ischemic stroke across geographical regions, sex, and ethnic groups (Howard et al. 2006). These factors include a history of hypertension or a blood pressure of more or equal to 160/90 mmHg, low levels of regular physical activity, a high ApoB to Apo-A1 ratio, diet, a high waist to hip ratio, psychological stress and depression, smoking, cardiac causes such as atrial fibrillation and previous myocardial infarction, high alcohol consumption and diabetes mellitus. Among these factors, self-reported hypertension, or blood pressure of more than 160/90 mmHg carried the strongest risk (Howard et al. 2006). Other potential risk factors include sleep apnea, chronic inflammation, periodontal disease, and chronic kidney disease (Redon et al. 2011). Some studies reported exposure to air pollution to cause an increase in stroke incidence (Asplund et al. 2009).

Pathophysiology of ischemic stroke

Overview

Ischemic stroke is defined by deficient nutrient and oxygen delivery to brain tissue triggered by arterial occlusion and downstream blood flow disruption usually caused by a thromboembolism (Campbell et al. 2019). In the acute stage, the affected brain tissue can be broadly categorized by the infarct core where the damage is irreversible and the ischemic penumbra where the tissue is still alive but at risk. Engagement of the cerebral collateral circulation is a crucial step in defining the relative size of these zones and in limiting the extension of the infarct core at the expense of the penumbra. Inflammation is rapidly initiated as blood flow disturbances and alteration of shear stress induce endothelial cell activation and the expression of P-selectin along with other molecules which mediate rolling of leukocytes and platelets on activated endothelial cells. Activation of the coagulation cascade, most likely by immune cells in early stages, triggers the activation of platelets and formation of platelet/fibrin plugs that can be further enforced by the release of extracellular DNA from

neutrophils and other cells. Extension of thrombosis in the microvasculature of the penumbra results in a loss of patency to accelerate the expansion of the infarct core and limit the efficiency of recanalization. Several studies have shown an early detrimental effect of T cells in coordinating these events through the activation of a "thrombo-inflammatory" process (Kleinschnitz et al. 2013)(Kraft et al. 2013). Neutrophils contribute to capillary plugging in the acute stage, initiated by early activation and vascular adhesion, and infiltrate brain tissue at later stages. BBB breakdown occurs gradually and involves loss of endothelial junctions primarily at later stages. Damaged brain cells release proinflammatory molecules and danger-associated molecular patterns, further promoting the activation of innate and adaptive immune cells and platelets. During the recovery phase (starting at day 3 to 4), macrophages infiltrate to remove dead tissue and promote some level of tissue repair. In the late or chronic phase (> day 7), adaptive immunity has been implicated in neural repair (Yoshimura and Ito 2020). My work and therefore my introduction will focus on the acute phase of ischemic stroke, primarily the first 24 hours after onset. Numerous studies have investigated the different actors during this stage with the perspective of developing novel therapeutic agents for ischemic stroke treatment.

Thrombotic occlusion of large cerebral arteries

Cerebral ischemia, which represents around 80% of all strokes, is triggered by the embolism of thrombi formed because of either atrial fibrillation or extracranial artery stenoses and rupture. Immediately after an embolus has occluded a cerebral blood vessel, the deficit in the delivery oxygen and glucose to brain tissue results in molecular, cellular, and clinical events, including clinically acute neurological deficits such as hemiparesis or aphasia, which are considered a medical emergency. When thrombus resolution is spontaneous it is referred to as a transient ischemic attack (TIA). While TIA symptoms are fully reversible, they are often warning signs of ischemic stroke. The ischemic penumbra is represented by the tissue surrounding the ischemic core which is not receiving adequate blood perfusion but at risk of infarction (Baron 2018). The concept "time is brain" and the treatment of stroke as a neurological emergency is based on the appreciation that more brain cells in the ischemic penumbra die every minute in the absence of treatment. The ischemic region is subjected to several deleterious metabolic processes initiated in the core and propagating to the neighboring tissue including excitotoxicity, oxidative stress, and inflammation which result in ischemic core extension and worse clinical outcome. Several molecular events are happening in the penumbral tissue during the acute phase of ischemic stroke extending the lesion core. These events are initiated by the decrease in local CBF that results in reduced activity of adenosine 5'-triphosphate and Na^+/k^+ pumps, increased extracellular glutamate and activation of glutamate-receptors, resulting in increased cytosolic calcium in neurons and glial cells. This in turn leads to the formation of oxygen free radicals via nitric oxide synthase activation, contributing to excitotoxicity (Belov Kirdajova et al. 2020). Advanced imaging techniques such as diffusion- and perfusion-weighted MRI and Computed tomography

perfusion are used clinically to identify the penumbra and rapidly select patients that are likely to respond to reperfusion therapies. This selection is based on a small core infarct and either a large volume of penumbral tissue or the presence of moderate or good collateral circulation.

Engagement of cerebral collaterals

The occlusion of a large cerebral artery results in the near immediate engagement of unidirectional blood flow in pial collaterals in the direction of the ischemic area. Subsequent dilatation of pial collaterals further improves perfusion of the ischemic penumbra, and collateral vessel blood pressure correlates with blood flow in ischemic areas (Morita et al. 1997) (Shima, Hossmann, and Date 1983). Based on observations in a rat model of experimental cerebral ischemia, it was suggested that pial arteries require only 12 seconds to reach maximal dilatation following ischemia induction, whereas in case of carotid artery occlusion several minutes are required (Morita et al. 1997). If a proportion of the penumbra is preserved even in the absence of reperfusion, collaterals can undergo outward remodeling to sustain higher blood flow. This process takes several days in rodents and longer time in humans. There is a great variability in the extent of pial collateralization between human individuals and between different strains of the animal species used to model stroke. When challenging 15 inbred strains of mice with the same experimental model of ischemic stroke and performing parallel analysis of the collateral circulation (number and diameter of collateral connections between ACA and PCA with MCA), Zhang et al demonstrated a significant inverse relationship between lesion size and collateral blood flow engagement in the MCA territory (Hua Zhang et al. 2010). Other studies suggested that a reduction in the number and diameter of pial collaterals, as well as an increase in their tortuosity, might explain an age-dependent effects on infarct size (J. Wang et al. 2011) (Faber et al. 2011). Collateral extent is also a significant predictor of stroke severity in human stroke patients (Liebeskind et al. 2014)(Menon, O'Brien, et al. 2013). In patients suffering acute MCAO and who received angiography exploration, it was concluded that retrograde perfusion in the ischemic territory varies significantly based on pial vascular collaterals number (Bang et al. 2008) (Hendrikse et al. 2005) (Menon, O'Brien, et al. 2013). Good collateral flow is positive prognostic marker associated with improved likelihood of major reperfusion, reduced infarct growth, and more successful outcome (Lima et al. 2010)(Miteff et al. 2009). With the use of MRI diffusion and perfusion imaging in combination with angiography, it has been demonstrated with collateral scoring during acute cerebral ischemia that patients with good collaterals have larger areas with only mild hypoperfusion and reduced lesion expansion within the penumbra (Bang et al. 2008). Common risk factors for stroke including metabolic syndrome, hyperuricemia and age are associated with poor pial collateral flow (Menon, Smith, et al. 2013).

Blood flow disturbance, endothelial activation, and loss of microvascular patency

Disturbed blood flow and alteration of shear stress are the first changes that endothelial cells and platelets are sensing in the ischemic penumbra. Endothelial cells respond by enhancing the expression of the adhesion molecule P-selectin, which initiates the rolling of circulating leukocytes and platelets at sites of tissue injury. Platelets also store P-selectin in α-granules, that are released immediately after platelet activation. Selectins play an important role in attracting circulating leukocytes to the endothelium mainly through the interaction with P-selectin glycoprotein ligand, which most leukocytes express. This process initiates cluster formation of leukocytes inducing intravascular plugging that further contributes to the ischemic lesion (De Meyer et al. 2016). Endothelial activation and cytokine release induce an increase in several other molecules including E-selectin, (Inter-Cellular Adhesion Molecule 1) ICAM-1 and (Vascular Cell Adhesion Molecule 1) VCAM-1, which regulate leukocyte recruitment, adhesion, and transmigration (Petrovic-Djergovic, Goonewardena, and Pinsky 2016). The coagulation cascade also becomes activated, resulting in the production of thrombin and thrombin-mediated activation of endothelial cells and platelets through protease-activated receptors (Delvaeye and Conway 2009)(Rezaie 2014). Thrombin can also directly disrupt endothelial barrier function (Amara et al. 2008). Furthermore, endothelial thrombomodulin and endothelial protein C receptor can be shed, impairing the anticoagulant and anti-inflammatory actions of activated protein C, ultimately enhancing coagulation activation, and inducing more inflammation. How the coagulation cascade becomes activated in the acute stage is not clear, but it is likely to involve the activation of the intrinsic cascade by neutrophil extracellular DNA, polyphosphates released by platelets and other cells, and tissue factor expressed by activated monocytes. At later stages, BBB disruption will expose plasma to astrocytes, which express high amounts of tissue factor (S. Wang et al. 2016).

Endothelial dysfunction

Although endothelial cells are more resistant to ischemia than cells in the surrounding parenchyma, they start to display signs of dysfunction soon after stroke onset. A lack of oxygen and nutrients in brain tissue triggers hallmarks of endothelial dysfunction including increased production of reactive oxygen species (ROS) and generation of superoxide, under the action of NO synthases (Kaneto et al. 2010)-(Victor et al. 2009). ROS includes oxygen radicals such as superoxide and hydroxyl radicals as well as non-radical derivatives of oxygen including hydrogen peroxide and ozone. Oxidative stress results from an imbalance between the activity of endogenous pro-oxidative enzymes such as nicotinamide adenine dinucleotide phosphate-oxidase (NADPH) oxidase and xanthine oxidase and anti-oxidative enzymes such as superoxide dismutase, glutathione peroxidase and heme oxygenase (Cahill and Redmond 2016) promoted by brain ischemia. Shear stress and cyclic stretch have been reported to modulate ROS production (Hsieh et al. 2014) and upregulate the expression of antioxidant

enzymes such as peroxiredoxin 1 (Mowbray et al. 2008). In contrast, decreased shear stress in ischemia was correlated with NADPH oxidase activation and ROS production (Chatterjee et al. 2012). Flow patterns are implicated in the regulation of the ROS/NO balance. Steady flow and high shear induce lower levels of ROS and greater NO bioavailability, which ultimately enhance the activity of key transcription factors such as nuclear factor erythroid-derived 2-like 2 and Krüppel-like Factor 2 to protect against oxidative damage and preserve endothelial function (Takabe, Warabi, and Noguchi 2011). On the other hand, disturbed blood flow results in higher ROS and lower NO bioavailability, promoting endothelial dysfunction (Cahill and Redmond 2016). Irregular flow enhances the activation of key transcription factors such as and AP-1 and NF-KB, which promote the expression of monocyte chemotactic protein 1 (MCP-1) and (ICAM-1) (Hsieh et al. 2014).

Thrombin, bradykinin and other acute inflammatory mediators can induce opening of endothelial junctions via Rho activation (Lum and Malik 1996), and vascular endothelial growth factor (VEGF) induces vascular permeability via NOS (Tilton et al. 1999)(Ashina et al. 2015). Fluid shear stress is also implicated in endothelial permeability regulation (Tarbell 2010). Indeed, it's not really the low wall shear stress that has elevated macromolecule permeability (LaMack et al. 2005), while laminar flow and high shear stress inhibit thrombosis and endothelial apoptosis (Berk et al. 2002).

The endothelium is covered by a negatively charged layer of membranous glycoproteins, proteoglycans and associated proteins with a thickness of around 100-750 nm referred to as the glycocalyx (Cahill and Redmond 2016). The glycocalyx protects the vascular wall against various insults (Alphonsus and Rodseth 2014) and its destruction has been reported after ischemic challenge (Rehm et al. 2007), during redox stress (Beresewicz, Czarnowska, and Maczewski 1998) and during vascular inflammation (Henry and Duling 2000). Loss of the glycocalyx has been correlated with increased endothelial permeability, platelet aggregation and loss of vascular responsiveness (Becker et al. 2010), while multiple vasculo-protective functions have been attributed to the glycocalyx including the fortification of endothelial barrier function (Huxley and Williams 2000), inhibition of coagulation and leukocytes adhesion (Constantinescu, Vink, and Spaan 2003), and mediation shear stress-induced NO release (Mochizuki et al. 2003)-(Kelly et al. 2006).

Platelets and the intrinsic coagulation cascade

The use of anti-platelets drugs such as aspirin is recommended within 48h after the onset of stroke symptoms to prevent recurrence (Sandercock et al. 2014). In patients receiving tPA thrombolysis the American Stroke Association 2018 guidelines recommend that anti-platelet treatments should be delayed for 24 hours (Powers et al. 2018). Platelets express the glycoprotein GP (GP)Ib-IX-V receptor complex, which binds von Willebrand factor (VWF), thus promoting platelet attachment to the injured blood vessel wall and thrombus growth in high shear stress environments (Berndt et al. 2001). VWF is released into circulation from endothelial cells and platelet α-granules, then immobilized at sites of endothelial damage or

activation (Kanaji et al. 2012). VWF binds on GPIbα but the dissociation rate of the GPIbα-VWF interaction is too rapid to enable firm platelet adhesion to the vessel wall or a growing thrombus. For firm adhesion other receptors need to be activated, such as GPVI, a platelet receptor for collagen and fibrin (Rayes, Watson, and Nieswandt 2019). Targeting GPVI provides protection in tMCAO models by both anti-GPVI antibody JAQ1 and recombinant soluble dimeric GPVI-Fc (Ungerer et al. 2013), indicating that GPVI-mediated platelet activation is an important step in the pathophysiology of ischemia-reperfusion injury in the brain. GPVI signaling also triggers the formation of procoagulant and pro-inflammatory microparticles and the release of inorganic polyphosphate (polyP), a powerful activator of coagulation factor XII (FXII), which initiates both the intrinsic coagulation cascade and the kallikrein–kinin system (Dütting, Bender, and Nieswandt 2012). Genetic deficiency in FXII and inhibition of activated FXII (FXIIa) are both strongly protective in tMCAO models without detectable effects on hemostasis or the risk of ICH. Further studies provided evidence that FXIIa-dependent activation of the kallikrein–kinin system, rather than thrombus formation, might be the critical FXII-driven activity that exacerbate thrombo-inflammation (Nickel et al. 2017). After activation and adhesion of platelets at sites of vessel wall injury, the formation of a stable thrombus requires amplification of the initial platelet response via platelet aggregation, which is mediated by GPIIb/IIIa (αIIbβ3 integrin) (Shattil, Kim, and Ginsberg 2010). Complete blockade of GPIIb/IIIa led to death from ICH after tMCAO in most young and aged mice (Bergmeier et al. 2002). Surprisingly, infarct sizes in the surviving animals were approximately the same as those in mice subjected to tMCAO and treated with control antibodies, suggesting that the treatment failed to provide protection (Kleinschnitz et al. 2007)(Kraft et al. 2015). A clinical trial of anti-GPIIb/IIIa treatment in patients suffering from ischemic stroke was stopped because of a dramatic increase in ICH in the treated group (Adams et al. 2008). This argues that the classical pathway of platelet activation in hemostasis and thrombosis is not critical for stroke progression after recanalization but is essential, together with granule release, for hemostasis in the ischemic brain (Deppermann et al. 2017). In contrast, engagement of the intrinsic coagulation cascade and bradykinin release through FXIIa and of platelets through GPIV is implicated in downstream microvascular thrombosis and brain injury but not required for brain hemostasis.

T cells and thrombo-inflammation

T cells contribute to both innate and adaptive immune responses. They are divided into two subsets, namely αβ and unconventional γδ T cells. T cell receptors of the αβ subset are heterodimers of the α and β chains, while γδ subset are heterodimers of the γ and δ chains. The αβ subset consist of CD4+ T helper cells involved in regulating the functions of phagocytes, granulocytes and CD8+ cytotoxic T lymphocytes as well as regulatory T cells (Treg) involved in regulating immune reactions. During ischemic stroke, soluble antigens leak to the blood or CSF and reach draining lymph nodes either directly or via infiltrated dendritic cells. There, they are presented by antigen-presenting cells and recognized by naïve T cells, which

are primed to proliferate and produce effector T cells and Tregs. T cell priming also occurs in the parenchyma, where antigens presented by microglia and dendritic cells encounter infiltrated naïve T cells. While T cells are known to infiltrate the parenchyma through the fenestrated capillaries of the Choroid plexus, γδ T cells have been reported to be preferentially located in the leptomeninges where they migrate from the intestines.

In the acute phase of ischemic stroke, thrombosis and microvascular dysfunction is enhanced by interaction between lymphocytes and platelets within the vasculature of the ischemic penumbra. T cells can interact with various receptors expressed on the activated endothelium, such as lymphocyte function antigen-1, macrophage antigen-1, and very late antigen-4 (Gregory J. del Zoppo and Mabuchi 2003). This has been suggested to induce microvascular dysfunction, impair capillary reperfusion, and aggravate the outcome of experimental stroke (Arumugam et al. 2004). In 2006, Yilmaz et al. reported that Rag1−/− mice, which lack mature functional T cells and B cells, are protected from brain injury and BBB disruption induced by tMCAO challenge (Yilmaz et al. 2006). Similar protection has been observed in models of ischemia/reperfusion (I/R) injury in other vascular beds, such as heart (Hofmann and Frantz 2016), kidney (Ysebaert et al. 2004) and liver (Zwacka et al. 1997), suggesting a general detrimental role of lymphocytes in the pathogenesis of I/R injury. Kleinschnitz et al. confirmed this protective role and demonstrated that adoptive transfer of T cells but not B cells into RAG1−/− mice reversed their neuroprotective status (Kleinschnitz et al. 2010). The presence of transgenic MHC class I ($CD8^+$)- or MHC class II ($CD4^+$) –restricted TCR of predefined antigen specificity was also sufficient to fully reconstitute susceptibility to experimental stroke, indicating that the ability of $CD4^+$ or $CD8^+$ T cells to recognize (auto)antigens is not a major determinant of stroke progression. In a subsequent study, the same group observed that adoptive transfer of Tregs into *Rag1*$^{-/-}$ mice exacerbated infarct size in a model of mild ischemic stroke (Kleinschnitz et al. 2013). Mice lacking Tregs also displayed a significant reduction in lesion size 24 hours after tMCAO (60 minutes) challenge. A prior study had shown that extent and time course of thrombus formation in *RAG1*$^{-/-}$ mice was not altered in a whole blood *in vitro* perfusion system under high shear flow conditions, nor *in vivo* after chemical injury of mesenteric arterioles (Nieswandt et al. 2001). On the other hand, activated T cells had been reported to interact with aggregated platelets (eg, via the CD40/CD40L), and promote intravascular thrombosis during ischemic stroke (N. Li 2008). Relative to primary resting T cells, natural Tregs demonstrate a higher adhesive susceptibility with platelets and activated cerebral endothelial cells in the context of ischemic stroke.

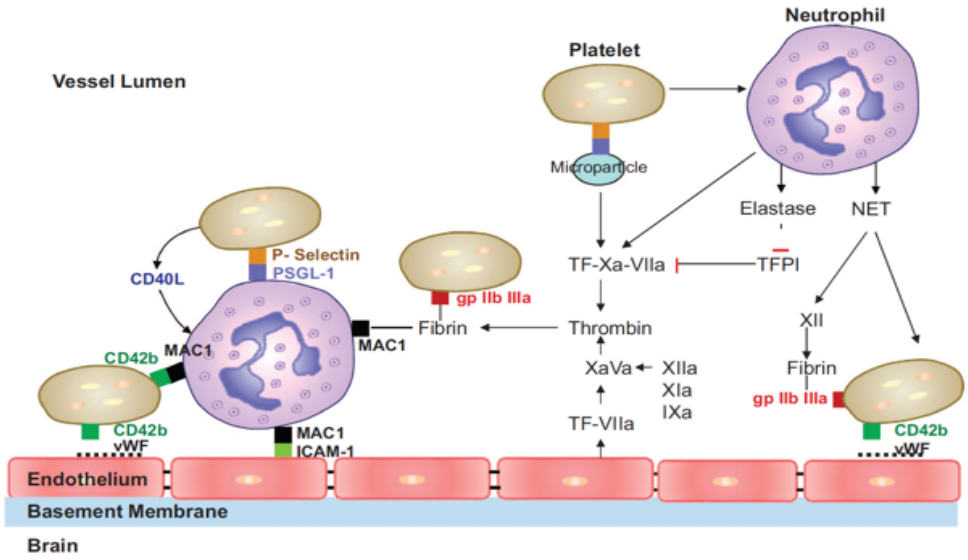

Figure 17. The role of neutrophils in thrombus formation. Neutrophils promote thrombosis through interactions with platelets, proteolytic cleavage of clotting factors (TFPI, coagulation factor X), and release of prothrombotic molecules (NETs and tissue factor). ICAM-1, intracellular adhesion molecule-1; MAC-1, macrophage 1 antigen; NET, neutrophil extracellular traps; PSGL-1, P-selectin glycoprotein ligand-1; TF, tissue factor; TFPI, tissue factor pathway inhibitor; vWF, von Willebrand factor. Reproduced with permission from (Jickling et al. 2015a).

Thrombo-inflammation is initiated during the acute phase of ischemic stroke and is a major contributing factor in the extension of the lesion core (Figure 17). Both microvascular dysfunction and exacerbated inflammation contribute to thrombo-inflammation. The work by Kleinschnitz and colleagues suggested that Tregs play an important role in this process. Accordingly, the presence of both Tregs and platelets was correlated with substantial reduction in CBF and increased brain fibrin levels compared with platelet-depleted mice. The immunological function of Tregs was not affected by platelet depletion, supporting platelet-Treg-associated microvascular dysfunction and thrombosis. Disabling either platelet GPIb, which is crucial for platelet binding to the endothelium during thrombosis, or its ligand VWF, with blocking antibodies or by genetic deletion resulted in significant infarct size reduction. Recently CD 84 was identified as the molecular link between T cells and platelets in the context of stroke (Schuhmann et al. 2020). *In vitro*, platelet-derived soluble CD84 enhanced the motility of wild-type but not Cd84−/− CD4+ T cells, suggesting that homophilic CD84 interactions drive this process. Evidence of platelet CD84 shedding was found in blood samples from patients suffering acute ischemic stroke, and high levels of platelet CD84 correlated with poor stroke outcome (Schuhmann et al. 2020). It has been suggested that during cerebral ischemia, platelets guide lymphocytes to vascular injury sites and vice versa (Nieswandt 2012). In conclusion, these data suggest that thrombo-inflammation triggered by interactions between TRegs and platelets accelerate the expansion of ischemic lesions by impairing microvascular patency in the acute phase of ischemic stroke. It should be noted that experimental evidence for a role for thrombo-inflammation in the pathology of ischemic stroke comes mainly from reperfusion models, suggesting that thrombo-inflammation may be an component of reperfusion injury.

Microglia and monocyte-derived macrophages

The role of microglia and monocyte-derived macrophages in ischemic stroke is more complex. On the one hand they have been reported to play a beneficial role during ischemic injury. Microglia are responsible for phagocytosis which is regulated by MER proto-oncogene tyrosine kinase, milk fat globule-epidermal growth factor 8 protein, and triggering receptor expressed on myeloid cell 2 expression (Neher et al. 2013). Ganciclovir, a prodrug nucleoside analogue that was developed in the 1970s as an antiviral treatment, was recently shown to potently inhibit microglial proliferation and neuroinflammation (Ding et al. 2014). Ganciclovir treatment exacerbated ischemic brain injury in mice that express herpes simplex virus-1 thymidine kinase in the myeloid lineage, along with a reduction in the expression of the neurotrophic cytokine insulin-like growth factor (Lalancette-Hébert et al. 2007). This effect was attributed to the depletion of proliferating microglia/macrophages. On the other hand, a high level of inflammatory monocytes in the circulation has been correlated with unfavorable clinical outcomes after stroke (Kaito et al. 2013). Monocytes may contribute to intravascular coagulation and microvascular clogging by releasing DNA and by triggering the extrinsic coagulation cascade via the expression of tissue factor. Once they infiltrate into the brain parenchyma they differentiate into macrophages and undergo polarization to classical proinflammatory M1, or alternative anti-inflammatory M2 macrophages, that may play divergent roles in stroke outcome (Hu et al. 2012) (Fumagalli et al. 2013).

Neutrophils in ischemic stroke

Intravascular adhesion of neutrophils can be observed very soon after onset of ischemic stroke and may contribute to capillary clogging (Figure 17). Early neutrophil-mediated clogging and obstruction of brain capillaries has been suggested to be a major cause of no-reflow in ischemic stroke despite successful thrombolysis (El Amki et al. 2020). Neutrophils also enhance inflammation and activate the intrinsic coagulation cascade through the release of neutrophil extracellular traps (NETs), thus further reducing tissue perfusion (G. J. del Zoppo et al. 1991)-(Dawson et al. 1996). At later stages, neutrophils are also implicated in BBB disruption by releasing matrix metalloproteinases (MMPs) (Rosell et al. 2008) (Ludewig et al. 2013), ROS and reactive nitrogen species (Garcia-Bonilla et al. 2014). Leukocyte trafficking is mediated by E-, L-, and P-selectins, (Yilmaz and Granger 2008). The selective blockade of E- or P-selectin improves neurological outcomes in rodent models of ischemic stroke (Huang et al. 2000) (Mocco et al. 2002). Similarly, a significant decrease in BBB breakdown was observed in P-selectin- deficient mice (A. Y. Jin et al. 2010). However, in a rabbit model of stroke anti-L-selectin antibody did not change the outcome (Yenari et al. 2001). ICAM-1 and VCAM-1, which are involved in the adhesion of neutrophils to the endothelial wall and promotion of extravasation into the brain tissue, have extensively been investigated in the context of cerebral ischemia. ICAM-1 expression peaks at 12–48 h post-stroke stroke both in rodents and in humans. ICAM-1 deficiency or inhibition in experimental stroke decreased leukocyte

infiltration and improved of stroke outcomes (Vemuganti, Dempsey, and Bowen 2004). However, a phase III clinical trial investigating the anti-ICAM-1 antibody enlimomab failed to show protection (Enlimomab Acute Stroke Trial Investigators 2001).

Sequential BBB breakdown

Substantial efforts have been made in recent years to understand the kinetics of cellular events occurring in the NVU during the acute phase of ischemic stroke (G. J. del Zoppo 2010). This includes studies conducted to elucidate the role and the contribution played by the cellular components of the BBB. One important question has been how viable ECs present in the penumbra gradually lose BBB properties in response to ischemic injury. The original dogma assumed that TJ complex disruption is the main cellular event in both early (<24) and late (>24) phases of BBB breakdown (Sandoval and Witt 2008)(Luissint et al. 2012). While it had been reported that TJ morphology was defective at 3hr after ischemia with reduced levels of Claudin5, Occludin, and Zona Occludens-1 (ZO-1) (Lossinsky and Shivers 2004) (Jiao et al. 2011), a 2013 study reported TJ morphology to be conserved despite profuse leak of tracers from blood vessels as late as 25 hours after embolic middle cerebral artery occlusion (MCA) (Krueger et al. 2013). A follow-up study by Knowland et al also failed to show TJ defects in the early phase of BBB disruption both by ultrastructural analysis and with the use of infused tracers (Knowland et al. 2014). In addition to paracellular barrier function, brain ECs maintain a transcellular transport through a limited number of endocytotic caveolae, which show a low rate of transcytosis under homeostasis (Nag 2003). Interestingly, the expression of Caveolin 1 (Cav1) and its phosphorylation state are increased as early as 2hr after stroke, prior to disassembly of TJ complexes and BBB breakdown (Nag, Venugopalan, and Stewart 2007) (Knowland et al. 2014). Temporal analysis of brain accumulation of tracers indicated that increased BBB permeability in the first 48 hours after tMCAO is driven mainly by transcellular pathways, whereas paracellular pathways dominate from 48 hours, consistent with the sequence of structural changes observed in ECs after reperfusion (Figure 18) (Knowland et al. 2014).

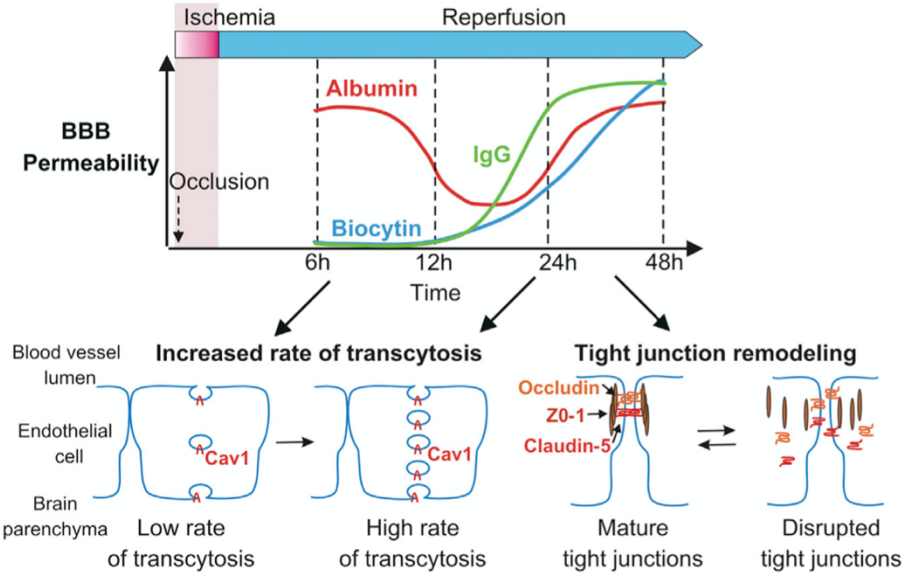

Figure 18. Schematic representation of increases in biocytin-TMR (blue), IgG (green), and alb-Alexa 594 (red) over time after t-MCAO. There is a nonlinear, gradual increase in biocytin-TMR and IgG permeability during stroke progression that becomes significant 24–48 hr after t-MCAO and correlates with the abundance of structural defects in TJs (i.e., junction remodeling). In contrast, alb-Alexa 594 uptake increases as early as 6 hr after t-MCAO, suggesting that endocytosis and transcytosis are increased in early phases of ischemic stroke. Upregulation of both Cav1-dependent and -independent endothelial transcytosis, followed by TJ disassembly, contribute to enhanced BBB permeability after t-MCAO. Reproduced with permission from (Knowland et al. 2014).

To evaluate the role of Cav1 in acute ischemic stroke, wild-type, and Cav1-deficient mice (which lack EC caveolae) were injected with Alexa 594 conjucated albumin to evaluate endocytosis and transcytosis and with biocytin-TMR to assess paracellular permeability after after tMCAO (30 minutes). Cav1 deficiency substantially reduced the amount of Alexa 594-albumin transported into the ipsilateral brain parenchyma at both 6 and 27 hours after tMCAO. On the other hand, paracellular permeability to biocytin-TMR and IgG leakage were significantly increased compared to wild-type (Knowland et al. 2014). Although the Knowland study argues for a role for transcellular vesicular transport in the acute phase, there is more recent data to suggest that TJ breakdown can also happen very early (Shi et al. 2016). Moreover, an alternative model has been proposed to suggest that the main mechanism of edema in ischemic stroke is a massive influx of CSF, not a loss of BBB permeability (Mestre et al. 2020). Thus, the mechanism of BBB breakdown and its importance for edema formation in the early stages of stroke remain controversial (Jiang et al. 2018).

BBB breakdown at late stages of ischemic stroke has been demonstrated to involve MMPs, which are calcium dependent zinc-endopeptidases of the metzincin superfamily (Stöcker et al. 1995). Structurally, MMPs contain a conserved Zn^{2+} binding motif in the catalytic domain and several conserved protein domains (Page-McCaw, Ewald, and Werb 2007). MMPs contribute to tissue morphogenesis, cell migration, angiogenesis, wound healing and cancer, where one of their important actions was considered to be the cleavage of extracellular matrix (ECM) proteins to allow cells to penetrate ECM barriers (Sternlicht and Werb

2001)(Sabeh et al. 2004). However, these studies were mainly based on *in vitro* experiments using excessive amounts of MMPs and remain controversial. In ischemic stroke, increased MMP is correlated with neuronal apoptosis, BBB breakdown, brain swelling, leukocyte extravasation and hemorrhagic transformation (Rosell et al. 2008). Increased activity of several MMPs (MMP-2, MMP-3, MMP-7, and MMP-9) has been linked to infarct growth. MMP-2 is constitutively expressed in the brain and contributes to BBB extracellular matrix disruption in early stages (withing 24 hours) of ischemic stroke (Gasche et al. 2001). In contrast, MMP-9 is an inducible enzyme which is secreted by activated microglia, macrophages, and infiltrating leukocytes, and linked to severe and irreversible BBB damage resulting in hemorrhagic transformation (Yang et al. 2007). High MMP-9 activity and serum levels were reported to be a predictor of poor stroke outcome (Zhong et al. 2017). Studies investigating the kinetics of MMP-9 expression after ischemic stroke indicating a highest upregulation 15-48 hours after stroke (Zhao et al. 2006). Genetic and pharmacological studies using MMP-9 deficiency and inhibition concluded a significant reduction in lesion size in transient experimental stroke models in mice (Asahi et al. 2001) (Gu et al. 2005). In contrast, genetic deficiency and pharmacological inhibition of MMP-2 was not successful in reducing infarct lesion in mice (Lucivero et al. 2007).

Ischemic Stroke modeling in rodents

Exploration of pathological mechanisms and novel pharmacological treatment strategies for human stroke relies on the use of animal models (Overgaard 1994). Rodents are the most widely used species in experimental stroke research. Several practical advantages promoted this choice, including relatively low costs for transportation, storage and feeding. Mice have been especially useful because of the availability of unique strains with different and well characterized collateral anatomy that can be genetically engineered to over- or under-express selected target genes, allowing the researcher to investigate molecular mechanisms of stroke. As discussed above, mice also form a complete circle of Willis (Sommer 2017). Nevertheless, one has always to keep in mind that the translation of animal model results on human disease has it limits. Failure to translate neuroprotection success from the laboratory to the clinical setting has also raised doubts about the utility of animal models of stroke (O'Collins et al. 2006). To improve the translational value of experimental studies performed in mice, recommendations are made to reduce the divergence between stroke model and the biological events in the context of human stroke (Fisher et al. 2009) (Stroke Therapy Academic Industry Roundtable (STAIR) 1999) .

Stroke Therapy Academic Industry Roundtable recommendations for stroke research

Despite considerable efforts and a multitude of successful preclinical studies, drugs, and concepts for acute stroke, only two treatments have been successfully translated to clinical practice. Strategies have failed in clinical trials for acute stroke treatment include 1026

neuroprotective agents (O'Collins et al. 2006), stem cells strategies (Borlongan 2019) as well as novel immunological treatments (Elkins et al. 2017). Analysis of this situation allows for the identification of some major culprits that will be discussed in this section. Some of the main elements that determine the quality of a preclinical study are the presence or absence of randomization of treated animals and control group, blinding of drug administration in the acute phase of experimental ischemic stroke induction, and blinding of the outcome assessment and analysis, as well as sample size calculation, which is also an important element in study quality design and reliability of the results (Sena et al. 2007). Another important limitation of animal models used for experimental stroke is the fact that experimental ischemia is most often induced in healthy animals while human stroke is usually diagnosed as a consequence of a natural evolution of underlying diseases or risk factors such as aging, hypertension, diabetes, and heart disease such as atrial fibrillation, and in the context co-medications (Shi, Mörike, and Klotz 2008). Another key point is the lack of direct correlation between the model used to induce experimental ischemic stroke and clinical situation; for instance, brain structure is not similar between human and rodents; the human brain contains higher proportion of white matter compared to the brain of rodents, which are widely used to model ischemic stroke in preclinal studies. The emergence of the neurovascular unit highlighted the lack of pertinence of strategies targeting only neuros to save the penumbra, as multiple cells are involved in the pathophysiologic process.

To reduce the barriers between preclinical animal studies and human clinical trials, the Stroke Therapy Academic Industry Roundtable (STAIR) published several recommendations to allow the development of acute stroke treatment that could be easily translated to clinical practice (Stroke Therapy Academic Industry Roundtable (STAIR) ; 1999). In 2009 an updated recommendation was published based on 10 years experience of preclinical studies (Fisher et al. 2009). Initial STAIR 1 recommended that preclinical studies should provide an adequate dose-response curve for any drug evaluated; define the time window of drug administration in a well-characterized model; be conducted in a blinded and physiologically controlled manner; include both permanent and transient occlusion models; and include acute and long term histological and functional outcomes. Moreover, initial rodent studies should ideally be repeated in gryencephalic species before moving into human clinical trials. O'Collins' systematic review in 2006 (O'Collins et al. 2006) concluded that the more a study design quality was improved with more adherence to STAIR 1 criteria the less the efficacy of the investigated neuroprotective agents. STAIR 1 recommendation has influenced scientists who are conducting studies exploring the acute treatment of ischemic stroke. For example, there are fewer studies that use pretreatment strategies of a potential neuroprotective agent now than before the publication of the 1999 recommendations. The 2009 STAIR 2 updates to the recommendations include a suggestion that a preclinical study should include a dose-response where the minimum effective and maximum of a drug concentration is determined identification of therapeutic window of efficacy of a potential drug using penumbral imaging based on perfusion/diffusion MRI mismatch and the use of multiple outcome measures

including histological assessment and behavioral evaluation acutely and long term at least 2 to 3 weeks after experimental ischemic stroke to address long-term benefit. Physiological monitoring should be routine in modeling ischemic stroke in order to introduce further exclusion critieria, such as when occlusion occurs but not reperfusion, resulting in larger infarct volume and high infarct size variability. It is therefore recommended to routinely monitor blood pressure, temperature, blood gases, and blood glucose, as well as cerebral blood flow using either doppler flow or perfusion imaging to document effective arterial occlusion and reperfusion. Providing proof of drug efficacy in multiple species is also suggested, for instance in rodents and rabbits, using both histological and behavioral outcome assessment. Inclusion and exclusion criteria should be provided and based on the monitoring of cerebral blood flow, physiological and other paramenters and the number of animals excluded from analysis based on these different criteria reported. Potential conflicts of interest and study funding should also be reported, along with information on study funding and the donation of drugs or equipment. Studies demonstrating positive effects in younger healthy animals should be followed by experiments conducted in aged animals and animals with comorbidities such as hypertension, diabetes, and hypercholesterolemia to mimic clinical situations including both male and female animals. It is also suggested that medication studies are designed to replicate the clinical situation in the presence of drugs usually administered both in the acute stage of ischemic stroke and for long-term comorbidities. Exploring relevant biomarkers using diffusion/perfusion MRI and serum markers of tissue damage is also recommended (Fisher et al. 2009). In conclusion STAIR recommendations to provide a robust data in preclinical research in the aim to facilitate results translation to clinical setting. In practice, however, it is difficult if not impossible to apply all these criteria to experimental studies.

Several rodent models of focal cerebral ischemia have been developed to mimic different conditions of human stroke (Koizumi et al. 1986) (Longa et al. 1989) (Tamura et al. 1981). In contrast to human stroke where manifestations are extremely diverse, experimental models result in more reproducible lesions, facilitating the analysis and exploration of stroke pathophysiology and the testing of pharmacological agents (Yamori et al. 1976). In addition, direct invasive access to brain tissue allows physiological, biochemical, genetic, and molecular investigations that would be impossible in human patients. While current imaging techniques used in the human stroke setting do not allow for the exploration of early pathological events occurring during ischemic stroke, animal models also offer the possibility of exploring this over time at the molecular and cellular level (Provenzale et al. 2003) (Hilger et al. 2004). These models also facilitate the exploration of vascular collaterals and brain perfusion. The development of new therapeutics and future success of preclinical stroke research rely in part partially on the careful selection of appropriate experimental stroke models. The most common rodent models of ischemic stroke will be discussed below.

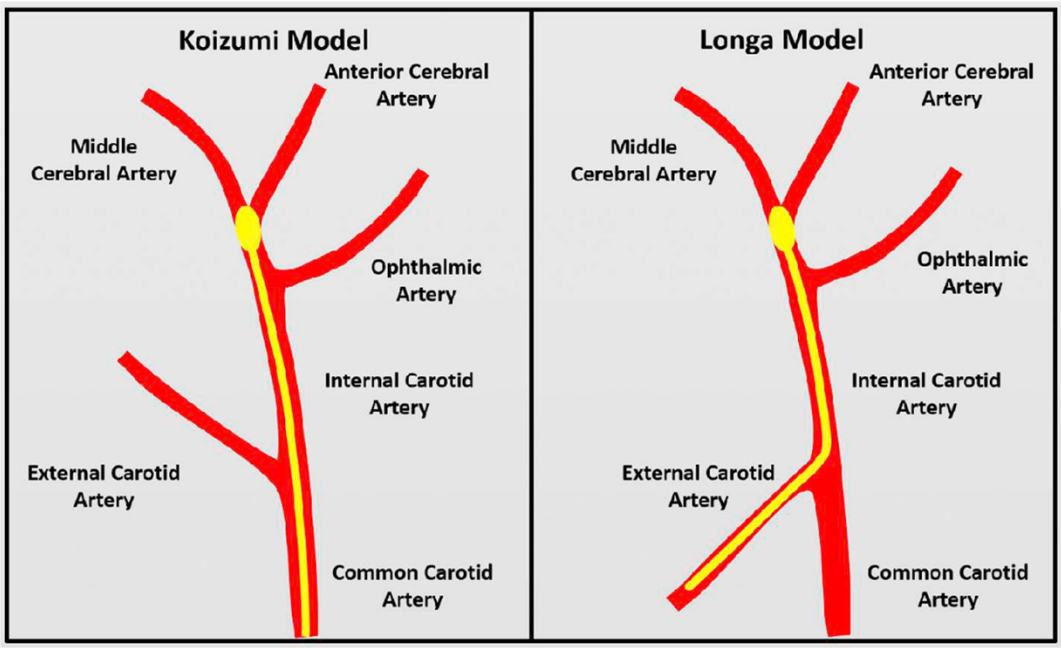

Figure 19. Two intraluminal filament methods can be used to achieve middle cerebral artery occlusion. The Longa method (right) has been deemed more useful for stroke research than the Koizumi method (left). The Longa method sees a much lower mortality rate post-surgery than that of the Koizumi. In the Longa method, the filament is inserted in the external carotid artery and is guided through the internal carotid artery to the middle cerebral artery, as opposed to insertion from the common carotid artery as seen in the Koizumi method. Reproduced with permission from (Barthels and Das, 2020).

As transient and permanent cerebral ischemia is most often triggered by occlusion of the MCA, focal ischemia is most commonly modeled experimentally by permanent or transient MCA occlusion (pMCAO and tMCAO, respectively) (S. Lee et al. 2014). Transient models reflect human stroke with mechanical, thrombolytic, or spontaneous reperfusion, and permanent models mimic clinical stroke without reperfusion. These models can be broadly separated according to the site of occlusion:

Proximal occlusion of the MCA at the level of its origin at the circle of Willis via the intraluminal suture technique (the so-called ‘’filament’’ or ‘’suture’’ model) is the most used model in experimental stroke research and is employed with and without reperfusion (Engel et al. 2011). It does not require craniectomy, limiting the potential for local structural damage and associated inflammation. It involves the introduction of a coated or heat blunted nylon filament into the common carotid artery (CCA) that is subsequently directed via the internal carotid artery (ICA) to the base of MCA at the level of the circle of Willis. The nylon filament can either be introduced directly into the CCA, which implies permanent CCA occlusion (Koizumi et al. 1986), or via the external carotid artery (ECA) to allowing the conservation of CCA perfusion (Longa et al. 1989) (Figure 20). The Longa method maintains the anatomic integrity required for efficient reperfusion (S. Liu et al. 2009). For both methods, blood flow monitoring in the MCA territory can be used to ensure sustained occlusion and efficient reperfusion (Schmid-Elsaesser et al. 1998). Careful retraction of the filament after a predetermined time that typically ranges from 30 minutes to 3-4 hours will produce

reperfusion with variable efficiency (tMCAO). The filament can also be left in place to model pMCAO. The reperfusion model imitates restoration of blood flow in humans after mechanical removal of a thromboembolic clot. Because of the involvement of the entire MCA territory including the lenticustriate arteries, the brain tissue affected by this model is extensive, frequently resulting in large infarcts, functional impairment, and a relatively high level of mortality.

In part to overcome these issues, focal ischemia is also frequently modeled through **distal MCAO** facilitated through direct MCA exposure by craniectomy and dura mater section (Tamura et al. 1981). The technique consists of removing the skull overlying the MCA downstream of the lenticustriate arteries after separating the parotid gland and temporalis muscle, transecting of the zygomatic arch. Permanent MCAO can then be induced by electrocoagulation followed by transection of the artery. Transient MCAO can be triggered using a microaneurysm clip, by hooks used to lift the MCA from the brain surface until blood flow is interrupted, by ligatures, by thrombin injection or by endothelin-1 (ET-1) injection or super-fusion (Yanagisawa, Kurihara, et al. 1988). Thrombosis can also be induced by extravascular application of ferric chloride soaked tissue paper or by intravascular photo-oxidation (Sugimori et al. 2004)(Ren et al. 2012). Thrombotic occlusion is commonly used to study thrombolytic interventions and approaches combining thrombolytic as well as neuroprotective drugs to treat the pathological condition of stroke (Nikitin et al. 2021). Photochemical models often target smaller MCA or ACA branches when combined with intravital microscopy due to practical considerations related to cranial window placement and imaging (V. M. Lee et al. 1996). ET-1 is a potent and long-acting vasoconstrictive peptide that can be applied directly onto the exposed MCA or as an intracerebral (stereotactic) injection. Its actions result in a sharp CBF reduction (70% - 90%) ensued by reperfusion over several hours. Lesions comparable pMCAO are observed if ET-1 is applied directly onto the MCA whereas semicircular infarct result from cortical injections. Compared to the proximal models, the distal models result in considerably smaller infarcts due to the vascular territories affected. While the proximal models involve thalamic, hypothalamic, hippocampal, and midbrain regions, the distal models spare these areas and involve frontal, parietal, temporal, and rostral occipital cortices, the underlying white matter, and a marginal part of the striatum (He et al. 1999). Distal models can be modified to consolidate ischemic damage by combining occlusion of the ipsilateral CCA with MCAO to reduce collateral blood flow.

The thromboembolic clot model models the clinical scenario and is not as well anatomically defined as the above models (Y. Chen et al. 2015). It consists of the application of spontaneously formed clots or thrombin-induced clots from autologous blood or direct injection of thrombin into the intracranial segment of the ICA to mimic the mechanism of vascular occlusion seen in a large proportion of human strokes. While this should make it suitable to investigate thrombolytic agents alone or in combination with neuroprotective drugs, it also has several limitations. Lesion sizes that results are more variable than most of

the distal and proximal models described above due to greater variability in the affected territory and the duration of occlusion. A high degree of autolysis inducing an early and uncontrollable reperfusion is observed, which ultimately make this model less sensitive and less suitable for validation of neuroprotective effects. Analysis of clot composition revealed that these are mainly composed of polymerized fibrin containing a low number of cells and platelets, which is different from human clots, which contain platelets, extracellular DNA from NETosis, and a significant accumulation of erythrocytes which together make these clots more stable (Niessen et al. 2003). Due to endogenous thrombolysis, spontaneous reopening of cortical micro vessels can be observed within 1 hour after clot injection, cortical vessels by 3 hours, and striatal vessels clear by 24 hours after thrombin injection. Moreover, the rate of cerebral hemorrhage and mortality is high (Kano et al. 2000).

Stroke Therapy Academic Industry Roundtable recommendations for stroke research

Despite considerable efforts and a multitude of successful preclinical studies, drugs, and concepts for acute stroke, only two treatments have been successfully translated to clinical practice. Strategies have failed in clinical trials for acute stroke treatment include 1026 neuroprotective agents (O'Collins et al. 2006), stem cells strategies (Borlongan 2019) as well as novel immunological treatments (Elkins et al. 2017). Analysis of this situation allows for the identification of some major culprits that will be discussed in this section. Some of the main elements that determine the quality of a preclinical study are the presence or absence of randomization of treated animals and control group, blinding of drug administration in the acute phase of experimental ischemic stroke induction, and blinding of the outcome assessment and analysis, as well as sample size calculation, which is also an important element in study quality design and reliability of the results (Sena et al. 2007). Another important limitation of animal models used for experimental stroke is the fact that experimental ischemia is most often induced in healthy animals while human stroke is usually diagnosed as a consequence of a natural evolution of underlying diseases or risk factors such as aging, hypertension, diabetes, and heart disease such as atrial fibrillation, and in the context co-medications (Shi, Mörike, and Klotz 2008). Another key point is the lack of direct correlation between the model used to induce experimental ischemic stroke and clinical situation; for instance, brain structure is not similar between human and rodents; the human brain contains higher proportion of white matter compared to the brain of rodents, which are widely used to model ischemic stroke in preclinal studies. The emergence of the neurovascular unit highlighted the lack of pertinence of strategies targeting only neuros to save the penumbra, as multiple cells are involved in the pathophysiologic process.

To reduce the barriers between preclinical animal studies and human clinical trials, the Stroke Therapy Academic Industry Roundtable (STAIR) published several recommendations to allow the development of acute stroke treatment that could be easily translated to clinical practice (Stroke Therapy Academic Industry Roundtable (STAIR) ; 1999). In 2009 an updated

recommendation was published based on 10 years experience of preclinical studies (Fisher et al. 2009). Initial STAIR 1 recommended that preclinical studies should provide an adequate dose-response curve for any drug evaluated; define the time window of drug administration in a well-characterized model; be conducted in a blinded and physiologically controlled manner; include both permanent and transient occlusion models; and include acute and long term histological and functional outcomes. Moreover, initial rodent studies should ideally be repeated in gryencephalic species before moving into human clinical trials. O'Collins' systematic review in 2006 (O'Collins et al. 2006) concluded that the more a study design quality was improved with more adherence to STAIR 1 criteria the less the efficacy of the investigated neuroprotective agents. STAIR 1 recommendation has influenced scientists who are conducting studies exploring the acute treatment of ischemic stroke. For example, there are fewer studies that use pretreatment strategies of a potential neuroprotective agent now than before the publication of the 1999 recommendations. The 2009 STAIR 2 updates to the recommendations include a suggestion that a preclinical study should include a dose-response where the minimum effective and maximum of a drug concentration is determined identification of therapeutic window of efficacy of a potential drug using penumbral imaging based on perfusion/diffusion MRI mismatch and the use of multiple outcome measures including histological assessment and behavioral evaluation acutely and long term at least 2 to 3 weeks after experimental ischemic stroke to address long-term benefit. Physiological monitoring should be routine in modeling ischemic stroke in order to introduce further exclusion critieria, such as when occlusion occurs but not reperfusion, resulting in larger infarct volume and high infarct size variability. It is therefore recommended to routinely monitor blood pressure, temperature, blood gases, and blood glucose, as well as cerebral blood flow using either doppler flow or perfusion imaging to document effective arterial occlusion and reperfusion. Providing proof of drug efficacy in multiple species is also suggested, for instance in rodents and rabbits, using both histological and behavioral outcome assessment. Inclusion and exclusion criteria should be provided and based on the monitoring of cerebral blood flow, physiological and other parameters and the number of animals excluded from analysis based on these different criteria reported. Potential conflicts of interest and study funding should also be reported, along with information on study funding and the donation of drugs or equipment. Studies demonstrating positive effects in younger healthy animals should be followed by experiments conducted in aged animals and animals with comorbidities such as hypertension, diabetes, and hypercholesterolemia to mimic clinical situations including both male and female animals. It is also suggested that medication studies are designed to replicate the clinical situation in the presence of drugs usually administered both in the acute stage of ischemic stroke and for long-term comorbidities. Exploring relevant biomarkers using diffusion/perfusion MRI and serum markers of tissue damage is also recommended (Fisher et al. 2009). In conclusion STAIR recommendations to provide a robust data in preclinical research in the aim to facilitate results translation to clinical setting. In practice, however, it is difficult if not impossible to apply all these criteria to experimental studies.

Chapter 4. Modulating Sphingosine 1-Phosphate Signaling in Stroke

Endogenous and pharmacological modulation of S1P receptor activity may impact the outcome of both ischemic and hemorrhagic stroke by actions on immune cells, vascular cells, and cells of the CNS. In the NVU, S1P receptors are expressed on endothelial cells, pericytes, neurons, astrocytes, and microglia (Vanlandewijck et al. 2018). S1PR modulation has been extensively studied in experimental models of ischemic and hemorrhagic stroke as well as in several small-scale clinical trials. In addition to addressing the efficacy and safety of FTY720 treatment, these studies have explored potential mechanisms of action of S1PR modulation using genetic and pharmacological tools. In this chapter I will provide an overview of these studies and a summary of the current state of S1PR modulation in ischemic stroke.

Efficacy and safety of Fingolimod treatment in ischemic stroke

Endogenous mechanisms of ischemic preconditioning have long been considered to be a potential source of novel targets for stroke treatment (Iadecola et al. 2011). One of the first indications for a role for S1P signaling in ischemic stroke came from a study by Wacker et al., who in 2009 investigated the role of Sphk isoforms in mediating ischemic tolerance induced by hypoxic preconditioning (HPC). HPC was shown to rapidly increase microvascular Sphk2 expression and activity (peaking at 2 hours) whereas Sphk1 expression was unchanged (Wacker, Park, and Gidday 2009). Sphk inhibition by dimethylsphingosine during HPC impaired the capacity of HPC to reduce infarct volumes, neurological deficits, and ipsilateral edema in mice challenged with tMCAO (60 minutes). Further suggesting a role for S1P signaling in HPC, FTY720 administration 48 hours before MCAO afforded ischemic tolerance similar to HPC. Moreover, when combined with HPC, FTY720 further increased protection, an increase that was reversed with dimethylsphingosine. These results suggest that hypoxia may mediate tolerance to ischemia by increasing Sphk2 activity and thus enhancing S1P production and activation of S1PRs. Interestingly, Sphks have also been shown to be critical for preconditioning protection in myocardial infarction, although Sphk1 was more important in that context (Vessey et al. 2011).

During the same period, several groups explored the capacity of FTY720 to improve the outcome of ischemic stroke when administered after MCAO. Czech et al. challenged C57Bl/6 mice with tMCAO (90 minutes) and administered FTY720 (1 mg/kg) via intraperitoneal (i.p.) injection at the onset of cerebral ischemia (Czech et al. 2009). FTY720 treatment reduced lesion size and improved neurological outcome at 24 after reperfusion. Shichita et al. challenged C57BL/6 mice with tMCAO (60 minutes) and administered FTY720 (1 mg/ kg) intravenously (i.v.) before reperfusion either as a single bolus, assessing infarct volume at 24 hours, or every 24 h for four consecutive days, assessing infarct volumes at day 4 (Shichita et al. 2009). FTY720 administration significantly reduced lesion size in both treatment protocols. Hasegawa et al. subjected male rats to tMCAO (120 minutes) and administered FTY720 i.p.

immediately after reperfusion (Hasegawa et al. 2010). At both 0.25 mg/kg and 1 mg/kg, FTY720 significantly reduced lesion size and improved neurological score at 24 and 72 hours. These studies argued that FTY720 reduces infarct size and improves neurological outcome in therapeutic protocols of ischemic stroke in both mice and rats.

The role of sphingosine kinases (Sphk)-1 and -2 and the capacity of FTY720 to induce protection were further investigated in the acute phase of ischemic stroke by Pfeilschifter et al. in 2011 (Pfeilschifter, Czech-Zechmeister, Sujak, Mirceska, et al. 2011). Using a 2-hour tMCAO ischemic model in mice, wild-type and knockout animals were administered FTY720 (1 mg/kg) i.p. directly after the occlusion of the MCA. Genetic deletion of Sphk2 but not Sphk1 increased ischemic lesion size and worsened neurological function 24 hours after tMCAO. The protective effect of FTY720 was conserved in Sphk1 (-/-) mice but not in Sphk2 (-/-) mice. This confirmed the important role of Sphk2-derived S1P for endogenous protection in cerebral ischemia, and (as FTY720 phosphorylation depends on Sphk2), it demonstrated that the protective effect of FTY720 is mediated via phospho-FTY720.

In a 2011 study, Wei et al. further explored the potential clinical utility of FTY720 by addressing if FTY720 improved long-term behavioral outcomes, whether delayed treatment was still effective and if FTY720 also provided protection in the absence of reperfusion (Wei et al. 2011). In a 90 minute tMCAO model in mice, administration of FTY720 (3mg/kg) 2 , 24 and 48 hours after reperfusion reduced infarct size, edema, and cell death in the core and peri-infarct area. FTY720 treatment also reduced the number of activated neutrophils and microglia/macrophages in the periinfarct area and ischemic core and reduced the number of ICAM-1-positive blood vessels in the periinfarct, ipsilateral intact and contralateral areas. FTY720 -treated mice developed smaller infarcts and performed better in behavioral tests up to 15 days after ischemia. The protective effect of FTY720 (1 mg/kg) was also observed in a thrombin-induced pMCAO model even with drug administration as late as 4 hours after ischemic challenge. FTY720 (1 mg/kg) injected i.p. 30 minutes after reperfusion also reduced infarct volumes 22 hours after reperfusion in rats subjected to 2 hours MCAO. This study emphasized the potential utility of FTY720 in a clinical context.

FTY720 induces strong lymphopenia that is sustained for more than 24 hours, raising a concern that FTY720 could increase the incidence of bacterial infection in ischemic stroke, where associated systemic immunodepression is already a clinical problem (Offner, Vandenbark, and Hurn 2009) (Langhorne et al. 2000) (Prass et al. 2003). However, Pheilschifter and colleagues reported no increase in bacterial infections in mice treated with FTY720 subjected to ischemic stroke (Pfeilschifter, Czech-Zechmeister, Sujak, Foerch, et al. 2011). In a later study by the same group, long-term effects of FTY720 were investigated (Brunkhorst et al. in 2013). Mice were challenged with a photothrombotic stroke model, and FTY720 treatment (1 mg/kg twice daily) initiated on day 3 and continued for 5 days. Thirty-one days later, a protective effect of FTY720 was demonstrated for long-term functional

outcome, with a substantial reduction in reactive astrogliosis along with larger post-synaptic densities. FTY720 treatment also induced an increase in the expression of vascular endothelial growth factor a (VEGFa). These studies further support the safety and efficacy of FTY720 treatment in a clinical scenario.

Further exploring the clinical utility and safety of FTY720, Campos et al. in (2013) investigated FTY720 as an adjunct to tPA using a mouse thromboembolic model involving local injection of thrombin into the MCA following a craniotomy (Campos et al. 2013). They found that FTY720 treatment (0.5 mg/kg) 45 minutes, 24 and 48 hours after thrombin improved neurological outcome and reduced infarct volumes at 24 and 48 hours. Interestingly, there was also less hemorrhagic transformation in mice that received FTY720. These results confirmed the efficacy of FTY720 in a thromboembolic occlusion model and suggested that FTY720 may not only be safe in conjunction with standard therapy, but also have the potential to reduce the risk of hemorrhagic transformation with delayed administration of tPA.

Nazari et al. (2016) investigated the effects of FTY720 on the impairment of learning and memory and hippocampal synaptic plasticity induced by tMCAO (60 minutes) in rats (Nazari et al. 2016). The animals received a first dose of FTY720 (0.5mg/Kg) or its vehicle i.p. 24 hours before surgery and then every other day for 7 days. FTY720 significantly reduced lesion size and memory impairment at 7 days. In addition, field potential recordings demonstrated a marked reduction in the induction of long-term potentiation. The results of this study demonstrated that tMCAO in rats impairs the retention of passive avoidance tasks and that multiple injections of FTY720 can reduce this impairment.

Although most published studies suggest efficacy and safety of FTY720 in ischemic stroke, there are also several studies that do not. In 2011, Liesz et al. showed that despite substantially reducing the number of T- and B-lymphocytes invading the brain, FTY720 administration did not improve outcome in mouse models of ischemic stroke (Liesz et al. 2011). No amelioration of infarct size, behavioral dysfunction or brain edema was observed 3 or 7 days after pMCAO nor 24 hours after 60 minutes tMCAO. FTY720 (1 mg/kg) was administered by oral gavage 48 hours before or 3 hours after pMCAO or daily starting 48 hours before tMCAO. It is unclear why no protection was observed in this study, but it is notable that Liesz et al. use a different route of administration (oral) and started treatment either well before or well after MCAO.

In a study parallel to that of Campos et al, Cai et al. challenged C57Bl/6 mice with tMCAO (3 hours) and administered vehicle, FTY720 (1 mg/kg i.p.), alteplase (10 mg/kg through intravenous infusion), or a combination of FTY720 and alteplase (n=18 mice per group) immediately prior to reperfusion (A. Cai et al. 2013). At 24 hours, the highest mortality rate (61 %) was observed in mice who received combination of FTY720 and thrombolysis, compared to mice treated with vehicle (33%), FTY720 alone (39%) or alteplase alone (44%).

There was no observed difference in functional neurological outcome between the four groups, and FTY720 did not improve the efficacy of thrombolysis nor preserve BBB integrity or reduce MMM9- activity. The Cai study differed from the Campos study mainly in the dose of FTY720 (higher) and the stroke model used (longer duration of ischemia).

Studies investigating the potential of S1PR modulation in aged mice and in the context of comorbidities have also had limited success. In 2019, Vogelgesang et al. used middle-aged mice (12-month-old male C57Bl/6) to investigate the treatment effect of siponimod (a second generation S1PR modulator that selectively binds both $S1PR_1$ and $S1PR_5$) on stroke outcome in a transient (45 minutes) model of cerebral ischemia (Vogelgesang et al. 2019). Mice received either siponimod (3 mg/kg) or vehicle i.p. directly after reperfusion and then daily for 5 days. Although siponimod induced sustained lymphopenia on day 7 and reduced T cell infiltration into the brain, there was no effect on brain lesion size on days 1, 3 or 7. These results could suggest that S1PR modulation is no longer effective in the aged population. It is notable however that siponimod is strongly desensitizing on $S1P_1$ (Grailhe et al. 2020) and that dosage used in this study was high. The study would have been more conclusive if the authors had shown protection in young mice with the same drug and under the same experimental conditions.

To address the efficacy of FTY720 in the context of diabetes comorbidity, Li et al. (2020) explored the effect of FTY720 after tMCAO (60 minutes) in mice rendered diabetic and hyperglycemic with a single bolus injection of streptozotocin 28 days prior to stroke modeling (W. Li et al. 2020). Immediately after reperfusion mice received either FTY720 (1 mg/kg) or vehicle i.p. Although FTY720 reduced the number of brain infiltrated inflammatory cells, lowered the level of TNF alpha mRNA and increased the Bcl-2/Bax ratio at 24 hours after reperfusion, it did not reduce apoptosis and it significantly aggravated brain edema. There was also a substantial reduction in the expression levels of TJ proteins Zo-1 and occludin. No statistically significant decrease in infarct volume was observed. Although the results of this study could suggest that $S1P_1$ modulation loses its efficacy in the context of diabetes, it also has several limitations. As for the study in aged mice, the authors did not perform parallel experiments on non-diabetic mice. They also provided evidence for strong $S1P_1$ desensitization in the cortex and striatum of the ipsilateral hemisphere. Moreover, while only 10 of 32 control mice survived untill 24 hours, 27 of 38 mice treated mice were alive at this time, suggesting a survival advantage in the treated group and a possible underestimation of the average infarct sizes in the control group.

Mechanism of action of Fingolimod protection in ischemic stroke

As previously discussed, FTY720 has a complex mechanism of action that involves both activating and inhibitory actions on 4 out of 5 S1P receptors, inhibition of Sphks, etc (Park and Im 2017) (Gupta et al. 2021). In one of the first studies on FTY720 efficacy discussed above,

Hasegawa et al observed that the $S1P_1$ selective agonist SEW2871 (5mg/kg) achieved similar neuroprotective effects to FTY720. This has been reproduced with SEW2871 and other $S1P_1$ selective agonists in subsequent studies and argues that FTY720 acts primarily through positive and/or negative modulation of $S1P_1$. As $S1P_1$ is expressed on astrocytes, neurons, ECs and lymphocytes and as most $S1P_1$ selective modulators, like FTY720, can both activate and desensitize the receptor, this suggests that FTY720 and $S1P_1$ selective modulators may act by disrupting $S1P_1$-dependent lymphocyte trafficking, by activating endothelial $S1P_1$ signaling, by modulating astrocyte activation or neuronal survival, or by several of these mechanisms. As discussed below, current literature does not clearly identify the cellular target of $S1P_1$ modulators, nor whether their principal action is by activation or by desensitization of $S1P_1$.

In their study of FTY720 efficacy and safety, Wei et al (2011) observed that FTY720 did not protect primary neurons against glutamate excitotoxicity or hydrogen peroxide, although it decreased ICAM-1 expression in brain ECs stimulated with TNFα (Wei et al. 2011). Hasegawa et al (2013) later explored the temporal profiles of $S1P_1$, Sphk1 and 2 on neurons in infarct and periinfarct cortices before, 6 and 24 hours tMCAO in rats (Hasegawa et al. 2013). Animals received either 0.25 mg/kg FTY720 or vehicle. Expression of $S1P_1$ and Sphk1&2 were reduced in the infarct cortex at 6 h and 24 hours after MCAO but remained present in the periinfarct cortex. FTY720 administration significantly improved behavioral outcome, and resulted in less brain damage compared with the vehicle and untreated group. Schuhmann et al. (2016) demonstrated that FTY720 treatment in male mice started before tMCAO and continued for 48 hours reduced infarct volume at day 1 and day 7 evaluated by significantly reduced lesion size and improved neurological outcomes compared to controls (Schuhmann et al. 2016). On the other hand, FTY720 treatment did not impact neuronal survival, astrogliosis, synaptogenesis or BDNF expression. Overall, these studies argue that although FTY720 may enter the brain and engage $S1P_1$ even at low doses, it is unlikely to act by a direct neuroprotective mechanism.

In a 2017 study Li et al. addressed the involvement of the S1P pathway in neuronal autophagy in context of ischemic stroke (Park and Im 2017). FTY720 significantly attenuated infarct volumes as previously demonstrated, and this was accompanied by reduced neuronal apoptosis on days 1 and 3 post stroke and amelioration of functional deficits. Furthermore, after ischemic stroke challenge, FTY720 decreased the induction of autophagosome proteins microtubule-associated protein 1, light chain 3 and Beclin 1 in a dose-dependent manner. FTY720 up-regulated the levels of expression of several proteins including the mammalian target of rapamycin and the 70-kDa ribosomal protein, S6 kinase-1. The nonspecific Sphk inhibitor N, N-dimethylsphingosine reversed the effect of FTY720 on mTOR signaling. These results indicated decrease in neuronal autophagy may be one mechanism by which modulation of the S1P signaling pathway by FTY720 attenuate ischemic brain injury in mice.
In 2013, Kraft et al. investigated the dependence of FTY720-mediated protection in cerebral ischemia on lymphocytes (Kraft et al. 2013). Transient MCAO was induced in wild-type and

lymphocyte-deficient Rag1$^{-/-}$ mice, and FTY720 (1 mg/kg) or vehicle administered immediately before reperfusion. Stroke outcome was assessed 24 hours later. FTY720 significantly reduced infarct size and improved functional outcome in wild-type mice on day 1 and day 3 after tMCAO, but this protective effect was lost in lymphocyte-deficient mice. Less lymphocytes were present in the cerebral vasculature of FTY720-treated wild-type mice. This, in turn, was suggested to explain reduced thrombosis and increased cerebral perfusion. However, FTY720 did not reduce BBB reakdown as assessed by Evans blue accumulation nor transendothelial immune cell trafficking after tMCAO in wild-type mice. FTY720 also had no protective effect on cultured neurons subjected to hypoxia, further arguing against direct neuroprotective effects of FTY720. These findings suggested that FTY720 provides benefit in ischemic stroke by induction of lymphopenia and concomitant reduction of microvascular thrombosis.

These conclusions were supported in a study by Brait et al, who in 2016 investigated the effect of the selective $S1P_1$ agonist LASW1238 in a 45 minute tMCAO model (Brait et al. 2016). Immediately after reperfusion mice received LASW1238 (3 or 10 mg/kg), FTY720 (1 mg/kg) or vehicle i.p. At 24 hours, a reduction in infarct volume was observed with both LASW1238 (10 mg/kg) and FTY720 (1 mg/kg) but not with LASW1238 (3 mg/kg). While LASW1238 (10 mg/kg) and FTY720 both induced prolonged lymphopenias, LASW1238 (3 mg/kg) induced only transient lymphopenia that resolved by 24 hours. Although the evidence was circumstantial, the authors concluded that prolonged lymphopenia is necessary to achieve protection with $S1P_1$ modulation.

Contrasting with this conclusion, Swendeman et al. demonstrated in 2017 that ApoM-Fc can afford protection similar to FTY720 in tMCAO without inducing even transient lymphopenia. In order to explore the therapeutic potential of S1P bound to its main plasma chaperone, ApoM, which is considered to both protect S1P from degradation and promote its EC-protective signaling, Swendeman et al developed recombinant ApoM-Fc as a soluble carrier for S1P. Strong protective effects of ApoM-Fc were demonstrated in both tMCAO and a myocardial infarction model. After 60 minutes of transient ischemia, mice were treated with PBS or ApoM-Fc immediately after reperfusion. ApoM-Fc substantially reduced both infarct size and edema and improved neurological scores at 24 hours. Treatment also reduced cerebrovascular permeability, evaluated by Evans blue dye leakage. On the other hand, ApoM-Fc did not impact the number of circulating lymphocytes. Accordingly, *in vitro* experiments showed that while capable of inducing strong protective signaling in cultured endothelial cell, ApoM-Fc–S1P triggered less internalization of $S1P_1$ than did albumin-S1P or FTY720-P. This study argued that S1P, most likely by positive modulation of EC $S1P_1$, can provide protection in ischemic stroke without impairing lymphocyte trafficking (Swendeman et al. 2017).

Takanori Yokota's group conducted two studies to address the impact of S1P signaling on the collateral vasculature. In 2015, Ichijo et al. investigated the effect of daily i.p. injections of

SEW2871 (5 mg/kg/day) for 7 days in C57Bl/6 mice subjected to unilateral common carotid occlusion (CCAO) and with or without (pMCAO) (Ichijo et al. 2015). They found that *S1pr1* mRNA levels and $S1P_1$ protein expression both increased significantly in ipsilateral leptomeningeal arteries at 7 and 14 days, along with an increase in cell growth and division in the ipsilateral leptomeningeal arteries after left CCAO. Fourteen days after CCAO, there was a significant increase in CBF and the diameter of leptomeningeal collateral vessels in mice treated with SEW2871, 5 mg/kg/day for 7 days after CCAO. The inverse $S1P_1$ agonist VPC23019 (0.5 mg/kg) inhibited the effect of SEW2871 on leptomeningeal collateral vessels, suggesting that the effect was $S1P_1$ specific. Infarct volumes were evaluated 7 days after combination of CCAO and pMCAO in mice treated with SEW2871 (5 mg/kg/day for 7 days), there was a reduction in infarct volumes with improvement in CBF, an increase in the diameter of ipsilateral leptomeningeal arteries along with less severe neurological status compared to control mice that received vehicle. The authors suggested that $S1P_1$ is a key regulator of leptomeningeal collateral recruitment at sites of increased shear stress, consistent with studies that reported that $S1P_1$ on ECs was essential in sensing fluid shear stress (Jung et al. 2012). Thus, $S1P_1$ agonism could be beneficial during the late phase of ischemic stroke by enhancing the capacity of shear stress to promote collateral function. In a follow-up study in 2017, Iwasawa et al. investigated the effect of daily i.p. administration of SEW2871 (5 mg/kg) to BALB/c mice after pMCAO (Iwasawa et al. 2018). They observed an early upregulation of $S1P_1$ expression on ECs of leptomeningeal arteries and capillaries at 6 hours after pMCAO, while an increase in $S1P_1$ expression on neurons was observed only after 24 hours. At 7 days after pMCAO, there was an increase in the number of leptomeningeal collateral arteries, improvement in CBF, a decrease in infarct volumes, and improvement of neurological outcome with shorter time to adhesive tape removal compared to mice receiving DMSO. At 6 hours after pMCAO, SEW2871 treatment increased the phosphorylation of eNOS, and at day 3 higher expression of TJ proteins zonula occludens-1 (ZO-1) and occludin was observed. Moreover, capillary density in the peri-infarct regions increased after daily administration of SEW2871, and at 7 days after pMCAO there was a promotion of monocyte/macrophage mobilization to the surface of ischemic cortex. The authors concluded that activation of EC $S1P_1$ in context of permanent ischemic stroke improves the leptomeningeal collateral circulation via eNOS, thereby promoting long term perfusion of the ischemic penumbra.

Intracerebral and subarachnoid hemorrhage

In addition to its protective effects in ischemic stroke models, $S1P_1$ modulation has been shown to provide protection in experimental models of intracerebral hemorrhage (ICH) and subarachnoid hemorrhage (SAH). These studies may support direct BBB actions of $S1P_1$ modulators.

In 2011 Rolland et al. investigated the impact of FTY720 (1 mg/kg i.p.) administration to CD-1 mice 1 h after injection of collagenase into the right basal ganglia to model ICH (Rolland et al. 2011). FTY720 reduced brain edema and improved neurological outcome at 24 and 72 h. In a follow-up study in 2012, they reported that FTY720 (1 mg/kg i.p.) administration either as a single bolus 1 hour after ICH-induction or daily administration 1, 24, and 48 hours after injury improved neurological outcome and reduced brain edema at 24 and 72h in both intra-striatal bacterial collagenase infusion and autologous blood models of ICH in CD-1 mice (Rolland et al. 2013). FTY720 administration resulted in strong lymphopenia and reduction in the expression of ICAM-1, interferon-γ, and interleukin-17 in the mouse brain at 72 hours post ICH. In a rat ICH model FTY720 improved long-term neurocognitive performance with attenuated spatial and motor learning deficits, less severe brain atrophy, and neuronal cell loss within the basal ganglia. They concluded that FTY720 modulates cerebral inflammation and reducing the infiltration of T cells to the brain tissue thereby reducing experimental ICH damage in the short and long term.

In support of these findings, Lu et al. showed that FTY720 provided protection also in a CD-1 mouse model of ICH, induced by injecting collagenase VII-S into the basal ganglia (Lu et al. 2014). Mice received FTY720 (0.5 mg/kg) 30 minutes after surgery and once daily for two days. FTY720 treatment significantly attenuated weight loss following ICH and reduced brain edema, measured three days after ICH. FTY720 also decreased the number of apoptotic cells and alleviated brain atrophy evaluated two weeks after ICH, and improved neurobehavioral functions assessed on day 3 and after 1 and 2 weeks after ICH. However, FTY720 did not change hematoma volume or the number of inflammatory (CD68-positive) cells.

More recently Bobinger et al. (2019) investigated the effect of siponimod administration on perihemorrhagic edema, neurological deficits, and survival in a mouse ICH model induced by intracranial injection of 0.075 U of bacterial collagenase (Bobinger et al. 2019). Siponimod (BAF-312) low dose (0.3 mg/kg) or high dose (3 mg/kg) was given either as a single bolus 30 minutes after the challenge or for 3 consecutive days starting 0.55, 24 and 48 hours after ICH induction. Perihemorrhagic edema formation was evaluated by MRI at 24 and 72 hours. Low dose siponimod reduced brain edema 24 hours after ICH as well as at 72 hours after multiple dosing. In contrast, no improvement was observed at 24 hours after high dose siponimod nor at 72 hours after single low dose or multiple high doses. Brain water content in the ipsilateral hemisphere at 72 hours was reduced after the administration of low, multiple low as well as

multiple high doses of siponimod. Multiple injections of low dose siponimod also improved survival at 10 days after ICH. This study provided the basis for a phase II clinical study of siponimod in ICH (see below).

As for ischemic stroke, not all studies confirm protective effects in ICH. In 2020 Diaz Diaz et al. investigated the efficacy of FTY720 in male and female C57BL/6 mice challenged with intrastriatal bacterial collagenase injection (Diaz Diaz et al. 2020). FTY720 (0.5mg/kg i.p.) administered 0.5, 24 and 72 hours after ICH induction improved survival and recovery in female mice. On the other hand, it did not decrease lesion volume or tissue loss, nor did it improve behavioral outcome despite decreases circulating lymphocyte counts. The authors argued that the variability of immune response between the mouse strains could explain the lack of efficacy of FTY720, as previous studies with FTY720 mostly used CD- 1 mice.

$S1P_2$ signaling in stroke

Most studies on S1PR modulation in ischemic and hemorrhagic stroke originate from studies demonstrating the efficacy of FTY720, which targets all S1PRs but $S1P_2$. Because of its coupling to G12/13 (vs. Gi for $S1P_1$), $S1P_2$ has been shown to play opposite roles to $S1P_1$ both in cultured cells and in several disease models (Cartier et al. 2020). This also appears to be the case for ischemic stroke. Interestingly, the expression of $S1P_2$ was higher in EC and astrocytes within neuroinflammatory disease-susceptible CNS regions of an inbred strain (SJL) of female mice, and in the white matter of female MS patients than in males, suggesting that the role of $S1P_2$ in the brain may be sex dependent. In mouse EAE models, $S1P_2$ function is responsible for the breakdown of adherens junctions, BBB leakage and chemokine-dependent inflammatory responses (Cruz-Orengo et al. 2014). Addressing if a similar mechanism may be engaged in ischemic stroke, Kim et al (2015) demonstrated that S1P2 is induced in vascular ECs after ischemia, and that both genetic and pharmacological inhibition of $S1P_2$ with the use JTE013 (30mg/kg) administered by gavage immediately after reperfusion in a tMCAO model (90 minutes), resulted in decreased MMP-9 activity in the ipsilateral hemisphere, lower gelatinase activity in cerebral micro vessels, reduced oedema formation, a striking reduction in ischemic lesion size and improved neurological scores (Kim et al. 2015). This argues that $S1P_2$ expression is induced during ischemia and that the receptor plays a disruptive role in ischemic and hemorrhagic stroke. It is interesting in this regard that Sphk2 deficiency exacerbates and Sphk1 deficiency has no impact on stroke outcome (Pfeilschifter, Czech-Zechmeister, Sujak, Mirceska, et al. 2011), arguing that S1P plays a net protective role in the context of ischemic stroke. Thus, there appears to be an important endogenous protective function of S1P signaling in the brain that overrides the disruptive roles mediated by $S1P_2$. This has so far not been described in genetic studies.

S1PR modulation in clinical stroke trials

Ischemic stroke

The safety of FTY720 for ischemic and hemorrhagic stroke has been investigated in several small-scale clinical trials that have also provided insight into possible efficacy. These studies, all conducted in China by the group of Fu-Dong Shi, suggested that FTY720 administration is safe and may improve neurological outcome both in the acute phase and at 3 months follow-up. Moreover, FTY720 coadministration with alteplase was found to reduced spontaneous hemorrhagic transformation in ischemic stroke.

A first study by Fu et al (2014) enrolled 22 patients with acute ischemic stroke with anterior cerebral circulation occlusion and not eligible for thrombolysis as onset of stroke had surpassed 4.5 hours (Fu, Zhang, et al. 2014). All patients received conventional stroke management (standard treatment adhered to current American Heart Association guidelines and half (n = 11) also received FTY720 (0.5 mg) orally once daily for 3 consecutive days between 6 and 72 h after the onset ischemic clinical symptoms. Patients in the FTY720 group presented lower circulating lymphocytes counts, as expected, as well as and better neurological recovery. At day 7, patients who received FTY720 showed less lesion enlargement evaluated by MRI. Importantly, no serious drug related adverse events were reported. The incidence of suspected lung infection was the same in the FTY720 treated group as in control patients, and ECG monitoring did not reveal cardiac arrhythmia or atrioventricular blocks. These results indicated safety and potential efficacy of FTY720 administration to ischemic stroke patients even late after disease onset.

In a follow-up study, Zhu et al. reported a multicenter randomized trial with a total of 47 patients, where 25 patients were assigned to alteplase alone and 22 patients treated with alteplase and oral FTY720 started within 4.5 hours of the onset symptoms (0.5mg daily for 3 consecutive days) (Z. Zhu et al. 2015). Patients who received FTY720 exhibited lower circulating lymphocytes, significantly smaller lesion volumes, less hemorrhagic transformation, and attenuated neurological deficits according to the NIHSS scale at day 1 and better neurological recovery at day 90. The group receiving FTY720 and alteplase showed 73 % good prognosis compared to 32% in patients who received alteplase alone. The incidence of suspected lung infection and urinary tract infection was similar in FTY720 combined treatment and patients who received only alteplase, infection signs were mild and resolved with brief antibiotic course, there was no cardiac arrhythmia or atrioventricular blocks detected with ECG monitoring. Interestingly, in patients treated with the combination of FTY720 and alteplase there was also no increase spontaneous bleeding, or the severity of hemorrhagic transformation compared to patients treated with alteplase alone. These observations extend on the Fu et al study to show that FTY720 remains safe and potentially efficacious in ischemic stroke patients when administered on top of alteplase.

In a third study by the same group, Tian et al. investigated the coadministration of FTY720 with alteplase in 46 patients suffering acute ischemic stroke in a delayed time window within 4.5 to 6 hours from symptoms onset after internal carotid artery or MCA proximal occlusion (Tian et al. 2018). Half or the patients received alteplase alone and the other half alteplase with FTY720 0.5 mg administered orally started just after imaging and continued for the next 3 days. Patients who received FTY720 with alteplase presented better clinical improvement at 24 hours and a more favorable neurological score at 90 days relative to those receiving alteplase alone. Imaging also reduced infarct growth at 24 hours and significantly improved recanalization and retrograde reperfusion of the affected territory through the collateral circulation. Six patients (26%) in the alteplase alone group experienced severe cerebral edema and brain herniation compared two patients (9%) treated with FTY720 plus alteplase. There was no significant difference in infection signs or other adverse events between the two groups. This study suggests that FTY720 may improve the efficacy and safety of delayed alteplase treatment by promoting retrograde collateral flow and the efficiency of recanalization and potentially reducing edema formation.

Intracerebral hemorrhage

The safety and efficacy of FTY720 was also been investigated in ICH patients by the group of Fu-Dong Shi in a study including a total of 23 patients (Fu, Hao, et al. 2014). While 12 patients received standard management, 11 patients received FTY720 (0.5mg p.o.) between 1 hour and no later than 72 hours after the onset of symptoms. FTY720 treated patients presented reduced neurological impairment compared to controls. This was associated with lower peripheral blood lymphocyte counts. The benefit on neurological outcome was maintained at 3 months. The FTY720 group also presented lower ICH-related lung infection. These results argue that FTY720 may also be beneficial for the treatment of ICH and further support its safety.

In 2017, Novartis Pharmaceuticals started a Phase 2 trial with 32 participants to investigate the efficacy, safety, and tolerability of siponimod compared to placebo in patients with ICH (ClinicalTrials.gov Identifier: NCT03338998). In addition to standard of care, ICH patients meeting study criteria were randomized at 1:1 ratio either to receive siponimod (10 mg) or placebo on daily administration for 7 days, then patients were followed for 76 days along with neurological status evaluation. Because of the COVID-19 pandemic recruitment for the trial was put on hold. However, after seven months and a negative initial analysis concluding for a lack of potential efficacy the trial was terminated by Novartis in June 2021.

Current status of S1PR modulation for stroke treatment

In summary, work from experimental models rodents as well as in small-scale clinical trials suggest that S1PR modulation could hold promise for both ischemic and hemorrhagic stroke (Dang et al. 2021) (Fu, Zhang, et al. 2014)(Fu, Hao, et al. 2014) (Z. Zhu et al. 2015)(Tian et al. 2018) (Dreikorn et al. 2018). Better understanding of the mechanism of action of $S1P_1$ and its modulators should facilitate the refinement of targeting strategies with the perspective of maximizing therapeutic benefit.

Observations from several experimental studies suggest that $S1P_1$ modulation could be beneficial in reducing infarct size and neurological outcome in ischemic stroke and that it can be efficacious even if applied in a clinically relevant time frame (Dang et al. 2021). This has been demonstrated in both permanent models and in transient filament- and thrombin-induced models of ischemic stroke and in both mice and rats. Most studies of safety argue that $S1P_1$ modulation will not increase the risk of spontaneous bleeding or infection, even if used in conjunction with alteplase. Whether $S1P_1$ modulation also has the capacity to reduce edema formation and preserve blood-brain barrier integrity is less clear, with as many studies demonstrating no protection or aggravation as those showing protection. Experiments in aged mice and mice with comorbidities indicate that $S1P_1$ modulation may lose its capacity to reduce ischemic damage with age and in the context of diabetes. Importantly, however, these studies are so far limited and could be compromised by the use of desensitizing agonists and doses. This argues for the need for more experimental research in accordance with the STAIR recommendations (Fisher et al. 2009), and may suggest that $S1P_1$ modulation, if efficacious in a real-world setting, may need to be based on careful patient selection. Small-scale clinical studies carried out so far are encouraging and argue that $S1P_1$ modulation may indeed be efficacious also in humans including aged individuals with comorbidities. The incidence of infections and other adverse events in patients treated with FTY720 was the same as in control groups, also supporting the safety of $S1P_1$ modulators. Thus, despite some negative studies, there is considerable evidence to suggest that $S1P_1$ modulation could be a promising new adjunct therapy for the treatment of ischemic stroke. $S1P_2$ could also be a promising target, but initial promising experimental work will need to be confirmed and expanded. Although there are fewer studies available, experimental studies also suggest that $S1P_1$ modulation could be useful for hemorrhagic stroke. The recent termination of a clinical trial with Siponimod is disappointing in this regard, but it is possible that lack of benefit was related to the choice of drug, treatment strategy, or patient selection.

Understanding the mechanism of action of $S1P_1$ modulators will be critical for further pursuing this class of drugs for stroke treatment and for optimal trial design. In this regard, experimental data are less conclusive. While there is limited support for direct actions on neurons and astrocytes and some studies suggest direct vasculoprotective actions, most argue or assume the principal mechanism of $S1P_1$ modulation in ischemic stroke to involve

sustained depletion of circulating lymphocytes and reduction of lymphocyte-mediated thrombo-inflammation (Dreikorn et al. 2018). Thrombo-inflammation is the result of the interaction of lymphocytes with ECs and platelets, which induce microvascular dysfunction resulting in loss of patency, reducing tissue perfusion and the supply of oxygen and nutrients, ultimately leading to the death of brain cells and secondary lesion size extension (Kraft et al. 2013). Interestingly, while FTY720 substantially reduces the abundance of most lymphocyte populations in peripheral blood, it increases the abundance of Tregs (Miller et al. 2016) (Sehrawat and Rouse 2008). As the role of lymphocytes in initiating thrombo-inflammation has been attributed to this T cell subset (Kleinschnitz et al. 2007), it is unclear how FTY720 treatment reduces thrombo-inflammation. Moreover, most studies demonstrating efficacy of FTY720 have used a dose range (0.2-1mg/kg) that is well below that required to fully desensitize $S1P_1$ in the brain endothelium (Yanagida et al. 2017). Studies showing no efficacy have often used relatively high doses and pre-treatment, in most cases demonstrated effective depletion of peripheral blood lymphocytes despite lack of efficacy, but rarely addressed endothelial $S1P_1$ desensitization. Finally, no study has shown efficacy of a direct $S1P_1$ antagonist, which should be equally efficacious at impairing lymphocyte functions, and ApoM-Fc is protective without inducing lymphopenia. Together these observations suggest that at least a component of the protection observed with $S1P_1$ modulators may involve vascular targeting, and that lack of efficacy in some studies could involve desensitization of $S1P_1$ on the brain endothelium. In this regard, there is good evidence that FTY720 activates $S1P_1$ *in vivo* in the dose range offering protection in ischemic stroke (Müller et al. 2011)(Oo et al. 2011) and that $S1P_1$ modulation reduces endothelial activation by inflammatory mediators and ischemia by decreasing the activation of NFkB and downstream targets such as ICAM-1. Such actions could also impact the no-reflow phenomenon generated by leukocyte plugging, recruitment of regulatory T cells and thrombo-inflammation, since leukocytes adhesion relies in part on the interaction between ß2-integrins on leukocytes and ICAM-1 on cerebral ECs (Wei et al. 2011). Thus, the reduction of leukocyte and platelet adhesion to the vessel wall, improved microvascular vessel patency and tissue perfusion observed with FTY720, although dependent on lymphocytes does not necessarily imply direct actions of FTY720 on lymphocytes (Kleinschnitz et al. 2013) (Kraft et al. 2013). Several studies have also suggested that FTY720 could act directly on the BBB to improve its stability, thus explaining its protective actions on brain edema and in hemorrhagic stroke. The capacity of $S1P_1$ modulators to improve collateral function and leptomeningeal collateral growth may also suggest direct actions on endothelial $S1P_1$. Thus, although $S1P_1$ modulation may provide protection in ischemic stroke in part by inducing lymphopenia, there is also ample evidence to suggest an EC-dependent mechanism of action. The reliance on a lymphocyte-dependent mechanism of action and the lack of sufficient consideration for endothelial receptor desensitization could indeed explain the poor outcome in some experimental studies and clinical trials.

It is notable from the review of the literature that although there is only one experimental study to suggest a role for $S1P_2$ in ischemic stroke, this was conducted with both

pharmacological and genetic tools (Kim et al. 2015). In contrast, despite considerable evidence for potential therapeutic benefit of targeting $S1P_1$, there have been no genetic studies performed to address the endogenous roles of $S1P_1$ signaling and the cellular targets $S1P_1$ modulators in ischemic stroke. This may be explained in part by the assumption that the mechanism of action of FTY720 in multiple sclerosis can be directly translated to stroke and in part by the need to conditionally target S1pr1 to bypass embryonic lethality.

Context and Objectives of the Thesis Project

It is well established that S1P plays critical roles in vascular and immune homeostasis and that $S1P_1$ plays a key role in mediating S1P signaling on both vascular and immune cells. It is also well established that $S1P_1$ targeting with FTY720 and $S1P_1$ selective modulators can provide protection in ischemic stroke. However, the endogenous roles of $S1P_1$ signaling in ischemic stroke have not been established, and the mechanism by which $S1P_1$ modulation provides protection in ischemic stroke remains a matter of debate. We reasoned that a better understanding of endogenous S1P signaling in the naïve brain vasculature and in response to ischemia would inform on future efforts to target this receptor in ischemic stroke.

The objectives of my PhD project were to use genetic and pharmacological tools in mice to:

1. Address endogenous roles of hematopoietic and endothelial $S1P_1$ in experimental ischemic stroke.
2. Determine how $S1P_1$ is engaged in the brain endothelium by its endogenous ligand.
3. Elucidate the mechanism by which endogenous $S1P_1$ signaling provides protection in ischemic stroke.
4. Identify the cellular target for pharmacological $S1P_1$ modulators in ischemic stroke.

My PhD project was part of a collaborative study conducted in the context of a transatlantic research network on S1P signaling in the neurovascular unit (SphingoNet). In this collaboration my main role was to model ischemic stroke. My specific contributions to the study are listed in the extended methods section that follows, where I also provide additional details about my work to adapt and improve stroke models in our laboratory.

Chapter 5. Extended Methods

In this chapter I will detail my contribution to the publication included in the Annex (Paper 1) (Nitzsche et al. 2021), provide information about the experimental stroke models used during my thesis work additional to what is provided in the Methods section of Paper 1 and discuss my efforts to overcome technical difficulties encountered.

Experimental ischemic stroke modeling in mice

In our study (Paper 1), stroke was modeled in 4 different laboratories by 5 different experimenters. Their affiliations, experimental models and specific contributions to stroke modeling are listed below:

Ammar Benarab
Camerer laboratory, Paris Cardiovascular Research Centre, Paris.
Experimental model 1: Distal pMCAO modeled by MCA electrocoagulation and dissection and exclusion based on hemorrhage and thermal injury.
Experimental model 2: Koizumi (CCA) proximal tMCAO model. No blood flow monitoring for experiments assessing infarct volume and exclusion based on survival, SAH and detectable infarct.
Contributed: Fig 1D, Fig 1F, Fig 2A tMCAO, Fig 2B, Fig 2D, Fig 2C tMCAO, Fig 2 F-G-H-I, Fig 4E, Fig 6 B-C, Fig 7A, Fig 8; A-B-C-D-E-F. Online Fig I B+C+D, online fig II L, online Fig IV A-B-C-D-E-F-G, online Fig VIII A+B.

Marine Poittevin
Kubis laboratory, Hôpital Lariboisière, Paris.
Camerer laboratory: Paris Cardiovascular Research Centre, Paris.
Experimental model: Distal pMCAO modeled by MCA electrocoagulation and dissection and exclusion based on hemorrhage.
Contributed: Fig 1A, Fig 1B, Fig 1C, Fig 3 D, Fig 4 A-B-C-D, Fig 6A. Online Fig II A+B+C

Hiroki Uchida
Sanchez laboratory, Weill Cornell Medical College, New York.
Experimental model: Longa (ECA filament entry) proximal tMCAO method with laser Speckle blood flow monitoring and exclusion based on occlusion/reperfusion criteria as well as death and hemorrhage.
Contributed: Figure 1E

Lidia Garcia-Bonilla and Giuseppe Faraco
Iadecola laboratory, Weill Cornell Medical College, New York.

Experimental model: Longa (ECA filament entry) proximal tMCAO model with transcranial Doppler probe blood flow monitoring and exclusion based on occlusion/reperfusion criteria as well as death and hemorrhage.
Contributed: Figure 5 I

Although experimental protocols and exclusion criteria were to some extent adapted between the laboratories, absolute values should not be compared across experiments.

In this collaboration, my main role was to adapt and improve stroke models in our lab and to model experimental ischemic stroke in mice by either transient or permanent occlusion of the MCA. I also administered pharmacological agents and carried out post-surgery care. In later stages of the project, I monitored cerebral blood flow with a laser doppler system to ensure appropriate MCA occlusion and adequate reperfusion after a predefined time of MCA occlusion. I also carried out neurological evaluation, brain harvesting, sectioning, coloration and stroke volume calculations. I worked with a postdoctoral fellow, a master student and our imaging platform to perform surgery on mice for which stroke lesions were imaged by different methods at different time points after occlusion. I calculated stroke volume and edema formation based on different MRI sequences.

In our laboratory we used two ischemic stroke models in mice in this study, one filament-based tMCAO model and one electrocoagulation-induced pMCAO model. I will discuss these models in detail below, including technical challenges encountered and the evolution of the models with time. Most importantly, I started modeling tMCAO with a model based on CCA filament introduction (Koizumi) without blood flow monitoring (Koizumi et al. 1986). To reduce variability between experiments, I continued to use this method for figures in the paper showing 2,3,5-Triphenyltetrazolium Chloride (TTC) based quantification of infarct volumes. However, due to limitations of the model, I experimented with different methods of blood flow monitoring and MCA occlusion that I will discuss below and that were used in subsequent pilot studies on $S1P_1$ modulation in comorbid mice.

Filament-induced distal tMCAO

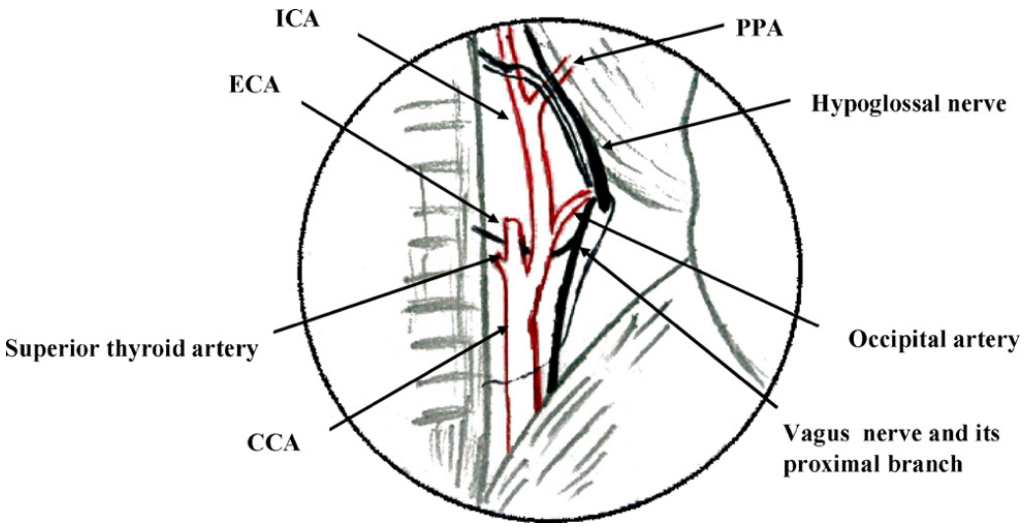

Figure 20. Schematic diagram of murine cervical neurovascular anatomy viewed through operating microscope. Immediately before entering digastric muscle, occipital artery is encircled by 4 nerve tracts including main branches of vagus and hypoglossal nerves. Branch of vagus nerve courses medially and ventrally near CCA bifurcation. Long, thin branch of hypoglossal nerve enters pre-tracheal muscles and runs laterally along vagus nerve under the omohyoid muscle. Reproduced with permission from (Chen et al., 2008).

Koisumi model description: Analgesia was applied to mice 30 minutes before starting the procedure through intraperitoneal (i.p.) injection of buprenorphine (0.1 mg/kg). A maintenance injection was given at 24 hours and 48 hours for longer term studies. Mice were anesthetized with 2% isoflurane (Minerve France). Following induction of anesthesia, isoflurane was reduced to 1.5%. In some experiments, a laser Doppler probe connected to a laser Doppler flowmeter (Moor instruments, Devon, UK) was used to monitor blood flow in the MCA territory. For this, an incision was made in the skin overlying the calvarium, the skin pulled laterally, and skull exposed, and the Doppler probe firmly glued to the skull to continuously monitor blood flow throughout the procedure. Then, the mouse was placed in supine position on a heating pad, the fur around the neck shaved and povidone iodine applied (Ansari et al. 2011). A 1.5 cm long midline incision was made in the neck and the common and external carotid arteries exposed by dissection (Figure 21). A silicon coated suture (Doccol Corporation) was inserted into the CCA of anesthetized mice and advanced until it obstructed the MCA. Once resistance was observed or a blood flow reduction of more than 80% observed, the suture was ligated and secured in place for between 40 and 90 minutes. In some cases, a laser Speckle contrast imager (Moor FLPI2, Moor instruments, Devon, UK) was used for two-dimensional evaluation of CBF (Ayata et al. 2004). This did not require surgical intervention. At the pre-determined time, the suture was gently withdrawn to allow reperfusion, the CCA ligated, the flow probe (when used) removed, and the skin incision closed. Core body temperature was maintained at 36-37°C, controlled by a thermostatic plate throughout the procedure. In the absence of blood flow monitoring, mice were allowed to wake up during the occlusion time while maintained under a heating lamp. Experiments

animals that showed uncontrolled surgery-induced bleeding, died prior to the pre-determined endpoint of 24 hours, for which brain damage was induced during tissue processing, or that displayed evidence of subarachnoid hemorrhage or no visible infarct were excluded from analysis of infarct volumes.

Post-operative care: After reperfusion, mice received 0.5 ml of warm saline subcutaneously for volume resuscitation. During the surgical procedures and 2 hours after reperfusion, animals were monitored, and body temperature was maintained first under a heat source and then in a humidified and heated small animal intensive care unit (R-Com Small Animal Pet Brooder) maintained between 36.5 – 37.5 °C. In experiments where mice were kept for more than 24 hours, mice were provided with humidified food pellets in a petri dish on cage floor and liquid food by oral gavage (0.5 ml 3 times daily). Each day food was freshly prepared (Lourbopoulos et al. 2017)**.**

Neurological evaluation in transient model: Neurologic examinations were carried using a modified Bederson scoring system as described by Kim et al (Kim et al. 2015), with slight modifications: 0: no deficit, 0.5: when held by tail, good extension of affected forelimb but weakness when grabbing the wires of the cage, 1: walking straight or ability to turn in both directions but when held by tail, unable to extend affected forelimb and torso turning to the ipsilateral side, 1.5: preference to walk in one direction, 2: unable to walk straight or to turn in both directions, circling to affected side when held by tail on the bench, 2.5: circling on the spot and walking circling, 3: spontaneous circling to the affected side (without going anywhere), 3.5: no movement, upon stimulation circling on the spot, 4: no spontaneous locomotor activity or barrel rolling.

Quantification of infarct volumes: After 24h, 72h or 7 days mice were sacrificed by cervical dislocation and the brain removed and observed for gross hemorrhage. Animals that exhibited subarachnoid hemorrhage or focal hemorrhage at the Circle of Willis were excluded. Brains were then cut into seven 1-mm-thick coronal sections using McIlwain tissue chopper (Campden Tissue Instruments). The brain slices were incubated for 15 minutes in a 2% solution of TTC and photographed with a camera connected to a LEICA stereomicroscope. Infarct volumes were then quantified by analysis of TTC brain slice images using Image J software (Bethesda, MD), by adding the infarcted areas in all sections and multiplying by the slice thickness (1 mm). To correct for edema, the volume of infarction was adjusted by the following calculation: Corrected Infarct Volume CIV % = contralateral hemisphere volume (ipsilateral volume-infarct volume)/contralateral volume hemisphere volume x 100 (Osborne et al. 1987). The infarct ratio (*I),* corrected for edema, was calculated by using the following equation: $I = (X - S)/Z$, where X is the area of infarct (mm2), S is brain swelling (mm2), S = Y - Z, Y is the area of the infarcted (ipsilateral) hemisphere slice (mm2) and Z is the area of the

non-infarcted (contralateral) hemisphere slices (mm2). The edema ratio was calculated with the following formula: E=(Y - Z)/Z (Kim et al. 2015).

Technical challenges encountered: Initial challenges with this model involved bleeding associated with the exposure and opening of the CCA and introduction of the nylon filament and occasional early lethality related to dissection of the vagus nerve. Later challenges involved the navigation of the filament to the base of the MCA to obtain infarcts and stabilization of the filament with sufficient tension to induce infarcts but not excessive pressure, which would result in arterial puncture and SAH. Despite successful surgery, mortality within the first 24 hours was also an important issue. This was associated with large infarcts or SAH and could be ameliorated to some degree by improvement of postoperative care, including temperature control and fluid resuscitation. Survival beyond 24 hours was a greater challenge and could be ameliorated but not eliminated by administration of liquid diet by oral gavage. Isolation and chopping of brains were also challenging, as infarcted regions of the brain parenchyma easily deteriorated either while the brain was sliced or during TTC staining. The slice quality improved with practice. Imaging TTC sections with good contrast and without reflection was another initial challenge that was overcome by scanning brain slices on a high-resolution photo scanner. Volume calculations were also challenging, with edema corrections introducing artifacts if brain slices were not fully perpendicular to the midline. The main challenge with this model was the variation in infarct size. This is discussed in further detail below.

Advantages and disadvantages of the model: Relative to the distal model, the use of a guided filament in this proximal model produces less injury and inflammation around the site of occlusion and the infarct core and avoids disruption of BBB integrity and intracranial pressure that can be induced by craniotomy. The filament also allows for easy reperfusion. Relative to the ECA entry-based Longa model discussed below, the CCA entry-based Koizumi model is easier to perform and considerably faster. However, it has several important limitations, even with blood flow monitoring. Because of the permanent occlusion of the CCA, blood flow is substantially reduced also in the ipsilateral ACA and PCA, making it less suitable for studying collateral function. If used as a permanent model, it is not useful for studying mechanisms that increase infarct size, as the infarcts already cover most of the MCA territory. Removal of the filament is frequently associated modest to poor reperfusion (discussed below). Combined with the proximal site of occlusion, this leads to large infarcts that can affect essential brain functions, such as the control of body temperature. Tissue damage associated with the surgical intervention and permanent impairment of ECA flow can damage the vagus nerve, induce tracheal edema, and paralyze muscles important for mastication and swallowing, rendering food intake and breathing difficult and mortality high.

Evolution of transient MCAO modeling

The Koizumi model: For the first tMCAO experiments performed in our laboratory we adapted a filament-based transient model of ischemic stroke from the Experimental Stroke Research Platform at the University of Caen. The method, described above, is also referred to as Koizumi model (Figure 20) (Koizumi et al. 1986). The model yielded variable results, with a substantial number of animals displaying no obvious ischemic lesions after TTC staining despite otherwise successful procedure. I next followed suggestions from the Doccol corporation to adjust the filament diameter to animal weight and experimented with the length of the filament coating. Although it did not eliminate the variability, adjusting filament diameter for animal weight and using longer coating surfaces (2-3 mm) yielded more consistent infarcts. As initial experiments in paper 1 were performed using this protocol before I had access to blood flow monitoring, we decided to continue to use this protocol for consistency. In parallel, I tried to ameliorate results by including blood flow monitoring and by experimenting with other surgical procedures.

Blood flow monitoring: Monitoring blood flow reduction after the placement of the suture was the most evident way to reduce variability in our studies. Laser Doppler Flowmetry (LDF) allows real-time monitoring of blood flow and significantly increases the accuracy of suture positioning and thus ensures obtaining consistent results. This is a noted advantage over the less precise techniques of feeling for resistance of the suture to be inserted, which is susceptible to the interference of anatomical variations (S. Lee et al. 2014) (Q. Cai et al. 2016). It also allows the exclusion of animals in which stable MCA occlusion and reperfusion is not obtained. Notably, while insufficient occlusion can reduce the infarct size, lack of reperfusion can increase the infarct size. When LDF is performed, animals are typically included only if the CBF decreases by 75-90% during occlusion and recovers up to 70% of baseline within 10 minutes after the start of reperfusion (Q. Cai et al. 2016). We tested both LDF and Laser Speckle flowmetry (LSF) devices from Moor Instruments.
LSF was tested first as it offered several important advantages to LDF: speed, as it did not require attachment of a flow probe to the scull of the animal, blood flow monitoring in two dimensions allowing for comparison between regions of MCA territory and between affected MCA territories, adjacent ACA territories as well as contralateral MCA territories, as well as the possibility of allowing the animals to move freely without anesthesia between occlusion and reperfusion. Despite these important advantages we acquired an LDF device, as LSF did not allow us to accurately compare blood flow post reperfusion to pre-and post-occlusion. After initial technical difficulties in gluing the flow probe stably to the scull, I was able to obtain consistent stable LDF recordings and monitor blood flow during and after surgery. With the Koizumi model this allowed me to observe a clear reduction in blood flow, a first drop seen after occlusion of the CCA and a second after the occlusion of the MCA (Figure 22). Although there was some variability in the degree and maintenance of occlusion, this had two important advantages: it allowed me to be more precise in placing the suture, thereby

increasing the success of occlusion, and reducing the incidence of SAH, and it allowed me to exclude mice with a blood flow reduction of less than 80%, eliminating the problem of observing animals with no infarcts. On the other hand, reperfusion was consistently poor, ranging from 0 to 50% of pre-occlusion values (Figure 22).

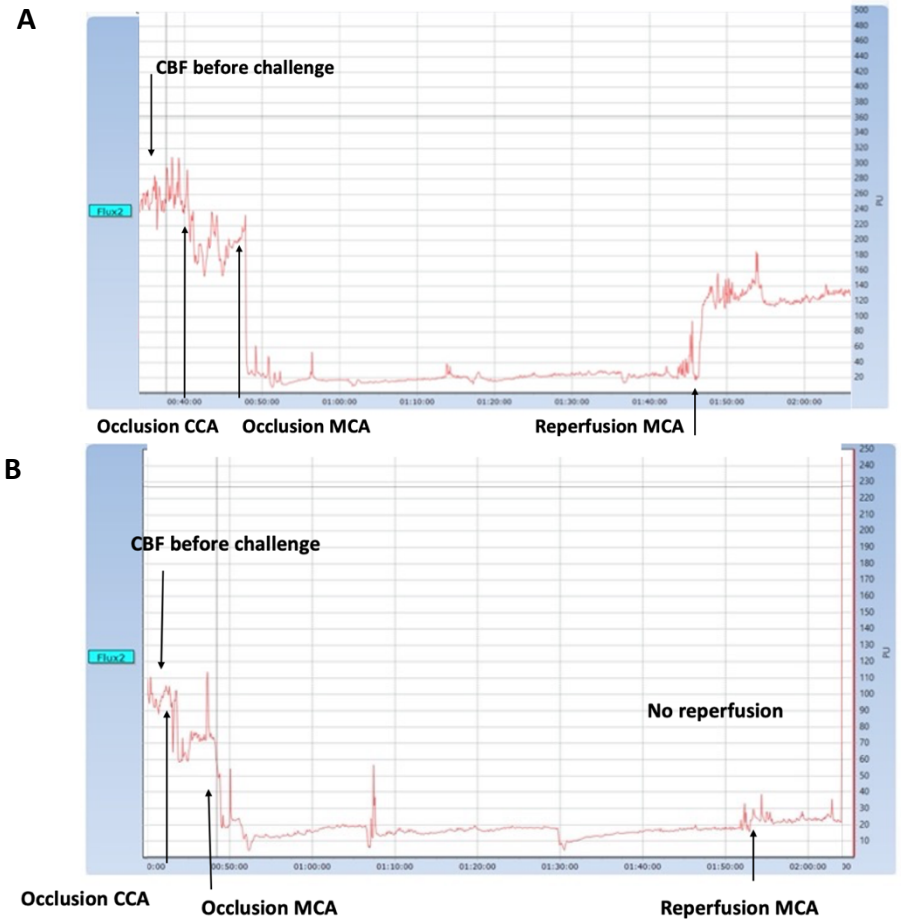

Figure 21. Cerebral blood flow monitoring in tMCAO: the Koizumi method. Tracings show representative LDF recordings from 60 minutes tMCAO with the Koizumi method in C57BL/6J mice. Arrows indicate the occlusion of the common cerebral artery (CCA) and the middle cerebral artery (MCA) and reperfusion of the MCA. Note that although MCA occlusion was effective and mostly relatively stable, reperfusion was consistently poor with this model, ranging from 0 to 50% of pre-occlusion values. **A** shows a mouse with a reperfusion rate of around 50% and **B** a mouse with a reperfusion rate of less than 10%.

This did not allow me to set reasonable reperfusion criteria, which are typically >70% of pre-occlusion values, and suggested I was modeling something closer to pMCAO than tMCAO. Moreover, probably because of the poor reperfusion and the long procedure times, I observed a substantial increase in mortality relative to the experiments performed without blood flow monitoring. These observations led us to reconsider the experimental model.

The Longa model: The intraluminal tMCAO model, first introduced by Koizumi, was later modified by Longa (Güzel et al. 2014). Unlike the Koizumi model, where the monofilament is passed through an incision in the CCA, the monofilament is passed through an incision in the

ECA before entry into the CCA in the Longa model (Figure 20). Although it has been reported that these methods provide similar results (Morris et al. 2016), the Longa model has the advantage that the CCA is left open after and in some cases during MCAO. By 2015, these methods and modifications thereof had been cited > 205 and > 8472 times, respectively, suggesting that use of the Longa method is far more prevalent (Smith et al. 2015)(Güzel et al. 2014). I therefore adapted the Longa method with the aim to improve collateral function and reperfusion, reduce infarct size, and improve recovery. In initially experiments I kept the CCA clamped during the MCA occlusion period. This resulted in better reperfusion than the Koizumi method, but it was still not as complete as frequently reported in the literature. A strong further increase in reperfusion with re-opening of the CCA after MCA reperfusion illustrated the benefit of not permanently occluding the CCA and the limited functionality of the circle of Willis in the C57BL/6 mouse strain (figure 23).

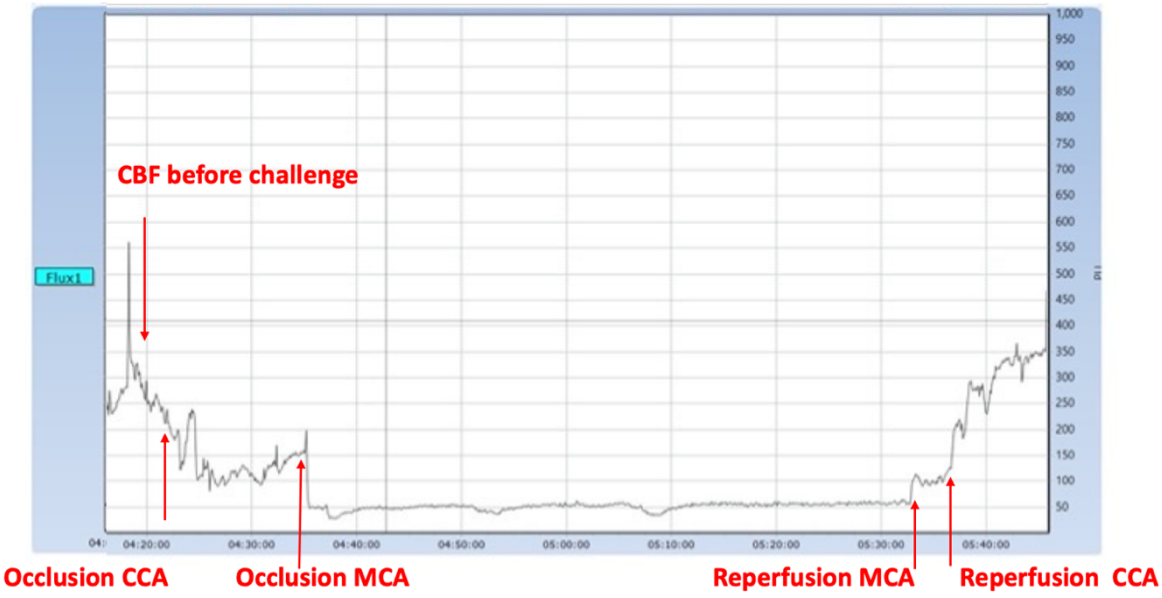

Figure 22. Cerebral blood flow monitoring in tMCAO: the Longa model. Tracing shows representative LDF recording from 60 minutes tMCAO with the Longa method in C57BL/6J mice. Arrows indicate the occlusion of the common cerebral artery (CCA) and the middle cerebral artery (MCA) and reperfusion of the MCA. Note that compared to the Koizumi method, a considerable further increase in reperfusion is observed when re-opening of the CCA following MCA reperfusion.

Observing this effect, we decided to keep the CCA open also during MCA occlusion. With this modification we observed a striking overall improvement relative to the Koizumi method, with robust reperfusion in most animals, often reaching pre-occlusion values. Animal recovery was also substantially improved despite even longer duration of the procedure and therefore anesthesia. However, despite these improvements, infarct size was surprisingly variable even in inbred C57BL/6 mice with similar occlusion and reperfusion efficiency. Operating time was also considerable, with exposure to anesthesia close to 2 hours for 60 minutes of tMCAO, and more animals were lost during surgery due to the complexity of the procedure.

Besides the surgical procedure, other factors known to contribute to infarct outcome variation, such as strain-related differences, filament type and size, body temperature, and anesthesia are discussed below.

Anesthesia: Exposure to isoflurane has a protective effect on lesion size (Yung et al. 2012). This could be a confounding factor in our studies, as S1P has been implicated in the protective effects of isoflurane (Altay et al. 2012)(Hillman et al. 2019). It is therefore possible that isoflurane exposure, especially the extended exposure necessary for LDF measurements, would mask beneficial effects of S1P signaling. This could also be a factor explaining the variability in effects of S1P modulators in preclinical studies. It is notable that most of the studies demonstrating protection with $S1P_1$ modulators do not use blood flow monitoring and extended anesthesia.

Body temperature: Body temperature is one of the essential factors affecting the extent of infarctions (S. Lee et al. 2014) (Xie, Kang, and Nedergaard 2016). Hypothermia decreases and hyperthermia increases the infarct size. To decrease variability, the mouse body temperature was maintained steady during the surgery and hypothermia was avoided after surgery.

Choice of filament: The literature on the filament model suggests that outcome is mainly influenced by the efficiency of occlusion. Insufficient occlusion, premature reperfusion, and/or filament dislodgment will either reduce or eliminate brain injury. Many types of filaments are applied in the MCAO model, including rubber-coated, flame-blunted, poly-L-Lysine coated, methyl methacarylate glue-coated, silicon resin-coated, and nail polish-coated monofilaments (Macleod et al. 2009)(S. Liu et al. 2009). Silicone-coated monofilaments are more expensive but appear to produce more consistent ischemic brain injuries and less occurrence of subarachnoid hemorrhage (SAH) (Guan et al. 2012). The adaptation of the diameter of silicone rubber-coated monofilament to animal size increases consistency. In my experience, it was nevertheless best to use animals between 25 and 30 grams, as SAH was more frequent in smaller animals and infarcts sizes more variable in larger animals despite adaptation of filament size. With regard to filament length, I first increased length from 1-2 mm to 9-10 mm to increase consistency. But when observing that this increase also resulted in larger infarcts and greater mortality, probably due to occlusion of other arterial branches, I returned to shorter filament coating (2-3 mm) in later experiments.

Surgical considerations: The pterygopalatine artery (PPA) supplies the ophthalmic artery and is therefore a very important artery branch of ICA. The dissection and the ligation of PPA to guarantee the insertion of the monofilament directly into the MCA is debated. It has been suggested that anatomizing the PPA is not an essential step of the MCAO model, and that elimination of this step can save time and improve survival (Güzel et al. 2014) (Ansari et al. 2011) (S. Lee et al. 2014). It is also important to avoid damage to the trachea, vagus nerve and nerve branches when exposing and ligating the CCA and ECA. Operation time is another factor

influencing the survival and success rate. After practice, the MCA occlusion procedure took 20 minutes for the Koizumi method and 30-40 minutes for the Longa method. For LDF measurements, an additional 35-40 minutes was needed for exposure of the skull and probe attachment, 10 minutes for pre-recording, and 20 minutes post-recording. When adding the occlusion time, which varied from 45-90 minutes, it would take a total of 135-200 minutes to perform the Longa method with LDF relative to 20 minutes for the Koizumi method without LDF. Besides the impact on the number of animals that could be done in a day, this substantially increased the risk of confounding effects of anesthesia-induced ischemic protection and had greater impact on overall animal health and recovery independent of infarct volume.

The use of LDF and adaptation of the Longa method improved the success rate of tMCAO but implied a considerable extension of surgery time and prolonged exposure of the animal to anesthesia, which is known to protect the brain parenchyma from the impact of ischemia. Despite practice and optimization of surgical procedures, variance in infarct size remained a challenge. It is unclear if this variance was due to variation of brain vascular anatomy even in inbred C57BL/s mice, the degree and stability of occlusion or other parameters. While this model may be inherently associated with large variance, a reduction in the duration of the procedure may be one way to improve consistency and reduce the number of animals required. As reperfusion was in most cases efficient with the Longa method, a practical compromise could be to perform LSF only for a few minutes beyond the MCA occlusion and not monitor reperfusion.

Electrocoagulation-induced distal pMCAO

Model description: Mice were anesthetized by isoflurane inhalation (initially 2%, followed by 1.5 to 1.8%). Body temperature was maintained with a heating plate. Under low-power magnification, the left temporal-parietal region of the head was shaved, and an incision was made between the orbit and the ear. A second incision was made on the temporal muscle, and the lateral aspect of the skull was exposed after reflecting the muscle forward permitting visualization of the MCA through the semi-translucent skull. A small hole (1-2 mm) was drilled into the outer surface of the skull just over the MCA (Technobox 810, Bien Air Dental SA, Bienne, Switzerland). The dura mater was removed with fine forceps and the left MCA occluded by electrocoagulation with bipolar forceps (Figure 24). After surgery, the wound was sutured, and the mice placed under a heating lamp until recovery from anesthesia and then in a humidified and heated recovery chamber during the first night. In one experiment in which animals were followed for 7 days, the ipsilateral common carotid artery was exposed and ligated under isoflurane (2%) anesthesia immediately prior to pMCAO in order to reduce collateral perfusion and thus increase the impact of MCA occlusion. Exclusion criteria included surgery-related injury (focal bleeding, drilling-induced brain damage, and thermal injury), tissue loss, and death.

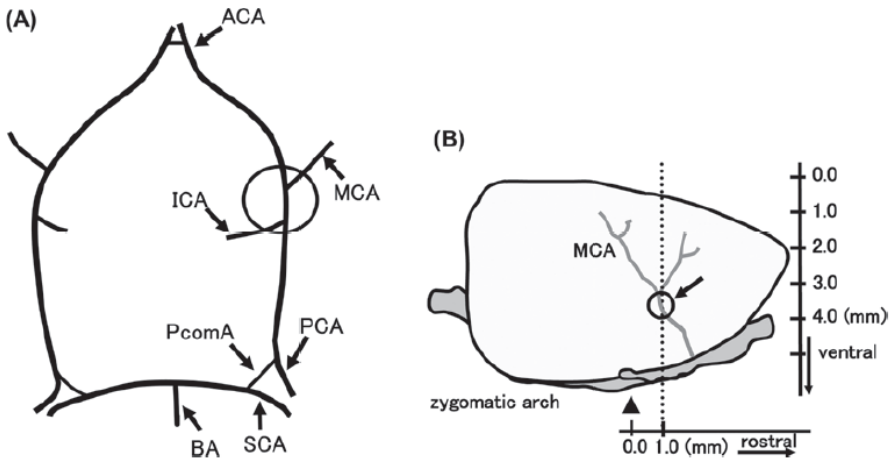

Figure 23. Schematic illustrations of the cerebral artery. (A) The portion of the ICA to the origin of the MCA (surrounded by a circle) is the target of occlusion in intraluminal thread models. (B) For the direct MCA occlusion method, a 1- to 2-mm burr hole is drilled in the frontal bone; the MCA exposed and coagulated. The burr hole is represented by a circle (and arrow), located 1 mm rostral to the fusion (an arrowhead) of the zygoma and squamosal bone on the zygoma arch, and about 3.5 mm ventral to the dorsal surface of brain. Abbreviations: anterior cerebral artery (ACA), middle cerebral artery (MCA), posterior cerebral artery (PCA), internal carotid artery (ICA), posterior communicating artery (PcomA), superior cerebellar artery (SCA), and basilar artery (BA) Reproduced with permission from (Kuraoka et al. 2009).

Technical challenges encountered: I encountered challenges at different stages of this procedure that were partially overcome with practice. The craniectomy performed by drilling can easily cause injury of the underlying cortex or rupture of underlying blood vessels. Intracranial pressure and BBB function can also be disturbed by the procedure. The next major difficulty I faced was burn injury in and sometimes even beyond the MCA territory. Such injury would also appear in sham operated mice in which the MCA was not occluded and was overcome with practice. The next difficulty was in the electrocoagulation and dissection of the MCA. Electrocoagulation required the addition of a drop of saline, and with excess saline I would also observe burn injuries. In some cases, several attempts were required to occlude the vessel, and some cases dissection revealed that occlusion had not been complete. Dissection could also be challenging when the MCA was more profound. These difficulties contributed to variability in infarct volumes in the pMCAO model but were all ameliorated with practice. The time of anesthesia and surgery was also substantially reduced with practice. Another contributor to variability that was not experimenter-dependent was the anatomy of the MCA branches. Even with consistency in the access location where the cranial opening was made, the location of bifurcations of MCA branches varied even in inbred mice. I also observed greater variability in infarct size in mice with mixed C57/129 genetic background. This could potentially be explained by anatomic differences in the MCA, the pial collaterals or the circle of Willis.

Advantages and disadvantages of the model: This model is complementary to the proximal tMCAO model and has several advantages, including the relative ease of the surgical procedure, limited exposure to anesthesia due to the rapidity of the procedure (8-15 minutes from start to finish for an experienced experimenter), rapid recovery of animals, 100 % penetrance of infarcts assured by MCA dissection, and low level of exclusion. The efficiency and relative reproducibility of the model is in part due to the fact that the exposed brain surface allows visual confirmation of successful MCAO. The very low mortality rate is probably because the infarct is restricted to the cortical area of the mouse brain and usually covers only a small proportion of the MCA territory as blood flow is unperturbed in the CCA and the circle of Willis, allowing for efficient collateral function in mouse strains that have good collateral development such as C57BL/6J and C57BL/6J:129SVJ used in our study. This model is therefore very well suited to study collateral function and has been used by the Faber group to demonstrate the importance of the collateral circulation for preservation of the ischemic penumbra in mice (Hua Zhang et al. 2010). In contrast, the proximal tMCAO model frequently affects the whole cortical aspect of the MCA territory, suggesting poor collateral function. The model can also be adapted to tMCAO by clamping or otherwise transiently occluding the MCA. However, this pMCAO model also has disadvantages. The small infarcts are beneficial for survival but also result in limited neurological impairment, that is not detectable with most neurological tests used in experimental stroke studies. Moreover, even if the small infarct volumes were well adapted to study exacerbation of infarct sizes in our knockout models, they were not as well adapted to study pharmacological protection. Other disadvantages we encountered in later experiments was that the anatomical location is not very well suited for imaging by intravital microscopy, and that the craniotomy alone was sufficient to substantially reduce blood flow in the MCA territory that could be visualized by laser Speckle. This in turn rendered laser Speckle unsuitable for blood flow monitoring in this model. Finally, local trauma and potential loss of intracranial pressure induced by cranial opening, electrocoagulation and MCA dissection as discussed above is likely to increase local inflammation in this model and induce some level of injury that is unrelated to MCA occlusion.

Chapter 6. Discussion

$S1P_1$ has been shown to be a potential therapeutic target in experimental ischemic and hemorrhagic stroke models as well as in small-scale clinical trials of ischemic and hemorrhagic stroke (Dreikorn et al. 2018)(Dang et al. 2021). The aim of our study was to provide insight into endogenous engagement and mechanism of action of $S1P_1$ signaling in ischemic stroke and to identify the cellular targets of $S1P_1$ modulators. Most studies using $S1P_1$ modulators in this context have aimed to downregulate $S1P_1$ receptors on lymphocytes and thus inhibit lymphocyte egress from secondary lymphoid organs, as lymphocytes have been considered to play a key role in the extension of thrombo-inflammation in the acute phase of ischemic stroke (Kraft et al. 2013). While selective deficiency of $S1P_1$ on lymphocytes induced strong lymphopenia and modest protection in a tMCAO model in our study, it had no impact in a pMCAO model. Moreover, selective deficiency of $S1P_1$ on EC had far greater impact, strongly exacerbating injury in both transient and permanent MCAO models. The enlargement of ischemic lesion size in $S1P_1$ ECKO mice could be explained by a rapid loss of BBB function and failure of cerebral collateral artery engagement due to impaired vasodilation and increased fibrin deposition in the poorly perfused microvasculature of the ischemic penumbra. An important role of $S1P_1$ in the regulation of endothelial functions in the brain was also observed under homeostasis. Consistent with these observations, $S1P_1$ modulation was no longer effective in mice lacking EC $S1P_1$. This highlighted the critical role played by ECs in the recovery for ischemic stroke and the importance of S1P signaling in regulating these functions.

Investigating the mechanisms of $S1P_1$ engagement, we were surprised to find that brain ECs require cell-autonomous ligand provision in the context of ischemic stroke, unlike in the lung, where circulating sources of S1P are critical for EC $S1P_1$ activation (Gazit et al. 2016). This appeared to be explained by polarization of $S1P_1$ away from the vascular lumen in most brain endothelial cells. Taken together, these observations suggested that the optimal strategy to maximize the benefit of engaging S1P signaling in the context of ischemic stroke would involve dual targeting of lymphocytes and ECs with BBB-penetrating $S1P_1$ agonists.

Our results suggest that loss of endothelial functions accelerates the extension of the infarct core in the ischemic cortex and that $S1P_1$ plays an important role in supporting these functions. We observed that $S1P_1$ plays a critical role in supporting vasodilatation of cerebral arteries in response to flow, in promoting BBB integrity and in maintaining the anti-inflammatory functions of the endothelium in the naïve brain. $S1pr1^{ECKO}$ mice failed to respond fully to acetylcholine - and hypercapnia-induced augmentation of regional blood flow, $S1pr1^{ECKO}$ cerebral arteries displayed impaired flow-mediated dilatation *ex vivo*, and an $S1P_1$ agonist increased CBF in wild-type but not in $S1pr1^{ECKO}$ mice. $S1pr1^{ECKO}$ mice also displayed impaired blood flow recovery and microvascular perfusion in the acute phase after pMCAO, arguing that $S1P_1$ actively regulates endothelial function during cerebral ischemia. On the other hand, normal responses to whisker stimulation argued against a critical role for

$S1P_1$ in neurovascular coupling. $S1P_1$ is known to regulate developmental angiogenesis by promoting the perfusion of newly formed vessels and contribute to flow-mediated dilatation of mesenteric arteries by supporting eNOS activity (Jung et al. 2012) (Cantalupo et al. 2017). Although this was not directly addressed in our study, it may suggest that $S1P_1$ acts at least in part through eNOS also in the mature brain vasculature. Together, these results suggest that endogenous $S1P_1$ signaling counteracts infarct enlargement through facilitating retrograde perfusion of the affected MCA territory via engagement of the cerebral collateral circulation.

We also confirmed a recently described defect in BBB integrity in naïve $S1pr1^{ECKO}$ mice (Yanagida et al. 2017). Although the defect was subtle compared to the defect in lung vascular integrity described in this model (Gazit et al. 2016), it suggested that $S1P_1$ may also play a role in maintaining BBB function in the ischemic brain. $S1pr1^{ECKO}$ mice indeed showed twice as much Evans Blue/albumin accumulation 24 hours after pMCAO as their littermate controls. MRI analysis also demonstrated dramatic edema within a few hours after 90 minutes tMCAO, which may explain high early mortality of $S1pr1^{ECKO}$ mice in this model. These results suggest a potential role for $S1P_1$ in regulating vesicular transport, as edema formation in acute phase of ischemic stroke primarily involves transcellular transport (Knowland et al. 2014). This would be consistent with a recent study demonstrating that ApoM-S1P regulates vesicular transport in pial arteries and penetrating arterioles through $S1P_1$ signaling (Mathiesen Janiurek et al. 2019). A second important endogenous role of $S1P_1$ in the brain endothelium may therefore be to support BBB integrity.

Another established role of $S1P_1$ signaling in the endothelium is to suppress endothelial activation. A functionally relevant readout for endothelial activation in this regard is the leukocyte adhesion molecule ICAM-1. $S1pr1^{ECKO}$ mice have been reported to show more ICAM-1 expression in the aorta (Galvani et al. 2015), and FTY720 has been described to suppress ICAM-1 expression in the brain endothelium after ischemic stroke (Wei et al. 2011). We also observed a significant increase in ICAM-1 expression in the naïve brain of $S1pr1^{ECKO}$ mice, supporting a potential contribution of $S1P_1$ in limiting endothelial activation and leukocyte adhesion. Surprisingly however, ICAM-1 expression did not further increase in $S1pr1^{ECKO}$ after ischemic challenge although it did increase in control mice. We also did not observe a notable difference in the early recruitment of neutrophils to the ischemic penumbra, nor an increase in hemorrhagic transformation, which involves leukocyte-mediated BBB destruction at later stages. Moreover, EC $S1P_1$ deficiency did not affect circulating markers of platelet activation or platelet recruitment after ischemic challenge. While these observations appear to argue against an important role for $S1P_1$ in suppressing EC activation, we observed a significant increase in microvascular fibrin deposition 3 hours after pMCAO in $S1pr1^{ECKO}$ mice. It remains unclear if $S1P_1$ plays a direct anticoagulant or profibrinolytic role in the endothelium or if increased fibrin deposition was a consequence of decreased microvascular perfusion. Regardless of mechanism, this indicates a critical role for

EC $S1P_1$ in maintenance of microvascular patency in the ischemic penumbra and argues that microvascular coagulation may contribute to collateral failure in $S1pr1^{ECKO}$ mice.

In summary, our results demonstrate an important role for endogenous endothelial $S1P_1$ signaling in counteracting ischemic lesion extension through three main functions including regulation of collateral CBF, BBB integrity and microvascular patency. Our result also suggests that $S1P_1$ in most ECs in the cerebral cortex is engaged through EC-autonomous S1P production during cerebral ischemia, possibly via the induction of *Sphk1* transcription in ECs in the acute phase. We also found evidence that $S1P_1$ is polarized on brain capillary ECs and therefore not exposed to circulating ligand. These observations have important implications for $S1P_1$ modulation for stroke therapy. As discussed above, many experimental and clinical studies exploring therapeutic $S1P_1$ modulation for stroke focus on inhibiting the function of lymphocyte $S1P_1$. Although our results support the hypothesis that this strategy may have some benefit in reducing thrombo-inflammation after reperfusion (Kleinschnitz et al. 2013), they mainly highlight the potential of activating and the risk of desensitizing EC $S1P_1$. It is worth noting that we observe a critical role for EC $S1P_1$ also in pMCAO models, where thrombo-inflammation is thought to be of less importance. Most $S1P_1$ modulators developed for clinical use and explored in stroke are designed to desensitize lymphocyte $S1P_1$, induce strong and sustained lymphopenia, and thereby optimize immune suppression. Our data indicate that to reach and activate endothelial $S1P_1$, an optimal drug also needs to cross the BBB.

In our study we investigated the therapeutic potential of the $S1P_1$-selective agonist CYM-5442 (Gonzalez-Cabrera et al. 2008). Although CYM-5442 is known to desensitize $S1P_1$ at high concentrations, it rapidly distributes to the brain while inducing only transient lymphopenia. We confirmed that CYM-5442 can cross the BBB to activate and $S1P_1$ reporter in capillary and venous ECs in the cerebral cortex. This was in contrast to RP-001, another potent and selective $S1P_1$ agonist, which only activated $S1P_1$ on brain capillaries when injected directly into the brain parenchyma. Both agonists induced equivalent transient lymphopenia, but only CYM-5442 provided protection in our pMCAO model. This protection was lost in $S1pr1^{ECKO}$ mice, demonstrating the need to target this receptor. These findings illustrated both the importance of EC $S1P_1$ for the therapeutic effects of $S1P_1$ modulators and the need for BBB penetration to reach $S1P_1$. Surprisingly, FTY720, which is known to cross the BBB at high concentrations, was also inefficient at activating the $S1P_1$ signaling reporter in brain capillaries in our protocol. This may be related to the fact that we addressed BBB crossing in the naïve brain. Given the strong protective effects for FTY720 and the relatively low doses at which it has been shown to be protective in ischemic stroke, we expect that FTY720 reaches and is primarily activating on EC $S1P_1$ at therapeutic doses. We nevertheless predict that a less desensitizing agonist could achieve a better overall outcome through promotion of endothelial $S1P_1$-mediated functions without requirement of sustained lymphopenia. Effective protection in a tMCAO model with ApoM-Fc, which does not induce even transient

lymphopenia, already suggests that it may be sufficient to target EC $S1P_1$ without targeting lymphocyte receptors (Swendeman et al. 2017).

Our study is in accordance with current literature suggesting that $S1P_1$ modulation may provide a promising therapeutic option for in ischemic stroke. It also provides important novel insight to suggest the importance of positively targeting the endothelial pool of $S1P_1$. As $S1P_1$ plays an important endogenous role during ischemic stroke, desensitization of endothelial receptors could aggravate outcome. This could indeed explain lack of efficacy or even detrimental results of $S1P_1$ modulators observed in some studies. On the other hand, sustained targeting lymphocyte receptors appears to have less importance. This should allow targeting strategies with minimal risk of post-stroke infections. Our study still has important limitations, and it is still a long way to go until we see $S1P_1$ modulators used clinically for stroke treatment. Most importantly, it was carried out in young male mice without comorbidities. Our experiments also targeted endothelial $S1P_1$ with intraperitoneal injection of drugs, while it is more common to use the intravenous route of administration in clinical practice. Most patients suffering ischemic stroke are elderly and have had prolonged exposure to one or several comorbidities, such as diabetes mellitus, hypercholesterolemia, and hypertension, which trigger endothelial dysfunction. Other groups have studied $S1P_1$ modulators in aged mice and with comorbidities, and results from these studies suggest that $S1P_1$ targeting could lose efficacy in this context. It is possible that those particular studies did not show efficacy due to experimental design, such as the use of high doses of desensitizing $S1P_1$ modulators, but it is also possible that the aged and dysfunctional endothelium is no longer responsive to $S1P_1$ modulators. It will therefore be important to expand on experimental and clinical studies on S1P modulation for the treatment of ischemic stroke, with more focus on endothelial activation and desensitization. Moreover, although FTY720 has been explored in combination with alteplase, any potential drug targeting endothelial $S1P_1$ more selectively must also be investigated in combination with alteplase if it is to be considered for clinical use (Tian et al. 2018). Another important limitation of our study is that we have addressed the mechanisms of action of $S1P_1$ in the context of endothelial specific deficiency in S1P production, export or $S1P_1$ signaling. Observations from endogenous signaling deficiency cannot be directly extrapolated to studies with $S1P_1$ agonists. Although we have also demonstrated that local administration of $S1P_1$ agonists can promote cerebral perfusion in naïve mice, we have not directly addressed if $S1P_1$ agonists can further promote tissue perfusion, BBB function or microvascular patency in the context of functional endogenous signaling.

Bibliography

Abbott, N. Joan, Lars Rönnbäck, and Elisabeth Hansson. 2006. "Astrocyte-Endothelial Interactions at the Blood-Brain Barrier." *Nature Reviews. Neuroscience* 7 (1): 41–53. https://doi.org/10.1038/nrn1824.

Adachi, Kunitomo, and Kenji Chiba. 2007. "FTY720 Story. Its Discovery and the Following Accelerated Development of Sphingosine 1-Phosphate Receptor Agonists as Immunomodulators Based on Reverse Pharmacology." *Perspectives in Medicinal Chemistry* 1 (September): 11–23.

Adams, Harold P., Mark B. Effron, James Torner, Antoni Dávalos, Judith Frayne, Philip Teal, Jacques Leclerc, et al. 2008. "Emergency Administration of Abciximab for Treatment of Patients with Acute Ischemic Stroke: Results of an International Phase III Trial: Abciximab in Emergency Treatment of Stroke Trial (AbESTT-II)." *Stroke* 39 (1): 87–99. https://doi.org/10.1161/STROKEAHA.106.476648.

Akhter, Md Zahid, Jagdish Chandra Joshi, Vijay Avin Balaji Ragunathrao, Mark Maienschein-Cline, Richard L. Proia, Asrar B. Malik, and Dolly Mehta. 2021. "Programming to S1PR1+ Endothelial Cells Promotes Restoration of Vascular Integrity." *Circulation Research* 129 (2): 221–36. https://doi.org/10.1161/CIRCRESAHA.120.318412.

Alemany, Regina, Chris J. van Koppen, Kerstin Danneberg, Michael Ter Braak, and Dagmar Meyer Zu Heringdorf. 2007. "Regulation and Functional Roles of Sphingosine Kinases." *Naunyn-Schmiedeberg's Archives of Pharmacology* 374 (5–6): 413–28. https://doi.org/10.1007/s00210-007-0132-3.

Allende, Maria L., Teiji Sasaki, Hiromichi Kawai, Ana Olivera, Yide Mi, Gerhild van Echten-Deckert, Richard Hajdu, et al. 2004. "Mice Deficient in Sphingosine Kinase 1 Are Rendered Lymphopenic by FTY720." *The Journal of Biological Chemistry* 279 (50): 52487–92. https://doi.org/10.1074/jbc.M406512200.

Allende, Maria L., Tadashi Yamashita, and Richard L. Proia. 2003. "G-Protein-Coupled Receptor S1P1 Acts within Endothelial Cells to Regulate Vascular Maturation." *Blood* 102 (10): 3665–67. https://doi.org/10.1182/blood-2003-02-0460.

Alphonsus, C. S., and R. N. Rodseth. 2014. "The Endothelial Glycocalyx: A Review of the Vascular Barrier." *Anaesthesia* 69 (7): 777–84. https://doi.org/10.1111/anae.12661.

Altay, Orhan, Hidenori Suzuki, Yu Hasegawa, Basak Caner, Paul R. Krafft, Mutsumi Fujii, Jiping Tang, and John H. Zhang. 2012. "Isoflurane Attenuates Blood-Brain Barrier Disruption in Ipsilateral Hemisphere after Subarachnoid Hemorrhage in Mice." *Stroke* 43 (9): 2513–16. https://doi.org/10.1161/STROKEAHA.112.661728.

Alvarez, Sergio E., Kuzhuvelil B. Harikumar, Nitai C. Hait, Jeremy Allegood, Graham M. Strub, Eugene Y. Kim, Michael Maceyka, et al. 2010.

"Sphingosine-1-Phosphate Is a Missing Cofactor for the E3 Ubiquitin Ligase TRAF2." *Nature* 465 (7301): 1084–88. https://doi.org/10.1038/nature09128.

Alves, Natascha G., Andrea N. Trujillo, Jerome W. Breslin, and Sarah Y. Yuan. 2019. "Sphingosine-1-Phosphate Reduces Hemorrhagic Shock and Resuscitation-Induced Microvascular Leakage by Protecting Endothelial Mitochondrial Integrity." *Shock (Augusta, Ga.)* 52 (4): 423–33. https://doi.org/10.1097/SHK.0000000000001280.

Amara, Umme, Daniel Rittirsch, Michael Flierl, Uwe Bruckner, Andreas Klos, Florian Gebhard, John D. Lambris, and Markus Huber-Lang. 2008. "Interaction between the Coagulation and Complement System." *Advances in Experimental Medicine and Biology* 632: 71–79. https://doi.org/10.1007/978-0-387-78952-1_6.

Ando, Joji, and Kimiko Yamamoto. 2011. "Effects of Shear Stress and Stretch on Endothelial Function." *Antioxidants & Redox Signaling* 15 (5): 1389–1403. https://doi.org/10.1089/ars.2010.3361.

Ansari, Saeed, Hassan Azari, Douglas J. McConnell, Aqeela Afzal, and J. Mocco. 2011. "Intraluminal Middle Cerebral Artery Occlusion (MCAO) Model for Ischemic Stroke with Laser Doppler Flowmetry Guidance in Mice." *Journal of Visualized Experiments: JoVE*, no. 51 (May): 2879. https://doi.org/10.3791/2879.

Argraves, Kelley M., Patrick J. Gazzolo, Eric M. Groh, Brent A. Wilkerson, Bryan S. Matsuura, Waleed O. Twal, Samar M. Hammad, and W. Scott Argraves. 2008. "High Density Lipoprotein-Associated Sphingosine 1-Phosphate Promotes Endothelial Barrier Function." *The Journal of Biological Chemistry* 283 (36): 25074–81. https://doi.org/10.1074/jbc.M801214200.

Arisaka, T., M. Mitsumata, M. Kawasumi, T. Tohjima, S. Hirose, and Y. Yoshida. 1995. "Effects of Shear Stress on Glycosaminoglycan Synthesis in Vascular Endothelial Cells." *Annals of the New York Academy of Sciences* 748 (January): 543–54. https://doi.org/10.1111/j.1749-6632.1994.tb17359.x.

Armitage, Glenn A., Kathryn G. Todd, Ashfaq Shuaib, and Ian R. Winship. 2010. "Laser Speckle Contrast Imaging of Collateral Blood Flow during Acute Ischemic Stroke." *Journal of Cerebral Blood Flow and Metabolism: Official Journal of the International Society of Cerebral Blood Flow and Metabolism* 30 (8): 1432–36. https://doi.org/10.1038/jcbfm.2010.73.

Armulik, Annika, Guillem Genové, Maarja Mäe, Maya H. Nisancioglu, Elisabet Wallgard, Colin Niaudet, Liqun He, et al. 2010. "Pericytes Regulate the Blood-Brain Barrier." *Nature* 468 (7323): 557–61. https://doi.org/10.1038/nature09522.

Arthur, F. E., R. R. Shivers, and P. D. Bowman. 1987. "Astrocyte-Mediated Induction of Tight Junctions in Brain Capillary Endothelium: An Efficient in Vitro Model." *Brain Research* 433 (1): 155–59. https://doi.org/10.1016/0165-3806(87)90075-7.

Arumugam, Thiruma V., James W. Salter, John H. Chidlow, Christie M. Ballantyne, Christopher G. Kevil, and D. Neil Granger. 2004. "Contributions of LFA-1 and Mac-1 to Brain Injury and Microvascular Dysfunction Induced by Transient Middle Cerebral Artery Occlusion." *American Journal of Physiology. Heart and Circulatory Physiology* 287 (6): H2555-2560. https://doi.org/10.1152/ajpheart.00588.2004.

Asahi, M., X. Wang, T. Mori, T. Sumii, J. C. Jung, M. A. Moskowitz, M. E. Fini, and E. H. Lo. 2001. "Effects of Matrix Metalloproteinase-9 Gene Knock-out on the Proteolysis of Blood-Brain Barrier and White Matter Components after Cerebral Ischemia." *The Journal of Neuroscience: The Official Journal of the Society for Neuroscience* 21 (19): 7724–32.

Ashina, Kohei, Yoshiki Tsubosaka, Koji Kobayashi, Keisuke Omori, and Takahisa Murata. 2015. "VEGF-Induced Blood Flow Increase Causes Vascular Hyper-Permeability in Vivo." *Biochemical and Biophysical Research Communications* 464 (2): 590–95. https://doi.org/10.1016/j.bbrc.2015.07.014.

Asplund, Kjell, Juha Karvanen, Simona Giampaoli, Pekka Jousilahti, Matti Niemelä, Grazyna Broda, Giancarlo Cesana, et al. 2009. "Relative Risks for Stroke by Age, Sex, and Population Based on Follow-up of 18 European Populations in the MORGAM Project." *Stroke* 40 (7): 2319–26. https://doi.org/10.1161/STROKEAHA.109.547869.

Ayata, Cenk, Andrew K. Dunn, Yasemin Gursoy-OZdemir, Zhihong Huang, David A. Boas, and Michael A. Moskowitz. 2004. "Laser Speckle Flowmetry for the Study of Cerebrovascular Physiology in Normal and Ischemic Mouse Cortex." *Journal of Cerebral Blood Flow and Metabolism: Official Journal of the International Society of Cerebral Blood Flow and Metabolism* 24 (7): 744–55. https://doi.org/10.1097/01.WCB.0000122745.72175.D5.

Bagher, P., and S. S. Segal. 2011. "Regulation of Blood Flow in the Microcirculation: Role of Conducted Vasodilation." *Acta Physiologica (Oxford, England)* 202 (3): 271–84. https://doi.org/10.1111/j.1748-1716.2010.02244.x.

Balabanov, R., and P. Dore-Duffy. 1998. "Role of the CNS Microvascular Pericyte in the Blood-Brain Barrier." *Journal of Neuroscience Research* 53 (6): 637–44. https://doi.org/10.1002/(SICI)1097-4547(19980915)53:6<637::AID-JNR1>3.0.CO;2-6.

Bang, O. Y., J. L. Saver, B. H. Buck, J. R. Alger, S. Starkman, B. Ovbiagele, D. Kim, et al. 2008. "Impact of Collateral Flow on Tissue Fate in Acute Ischaemic Stroke." *Journal of Neurology, Neurosurgery, and Psychiatry* 79 (6): 625–29. https://doi.org/10.1136/jnnp.2007.132100.

Baron, Jean-Claude. 2018. "Protecting the Ischaemic Penumbra as an Adjunct to Thrombectomy for Acute Stroke." *Nature Reviews. Neurology* 14 (6): 325–37. https://doi.org/10.1038/s41582-018-0002-2.

Becker, Bernhard F., Daniel Chappell, Dirk Bruegger, Thorsten Annecke, and Matthias Jacob. 2010. "Therapeutic Strategies Targeting the Endothelial

Glycocalyx: Acute Deficits, but Great Potential." *Cardiovascular Research* 87 (2): 300–310. https://doi.org/10.1093/cvr/cvq137.

Behjati, Mohaddeseh, Masoud Etemadifar, and Morteza Abdar Esfahani. 2014. "Cardiovascular Effects of Fingolimod: A Review Article." *Iranian Journal of Neurology* 13 (3): 119–26.

Bell, Robert D., Ethan A. Winkler, Itender Singh, Abhay P. Sagare, Rashid Deane, Zhenhua Wu, David M. Holtzman, et al. 2012. "Apolipoprotein E Controls Cerebrovascular Integrity via Cyclophilin A." *Nature* 485 (7399): 512–16. https://doi.org/10.1038/nature11087.

Belov Kirdajova, Denisa, Jan Kriska, Jana Tureckova, and Miroslava Anderova. 2020. "Ischemia-Triggered Glutamate Excitotoxicity From the Perspective of Glial Cells." *Frontiers in Cellular Neuroscience* 14: 51. https://doi.org/10.3389/fncel.2020.00051.

Beresewicz, A., E. Czarnowska, and M. Maczewski. 1998. "Ischemic Preconditioning and Superoxide Dismutase Protect against Endothelial Dysfunction and Endothelium Glycocalyx Disruption in the Postischemic Guinea-Pig Hearts." *Molecular and Cellular Biochemistry* 186 (1–2): 87–97.

Bergmeier, Wolfgang, Valerie Schulte, Gero Brockhoff, Ulrich Bier, Hubert Zirngibl, and Bernhard Nieswandt. 2002. "Flow Cytometric Detection of Activated Mouse Integrin AlphaIIbbeta3 with a Novel Monoclonal Antibody." *Cytometry* 48 (2): 80–86. https://doi.org/10.1002/cyto.10114.

Berk, Bradford C., Wang Min, Chen Yan, James Surapisitchat, Yingmei Liu, and Ryan Hoefen. 2002. "Atheroprotective Mechanisms Activated by Fluid Shear Stress in Endothelial Cells." *Drug News & Perspectives* 15 (3): 133–39. https://doi.org/10.1358/dnp.2002.15.3.704684.

Bermejo-Martin, Jesus F., Marta Martín-Fernandez, Cristina López-Mestanza, Patricia Duque, and Raquel Almansa. 2018. "Shared Features of Endothelial Dysfunction between Sepsis and Its Preceding Risk Factors (Aging and Chronic Disease)." *Journal of Clinical Medicine* 7 (11). https://doi.org/10.3390/jcm7110400.

Berndt, M. C., Y. Shen, S. M. Dopheide, E. E. Gardiner, and R. K. Andrews. 2001. "The Vascular Biology of the Glycoprotein Ib-IX-V Complex." *Thrombosis and Haemostasis* 86 (1): 178–88.

Bettger, Janet Prvu, Xin Zhao, Cheryl Bushnell, Louise Zimmer, Wenqin Pan, Linda S. Williams, and Eric D. Peterson. 2014. "The Association between Socioeconomic Status and Disability after Stroke: Findings from the Adherence EValuation After Ischemic Stroke Longitudinal (AVAIL) Registry." *BMC Public Health* 14 (March): 281. https://doi.org/10.1186/1471-2458-14-281.

Bobinger, Tobias, Anatol Manaenko, Petra Burkardt, Vanessa Beuscher, Maximilian I. Sprügel, Sebastian S. Roeder, Tobias Bäuerle, et al. 2019. "Siponimod (BAF-312) Attenuates Perihemorrhagic Edema And Improves Survival in Experimental

Intracerebral Hemorrhage." *Stroke* 50 (11): 3246–54. https://doi.org/10.1161/STROKEAHA.119.027134.

Bobryshev, Yuri V., Nikita G. Nikiforov, Natalia V. Elizova, and Alexander N. Orekhov. 2017. "Macrophages and Their Contribution to the Development of Atherosclerosis." *Results and Problems in Cell Differentiation* 62: 273–98. https://doi.org/10.1007/978-3-319-54090-0_11.

Brait, Vanessa H., Gema Tarrasón, Amadeu Gavaldà, Núria Godessart, and Anna M. Planas. 2016. "Selective Sphingosine 1-Phosphate Receptor 1 Agonist Is Protective Against Ischemia/Reperfusion in Mice." *Stroke* 47 (12): 3053–56. https://doi.org/10.1161/STROKEAHA.116.015371.

Brinkmann, Volker, Andreas Billich, Thomas Baumruker, Peter Heining, Robert Schmouder, Gordon Francis, Shreeram Aradhye, and Pascale Burtin. 2010. "Fingolimod (FTY720): Discovery and Development of an Oral Drug to Treat Multiple Sclerosis." *Nature Reviews. Drug Discovery* 9 (11): 883–97. https://doi.org/10.1038/nrd3248.

Brinkmann, Volker, and Kevin R. Lynch. 2002. "FTY720: Targeting G-Protein-Coupled Receptors for Sphingosine 1-Phosphate in Transplantation and Autoimmunity." *Current Opinion in Immunology* 14 (5): 569–75. https://doi.org/10.1016/s0952-7915(02)00374-6.

Brozici, Mariana, Albert van der Zwan, and Berend Hillen. 2003. "Anatomy and Functionality of Leptomeningeal Anastomoses: A Review." *Stroke* 34 (11): 2750–62. https://doi.org/10.1161/01.STR.0000095791.85737.65.

Burg, Nathalie, Steven Swendeman, Stefan Worgall, Timothy Hla, and Jane E. Salmon. 2018. "Sphingosine 1-Phosphate Receptor 1 Signaling Maintains Endothelial Cell Barrier Function and Protects Against Immune Complex-Induced Vascular Injury." *Arthritis & Rheumatology (Hoboken, N.J.)* 70 (11): 1879–89. https://doi.org/10.1002/art.40558.

Cahill, Paul A., and Eileen M. Redmond. 2016. "Vascular Endothelium - Gatekeeper of Vessel Health." *Atherosclerosis* 248 (May): 97–109. https://doi.org/10.1016/j.atherosclerosis.2016.03.007.

Cai, Aijia, Frieder Schlunk, Ferdinand Bohmann, Sepide Kashefiolasl, Robert Brunkhorst, Christian Foerch, and Waltraud Pfeilschifter. 2013. "Coadministration of FTY720 and Rt-PA in an Experimental Model of Large Hemispheric Stroke-No Influence on Functional Outcome and Blood-Brain Barrier Disruption." *Experimental & Translational Stroke Medicine* 5 (1): 11. https://doi.org/10.1186/2040-7378-5-11.

Cai, Qiang, Gang Xu, Junhui Liu, Long Wang, Gang Deng, Jun Liu, and Zhibiao Chen. 2016. "A Modification of Intraluminal Middle Cerebral Artery Occlusion/Reperfusion Model for Ischemic Stroke with Laser Doppler Flowmetry Guidance in Mice." *Neuropsychiatric Disease and Treatment* 12: 2851–58. https://doi.org/10.2147/NDT.S118531.

Callera, Glaucia, Rita Tostes, Carmine Savoia, M. N. Muscara, and Rhian M. Touyz. 2007. "Vasoactive Peptides in Cardiovascular (Patho)Physiology." *Expert Review of Cardiovascular Therapy* 5 (3): 531–52.

https://doi.org/10.1586/14779072.5.3.531.

Camerer, Eric, Jean B. Regard, Ivo Cornelissen, Yoga Srinivasan, Daniel N. Duong, Daniel Palmer, Trung H. Pham, Jinny S. Wong, Rajita Pappu, and Shaun R. Coughlin. 2009. "Sphingosine-1-Phosphate in the Plasma Compartment Regulates Basal and Inflammation-Induced Vascular Leak in Mice." *The Journal of Clinical Investigation* 119 (7): 1871–79. https://doi.org/10.1172/jci38575.

Campbell, Bruce C. V., Deidre A. De Silva, Malcolm R. Macleod, Shelagh B. Coutts, Lee H. Schwamm, Stephen M. Davis, and Geoffrey A. Donnan. 2019. "Ischaemic Stroke." *Nature Reviews. Disease Primers* 5 (1): 70. https://doi.org/10.1038/s41572-019-0118-8.

Campos, Francisco, Tao Qin, José Castillo, Ji Hae Seo, Ken Arai, Eng H. Lo, and Christian Waeber. 2013. "Fingolimod Reduces Hemorrhagic Transformation Associated with Delayed Tissue Plasminogen Activator Treatment in a Mouse Thromboembolic Model." *Stroke* 44 (2): 505–11. https://doi.org/10.1161/STROKEAHA.112.679043.

Cannavo, Alessandro, Daniela Liccardo, Klara Komici, Graziamaria Corbi, Claudio de Lucia, Grazia D. Femminella, Andrea Elia, et al. 2017. "Sphingosine Kinases and Sphingosine 1-Phosphate Receptors: Signaling and Actions in the Cardiovascular System." *Frontiers in Pharmacology* 8: 556. https://doi.org/10.3389/fphar.2017.00556.

Cantalupo, Anna, Antonella Gargiulo, Elona Dautaj, Catherine Liu, Yi Zhang, Timothy Hla, and Annarita Di Lorenzo. 2017. "S1PR1 (Sphingosine-1-Phosphate Receptor 1) Signaling Regulates Blood Flow and Pressure." *Hypertension (Dallas, Tex.: 1979)* 70 (2): 426–34. https://doi.org/10.1161/HYPERTENSIONAHA.117.09088.

Cantalupo, Anna, Yi Zhang, Milankumar Kothiya, Sylvain Galvani, Hideru Obinata, Mariarosaria Bucci, Frank J. Giordano, Xian-Cheng Jiang, Timothy Hla, and Annarita Di Lorenzo. 2015. "Nogo-B Regulates Endothelial Sphingolipid Homeostasis to Control Vascular Function and Blood Pressure." *Nature Medicine* 21 (9): 1028–37. https://doi.org/10.1038/nm.3934.

Cartier, Andreane, and Timothy Hla. 2019. "Sphingosine 1-Phosphate: Lipid Signaling in Pathology and Therapy." *Science (New York, N.Y.)* 366 (6463). https://doi.org/10.1126/science.aar5551.

Cartier, Andreane, Tani Leigh, Catherine H. Liu, and Timothy Hla. 2020. "Endothelial Sphingosine 1-Phosphate Receptors Promote Vascular Normalization and Antitumor Therapy." *Proceedings of the National Academy of Sciences of the United States of America* 117 (6): 3157–66. https://doi.org/10.1073/pnas.1906246117.

Chandrakanthan, Madhuvanthi, Toan Quoc Nguyen, Zafrul Hasan, Sneha Muralidharan, Thiet Minh Vu, Aaron Wei Liang Li, Uyen Thanh Nha Le, et al. 2021. "Deletion of Mfsd2b Impairs Thrombotic Functions of Platelets." *Nature Communications* 12 (1): 2286. https://doi.org/10.1038/s41467-021-22642-x.

Chatterjee, Shampa, Elizabeth A. Browning, NanKang Hong, Kris DeBolt, Elena M. Sorokina, Weidong Liu, Morris J. Birnbaum, and Aron B. Fisher. 2012. "Membrane Depolarization Is the Trigger for PI3K/Akt Activation and Leads to the Generation of ROS." *American Journal of Physiology. Heart and Circulatory Physiology* 302 (1): H105-114. https://doi.org/10.1152/ajpheart.00298.2011.

Chatzizisis, Yiannis S., Ahmet Umit Coskun, Michael Jonas, Elazer R. Edelman, Charles L. Feldman, and Peter H. Stone. 2007. "Role of Endothelial Shear Stress in the Natural History of Coronary Atherosclerosis and Vascular Remodeling: Molecular, Cellular, and Vascular Behavior." *Journal of the American College of Cardiology* 49 (25): 2379–93. https://doi.org/10.1016/j.jacc.2007.02.059.

Chen, Jing, Neil Ingham, John Kelly, Shalini Jadeja, David Goulding, Johanna Pass, Vinit B. Mahajan, et al. 2014. "Spinster Homolog 2 (Spns2) Deficiency Causes Early Onset Progressive Hearing Loss." *PLoS Genetics* 10 (10): e1004688. https://doi.org/10.1371/journal.pgen.1004688.

Chen, Yingxin, Wenbin Zhu, Wenri Zhang, Nicole Libal, Stephanie J. Murphy, Halina Offner, and Nabil J. Alkayed. 2015. "A Novel Mouse Model of Thromboembolic Stroke." *Journal of Neuroscience Methods* 256 (December): 203–11. https://doi.org/10.1016/j.jneumeth.2015.09.013.

Christoffersen, Christina, Lars Bo Nielsen, Olof Axler, Astra Andersson, Anders H. Johnsen, and Björn Dahlbäck. 2006. "Isolation and Characterization of Human Apolipoprotein M-Containing Lipoproteins." *Journal of Lipid Research* 47 (8): 1833–43. https://doi.org/10.1194/jlr.M600055-JLR200.

Christoffersen, Christina, Hideru Obinata, Sunil B. Kumaraswamy, Sylvain Galvani, Josefin Ahnström, Madhumati Sevvana, Claudia Egerer-Sieber, et al. 2011. "Endothelium-Protective Sphingosine-1-Phosphate Provided by HDL-Associated Apolipoprotein M." *Proceedings of the National Academy of Sciences of the United States of America* 108 (23): 9613–18. https://doi.org/10.1073/pnas.1103187108.

Chun, Jerold, Gavin Giovannoni, and Samuel F. Hunter. 2021. "Sphingosine 1-Phosphate Receptor Modulator Therapy for Multiple Sclerosis: Differential Downstream Receptor Signalling and Clinical Profile Effects." *Drugs* 81 (2): 207–31. https://doi.org/10.1007/s40265-020-01431-8.

Chung, Alicia S., and Napoleone Ferrara. 2011. "Developmental and Pathological Angiogenesis." *Annual Review of Cell and Developmental Biology* 27: 563–84. https://doi.org/10.1146/annurev-cellbio-092910-154002.

Claesson-Welsh, Lena, Elisabetta Dejana, and Donald M. McDonald. 2021. "Permeability of the Endothelial Barrier: Identifying and Reconciling Controversies." *Trends in Molecular Medicine* 27 (4): 314–31. https://doi.org/10.1016/j.molmed.2020.11.006.

Constantinescu, Alina A., Hans Vink, and Jos A. E. Spaan. 2003. "Endothelial Cell Glycocalyx Modulates Immobilization of Leukocytes at the

Endothelial Surface." *Arteriosclerosis, Thrombosis, and Vascular Biology* 23 (9): 1541–47. https://doi.org/10.1161/01.ATV.0000085630.24353.3D.

Cordonnier, Charlotte, Nikola Sprigg, Else Charlotte Sandset, Aleksandra Pavlovic, Katharina S. Sunnerhagen, Valeria Caso, Hanne Christensen, and Women Initiative for Stroke in Europe (WISE) group. 2017. "Stroke in Women - from Evidence to Inequalities." *Nature Reviews. Neurology* 13 (9): 521–32. https://doi.org/10.1038/nrneurol.2017.95.

Cruz-Orengo, Lillian, Brian P. Daniels, Denise Dorsey, Sarah Alison Basak, José G. Grajales-Reyes, Erin E. McCandless, Laura Piccio, et al. 2014. "Enhanced Sphingosine-1-Phosphate Receptor 2 Expression Underlies Female CNS Autoimmunity Susceptibility." *The Journal of Clinical Investigation* 124 (6): 2571–84. https://doi.org/10.1172/JCI73408.

Cui, Hong, Yasuo Okamoto, Kazuaki Yoshioka, Wa Du, Noriko Takuwa, Wei Zhang, Masahide Asano, Toshishige Shibamoto, and Yoh Takuwa. 2013. "Sphingosine-1-Phosphate Receptor 2 Protects against Anaphylactic Shock through Suppression of Endothelial Nitric Oxide Synthase in Mice." *The Journal of Allergy and Clinical Immunology* 132 (5): 1205-1214.e9. https://doi.org/10.1016/j.jaci.2013.07.026.

Cullen, John P., Suzanne M. Nicholl, Shariq Sayeed, James V. Sitzmann, S. Steve Okada, Paul A. Cahill, and Eileen M. Redmond. 2004. "Plasminogen Activator Inhibitor-1 Deficiency Enhances Flow-Induced Smooth Muscle Cell Migration." *Thrombosis Research* 114 (1): 57–65. https://doi.org/10.1016/j.thromres.2004.05.003.

Czech, Bozena, Waltraud Pfeilschifter, Niloufar Mazaheri-Omrani, Marc André Strobel, Timo Kahles, Tobias Neumann-Haefelin, Abdelhaq Rami, Andrea Huwiler, and Josef Pfeilschifter. 2009. "The Immunomodulatory Sphingosine 1-Phosphate Analog FTY720 Reduces Lesion Size and Improves Neurological Outcome in a Mouse Model of Cerebral Ischemia." *Biochemical and Biophysical Research Communications* 389 (2): 251–56. https://doi.org/10.1016/j.bbrc.2009.08.142.

Daneman, Richard, and Alexandre Prat. 2015. "The Blood-Brain Barrier." *Cold Spring Harbor Perspectives in Biology* 7 (1): a020412. https://doi.org/10.1101/cshperspect.a020412.

Daneman, Richard, Lu Zhou, Amanuel A. Kebede, and Ben A. Barres. 2010. "Pericytes Are Required for Blood-Brain Barrier Integrity during Embryogenesis." *Nature* 468 (7323): 562–66. https://doi.org/10.1038/nature09513.

Dang, Chun, Yaoheng Lu, Qian Li, Chunyang Wang, and Xiaofeng Ma. 2021. "Efficacy of the Sphingosine-1-Phosphate Receptor Agonist Fingolimod in Animal Models of Stroke: An Updated Meta-Analysis." *The International Journal of Neuroscience* 131 (1): 85–94. https://doi.org/10.1080/00207454.2020.1733556.

Dawson, D. A., C. A. Ruetzler, T. M. Carlos, P. M. Kochanek, and J. M. Hallenbeck. 1996. "Polymorphonuclear Leukocytes

and Microcirculatory Perfusion in Acute Stroke in the SHR." *The Keio Journal of Medicine* 45 (3): 248–52; discussion 252-253. https://doi.org/10.2302/kjm.45.248.

De Meyer, Simon F., Frederik Denorme, Friederike Langhauser, Eva Geuss, Felix Fluri, and Christoph Kleinschnitz. 2016. "Thromboinflammation in Stroke Brain Damage." *Stroke* 47 (4): 1165–72. https://doi.org/10.1161/STROKEAHA.115.011238.

Delvaeye, Mieke, and Edward M. Conway. 2009. "Coagulation and Innate Immune Responses: Can We View Them Separately?" *Blood* 114 (12): 2367–74. https://doi.org/10.1182/blood-2009-05-199208.

Dente, C. J., C. P. Steffes, C. Speyer, and J. G. Tyburski. 2001. "Pericytes Augment the Capillary Barrier in in Vitro Cocultures." *The Journal of Surgical Research* 97 (1): 85–91. https://doi.org/10.1006/jsre.2001.6117.

Deppermann, Carsten, Peter Kraft, Julia Volz, Michael K. Schuhmann, Sarah Beck, Karen Wolf, David Stegner, Guido Stoll, and Bernhard Nieswandt. 2017. "Platelet Secretion Is Crucial to Prevent Bleeding in the Ischemic Brain but Not in the Inflamed Skin or Lung in Mice." *Blood* 129 (12): 1702–6. https://doi.org/10.1182/blood-2016-12-750711.

Diamond, S. L., S. G. Eskin, and L. V. McIntire. 1989. "Fluid Flow Stimulates Tissue Plasminogen Activator Secretion by Cultured Human Endothelial Cells." *Science (New York, N.Y.)* 243 (4897): 1483–85. https://doi.org/10.1126/science.2467379.

Diaz Diaz, Andrea C., Jennifer A. Shearer, Kyle Malone, and Christian Waeber. 2020. "Acute Treatment With Fingolimod Does Not Confer Long-Term Benefit in a Mouse Model of Intracerebral Haemorrhage." *Frontiers in Pharmacology* 11: 613103. https://doi.org/10.3389/fphar.2020.613103.

Ding, Zhaoqing, Vidhu Mathur, Peggy P. Ho, Michelle L. James, Kurt M. Lucin, Aileen Hoehne, Haitham Alabsi, et al. 2014. "Antiviral Drug Ganciclovir Is a Potent Inhibitor of Microglial Proliferation and Neuroinflammation." *The Journal of Experimental Medicine* 211 (2): 189–98. https://doi.org/10.1084/jem.20120696.

Dreikorn, Mirjam, Zeljko Milacic, Vladimir Pavlovic, Sven G. Meuth, Christoph Kleinschnitz, and Peter Kraft. 2018. "Immunotherapy of Experimental and Human Stroke with Agents Approved for Multiple Sclerosis: A Systematic Review." *Therapeutic Advances in Neurological Disorders* 11: 1756286418770626. https://doi.org/10.1177/1756286418770626.

Duchemin, Sonia, Michaël Boily, Nataliya Sadekova, and Hélène Girouard. 2012. "The Complex Contribution of NOS Interneurons in the Physiology of Cerebrovascular Regulation." *Frontiers in Neural Circuits* 6: 51. https://doi.org/10.3389/fncir.2012.00051.

Dütting, Sebastian, Markus Bender, and Bernhard Nieswandt. 2012. "Platelet GPVI: A Target for Antithrombotic Therapy?!" *Trends in Pharmacological Sciences* 33 (11):

583–90. https://doi.org/10.1016/j.tips.2012.07.004.

El Amki, Mohamad, Chaim Glück, Nadine Binder, William Middleham, Matthias T. Wyss, Tobias Weiss, Hanna Meister, et al. 2020. "Neutrophils Obstructing Brain Capillaries Are a Major Cause of No-Reflow in Ischemic Stroke." *Cell Reports* 33 (2): 108260. https://doi.org/10.1016/j.celrep.2020.108260.

Eltanahy, Ahmed M., Yara A. Koluib, and Albert Gonzales. 2021. "Pericytes: Intrinsic Transportation Engineers of the CNS Microcirculation." *Frontiers in Physiology* 12: 719701. https://doi.org/10.3389/fphys.2021.719701.

Engel, Odilo, Sabine Kolodziej, Ulrich Dirnagl, and Vincent Prinz. 2011. "Modeling Stroke in Mice - Middle Cerebral Artery Occlusion with the Filament Model." *Journal of Visualized Experiments: JoVE*, no. 47 (January): 2423. https://doi.org/10.3791/2423.

Engelbrecht, Eric, Michel V. Levesque, Liqun He, Michael Vanlandewijck, Anja Nitzsche, Hira Niazi, Andrew Kuo, et al. 2020. "Sphingosine 1-Phosphate-Regulated Transcriptomes in Heterogenous Arterial and Lymphatic Endothelium of the Aorta." *ELife* 9 (February): e52690. https://doi.org/10.7554/eLife.52690.

Enlimomab Acute Stroke Trial Investigators. 2001. "Use of Anti-ICAM-1 Therapy in Ischemic Stroke: Results of the Enlimomab Acute Stroke Trial." *Neurology* 57 (8): 1428–34. https://doi.org/10.1212/wnl.57.8.1428.

Etemadi, Nima, Michael Chopin, Holly Anderton, Maria C. Tanzer, James A. Rickard, Waruni Abeysekera, Cathrine Hall, et al. 2015. "TRAF2 Regulates TNF and NF-KB Signalling to Suppress Apoptosis and Skin Inflammation Independently of Sphingosine Kinase 1." *ELife* 4 (December): e10592. https://doi.org/10.7554/eLife.10592.

Faber, James E., Hua Zhang, Roberta M. Lassance-Soares, Pranay Prabhakar, Amir H. Najafi, Mary Susan Burnett, and Stephen E. Epstein. 2011. "Aging Causes Collateral Rarefaction and Increased Severity of Ischemic Injury in Multiple Tissues." *Arteriosclerosis, Thrombosis, and Vascular Biology* 31 (8): 1748–56. https://doi.org/10.1161/ATVBAHA.111.227314.

Fang, Chao, Ganlan Bian, Pan Ren, Jie Xiang, Jun Song, Caiyong Yu, Qian Zhang, et al. 2018. "S1P Transporter SPNS2 Regulates Proper Postnatal Retinal Morphogenesis." *FASEB Journal: Official Publication of the Federation of American Societies for Experimental Biology* 32 (7): 3597–3613. https://doi.org/10.1096/fj.201701116R.

Feigin, Valery L., Rita V. Krishnamurthi, Priya Parmar, Bo Norrving, George A. Mensah, Derrick A. Bennett, Suzanne Barker-Collo, et al. 2015. "Update on the Global Burden of Ischemic and Hemorrhagic Stroke in 1990-2013: The GBD 2013 Study." *Neuroepidemiology* 45 (3): 161–76. https://doi.org/10.1159/000441085.

Fellows, Kelly, Tomas Uher, Richard W. Browne, Bianca Weinstock-Guttman, Dana Horakova, Helena Posova, Manuela Vaneckova, et al. 2015. "Protective Associations of HDL with Blood-Brain Barrier Injury

in Multiple Sclerosis Patients." *Journal of Lipid Research* 56 (10): 2010–18. https://doi.org/10.1194/jlr.M060970.

Figley, Chase R., and Patrick W. Stroman. 2011. "The Role(s) of Astrocytes and Astrocyte Activity in Neurometabolism, Neurovascular Coupling, and the Production of Functional Neuroimaging Signals." *The European Journal of Neuroscience* 33 (4): 577–88. https://doi.org/10.1111/j.1460-9568.2010.07584.x.

Filosa, Jessica A., and Jennifer A. Iddings. 2013. "Astrocyte Regulation of Cerebral Vascular Tone." *American Journal of Physiology. Heart and Circulatory Physiology* 305 (5): H609-619. https://doi.org/10.1152/ajpheart.00359.2013.

Fisher, Marc. 2004. "The Ischemic Penumbra: Identification, Evolution and Treatment Concepts." *Cerebrovascular Diseases (Basel, Switzerland)* 17 Suppl 1: 1–6. https://doi.org/10.1159/000074790.

Fisher, Marc, Giora Feuerstein, David W. Howells, Patricia D. Hurn, Thomas A. Kent, Sean I. Savitz, Eng H. Lo, and STAIR Group. 2009. "Update of the Stroke Therapy Academic Industry Roundtable Preclinical Recommendations." *Stroke* 40 (6): 2244–50. https://doi.org/10.1161/STROKEAHA.108.541128.

Fleming, Jonathan K., Thomas R. Glass, Steve J. Lackie, and Jonathan M. Wojciak. 2016. "A Novel Approach for Measuring Sphingosine-1-Phosphate and Lysophosphatidic Acid Binding to Carrier Proteins Using Monoclonal Antibodies and the Kinetic Exclusion Assay." *Journal of Lipid Research* 57 (9): 1737–47. https://doi.org/10.1194/jlr.D068866.

Forrest, M., S.-Y. Sun, R. Hajdu, J. Bergstrom, D. Card, G. Doherty, J. Hale, et al. 2004. "Immune Cell Regulation and Cardiovascular Effects of Sphingosine 1-Phosphate Receptor Agonists in Rodents Are Mediated via Distinct Receptor Subtypes." *The Journal of Pharmacology and Experimental Therapeutics* 309 (2): 758–68. https://doi.org/10.1124/jpet.103.062828.

Fryer, Ryan M., Akalushi Muthukumarana, Paul C. Harrison, Suzanne Nodop Mazurek, Rong Rhonda Chen, Kyle E. Harrington, Roger M. Dinallo, et al. 2012. "The Clinically-Tested S1P Receptor Agonists, FTY720 and BAF312, Demonstrate Subtype-Specific Bradycardia ($S1P_1$) and Hypertension ($S1P_3$) in Rat." *PloS One* 7 (12): e52985. https://doi.org/10.1371/journal.pone.0052985.

Fu, Ying, Junwei Hao, Ningnannan Zhang, Li Ren, Na Sun, Yu-Jing Li, Yaping Yan, DeRen Huang, Chunshui Yu, and Fu-Dong Shi. 2014. "Fingolimod for the Treatment of Intracerebral Hemorrhage: A 2-Arm Proof-of-Concept Study." *JAMA Neurology* 71 (9): 1092–1101. https://doi.org/10.1001/jamaneurol.2014.1065.

Fu, Ying, Ningnannan Zhang, Li Ren, Yaping Yan, Na Sun, Yu-Jing Li, Wei Han, et al. 2014. "Impact of an Immune Modulator Fingolimod on Acute Ischemic Stroke." *Proceedings of the National Academy of Sciences of the United States of America* 111 (51): 18315–20.

https://doi.org/10.1073/pnas.1416166111.

Fukai, Tohru, and Masuko Ushio-Fukai. 2011. “Superoxide Dismutases: Role in Redox Signaling, Vascular Function, and Diseases.” *Antioxidants & Redox Signaling* 15 (6): 1583–1606. https://doi.org/10.1089/ars.2011.3999.

Fukuhara, Shigetomo, Szandor Simmons, Shunsuke Kawamura, Asuka Inoue, Yasuko Orba, Takeshi Tokudome, Yuji Sunden, et al. 2012. “The Sphingosine-1-Phosphate Transporter Spns2 Expressed on Endothelial Cells Regulates Lymphocyte Trafficking in Mice.” *The Journal of Clinical Investigation* 122 (4): 1416–26. https://doi.org/10.1172/JCI60746.

Fumagalli, Stefano, Carlo Perego, Fabrizio Ortolano, and Maria-Grazia De Simoni. 2013. “CX3CR1 Deficiency Induces an Early Protective Inflammatory Environment in Ischemic Mice.” *Glia* 61 (6): 827–42. https://doi.org/10.1002/glia.22474.

Furchgott, R. F., and P. M. Vanhoutte. 1989. “Endothelium-Derived Relaxing and Contracting Factors.” *FASEB Journal: Official Publication of the Federation of American Societies for Experimental Biology* 3 (9): 2007–18.

Gaengel, Konstantin, Guillem Genové, Annika Armulik, and Christer Betsholtz. 2009. “Endothelial-Mural Cell Signaling in Vascular Development and Angiogenesis.” *Arteriosclerosis, Thrombosis, and Vascular Biology* 29 (5): 630–38. https://doi.org/10.1161/ATVBAHA.107.161521.

Gaengel, Konstantin, Colin Niaudet, Kazuhiro Hagikura, Bàrbara Laviña, Bàrbara Laviña Siemsen, Lars Muhl, Jennifer J. Hofmann, et al. 2012. “The Sphingosine-1-Phosphate Receptor S1PR1 Restricts Sprouting Angiogenesis by Regulating the Interplay between VE-Cadherin and VEGFR2.” *Developmental Cell* 23 (3): 587–99. https://doi.org/10.1016/j.devcel.2012.08.005.

Galvani, Sylvain, Marie Sanson, Victoria A. Blaho, Steven L. Swendeman, Hideru Obinata, Heather Conger, Björn Dahlbäck, et al. 2015. “HDL-Bound Sphingosine 1-Phosphate Acts as a Biased Agonist for the Endothelial Cell Receptor S1P1 to Limit Vascular Inflammation.” *Science Signaling* 8 (389): ra79. https://doi.org/10.1126/scisignal.aaa2581.

Garcia-Bonilla, Lidia, Jamie M. Moore, Gianfranco Racchumi, Ping Zhou, Jason M. Butler, Costantino Iadecola, and Josef Anrather. 2014. “Inducible Nitric Oxide Synthase in Neutrophils and Endothelium Contributes to Ischemic Brain Injury in Mice.” *Journal of Immunology (Baltimore, Md.: 1950)* 193 (5): 2531–37. https://doi.org/10.4049/jimmunol.1400918.

Gasche, Y., J. C. Copin, T. Sugawara, M. Fujimura, and P. H. Chan. 2001. “Matrix Metalloproteinase Inhibition Prevents Oxidative Stress-Associated Blood-Brain Barrier Disruption after Transient Focal Cerebral Ischemia.” *Journal of Cerebral Blood Flow and Metabolism: Official Journal of the International Society of Cerebral Blood Flow and Metabolism* 21 (12): 1393–1400. https://doi.org/10.1097/00004647-200112000-00003.

Gazit, Salomé L., Boubacar Mariko, Patrice Thérond, Benoit Decouture, Yuquan Xiong, Ludovic Couty, Philippe Bonnin, et al. 2016. "Platelet and Erythrocyte Sources of S1P Are Redundant for Vascular Development and Homeostasis, but Both Rendered Essential After Plasma S1P Depletion in Anaphylactic Shock." *Circulation Research* 119 (8): e110-126. https://doi.org/10.1161/CIRCRESAHA.116.308929.

GBD 2015 Mortality and Causes of Death Collaborators. 2016. "Global, Regional, and National Life Expectancy, All-Cause Mortality, and Cause-Specific Mortality for 249 Causes of Death, 1980-2015: A Systematic Analysis for the Global Burden of Disease Study 2015." *Lancet (London, England)* 388 (10053): 1459–1544. https://doi.org/10.1016/S0140-6736(16)31012-1.

Giesen, P. L., B. S. Fyfe, J. T. Fallon, M. Roque, M. Mendlowitz, M. Rossikhina, A. Guha, J. J. Badimon, Y. Nemerson, and M. B. Taubman. 2000. "Intimal Tissue Factor Activity Is Released from the Arterial Wall after Injury." *Thrombosis and Haemostasis* 83 (4): 622–28.

Gilbert, P., J. Tremblay, and E. Thorin. 2001. "Endothelium-Derived Endothelin-1 Reduces Cerebral Artery Sensitivity to Nitric Oxide by a Protein Kinase C-Independent Pathway." *Stroke* 32 (10): 2351–55. https://doi.org/10.1161/hs1001.096007.

Gimbrone, Michael A., and Guillermo García-Cardeña. 2016. "Endothelial Cell Dysfunction and the Pathobiology of Atherosclerosis." *Circulation Research* 118 (4): 620–36. https://doi.org/10.1161/CIRCRESAHA.115.306301.

Gkaliagkousi, Eugenia, and Albert Ferro. 2011. "Nitric Oxide Signalling in the Regulation of Cardiovascular and Platelet Function." *Frontiers in Bioscience (Landmark Edition)* 16 (January): 1873–97. https://doi.org/10.2741/3828.

Go, Alan S., Dariush Mozaffarian, Véronique L. Roger, Emelia J. Benjamin, Jarett D. Berry, Michael J. Blaha, Shifan Dai, et al. 2014. "Heart Disease and Stroke Statistics--2014 Update: A Report from the American Heart Association." *Circulation* 129 (3): e28–292. https://doi.org/10.1161/01.cir.0000441139.02102.80.

Gonzalez-Cabrera, Pedro J., Euijung Jo, M. Germana Sanna, Steven Brown, Nora Leaf, David Marsolais, Marie-Therese Schaeffer, et al. 2008. "Full Pharmacological Efficacy of a Novel S1P1 Agonist That Does Not Require S1P-like Headgroup Interactions." *Molecular Pharmacology* 74 (5): 1308–18. https://doi.org/10.1124/mol.108.049783.

Gordon, Grant R. J., Clare Howarth, and Brian A. MacVicar. 2011. "Bidirectional Control of Arteriole Diameter by Astrocytes." *Experimental Physiology* 96 (4): 393–99. https://doi.org/10.1113/expphysiol.2010.053132.

Govers, R., and T. J. Rabelink. 2001. "Cellular Regulation of Endothelial Nitric Oxide Synthase." *American Journal of Physiology. Renal Physiology* 280 (2): F193-206. https://doi.org/10.1152/ajprenal.2001.280.2.F193.

Grailhe, Patrick, Asma Boutarfa-Madec, Philippe Beauverger, Philip Janiak,

and Ashfaq A. Parkar. 2020. “A Label-Free Impedance Assay in Endothelial Cells Differentiates the Activation and Desensitization Properties of Clinical S1P1 Agonists.” *FEBS Open Bio* 10 (10): 2010–20. https://doi.org/10.1002/2211-5463.12951.

Gu, Zezong, Jiankun Cui, Stephen Brown, Rafael Fridman, Shahriar Mobashery, Alex Y. Strongin, and Stuart A. Lipton. 2005. “A Highly Specific Inhibitor of Matrix Metalloproteinase-9 Rescues Laminin from Proteolysis and Neurons from Apoptosis in Transient Focal Cerebral Ischemia.” *The Journal of Neuroscience: The Official Journal of the Society for Neuroscience* 25 (27): 6401–8. https://doi.org/10.1523/JNEUROSCI.1563-05.2005.

Guan, Yongjing, Yongting Wang, Falei Yuan, Haiyan Lu, Yuqi Ren, Tiqiao Xiao, Kemin Chen, David A. Greenberg, Kunlin Jin, and Guo-Yuan Yang. 2012. “Effect of Suture Properties on Stability of Middle Cerebral Artery Occlusion Evaluated by Synchrotron Radiation Angiography.” *Stroke* 43 (3): 888–91. https://doi.org/10.1161/STROKEAHA.111.636456.

Gupta, Preeti, Aaliya Taiyab, Afzal Hussain, Mohamed F. Alajmi, Asimul Islam, and Md Imtaiyaz Hassan. 2021. “Targeting the Sphingosine Kinase/Sphingosine-1-Phosphate Signaling Axis in Drug Discovery for Cancer Therapy.” *Cancers* 13 (8): 1898. https://doi.org/10.3390/cancers13081898.

Gustavsson, Anders, Mikael Svensson, Frank Jacobi, Christer Allgulander, Jordi Alonso, Ettore Beghi, Richard Dodel, et al. 2011. “Cost of Disorders of the Brain in Europe 2010.” *European Neuropsychopharmacology: The Journal of the European College of Neuropsychopharmacology* 21 (10): 718–79. https://doi.org/10.1016/j.euroneuro.2011.08.008.

Güzel, Aslan, Roland Rölz, Guido Nikkhah, Ulf D. Kahlert, and Jaroslaw Maciaczyk. 2014. “A Microsurgical Procedure for Middle Cerebral Artery Occlusion by Intraluminal Monofilament Insertion Technique in the Rat: A Special Emphasis on the Methodology.” *Experimental & Translational Stroke Medicine* 6: 6. https://doi.org/10.1186/2040-7378-6-6.

Hait, Nitai C., Jeremy Allegood, Michael Maceyka, Graham M. Strub, Kuzhuvelil B. Harikumar, Sandeep K. Singh, Cheng Luo, et al. 2009. “Regulation of Histone Acetylation in the Nucleus by Sphingosine-1-Phosphate.” *Science (New York, N.Y.)* 325 (5945): 1254–57. https://doi.org/10.1126/science.1176709.

Hakomori, S. 2000. “Traveling for the Glycosphingolipid Path.” *Glycoconjugate Journal* 17 (7–9): 627–47. https://doi.org/10.1023/a:1011086929064.

Halbgebauer, Rebecca, Christian K. Braun, Stephanie Denk, Benjamin Mayer, Paolo Cinelli, Peter Radermacher, Guido A. Wanner, et al. 2018. “Hemorrhagic Shock Drives Glycocalyx, Barrier and Organ Dysfunction Early after Polytrauma.” *Journal of Critical Care* 44 (April): 229–37.

https://doi.org/10.1016/j.jcrc.2017.11.025.

Hale, Jeffrey J., Christopher L. Lynch, William Neway, Sander G. Mills, Richard Hajdu, Carol Ann Keohane, Mark J. Rosenbach, et al. 2004. "A Rational Utilization of High-Throughput Screening Affords Selective, Orally Bioavailable 1-Benzyl-3-Carboxyazetidine Sphingosine-1-Phosphate-1 Receptor Agonists." *Journal of Medicinal Chemistry* 47 (27): 6662–65. https://doi.org/10.1021/jm0492507.

Hasegawa, Yu, Hidenori Suzuki, Orhan Altay, William Rolland, and John H. Zhang. 2013. "Role of the Sphingosine Metabolism Pathway on Neurons against Experimental Cerebral Ischemia in Rats." *Translational Stroke Research* 4 (5): 524–32. https://doi.org/10.1007/s12975-013-0260-7.

Hasegawa, Yu, Hidenori Suzuki, Takumi Sozen, William Rolland, and John H. Zhang. 2010. "Activation of Sphingosine 1-Phosphate Receptor-1 by FTY720 Is Neuroprotective after Ischemic Stroke in Rats." *Stroke* 41 (2): 368–74. https://doi.org/10.1161/STROKEAHA.109.568899.

Hawkins, Brian T., and Thomas P. Davis. 2005. "The Blood-Brain Barrier/Neurovascular Unit in Health and Disease." *Pharmacological Reviews* 57 (2): 173–85. https://doi.org/10.1124/pr.57.2.4.

He, Z., T. Yamawaki, S. Yang, A. L. Day, J. W. Simpkins, and H. Naritomi. 1999. "Experimental Model of Small Deep Infarcts Involving the Hypothalamus in Rats: Changes in Body Temperature and Postural Reflex." *Stroke* 30 (12): 2743–51; discussion 2751. https://doi.org/10.1161/01.str.30.12.2743.

Helenius, G., S. H. Hagvall, M. Esguerra, H. Fink, R. Soderberg, and B. Risberg. 2008. "Effect of Shear Stress on the Expression of Coagulation and Fibrinolytic Factors in Both Smooth Muscle and Endothelial Cells in a Co-Culture Model." *European Surgical Research. Europaische Chirurgische Forschung. Recherches Chirurgicales Europeennes* 40 (4): 325–32. https://doi.org/10.1159/000118028.

Hemmings, Denise G. 2006. "Signal Transduction Underlying the Vascular Effects of Sphingosine 1-Phosphate and Sphingosylphosphorylcholine." *Naunyn-Schmiedeberg's Archives of Pharmacology* 373 (1): 18–29. https://doi.org/10.1007/s00210-006-0046-5.

Hendrikse, Jeroen, A. Fleur van Raamt, Yolanda van der Graaf, Willem P. T. M. Mali, and Jeroen van der Grond. 2005. "Distribution of Cerebral Blood Flow in the Circle of Willis." *Radiology* 235 (1): 184–89. https://doi.org/10.1148/radiol.2351031799.

Henry, C. B., and B. R. Duling. 2000. "TNF-Alpha Increases Entry of Macromolecules into Luminal Endothelial Cell Glycocalyx." *American Journal of Physiology. Heart and Circulatory Physiology* 279 (6): H2815-2823. https://doi.org/10.1152/ajpheart.2000.279.6.H2815.

Hilger, Thomas, James A. Blunk, Mathias Hoehn, Günter Mies, and Per Wester. 2004. "Characterization of a

Novel Chronic Photothrombotic Ring Stroke Model in Rats by Magnetic Resonance Imaging, Biochemical Imaging, and Histology." *Journal of Cerebral Blood Flow and Metabolism: Official Journal of the International Society of Cerebral Blood Flow and Metabolism* 24 (7): 789–97. https://doi.org/10.1097/01.WCB.0000123905.17746.DB.

Hillman, Tyler C., Nathanael Matei, Jiping Tang, and John H. Zhang. 2019. "Developing a Standardized System of Exposure and Intervention Endpoints for Isoflurane in Preclinical Stroke Models." *Medical Gas Research* 9 (1): 46–51. https://doi.org/10.4103/2045-9912.254640.

Hisano, Yu, Naoki Kobayashi, Atsuo Kawahara, Akihito Yamaguchi, and Tsuyoshi Nishi. 2011. "The Sphingosine 1-Phosphate Transporter, SPNS2, Functions as a Transporter of the Phosphorylated Form of the Immunomodulating Agent FTY720." *The Journal of Biological Chemistry* 286 (3): 1758–66. https://doi.org/10.1074/jbc.M110.171116.

Hoefer, Imo E., Brigit den Adel, and Mat J. A. P. Daemen. 2013. "Biomechanical Factors as Triggers of Vascular Growth." *Cardiovascular Research* 99 (2): 276–83. https://doi.org/10.1093/cvr/cvt089.

Hofmann, Ulrich, and Stefan Frantz. 2016. "Role of T-Cells in Myocardial Infarction." *European Heart Journal* 37 (11): 873–79. https://doi.org/10.1093/eurheartj/ehv639.

Hovingh, G. Kees, Daniel J. Rader, and Robert A. Hegele. 2015. "HDL Re-Examined." *Current Opinion in Lipidology* 26 (2): 127–32. https://doi.org/10.1097/MOL.0000000000000161.

Howard, George, Ron Prineas, Claudia Moy, Mary Cushman, Martha Kellum, Ella Temple, Andra Graham, and Virginia Howard. 2006. "Racial and Geographic Differences in Awareness, Treatment, and Control of Hypertension: The REasons for Geographic And Racial Differences in Stroke Study." *Stroke* 37 (5): 1171–78. https://doi.org/10.1161/01.STR.0000217222.09978.ce.

Hsieh, Hsyue-Jen, Ching-Ann Liu, Bin Huang, Anne Hh Tseng, and Danny Ling Wang. 2014. "Shear-Induced Endothelial Mechanotransduction: The Interplay between Reactive Oxygen Species (ROS) and Nitric Oxide (NO) and the Pathophysiological Implications." *Journal of Biomedical Science* 21 (January): 3. https://doi.org/10.1186/1423-0127-21-3.

Hu, Xiaoming, Peiying Li, Yanling Guo, Haiying Wang, Rehana K. Leak, Songela Chen, Yanqin Gao, and Jun Chen. 2012. "Microglia/Macrophage Polarization Dynamics Reveal Novel Mechanism of Injury Expansion after Focal Cerebral Ischemia." *Stroke* 43 (11): 3063–70. https://doi.org/10.1161/STROKEAHA.112.659656.

Huang, J., T. F. Choudhri, C. J. Winfree, R. A. McTaggart, S. Kiss, J. Mocco, L. J. Kim, et al. 2000. "Postischemic Cerebrovascular E-Selectin Expression Mediates Tissue Injury in Murine Stroke." *Stroke* 31 (12): 3047–53.

Huxley, V. H., and D. A. Williams. 2000. "Role of a Glycocalyx on Coronary Arteriole Permeability to Proteins:

Evidence from Enzyme Treatments." *American Journal of Physiology. Heart and Circulatory Physiology* 278 (4): H1177-1185. https://doi.org/10.1152/ajpheart.2000.278.4.H1177.

Iadecola, Costantino, Timo Kahles, Eduardo F. Gallo, and Josef Anrather. 2011. "Neurovascular Protection by Ischaemic Tolerance: Role of Nitric Oxide." *The Journal of Physiology* 589 (17): 4137–45. https://doi.org/10.1113/jphysiol.2011.210831.

Ichijo, Masahiko, Satoru Ishibashi, Fuying Li, Daishi Yui, Kazunori Miki, Hidehiro Mizusawa, and Takanori Yokota. 2015. "Sphingosine-1-Phosphate Receptor-1 Selective Agonist Enhances Collateral Growth and Protects against Subsequent Stroke." *PloS One* 10 (9): e0138029. https://doi.org/10.1371/journal.pone.0138029.

Igarashi, J., S. G. Bernier, and T. Michel. 2001. "Sphingosine 1-Phosphate and Activation of Endothelial Nitric-Oxide Synthase. Differential Regulation of Akt and MAP Kinase Pathways by EDG and Bradykinin Receptors in Vascular Endothelial Cells." *The Journal of Biological Chemistry* 276 (15): 12420–26. https://doi.org/10.1074/jbc.M008375200.

Igarashi, Junsuke, and Thomas Michel. 2009. "Sphingosine-1-Phosphate and Modulation of Vascular Tone." *Cardiovascular Research* 82 (2): 212–20. https://doi.org/10.1093/cvr/cvp064.

Igarashi, Nobuaki, Taro Okada, Shun Hayashi, Toshitada Fujita, Saleem Jahangeer, and Shun-ichi Nakamura. 2003. "Sphingosine Kinase 2 Is a Nuclear Protein and Inhibits DNA Synthesis." *The Journal of Biological Chemistry* 278 (47): 46832–39. https://doi.org/10.1074/jbc.M306577200.

Igarashi, Y., and Y. Yatomi. 1998. "Sphingosine 1-Phosphate Is a Blood Constituent Released from Activated Platelets, Possibly Playing a Variety of Physiological and Pathophysiological Roles." *Acta Biochimica Polonica* 45 (2): 299–309.

Ignarro, L. J., R. E. Byrns, G. M. Buga, and K. S. Wood. 1987. "Endothelium-Derived Relaxing Factor from Pulmonary Artery and Vein Possesses Pharmacologic and Chemical Properties Identical to Those of Nitric Oxide Radical." *Circulation Research* 61 (6): 866–79. https://doi.org/10.1161/01.res.61.6.866.

Intapad, Suttira. 2019. "Sphingosine-1-Phosphate Signaling in Blood Pressure Regulation." *American Journal of Physiology. Renal Physiology* 317 (3): F638–40. https://doi.org/10.1152/ajprenal.00572.2018.

Ito, Kiyoharu, Yoshihiro Anada, Motohiro Tani, Mika Ikeda, Takamitsu Sano, Akio Kihara, and Yasuyuki Igarashi. 2007. "Lack of Sphingosine 1-Phosphate-Degrading Enzymes in Erythrocytes." *Biochemical and Biophysical Research Communications* 357 (1): 212–17. https://doi.org/10.1016/j.bbrc.2007.03.123.

Iwasawa, Eri, Satoru Ishibashi, Motohiro Suzuki, FuYing Li, Masahiko Ichijo, Kazunori Miki, and Takanori Yokota. 2018. "Sphingosine-1-Phosphate Receptor 1 Activation Enhances Leptomeningeal Collateral Development and Improves Outcome after Stroke in Mice."

Journal of Stroke and Cerebrovascular Diseases: The Official Journal of National Stroke Association 27 (5): 1237–51. https://doi.org/10.1016/j.jstrokecerebrovasdis.2017.11.040.

Jackson, Shaun P. 2011. "Arterial Thrombosis--Insidious, Unpredictable and Deadly." *Nature Medicine* 17 (11): 1423–36. https://doi.org/10.1038/nm.2515.

Jiang, Xiaoyan, Anuska V. Andjelkovic, Ling Zhu, Tuo Yang, Michael V. L. Bennett, Jun Chen, Richard F. Keep, and Yejie Shi. 2018. "Blood-Brain Barrier Dysfunction and Recovery after Ischemic Stroke." *Progress in Neurobiology* 163–164 (May): 144–71. https://doi.org/10.1016/j.pneurobio.2017.10.001.

Jiao, Haixia, Zhenhua Wang, Yunhui Liu, Ping Wang, and Yixue Xue. 2011. "Specific Role of Tight Junction Proteins Claudin-5, Occludin, and ZO-1 of the Blood-Brain Barrier in a Focal Cerebral Ischemic Insult." *Journal of Molecular Neuroscience: MN* 44 (2): 130–39. https://doi.org/10.1007/s12031-011-9496-4.

Jin, Albert Y., Ursula I. Tuor, David Rushforth, Jaspreet Kaur, Robert N. Muller, Jodie Lee Petterson, Sébastien Boutry, and Philip A. Barber. 2010. "Reduced Blood Brain Barrier Breakdown in P-Selectin Deficient Mice Following Transient Ischemic Stroke: A Future Therapeutic Target for Treatment of Stroke." *BMC Neuroscience* 11 (February): 12. https://doi.org/10.1186/1471-2202-11-12.

Jin, Richard C., Barbara Voetsch, and Joseph Loscalzo. 2005. "Endogenous Mechanisms of Inhibition of Platelet Function." *Microcirculation (New York, N.Y.: 1994)* 12 (3): 247–58. https://doi.org/10.1080/10739680590925493.

Jo, Euijung, Barun Bhhatarai, Emanuela Repetto, Miguel Guerrero, Sean Riley, Steven J. Brown, Yasushi Kohno, Edward Roberts, Stephan C. Schürer, and Hugh Rosen. 2012. "Novel Selective Allosteric and Bitopic Ligands for the S1P(3) Receptor." *ACS Chemical Biology* 7 (12): 1975–83. https://doi.org/10.1021/cb300392z.

Johnson, Barbara H., Machaon M. Bonafede, and Crystal Watson. 2016. "Short- and Longer-Term Health-Care Resource Utilization and Costs Associated with Acute Ischemic Stroke." *ClinicoEconomics and Outcomes Research: CEOR* 8: 53–61. https://doi.org/10.2147/CEOR.S95662.

Jozefczuk, E., T. J. Guzik, and M. Siedlinski. 2020. "Significance of Sphingosine-1-Phosphate in Cardiovascular Physiology and Pathology." *Pharmacological Research* 156 (June): 104793. https://doi.org/10.1016/j.phrs.2020.104793.

Jung, Bongnam, Hideru Obinata, Sylvain Galvani, Karen Mendelson, Bi-sen Ding, Athanasia Skoura, Bernd Kinzel, et al. 2012. "Flow-Regulated Endothelial S1P Receptor-1 Signaling Sustains Vascular Development." *Developmental Cell* 23 (3): 600–610. https://doi.org/10.1016/j.devcel.2012.07.015.

Kaito, Muichi, Shin-Ichi Araya, Yuichiro Gondo, Michiyo Fujita, Naomi Minato, Megumi Nakanishi, and Makoto Matsui. 2013. "Relevance of Distinct Monocyte Subsets to

Clinical Course of Ischemic Stroke Patients." *PloS One* 8 (8): e69409. https://doi.org/10.1371/journal.pone.0069409.

Kanaji, S., S. A. Fahs, Q. Shi, S. L. Haberichter, and R. R. Montgomery. 2012. "Contribution of Platelet vs. Endothelial VWF to Platelet Adhesion and Hemostasis." *Journal of Thrombosis and Haemostasis: JTH* 10 (8): 1646–52. https://doi.org/10.1111/j.1538-7836.2012.04797.x.

Kaneto, Hideaki, Naoto Katakami, Munehide Matsuhisa, and Taka-aki Matsuoka. 2010. "Role of Reactive Oxygen Species in the Progression of Type 2 Diabetes and Atherosclerosis." *Mediators of Inflammation* 2010: 453892. https://doi.org/10.1155/2010/453892.

Kano, T., Y. Katayama, E. Tejima, and E. H. Lo. 2000. "Hemorrhagic Transformation after Fibrinolytic Therapy with Tissue Plasminogen Activator in a Rat Thromboembolic Model of Stroke." *Brain Research* 854 (1–2): 245–48. https://doi.org/10.1016/s0006-8993(99)02276-3.

Kappos, Ludwig, Amit Bar-Or, Bruce A. C. Cree, Robert J. Fox, Gavin Giovannoni, Ralf Gold, Patrick Vermersch, et al. 2018. "Siponimod versus Placebo in Secondary Progressive Multiple Sclerosis (EXPAND): A Double-Blind, Randomised, Phase 3 Study." *Lancet (London, England)* 391 (10127): 1263–73. https://doi.org/10.1016/S0140-6736(18)30475-6.

Katan, Mira, and Andreas Luft. 2018. "Global Burden of Stroke." *Seminars in Neurology* 38 (2): 208–11. https://doi.org/10.1055/s-0038-1649503.

Kawahara, Atsuo, Tsuyoshi Nishi, Yu Hisano, Hajime Fukui, Akihito Yamaguchi, and Naoki Mochizuki. 2009. "The Sphingolipid Transporter Spns2 Functions in Migration of Zebrafish Myocardial Precursors." *Science (New York, N.Y.)* 323 (5913): 524–27. https://doi.org/10.1126/science.1167449.

Keaney, James, and Matthew Campbell. 2015. "The Dynamic Blood-Brain Barrier." *FEBS Journal* 282 (21): 4067–79. https://doi.org/10.1111/febs.13412.

Kelly, R., T. Ruane-O'Hora, M. I. M. Noble, A. J. Drake-Holland, and H. M. Snow. 2006. "Differential Inhibition by Hyperglycaemia of Shear Stress- but Not Acetylcholine-Mediated Dilatation in the Iliac Artery of the Anaesthetized Pig." *The Journal of Physiology* 573 (Pt 1): 133–45. https://doi.org/10.1113/jphysiol.2006.106500.

Kelly-Hayes, Margaret, Alexa Beiser, Carlos S. Kase, Amy Scaramucci, Ralph B. D'Agostino, and Philip A. Wolf. 2003. "The Influence of Gender and Age on Disability Following Ischemic Stroke: The Framingham Study." *Journal of Stroke and Cerebrovascular Diseases: The Official Journal of National Stroke Association* 12 (3): 119–26. https://doi.org/10.1016/S1052-3057(03)00042-9.

Kerage, D., D. N. Brindley, and D. G. Hemmings. 2014. "Review: Novel Insights into the Regulation of Vascular Tone by Sphingosine 1-Phosphate." *Placenta* 35 Suppl (February): S86-92. https://doi.org/10.1016/j.placenta.2013.12.006.

Kim, Gab Seok, Li Yang, Guoqi Zhang, Honggang Zhao, Magdy Selim, Louise D. McCullough, Michael J. Kluk, and Teresa Sanchez. 2015. "Critical Role of Sphingosine-1-Phosphate Receptor-2 in the Disruption of Cerebrovascular Integrity in Experimental Stroke." *Nature Communications* 6 (August): 7893. https://doi.org/10.1038/ncomms8893.

Kimura, Takao, Koichi Sato, Enkhzol Malchinkhuu, Hideaki Tomura, Kenichi Tamama, Atsushi Kuwabara, Masami Murakami, and Fumikazu Okajima. 2003. "High-Density Lipoprotein Stimulates Endothelial Cell Migration and Survival through Sphingosine 1-Phosphate and Its Receptors." *Arteriosclerosis, Thrombosis, and Vascular Biology* 23 (7): 1283–88. https://doi.org/10.1161/01.ATV.0000079011.67194.5A.

Kleinschnitz, Christoph, Peter Kraft, Angela Dreykluft, Ina Hagedorn, Kerstin Göbel, Michael K. Schuhmann, Friederike Langhauser, et al. 2013. "Regulatory T Cells Are Strong Promoters of Acute Ischemic Stroke in Mice by Inducing Dysfunction of the Cerebral Microvasculature." *Blood* 121 (4): 679–91. https://doi.org/10.1182/blood-2012-04-426734.

Kleinschnitz, Christoph, Miroslava Pozgajova, Mirko Pham, Martin Bendszus, Bernhard Nieswandt, and Guido Stoll. 2007. "Targeting Platelets in Acute Experimental Stroke: Impact of Glycoprotein Ib, VI, and IIb/IIIa Blockade on Infarct Size, Functional Outcome, and Intracranial Bleeding." *Circulation* 115 (17): 2323–30. https://doi.org/10.1161/CIRCULATIONAHA.107.691279.

Kleinschnitz, Christoph, Nicholas Schwab, Peter Kraft, Ina Hagedorn, Angela Dreykluft, Tobias Schwarz, Madeleine Austinat, Bernhard Nieswandt, Heinz Wiendl, and Guido Stoll. 2010. "Early Detrimental T-Cell Effects in Experimental Cerebral Ischemia Are Neither Related to Adaptive Immunity nor Thrombus Formation." *Blood* 115 (18): 3835–42. https://doi.org/10.1182/blood-2009-10-249078.

Kleuser, Burkhard. 2018. "Divergent Role of Sphingosine 1-Phosphate in Liver Health and Disease." *International Journal of Molecular Sciences* 19 (3): E722. https://doi.org/10.3390/ijms19030722.

Kluk, Michael J., and Timothy Hla. 2002. "Signaling of Sphingosine-1-Phosphate via the S1P/EDG-Family of G-Protein-Coupled Receptors." *Biochimica Et Biophysica Acta* 1582 (1–3): 72–80. https://doi.org/10.1016/s1388-1981(02)00139-7.

Knowland, Daniel, Ahmet Arac, Kohei J. Sekiguchi, Martin Hsu, Sarah E. Lutz, John Perrino, Gary K. Steinberg, Ben A. Barres, Axel Nimmerjahn, and Dritan Agalliu. 2014. "Stepwise Recruitment of Transcellular and Paracellular Pathways Underlies Blood-Brain Barrier Breakdown in Stroke." *Neuron* 82 (3): 603–17. https://doi.org/10.1016/j.neuron.2014.03.003.

Koizumi Jin-ichi, Yoshida Yoji, Nakazawa Teiji, and Ooneda Genju. 1986. "Experimental studies of ischemic brain edema." *Nosotchu* 8 (1): 1–8. https://doi.org/10.3995/jstroke.8.1.

Komarova, Yulia A., Kevin Kruse, Dolly Mehta, and Asrar B. Malik. 2017. "Protein Interactions at Endothelial Junctions and Signaling Mechanisms Regulating Endothelial Permeability." *Circulation Research* 120 (1): 179–206. https://doi.org/10.1161/CIRCRESAHA.116.306534.

Komarova, Yulia A., Dolly Mehta, and Asrar B. Malik. 2007. "Dual Regulation of Endothelial Junctional Permeability." *Science's STKE: Signal Transduction Knowledge Environment* 2007 (412): re8. https://doi.org/10.1126/stke.412200 7re8.

Kono, Mari, Yide Mi, Yujing Liu, Teiji Sasaki, Maria Laura Allende, Yun-Ping Wu, Tadashi Yamashita, and Richard L. Proia. 2004. "The Sphingosine-1-Phosphate Receptors S1P1, S1P2, and S1P3 Function Coordinately during Embryonic Angiogenesis." *The Journal of Biological Chemistry* 279 (28): 29367–73. https://doi.org/10.1074/jbc.M4039 37200.

Kraft, Peter, Eva Göb, Michael K. Schuhmann, Kerstin Göbel, Carsten Deppermann, Ina Thielmann, Alexander M. Herrmann, et al. 2013. "FTY720 Ameliorates Acute Ischemic Stroke in Mice by Reducing Thrombo-Inflammation but Not by Direct Neuroprotection." *Stroke* 44 (11): 3202–10. https://doi.org/10.1161/STROKEAHA.113.002880.

Kraft, Peter, Michael K. Schuhmann, Felix Fluri, Kristina Lorenz, Alma Zernecke, Guido Stoll, Bernhard Nieswandt, and Christoph Kleinschnitz. 2015. "Efficacy and Safety of Platelet Glycoprotein Receptor Blockade in Aged and Comorbid Mice With Acute Experimental Stroke." *Stroke* 46 (12): 3502–6. https://doi.org/10.1161/STROKEAHA.115.011114.

Krishnamurthi, Rita V., Valery L. Feigin, Mohammad H. Forouzanfar, George A. Mensah, Myles Connor, Derrick A. Bennett, Andrew E. Moran, et al. 2013. "Global and Regional Burden of First-Ever Ischaemic and Haemorrhagic Stroke during 1990-2010: Findings from the Global Burden of Disease Study 2010." *The Lancet. Global Health* 1 (5): e259-281. https://doi.org/10.1016/S2214-109X(13)70089-5.

Krock, Bryan L., Nicolas Skuli, and M. Celeste Simon. 2011. "Hypoxia-Induced Angiogenesis: Good and Evil." *Genes & Cancer* 2 (12): 1117–33. https://doi.org/10.1177/194760191 1423654.

Kroetsch, Jeffrey T., and Steffen-Sebastian Bolz. 2013. "The TNF-α/Sphingosine-1-Phosphate Signaling Axis Drives Myogenic Responsiveness in Heart Failure." *Journal of Vascular Research* 50 (3): 177–85. https://doi.org/10.1159/000350528 .

Krueger, Martin, Wolfgang Härtig, Andreas Reichenbach, Ingo Bechmann, and Dominik Michalski. 2013. "Blood-Brain Barrier Breakdown after Embolic Stroke in Rats Occurs without Ultrastructural Evidence for Disrupting Tight Junctions." Edited by Stefan Liebner. *PLoS ONE* 8 (2): e56419. https://doi.org/10.1371/journal.pone.0056419.

Kurano, Makoto, Koichi Tsuneyama, Yuki Morimoto, Tomo Shimizu, Masahiro Jona, Hidetoshi Kassai, Kazuki

Nakao, Atsu Aiba, and Yutaka Yatomi. 2018. “Apolipoprotein M Protects Lipopolysaccharide-Treated Mice from Death and Organ Injury.” *Thrombosis and Haemostasis* 118 (6): 1021–35. https://doi.org/10.1055/s-0038-1641750.

Lacolley, Patrick, Véronique Regnault, Antonino Nicoletti, Zhenlin Li, and Jean-Baptiste Michel. 2012. “The Vascular Smooth Muscle Cell in Arterial Pathology: A Cell That Can Take on Multiple Roles.” *Cardiovascular Research* 95 (2): 194–204. https://doi.org/10.1093/cvr/cvs135.

Lalancette-Hébert, Mélanie, Geneviève Gowing, Alain Simard, Yuan Cheng Weng, and Jasna Kriz. 2007. “Selective Ablation of Proliferating Microglial Cells Exacerbates Ischemic Injury in the Brain.” *The Journal of Neuroscience: The Official Journal of the Society for Neuroscience* 27 (10): 2596–2605. https://doi.org/10.1523/JNEUROSCI.5360-06.2007.

LaMack, Jeffrey A., Heather A. Himburg, Xue-Mei Li, and Morton H. Friedman. 2005. “Interaction of Wall Shear Stress Magnitude and Gradient in the Prediction of Arterial Macromolecular Permeability.” *Annals of Biomedical Engineering* 33 (4): 457–64. https://doi.org/10.1007/s10439-005-2500-9.

Langhorne, P., D. J. Stott, L. Robertson, J. MacDonald, L. Jones, C. McAlpine, F. Dick, G. S. Taylor, and G. Murray. 2000. “Medical Complications after Stroke: A Multicenter Study.” *Stroke* 31 (6): 1223–29. https://doi.org/10.1161/01.str.31.6.1223.

Lecrux, C., and E. Hamel. 2016. “Neuronal Networks and Mediators of Cortical Neurovascular Coupling Responses in Normal and Altered Brain States.” *Philosophical Transactions of the Royal Society of London. Series B, Biological Sciences* 371 (1705): 20150350. https://doi.org/10.1098/rstb.2015.0350.

Lee, M. J., S. Thangada, K. P. Claffey, N. Ancellin, C. H. Liu, M. Kluk, M. Volpi, R. I. Sha’afi, and T. Hla. 1999. “Vascular Endothelial Cell Adherens Junction Assembly and Morphogenesis Induced by Sphingosine-1-Phosphate.” *Cell* 99 (3): 301–12. https://doi.org/10.1016/s0092-8674(00)81661-x.

Lee, M. J., J. R. Van Brocklyn, S. Thangada, C. H. Liu, A. R. Hand, R. Menzeleev, S. Spiegel, and T. Hla. 1998. “Sphingosine-1-Phosphate as a Ligand for the G Protein-Coupled Receptor EDG-1.” *Science (New York, N.Y.)* 279 (5356): 1552–55. https://doi.org/10.1126/science.279.5356.1552.

Lee, Seunghoon, Yunkyung Hong, Sookyoung Park, Sang-Rae Lee, Kyu-Tae Chang, and Yonggeun Hong. 2014. “Comparison of Surgical Methods of Transient Middle Cerebral Artery Occlusion between Rats and Mice.” *The Journal of Veterinary Medical Science* 76 (12): 1555–61. https://doi.org/10.1292/jvms.14-0258.

Lee, V. M., N. G. Burdett, A. Carpenter, L. D. Hall, P. S. Pambakian, S. Patel, N. I. Wood, and M. F. James. 1996. “Evolution of Photochemically Induced Focal Cerebral Ischemia in the Rat. Magnetic Resonance Imaging and Histology.” *Stroke* 27

(11): 2110–18; discussion 2118-2119. https://doi.org/10.1161/01.str.27.11.2110.

Levkau, Bodo, Sven Hermann, Gregor Theilmeier, Markus van der Giet, Jerold Chun, Otmar Schober, and Michael Schäfers. 2004. "High-Density Lipoprotein Stimulates Myocardial Perfusion in Vivo." *Circulation* 110 (21): 3355–59. https://doi.org/10.1161/01.CIR.0000147827.43912.AE.

Li, Nailin. 2008. "Platelet-Lymphocyte Cross-Talk." *Journal of Leukocyte Biology* 83 (5): 1069–78. https://doi.org/10.1189/jlb.0907615.

Li, Wanlu, Tingting He, Lu Jiang, Rubing Shi, Yaying Song, Muyassar Mamtilahun, Yuanyuan Ma, et al. 2020. "Fingolimod Inhibits Inflammation but Exacerbates Brain Edema in the Acute Phases of Cerebral Ischemia in Diabetic Mice." *Frontiers in Neuroscience* 14: 842. https://doi.org/10.3389/fnins.2020.00842.

Li, Xiao, Ming-Huan Wang, Chuan Qin, Wen-Hui Fan, Dai-Shi Tian, and Jun-Li Liu. 2017. "Fingolimod Suppresses Neuronal Autophagy through the MTOR/P70S6K Pathway and Alleviates Ischemic Brain Damage in Mice." *PloS One* 12 (11): e0188748. https://doi.org/10.1371/journal.pone.0188748.

Liebeskind, David S., Thomas A. Tomsick, Lydia D. Foster, Sharon D. Yeatts, Janice Carrozzella, Andrew M. Demchuk, Tudor G. Jovin, et al. 2014. "Collaterals at Angiography and Outcomes in the Interventional Management of Stroke (IMS) III Trial." *Stroke* 45 (3): 759–64. https://doi.org/10.1161/STROKEAHA.113.004072.

Liebner, S., A. Fischmann, G. Rascher, F. Duffner, E. H. Grote, H. Kalbacher, and H. Wolburg. 2000. "Claudin-1 and Claudin-5 Expression and Tight Junction Morphology Are Altered in Blood Vessels of Human Glioblastoma Multiforme." *Acta Neuropathologica* 100 (3): 323–31. https://doi.org/10.1007/s004010000180.

Lien, Y.-Hh, K.-C. Yong, C. Cho, S. Igarashi, and L.-W. Lai. 2006. "S1P(1)-Selective Agonist, SEW2871, Ameliorates Ischemic Acute Renal Failure." *Kidney International* 69 (9): 1601–8. https://doi.org/10.1038/sj.ki.5000360.

Liesz, Arthur, Li Sun, Wei Zhou, Sönke Schwarting, Eva Mracsko, Markus Zorn, Henrike Bauer, Clemens Sommer, and Roland Veltkamp. 2011. "FTY720 Reduces Post-Ischemic Brain Lymphocyte Influx but Does Not Improve Outcome in Permanent Murine Cerebral Ischemia." *PloS One* 6 (6): e21312. https://doi.org/10.1371/journal.pone.0021312.

Lima, Fabricio O., Karen L. Furie, Gisele S. Silva, Michael H. Lev, Erica C. S. Camargo, Aneesh B. Singhal, Gordon J. Harris, et al. 2010. "The Pattern of Leptomeningeal Collaterals on CT Angiography Is a Strong Predictor of Long-Term Functional Outcome in Stroke Patients with Large Vessel Intracranial Occlusion." *Stroke* 41 (10): 2316–22. https://doi.org/10.1161/STROKEAHA.110.592303.

Lipton, P. 1999. "Ischemic Cell Death in Brain Neurons." *Physiological Reviews* 79 (4): 1431–1568. https://doi.org/10.1152/physrev.1999.79.4.1431.

Liu, H., M. Sugiura, V. E. Nava, L. C. Edsall, K. Kono, S. Poulton, S. Milstien, T. Kohama, and S. Spiegel. 2000. "Molecular Cloning and Functional Characterization of a Novel Mammalian Sphingosine Kinase Type 2 Isoform." *The Journal of Biological Chemistry* 275 (26): 19513–20. https://doi.org/10.1074/jbc.M002759200.

Liu, Shimin, Gehua Zhen, Bruno P. Meloni, Kym Campbell, and H. Richard Winn. 2009. "RODENT STROKE MODEL GUIDELINES FOR PRECLINICAL STROKE TRIALS (1ST EDITION)." *Journal of Experimental Stroke & Translational Medicine* 2 (2): 2–27. https://doi.org/10.6030/1939-067x-2.2.2.

Liu, Y., R. Wada, T. Yamashita, Y. Mi, C. X. Deng, J. P. Hobson, H. M. Rosenfeldt, et al. 2000. "Edg-1, the G Protein-Coupled Receptor for Sphingosine-1-Phosphate, Is Essential for Vascular Maturation." *The Journal of Clinical Investigation* 106 (8): 951–61. https://doi.org/10.1172/JCI10905.

Longa, E. Z., P. R. Weinstein, S. Carlson, and R. Cummins. 1989. "Reversible Middle Cerebral Artery Occlusion without Craniectomy in Rats." *Stroke* 20 (1): 84–91. https://doi.org/10.1161/01.str.20.1.84.

Lorenz, John N., Lois J. Arend, Rachel Robitz, Richard J. Paul, and A. John MacLennan. 2007. "Vascular Dysfunction in S1P2 Sphingosine 1-Phosphate Receptor Knockout Mice." *American Journal of Physiology. Regulatory, Integrative and Comparative Physiology* 292 (1): R440-446. https://doi.org/10.1152/ajpregu.00085.2006.

Lossinsky, A. S., and R. R. Shivers. 2004. "Structural Pathways for Macromolecular and Cellular Transport across the Blood-Brain Barrier during Inflammatory Conditions. Review." *Histology and Histopathology* 19 (2): 535–64. https://doi.org/10.14670/HH-19.535.

Lourbopoulos, Athanasios, Uta Mamrak, Stefan Roth, Matilde Balbi, Joshua Shrouder, Arthur Liesz, Farida Hellal, and Nikolaus Plesnila. 2017. "Inadequate Food and Water Intake Determine Mortality Following Stroke in Mice." *Journal of Cerebral Blood Flow & Metabolism* 37 (6): 2084–97. https://doi.org/10.1177/0271678X16660986.

Lu, Lei, Arnavaz Hajizadeh Barfejani, Tao Qin, Qiang Dong, Cenk Ayata, and Christian Waeber. 2014. "Fingolimod Exerts Neuroprotective Effects in a Mouse Model of Intracerebral Hemorrhage." *Brain Research* 1555 (March): 89–96. https://doi.org/10.1016/j.brainres.2014.01.048.

Lucivero, V., M. Prontera, D. M. Mezzapesa, M. Petruzzellis, M. Sancilio, A. Tinelli, D. Di Noia, M. Ruggieri, and F. Federico. 2007. "Different Roles of Matrix Metalloproteinases-2 and -9 after Human Ischaemic Stroke." *Neurological Sciences* 28 (4): 165–70. https://doi.org/10.1007/s10072-007-0814-0.

Ludewig, Peter, Jan Sedlacik, Mathias Gelderblom, Christian Bernreuther, Yücel Korkusuz, Christoph Wagener, Christian Gerloff, Jens Fiehler, Tim Magnus, and Andrea Kristina Horst. 2013. "Carcinoembryonic Antigen-Related Cell Adhesion Molecule 1

Inhibits MMP-9-Mediated Blood-Brain-Barrier Breakdown in a Mouse Model for Ischemic Stroke." *Circulation Research* 113 (8): 1013–22. https://doi.org/10.1161/CIRCRESAHA.113.301207.

Luissint, Anny-Claude, Cédric Artus, Fabienne Glacial, Kayathiri Ganeshamoorthy, and Pierre-Olivier Couraud. 2012. "Tight Junctions at the Blood Brain Barrier: Physiological Architecture and Disease-Associated Dysregulation." *Fluids and Barriers of the CNS* 9 (1): 23. https://doi.org/10.1186/2045-8118-9-23.

Lum, H., and A. B. Malik. 1996. "Mechanisms of Increased Endothelial Permeability." *Canadian Journal of Physiology and Pharmacology* 74 (7): 787–800. https://doi.org/10.1139/y96-081.

Lum, H., A. Siflinger-Birnboim, F. Blumenstock, and A. B. Malik. 1991. "Serum Albumin Decreases Transendothelial Permeability to Macromolecules." *Microvascular Research* 42 (1): 91–102. https://doi.org/10.1016/0026-2862(91)90077-o.

Ma, Vincent Y., Leighton Chan, and Kadir J. Carruthers. 2014. "Incidence, Prevalence, Costs, and Impact on Disability of Common Conditions Requiring Rehabilitation in the United States: Stroke, Spinal Cord Injury, Traumatic Brain Injury, Multiple Sclerosis, Osteoarthritis, Rheumatoid Arthritis, Limb Loss, and Back Pain." *Archives of Physical Medicine and Rehabilitation* 95 (5): 986-995.e1. https://doi.org/10.1016/j.apmr.2013.10.032.

Maceyka, Michael, and Sarah Spiegel. 2014. "Sphingolipid Metabolites in Inflammatory Disease." *Nature* 510 (7503): 58–67. https://doi.org/10.1038/nature13475.

Mackman, N. 2009. "The Many Faces of Tissue Factor." *Journal of Thrombosis and Haemostasis: JTH* 7 Suppl 1 (July): 136–39. https://doi.org/10.1111/j.1538-7836.2009.03368.x.

Macleod, Malcolm R., Marc Fisher, Victoria O'Collins, Emily S. Sena, Ulrich Dirnagl, Philip M. W. Bath, Alistair Buchan, et al. 2009. "Good Laboratory Practice: Preventing Introduction of Bias at the Bench." *Stroke* 40 (3): e50-52. https://doi.org/10.1161/STROKEAHA.108.525386.

MacVicar, Brian A., and Eric A. Newman. 2015. "Astrocyte Regulation of Blood Flow in the Brain." *Cold Spring Harbor Perspectives in Biology* 7 (5): a020388. https://doi.org/10.1101/cshperspect.a020388.

Mahler, M.-P., K. Züger, K. Kaspar, A. Haefeli, W. Jenni, T. Leniger, and J. H. Beer. 2008. "A Cost Analysis of the First Year after Stroke - Early Triage and Inpatient Rehabilitation May Reduce Long Term Costs." *Swiss Medical Weekly* 138 (31–32): 459–65. https://doi.org/2008/31/smw-11845.

Mandala, Suzanne, Richard Hajdu, James Bergstrom, Elizabeth Quackenbush, Jenny Xie, James Milligan, Rosemary Thornton, et al. 2002. "Alteration of Lymphocyte Trafficking by Sphingosine-1-Phosphate Receptor Agonists." *Science (New York, N.Y.)* 296 (5566): 346–49. https://doi.org/10.1126/science.1070238.

Mathiesen Janiurek, Mette, Rana Soylu-Kucharz, Christina Christoffersen, Krzysztof Kucharz, and Martin Lauritzen. 2019a. “Apolipoprotein M-Bound Sphingosine-1-Phosphate Regulates Blood–Brain Barrier Paracellular Permeability and Transcytosis.” *ELife* 8 (November): e49405. https://doi.org/10.7554/eLife.49405.

———. 2019b. “Apolipoprotein M-Bound Sphingosine-1-Phosphate Regulates Blood–Brain Barrier Paracellular Permeability and Transcytosis.” *ELife* 8 (November): e49405. https://doi.org/10.7554/eLife.49405.

———. 2019c. “Apolipoprotein M-Bound Sphingosine-1-Phosphate Regulates Blood–Brain Barrier Paracellular Permeability and Transcytosis.” *ELife* 8 (November): e49405. https://doi.org/10.7554/eLife.49405.

Mathiisen, Thomas Misje, Knut Petter Lehre, Niels Christian Danbolt, and Ole Petter Ottersen. 2010. “The Perivascular Astroglial Sheath Provides a Complete Covering of the Brain Microvessels: An Electron Microscopic 3D Reconstruction.” *Glia* 58 (9): 1094–1103. https://doi.org/10.1002/glia.20990.

McConnell, Heather L., Cymon N. Kersch, Randall L. Woltjer, and Edward A. Neuwelt. 2017. “The Translational Significance of the Neurovascular Unit.” *The Journal of Biological Chemistry* 292 (3): 762–70. https://doi.org/10.1074/jbc.R116.760215.

Meissner, Anja, Francesc Miro, Francesc Jiménez-Altayó, Andrés Jurado, Elisabet Vila, and Anna M. Planas. 2017. “Sphingosine-1-Phosphate Signalling-a Key Player in the Pathogenesis of Angiotensin II-Induced Hypertension.” *Cardiovascular Research* 113 (2): 123–33. https://doi.org/10.1093/cvr/cvw256.

Meissner, Anja, Jingli Yang, Jeffrey T. Kroetsch, Meghan Sauvé, Hendrik Dax, Abdul Momen, M. Hossein Noyan-Ashraf, et al. 2012. “Tumor Necrosis Factor-α-Mediated Downregulation of the Cystic Fibrosis Transmembrane Conductance Regulator Drives Pathological Sphingosine-1-Phosphate Signaling in a Mouse Model of Heart Failure.” *Circulation* 125 (22): 2739–50. https://doi.org/10.1161/CIRCULATIONAHA.111.047316.

Mendoza, Alejandra, Béatrice Bréart, Willy D. Ramos-Perez, Lauren A. Pitt, Michael Gobert, Manjula Sunkara, Juan J. Lafaille, Andrew J. Morris, and Susan R. Schwab. 2012. “The Transporter Spns2 Is Required for Secretion of Lymph but Not Plasma Sphingosine-1-Phosphate.” *Cell Reports* 2 (5): 1104–10. https://doi.org/10.1016/j.celrep.2012.09.021.

Menon, Bijoy K., Billy O’Brien, Andrew Bivard, Neil J. Spratt, Andrew M. Demchuk, Ferdinand Miteff, Xuewen Lu, Christopher Levi, and Mark W. Parsons. 2013. “Assessment of Leptomeningeal Collaterals Using Dynamic CT Angiography in Patients with Acute Ischemic Stroke.” *Journal of Cerebral Blood Flow and Metabolism: Official Journal of the International Society of Cerebral Blood Flow and Metabolism* 33 (3): 365–71. https://doi.org/10.1038/jcbfm.2012.171.

Menon, Bijoy K., Eric E. Smith, Shelagh B. Coutts, Donald G. Welsh, James E. Faber, Mayank Goyal, Michael D. Hill, et al. 2013. "Leptomeningeal Collaterals Are Associated with Modifiable Metabolic Risk Factors." *Annals of Neurology* 74 (2): 241–48. https://doi.org/10.1002/ana.23906.

Mestre, Humberto, Ting Du, Amanda M. Sweeney, Guojun Liu, Andrew J. Samson, Weiguo Peng, Kristian Nygaard Mortensen, et al. 2020. "Cerebrospinal Fluid Influx Drives Acute Ischemic Tissue Swelling." *Science (New York, N.Y.)* 367 (6483): eaax7171. https://doi.org/10.1126/science.aax7171.

Metea, Monica R., and Eric A. Newman. 2006. "Glial Cells Dilate and Constrict Blood Vessels: A Mechanism of Neurovascular Coupling." *The Journal of Neuroscience: The Official Journal of the Society for Neuroscience* 26 (11): 2862–70. https://doi.org/10.1523/JNEUROSCI.4048-05.2006.

Miller, David C., Karen B. Whittington, David D. Brand, Karen A. Hasty, and Edward F. Rosloniec. 2016. "The CII-Specific Autoimmune T-Cell Response Develops in the Presence of FTY720 but Is Regulated by Enhanced Treg Cells That Inhibit the Development of Autoimmune Arthritis." *Arthritis Research & Therapy* 18 (January): 8. https://doi.org/10.1186/s13075-015-0909-6.

Mineo, Chieko. 2020. "Lipoprotein Receptor Signalling in Atherosclerosis." *Cardiovascular Research* 116 (7): 1254–74. https://doi.org/10.1093/cvr/cvz338.

Miteff, Ferdinand, Christopher R. Levi, Grant A. Bateman, Neil Spratt, Patrick McElduff, and Mark W. Parsons. 2009. "The Independent Predictive Utility of Computed Tomography Angiographic Collateral Status in Acute Ischaemic Stroke." *Brain: A Journal of Neurology* 132 (Pt 8): 2231–38. https://doi.org/10.1093/brain/awp155.

Mizugishi, Kiyomi, Tadashi Yamashita, Ana Olivera, Georgina F. Miller, Sarah Spiegel, and Richard L. Proia. 2005. "Essential Role for Sphingosine Kinases in Neural and Vascular Development." *Molecular and Cellular Biology* 25 (24): 11113–21. https://doi.org/10.1128/MCB.25.24.11113-11121.2005.

Moccia, Francesco, Sharon Negri, Mudhir Shekha, Pawan Faris, and Germano Guerra. 2019. "Endothelial Ca2+ Signaling, Angiogenesis and Vasculogenesis: Just What It Takes to Make a Blood Vessel." *International Journal of Molecular Sciences* 20 (16). https://doi.org/10.3390/ijms20163962.

Mocco, J., Tanvir Choudhri, Judy Huang, Elisabeth Harfeldt, Lyubov Efros, Corine Klingbeil, Vladimir Vexler, et al. 2002. "HuEP5C7 as a Humanized Monoclonal Anti-E/P-Selectin Neurovascular Protective Strategy in a Blinded Placebo-Controlled Trial of Nonhuman Primate Stroke." *Circulation Research* 91 (10): 907–14. https://doi.org/10.1161/01.res.0000042063.15901.20.

Mochizuki, Seiichi, Hans Vink, Osamu Hiramatsu, Tatsuya Kajita, Fumiyuki Shigeto, Jos A. E. Spaan, and Fumihiko Kajiya. 2003. "Role of Hyaluronic Acid Glycosaminoglycans in Shear-Induced Endothelium-Derived Nitric Oxide Release."

American Journal of Physiology. Heart and Circulatory Physiology 285 (2): H722-726. https://doi.org/10.1152/ajpheart.00691.2002.

Moncada, S., and E. A. Higgs. 1991. "Endogenous Nitric Oxide: Physiology, Pathology and Clinical Relevance." *European Journal of Clinical Investigation* 21 (4): 361–74. https://doi.org/10.1111/j.1365-2362.1991.tb01383.x.

Morita, Y., Y. Fukuuchi, A. Koto, N. Suzuki, K. Isozumi, J. Gotoh, T. Shimizu, M. Takao, and M. Aoyama. 1997. "Rapid Changes in Pial Arterial Diameter and Cerebral Blood Flow Caused by Ipsilateral Carotid Artery Occlusion in Rats." *The Keio Journal of Medicine* 46 (3): 120–27. https://doi.org/10.2302/kjm.46.120.

Morris, Gary P., Amanda L. Wright, Richard P. Tan, Amadeus Gladbach, Lars M. Ittner, and Bryce Vissel. 2016. "A Comparative Study of Variables Influencing Ischemic Injury in the Longa and Koizumi Methods of Intraluminal Filament Middle Cerebral Artery Occlusion in Mice." *PloS One* 11 (2): e0148503. https://doi.org/10.1371/journal.pone.0148503.

Mowbray, Amy L., Dong-Hoon Kang, Sue Goo Rhee, Sang Won Kang, and Hanjoong Jo. 2008. "Laminar Shear Stress Up-Regulates Peroxiredoxins (PRX) in Endothelial Cells: PRX 1 as a Mechanosensitive Antioxidant." *The Journal of Biological Chemistry* 283 (3): 1622–27. https://doi.org/10.1074/jbc.M707985200.

Müller, Holger Christian, Andreas Christian Hocke, Katharina Hellwig, Birgitt Gutbier, Harm Peters, Stefanie Maria Schönrock, Thomas Tschernig, et al. 2011. "The Sphingosine-1 Phosphate Receptor Agonist FTY720 Dose Dependently Affected Endothelial Integrity in Vitro and Aggravated Ventilator-Induced Lung Injury in Mice." *Pulmonary Pharmacology & Therapeutics* 24 (4): 377–85. https://doi.org/10.1016/j.pupt.2011.01.017.

Mulligan, Sean J., and Brian A. MacVicar. 2004. "Calcium Transients in Astrocyte Endfeet Cause Cerebrovascular Constrictions." *Nature* 431 (7005): 195–99. https://doi.org/10.1038/nature02827.

Muoio, V., P. B. Persson, and M. M. Sendeski. 2014. "The Neurovascular Unit - Concept Review." *Acta Physiologica (Oxford, England)* 210 (4): 790–98. https://doi.org/10.1111/apha.12250.

Murata, Kyoko, Shiro Hinotsu, Nobutake Sadamasa, Kazumichi Yoshida, Sen Yamagata, Shoji Asari, Susumu Miyamoto, and Koji Kawakami. 2017. "Healthcare Resource Utilization and Clinical Outcomes Associated with Acute Care and Inpatient Rehabilitation of Stroke Patients in Japan." *International Journal for Quality in Health Care: Journal of the International Society for Quality in Health Care* 29 (1): 26–31. https://doi.org/10.1093/intqhc/mzw127.

Murata, N., K. Sato, J. Kon, H. Tomura, M. Yanagita, A. Kuwabara, M. Ui, and F. Okajima. 2000. "Interaction of Sphingosine 1-Phosphate with Plasma Components, Including Lipoproteins, Regulates the Lipid Receptor-Mediated Actions." *The*

Biochemical Journal 352 Pt 3 (December): 809–15.

Murata, T., Y. Nakashima, C. Yasunaga, K. Maeda, and K. Sueishi. 1991. "Extracellular and Cell-Associated Localizations of Plasminogen Activators and Plasminogen Activator Inhibitor-1 in Cultured Endothelium." *Experimental and Molecular Pathology* 55 (2): 105–18. https://doi.org/10.1016/0014-4800(91)90046-z.

Nag, Sukriti. 2003. "Morphology and Molecular Properties of Cellular Components of Normal Cerebral Vessels." *Methods in Molecular Medicine* 89: 3–36. https://doi.org/10.1385/1-59259-419-0:3.

Nag, Sukriti, Roopa Venugopalan, and Duncan J. Stewart. 2007. "Increased Caveolin-1 Expression Precedes Decreased Expression of Occludin and Claudin-5 during Blood-Brain Barrier Breakdown." *Acta Neuropathologica* 114 (5): 459–69. https://doi.org/10.1007/s00401-007-0274-x.

Nagy, Janice A., Laura Benjamin, Huiyan Zeng, Ann M. Dvorak, and Harold F. Dvorak. 2008. "Vascular Permeability, Vascular Hyperpermeability and Angiogenesis." *Angiogenesis* 11 (2): 109–19. https://doi.org/10.1007/s10456-008-9099-z.

Narumiya, S., Y. Sugimoto, and F. Ushikubi. 1999. "Prostanoid Receptors: Structures, Properties, and Functions." *Physiological Reviews* 79 (4): 1193–1226. https://doi.org/10.1152/physrev.1999.79.4.1193.

Nava, Eduardo, and Silvia Llorens. 2019. "The Local Regulation of Vascular Function: From an Inside-Outside to an Outside-Inside Model." *Frontiers in Physiology* 10: 729. https://doi.org/10.3389/fphys.2019.00729.

Nazari, Maryam, Somaye Keshavarz, Ali Rafati, Mohammad Reza Namavar, and Masoud Haghani. 2016. "Fingolimod (FTY720) Improves Hippocampal Synaptic Plasticity and Memory Deficit in Rats Following Focal Cerebral Ischemia." *Brain Research Bulletin* 124 (June): 95–102. https://doi.org/10.1016/j.brainresbull.2016.04.004.

Neher, Jonas J., Julius V. Emmrich, Michael Fricker, Palwinder K. Mander, Clotilde Théry, and Guy C. Brown. 2013. "Phagocytosis Executes Delayed Neuronal Death after Focal Brain Ischemia." *Proceedings of the National Academy of Sciences of the United States of America* 110 (43): E4098-4107. https://doi.org/10.1073/pnas.1308679110.

Nicholls, Stephen J., and Adam J. Nelson. 2019. "HDL and Cardiovascular Disease." *Pathology* 51 (2): 142–47. https://doi.org/10.1016/j.pathol.2018.10.017.

Nickel, Katrin F., Andy T. Long, Tobias A. Fuchs, Lynn M. Butler, and Thomas Renné. 2017. "Factor XII as a Therapeutic Target in Thromboembolic and Inflammatory Diseases." *Arteriosclerosis, Thrombosis, and Vascular Biology* 37 (1): 13–20. https://doi.org/10.1161/ATVBAHA.116.308595.

Niessen, Frank, Thomas Hilger, Mathias Hoehn, and Konstantin-A. Hossmann. 2003. "Differences in Clot Preparation Determine Outcome of Recombinant Tissue Plasminogen Activator Treatment in

Experimental Thromboembolic Stroke." *Stroke* 34 (8): 2019–24. https://doi.org/10.1161/01.STR.0000080941.73934.30.

Nieswandt, B. 2012. "Platelets Guide Lymphocytes to Vascular Injury Sites." *Thrombosis and Haemostasis* 108 (2): 207. https://doi.org/10.1160/TH12-07-0450.

Nieswandt, B., C. Brakebusch, W. Bergmeier, V. Schulte, D. Bouvard, R. Mokhtari-Nejad, T. Lindhout, J. W. Heemskerk, H. Zirngibl, and R. Fässler. 2001. "Glycoprotein VI but Not Alpha2beta1 Integrin Is Essential for Platelet Interaction with Collagen." *The EMBO Journal* 20 (9): 2120–30. https://doi.org/10.1093/emboj/20.9.2120.

Nigris, Filomena de, Lilach O. Lerman, Sharon Williams Ignarro, Giacomo Sica, Amir Lerman, Wulf Palinski, Louis J. Ignarro, and Claudio Napoli. 2003. "Beneficial Effects of Antioxidants and L-Arginine on Oxidation-Sensitive Gene Expression and Endothelial NO Synthase Activity at Sites of Disturbed Shear Stress." *Proceedings of the National Academy of Sciences of the United States of America* 100 (3): 1420–25. https://doi.org/10.1073/pnas.0237367100.

Nikitin, Dmitri, Seungbum Choi, Jan Mican, Martin Toul, Wi-Sun Ryu, Jiri Damborsky, Robert Mikulik, and Dong-Eog Kim. 2021. "Development and Testing of Thrombolytics in Stroke." *Journal of Stroke* 23 (1): 12–36. https://doi.org/10.5853/jos.2020.03349.

Nitzsche, Anja, Marine Poittevin, Ammar Benarab, Philippe Bonnin, Giuseppe Faraco, Hiroki Uchida, Julie Favre, et al. 2021. "Endothelial S1P $_1$ Signaling Counteracts Infarct Expansion in Ischemic Stroke." *Circulation Research* 128 (3): 363–82. https://doi.org/10.1161/CIRCRESAHA.120.316711.

Nofer, Jerzy-Roch, Markus van der Giet, Markus Tölle, Iza Wolinska, Karin von Wnuck Lipinski, Hideo A. Baba, Uwe J. Tietge, et al. 2004. "HDL Induces NO-Dependent Vasorelaxation via the Lysophospholipid Receptor S1P3." *The Journal of Clinical Investigation* 113 (4): 569–81. https://doi.org/10.1172/JCI18004.

Obinata, Hideru, Andrew Kuo, Yukata Wada, Steven Swendeman, Catherine H. Liu, Victoria A. Blaho, Rieko Nagumo, Kenichi Satoh, Takashi Izumi, and Timothy Hla. 2019. "Identification of ApoA4 as a Sphingosine 1-Phosphate Chaperone in ApoM- and Albumin-Deficient Mice." *Journal of Lipid Research* 60 (11): 1912–21. https://doi.org/10.1194/jlr.RA119000277.

O'Collins, Victoria E., Malcolm R. Macleod, Geoffrey A. Donnan, Laura L. Horky, Bart H. van der Worp, and David W. Howells. 2006. "1,026 Experimental Treatments in Acute Stroke." *Annals of Neurology* 59 (3): 467–77. https://doi.org/10.1002/ana.20741.

O'Connor, Rory J., Rushdy Beden, Andrew Pilling, and M. Anne Chamberlain. 2011. "What Reductions in Dependency Costs Result from Treatment in an Inpatient Neurological Rehabilitation Unit for People with Stroke?" *Clinical Medicine (London, England)* 11 (1): 40–43. https://doi.org/10.7861/clinmedicine.11-1-40.

Offner, H., A. A. Vandenbark, and P. D. Hurn. 2009. “Effect of Experimental Stroke on Peripheral Immunity: CNS Ischemia Induces Profound Immunosuppression.” *Neuroscience* 158 (3): 1098–1111. https://doi.org/10.1016/j.neuroscience.2008.05.033.

Olivera, A., and S. Spiegel. 1993. “Sphingosine-1-Phosphate as Second Messenger in Cell Proliferation Induced by PDGF and FCS Mitogens.” *Nature* 365 (6446): 557–60. https://doi.org/10.1038/365557a0.

Oo, Myat Lin, Sung-Hee Chang, Shobha Thangada, Ming-Tao Wu, Karim Rezaul, Victoria Blaho, Sun-Il Hwang, David K. Han, and Timothy Hla. 2011. “Engagement of $S1P_1$-Degradative Mechanisms Leads to Vascular Leak in Mice.” *The Journal of Clinical Investigation* 121 (6): 2290–2300. https://doi.org/10.1172/JCI45403.

Opal, S. M., and T. van der Poll. 2015. “Endothelial Barrier Dysfunction in Septic Shock.” *Journal of Internal Medicine* 277 (3): 277–93. https://doi.org/10.1111/joim.12331.

Osada, Makoto, Yutaka Yatomi, Tsukasa Ohmori, Hitoshi Ikeda, and Yukio Ozaki. 2002. “Enhancement of Sphingosine 1-Phosphate-Induced Migration of Vascular Endothelial Cells and Smooth Muscle Cells by an EDG-5 Antagonist.” *Biochemical and Biophysical Research Communications* 299 (3): 483–87. https://doi.org/10.1016/s0006-291x(02)02671-2.

Osborne, K. A., T. Shigeno, A. M. Balarsky, I. Ford, J. McCulloch, G. M. Teasdale, and D. I. Graham. 1987. “Quantitative Assessment of Early Brain Damage in a Rat Model of Focal Cerebral Ischaemia.” *Journal of Neurology, Neurosurgery, and Psychiatry* 50 (4): 402–10. https://doi.org/10.1136/jnnp.50.4.402.

Overgaard, K. 1994. “Thrombolytic Therapy in Experimental Embolic Stroke.” *Cerebrovascular and Brain Metabolism Reviews* 6 (3): 257–86.

Page-McCaw, Andrea, Andrew J. Ewald, and Zena Werb. 2007. “Matrix Metalloproteinases and the Regulation of Tissue Remodelling.” *Nature Reviews. Molecular Cell Biology* 8 (3): 221–33. https://doi.org/10.1038/nrm2125.

Paik, Ji-Hye, Athanasia Skoura, Sung-Suk Chae, Ann E. Cowan, David K. Han, Richard L. Proia, and Timothy Hla. 2004. “Sphingosine 1-Phosphate Receptor Regulation of N-Cadherin Mediates Vascular Stabilization.” *Genes & Development* 18 (19): 2392–2403. https://doi.org/10.1101/gad.1227804.

Pan, Shifeng, Yuan Mi, Charles Pally, Christian Beerli, Alice Chen, Danilo Guerini, Klaus Hinterding, et al. 2006. “A Monoselective Sphingosine-1-Phosphate Receptor-1 Agonist Prevents Allograft Rejection in a Stringent Rat Heart Transplantation Model.” *Chemistry & Biology* 13 (11): 1227–34. https://doi.org/10.1016/j.chembiol.2006.09.017.

Pappu, Rajita, Susan R. Schwab, Ivo Cornelissen, João P. Pereira, Jean B. Regard, Ying Xu, Eric Camerer, et al. 2007. “Promotion of Lymphocyte Egress into Blood and Lymph by Distinct Sources of Sphingosine-1-Phosphate.” *Science (New York, N.Y.)* 316 (5822): 295–98. https://doi.org/10.1126/science.1139221.

Park, Soo-Jin, and Dong-Soon Im. 2017. "Sphingosine 1-Phosphate Receptor Modulators and Drug Discovery." *Biomolecules & Therapeutics* 25 (1): 80–90. https://doi.org/10.4062/biomolther.2016.160.

Paugh, Steven W., Shawn G. Payne, Suzanne E. Barbour, Sheldon Milstien, and Sarah Spiegel. 2003. "The Immunosuppressant FTY720 Is Phosphorylated by Sphingosine Kinase Type 2." *FEBS Letters* 554 (1–2): 189–93. https://doi.org/10.1016/s0014-5793(03)01168-2.

Petrovic-Djergovic, Danica, Sascha N. Goonewardena, and David J. Pinsky. 2016. "Inflammatory Disequilibrium in Stroke." *Circulation Research* 119 (1): 142–58. https://doi.org/10.1161/CIRCRESAHA.116.308022.

Petzold, Gabor C., and Venkatesh N. Murthy. 2011. "Role of Astrocytes in Neurovascular Coupling." *Neuron* 71 (5): 782–97. https://doi.org/10.1016/j.neuron.2011.08.009.

Pfeilschifter, Waltraud, Bożena Czech-Zechmeister, Marian Sujak, Christian Foerch, Thomas A. Wichelhaus, and Josef Pfeilschifter. 2011. "Treatment with the Immunomodulator FTY720 Does Not Promote Spontaneous Bacterial Infections after Experimental Stroke in Mice." *Experimental & Translational Stroke Medicine* 3 (March): 2. https://doi.org/10.1186/2040-7378-3-2.

Pfeilschifter, Waltraud, Bożena Czech-Zechmeister, Marian Sujak, Ana Mirceska, Alexander Koch, Abdelhaq Rami, Helmuth Steinmetz, Christian Foerch, Andrea Huwiler, and Josef Pfeilschifter. 2011. "Activation of Sphingosine Kinase 2 Is an Endogenous Protective Mechanism in Cerebral Ischemia." *Biochemical and Biophysical Research Communications* 413 (2): 212–17. https://doi.org/10.1016/j.bbrc.2011.08.070.

Pitson, Stuart M., Paul A. B. Moretti, Julia R. Zebol, Helen E. Lynn, Pu Xia, Mathew A. Vadas, and Binks W. Wattenberg. 2003. "Activation of Sphingosine Kinase 1 by ERK1/2-Mediated Phosphorylation." *The EMBO Journal* 22 (20): 5491–5500. https://doi.org/10.1093/emboj/cdg540.

Poirier, Bruno, Veronique Briand, Dieter Kadereit, Matthias Schäfer, Paulus Wohlfart, Marie-Claire Philippo, Dominique Caillaud, et al. 2020. "A G Protein-Biased S1P1 Agonist, SAR247799, Protects Endothelial Cells without Affecting Lymphocyte Numbers." *Science Signaling* 13 (634): eaax8050. https://doi.org/10.1126/scisignal.aax8050.

Potente, Michael, Holger Gerhardt, and Peter Carmeliet. 2011. "Basic and Therapeutic Aspects of Angiogenesis." *Cell* 146 (6): 873–87. https://doi.org/10.1016/j.cell.2011.08.039.

Powers, William J., Alejandro A. Rabinstein, Teri Ackerson, Opeolu M. Adeoye, Nicholas C. Bambakidis, Kyra Becker, José Biller, et al. 2018. "2018 Guidelines for the Early Management of Patients With Acute Ischemic Stroke: A Guideline for Healthcare Professionals From the American Heart Association/American Stroke Association." *Stroke* 49 (3): e46–110.

https://doi.org/10.1161/STR.0000000000000158.

Pradhan, Sanjeev, and Bauer Sumpio. 2004. "Molecular and Biological Effects of Hemodynamics on Vascular Cells." *Frontiers in Bioscience: A Journal and Virtual Library* 9 (September): 3276–85. https://doi.org/10.2741/1480.

Prass, Konstantin, Christian Meisel, Conny Höflich, Johann Braun, Elke Halle, Tilo Wolf, Karsten Ruscher, et al. 2003. "Stroke-Induced Immunodeficiency Promotes Spontaneous Bacterial Infections and Is Mediated by Sympathetic Activation Reversal by Poststroke T Helper Cell Type 1-like Immunostimulation." *The Journal of Experimental Medicine* 198 (5): 725–36. https://doi.org/10.1084/jem.20021098.

Proia, Richard L., and Timothy Hla. 2015. "Emerging Biology of Sphingosine-1-Phosphate: Its Role in Pathogenesis and Therapy." *The Journal of Clinical Investigation* 125 (4): 1379–87. https://doi.org/10.1172/JCI76369.

Provenzale, James M., Reza Jahan, Thomas P. Naidich, and Allan J. Fox. 2003. "Assessment of the Patient with Hyperacute Stroke: Imaging and Therapy." *Radiology* 229 (2): 347–59. https://doi.org/10.1148/radiol.2292020402.

Quancard, Jean, Birgit Bollbuck, Philipp Janser, Daniela Angst, Frédéric Berst, Peter Buehlmayer, Markus Streiff, et al. 2012. "A Potent and Selective S1P(1) Antagonist with Efficacy in Experimental Autoimmune Encephalomyelitis." *Chemistry & Biology* 19 (9): 1142–51. https://doi.org/10.1016/j.chembiol.2012.07.016.

Rader, Daniel J., and Alan R. Tall. 2012. "The Not-so-Simple HDL Story: Is It Time to Revise the HDL Cholesterol Hypothesis?" *Nature Medicine* 18 (9): 1344–46. https://doi.org/10.1038/nm.2937.

Rayes, Julie, Steve P. Watson, and Bernhard Nieswandt. 2019. "Functional Significance of the Platelet Immune Receptors GPVI and CLEC-2." *The Journal of Clinical Investigation* 129 (1): 12–23. https://doi.org/10.1172/JCI122955.

Redon, Josep, Michael H. Olsen, Richard S. Cooper, Oscar Zurriaga, Miguel A. Martinez-Beneito, Stephane Laurent, Renata Cifkova, Antonio Coca, and Guiseppe Mancia. 2011. "Stroke Mortality and Trends from 1990 to 2006 in 39 Countries from Europe and Central Asia: Implications for Control of High Blood Pressure." *European Heart Journal* 32 (11): 1424–31. https://doi.org/10.1093/eurheartj/ehr045.

Reese, T. S., and M. J. Karnovsky. 1967. "Fine Structural Localization of a Blood-Brain Barrier to Exogenous Peroxidase." *The Journal of Cell Biology* 34 (1): 207–17. https://doi.org/10.1083/jcb.34.1.207.

Rehm, Markus, Dirk Bruegger, Frank Christ, Peter Conzen, Manfred Thiel, Matthias Jacob, Daniel Chappell, et al. 2007. "Shedding of the Endothelial Glycocalyx in Patients Undergoing Major Vascular Surgery with Global and Regional Ischemia." *Circulation* 116 (17): 1896–1906. https://doi.org/10.1161/CIRCULATIONAHA.106.684852.

Reinhard, Nathalie R., Marieke Mastop, Taofei Yin, Yi Wu, Esmeralda K.

Bosma, Theodorus W. J. Gadella, Joachim Goedhart, and Peter L. Hordijk. 2017. “The Balance between Gαi-Cdc42/Rac and Gα12/13-RhoA Pathways Determines Endothelial Barrier Regulation by Sphingosine-1-Phosphate.” *Molecular Biology of the Cell* 28 (23): 3371–82. https://doi.org/10.1091/mbc.E17-03-0136.

Ren, Ming, Zi-Jing Lin, Hai Qian, Gourav Roy Choudhury, Ran Liu, Hanli Liu, and Shao-Hua Yang. 2012. “Embolic Middle Cerebral Artery Occlusion Model Using Thrombin and Fibrinogen Composed Clots in Rat.” *Journal of Neuroscience Methods* 211 (2): 296–304. https://doi.org/10.1016/j.jneumeth.2012.09.006.

Reymond, Nicolas, Bárbara Borda d’Água, and Anne J. Ridley. 2013. “Crossing the Endothelial Barrier during Metastasis.” *Nature Reviews. Cancer* 13 (12): 858–70. https://doi.org/10.1038/nrc3628.

Rezaie, Alireza R. 2014. “Protease-Activated Receptor Signalling by Coagulation Proteases in Endothelial Cells.” *Thrombosis and Haemostasis* 112 (5): 876–82. https://doi.org/10.1160/TH14-02-0167.

Riha, Gordon M., Peter H. Lin, Alan B. Lumsden, Qizhi Yao, and Changyi Chen. 2005. “Roles of Hemodynamic Forces in Vascular Cell Differentiation.” *Annals of Biomedical Engineering* 33 (6): 772–79. https://doi.org/10.1007/s10439-005-3310-9.

Rolland, William B., Tim Lekic, Paul R. Krafft, Yu Hasegawa, Orhan Altay, Richard Hartman, Robert Ostrowski, Anatol Manaenko, Jiping Tang, and John H. Zhang. 2013. “Fingolimod Reduces Cerebral Lymphocyte Infiltration in Experimental Models of Rodent Intracerebral Hemorrhage.” *Experimental Neurology* 241 (March): 45–55. https://doi.org/10.1016/j.expneurol.2012.12.009.

Rolland, William B., Anatol Manaenko, Tim Lekic, Yu Hasegawa, Robert Ostrowski, Jiping Tang, and John H. Zhang. 2011. “FTY720 Is Neuroprotective and Improves Functional Outcomes after Intracerebral Hemorrhage in Mice.” *Acta Neurochirurgica. Supplement* 111: 213–17. https://doi.org/10.1007/978-3-7091-0693-8_36.

Rosell, Anna, Eloy Cuadrado, Arantxa Ortega-Aznar, Mar Hernández-Guillamon, Eng H. Lo, and Joan Montaner. 2008. “MMP-9-Positive Neutrophil Infiltration Is Associated to Blood-Brain Barrier Breakdown and Basal Lamina Type IV Collagen Degradation during Hemorrhagic Transformation after Human Ischemic Stroke.” *Stroke* 39 (4): 1121–26. https://doi.org/10.1161/STROKEAHA.107.500868.

Roy, Reshmi, Alaa A. Alotaibi, and Mark S. Freedman. 2021. “Sphingosine 1-Phosphate Receptor Modulators for Multiple Sclerosis.” *CNS Drugs* 35 (4): 385–402. https://doi.org/10.1007/s40263-021-00798-w.

Ruggeri, Zaverio M. 2002. “Platelets in Atherothrombosis.” *Nature Medicine* 8 (11): 1227–34. https://doi.org/10.1038/nm1102-1227.

Sabeh, Farideh, Ichiro Ota, Kenn Holmbeck, Henning Birkedal-Hansen, Paul Soloway, Milagros Balbin, Carlos Lopez-Otin, et al. 2004. “Tumor Cell

Traffic through the Extracellular Matrix Is Controlled by the Membrane-Anchored Collagenase MT1-MMP." *The Journal of Cell Biology* 167 (4): 769–81. https://doi.org/10.1083/jcb.200408028.

Salomone, S., E. M. Potts, S. Tyndall, P. C. Ip, J. Chun, V. Brinkmann, and C. Waeber. 2008. "Analysis of Sphingosine 1-Phosphate Receptors Involved in Constriction of Isolated Cerebral Arteries with Receptor Null Mice and Pharmacological Tools." *British Journal of Pharmacology* 153 (1): 140–47. https://doi.org/10.1038/sj.bjp.0707581.

Salomone, Salvatore, Shin-ichi Yoshimura, Uwe Reuter, Melissa Foley, Sunu S. Thomas, Michael A. Moskowitz, and Christian Waeber. 2003. "S1P3 Receptors Mediate the Potent Constriction of Cerebral Arteries by Sphingosine-1-Phosphate." *European Journal of Pharmacology* 469 (1–3): 125–34. https://doi.org/10.1016/s0014-2999(03)01731-x.

Sammani, Saad, Liliana Moreno-Vinasco, Tamara Mirzapoiazova, Patrick A. Singleton, Eddie T. Chiang, Carrie L. Evenoski, Ting Wang, et al. 2010. "Differential Effects of Sphingosine 1-Phosphate Receptors on Airway and Vascular Barrier Function in the Murine Lung." *American Journal of Respiratory Cell and Molecular Biology* 43 (4): 394–402. https://doi.org/10.1165/rcmb.2009-0223OC.

Sanchez, Teresa, Athanasia Skoura, Ming Tao Wu, Brian Casserly, Elizabeth O. Harrington, and Timothy Hla. 2007. "Induction of Vascular Permeability by the Sphingosine-1-Phosphate Receptor-2 (S1P2R) and Its Downstream Effectors ROCK and PTEN." *Arteriosclerosis, Thrombosis, and Vascular Biology* 27 (6): 1312–18. https://doi.org/10.1161/ATVBAHA.107.143735.

Sandercock, Peter A. G., Carl Counsell, Mei-Chiun Tseng, and Emanuela Cecconi. 2014. "Oral Antiplatelet Therapy for Acute Ischaemic Stroke." *The Cochrane Database of Systematic Reviews*, no. 3 (March): CD000029. https://doi.org/10.1002/14651858.CD000029.pub3.

Sandoval, Karin E., and Ken A. Witt. 2008. "Blood-Brain Barrier Tight Junction Permeability and Ischemic Stroke." *Neurobiology of Disease* 32 (2): 200–219. https://doi.org/10.1016/j.nbd.2008.08.005.

Sanna, M. Germana, Jiayu Liao, Euijung Jo, Christopher Alfonso, Min-Young Ahn, Melissa S. Peterson, Bill Webb, et al. 2004. "Sphingosine 1-Phosphate (S1P) Receptor Subtypes S1P1 and S1P3, Respectively, Regulate Lymphocyte Recirculation and Heart Rate." *The Journal of Biological Chemistry* 279 (14): 13839–48. https://doi.org/10.1074/jbc.M311743200.

Sá-Pereira, Inês, Dora Brites, and Maria Alexandra Brito. 2012. "Neurovascular Unit: A Focus on Pericytes." *Molecular Neurobiology* 45 (2): 327–47. https://doi.org/10.1007/s12035-012-8244-2.

Saver, Jeffrey L., Mayank Goyal, Aad van der Lugt, Bijoy K. Menon, Charles B. L. M. Majoie, Diederik W. Dippel, Bruce C. Campbell, et al. 2016. "Time to Treatment With Endovascular Thrombectomy and Outcomes From Ischemic Stroke: A

Meta-Analysis." *JAMA* 316 (12): 1279–88. https://doi.org/10.1001/jama.2016.13647.

Schaeffer, Samantha, and Costantino Iadecola. 2021. "Revisiting the Neurovascular Unit." *Nature Neuroscience* 24 (9): 1198–1209. https://doi.org/10.1038/s41593-021-00904-7.

Schäfer, Andreas, and Johann Bauersachs. 2008. "Endothelial Dysfunction, Impaired Endogenous Platelet Inhibition and Platelet Activation in Diabetes and Atherosclerosis." *Current Vascular Pharmacology* 6 (1): 52–60. https://doi.org/10.2174/157016108783331295.

Scherer, Elias Q., Jingli Yang, Martin Canis, Katrin Reimann, Karolina Ivanov, Christian D. Diehl, Peter H. Backx, et al. 2010. "Tumor Necrosis Factor-α Enhances Microvascular Tone and Reduces Blood Flow in the Cochlea via Enhanced Sphingosine-1-Phosphate Signaling." *Stroke* 41 (11): 2618–24. https://doi.org/10.1161/STROKEAHA.110.593327.

Schmid-Elsaesser, R., S. Zausinger, E. Hungerhuber, A. Baethmann, and H. J. Reulen. 1998. "A Critical Reevaluation of the Intraluminal Thread Model of Focal Cerebral Ischemia: Evidence of Inadvertent Premature Reperfusion and Subarachnoid Hemorrhage in Rats by Laser-Doppler Flowmetry." *Stroke* 29 (10): 2162–70. https://doi.org/10.1161/01.str.29.10.2162.

Schuchardt, Mirjam, Markus Tölle, Jasmin Prüfer, and Markus van der Giet. 2011. "Pharmacological Relevance and Potential of Sphingosine 1-Phosphate in the Vascular System." *British Journal of Pharmacology* 163 (6): 1140–62. https://doi.org/10.1111/j.1476-5381.2011.01260.x.

Schuhmann, Michael K., Milos Krstic, Christoph Kleinschnitz, and Felix Fluri. 2016. "Fingolimod (FTY720) Reduces Cortical Infarction and Neurological Deficits During Ischemic Stroke Through Potential Maintenance of Microvascular Patency." *Current Neurovascular Research* 13 (4): 277–82. https://doi.org/10.2174/1567202613666160823152446.

Schuhmann, Michael K., Guido Stoll, Michael Bieber, Timo Vögtle, Sebastian Hofmann, Vanessa Klaus, Peter Kraft, et al. 2020. "CD84 Links T Cell and Platelet Activity in Cerebral Thrombo-Inflammation in Acute Stroke." *Circulation Research* 127 (8): 1023–35. https://doi.org/10.1161/CIRCRESAHA.120.316655.

Schwab, Susan R., João P. Pereira, Mehrdad Matloubian, Ying Xu, Yong Huang, and Jason G. Cyster. 2005. "Lymphocyte Sequestration through S1P Lyase Inhibition and Disruption of S1P Gradients." *Science (New York, N.Y.)* 309 (5741): 1735–39. https://doi.org/10.1126/science.1113640.

Sehrawat, Sharvan, and Barry T. Rouse. 2008. "Anti-Inflammatory Effects of FTY720 against Viral-Induced Immunopathology: Role of Drug-Induced Conversion of T Cells to Become Foxp3+ Regulators." *Journal of Immunology (Baltimore, Md.: 1950)* 180 (11): 7636–47. https://doi.org/10.4049/jimmunol.180.11.7636.

Seiffert, Ernst, Jens P. Dreier, Sebastian Ivens, Ingo Bechmann, Oren Tomkins, Uwe Heinemann, and Alon

Friedman. 2004. “Lasting Blood-Brain Barrier Disruption Induces Epileptic Focus in the Rat Somatosensory Cortex.” *The Journal of Neuroscience: The Official Journal of the Society for Neuroscience* 24 (36): 7829–36. https://doi.org/10.1523/JNEUROSCI.1751-04.2004.

Shattil, Sanford J., Chungho Kim, and Mark H. Ginsberg. 2010. “The Final Steps of Integrin Activation: The End Game.” *Nature Reviews. Molecular Cell Biology* 11 (4): 288–300. https://doi.org/10.1038/nrm2871.

Shen, Hongying, Francesca Giordano, Yumei Wu, Jason Chan, Chen Zhu, Ira Milosevic, Xudong Wu, et al. 2014. “Coupling between Endocytosis and Sphingosine Kinase 1 Recruitment.” *Nature Cell Biology* 16 (7): 652–62. https://doi.org/10.1038/ncb2987.

Shi, Yejie, Lili Zhang, Hongjian Pu, Leilei Mao, Xiaoming Hu, Xiaoyan Jiang, Na Xu, et al. 2016. “Rapid Endothelial Cytoskeletal Reorganization Enables Early Blood–Brain Barrier Disruption and Long-Term Ischaemic Reperfusion Brain Injury.” *Nature Communications* 7 (1): 10523. https://doi.org/10.1038/ncomms10523.

Shichita, Takashi, Yuki Sugiyama, Hiroaki Ooboshi, Hiroshi Sugimori, Ryusuke Nakagawa, Ichiro Takada, Toru Iwaki, et al. 2009. “Pivotal Role of Cerebral Interleukin-17-Producing GammadeltaT Cells in the Delayed Phase of Ischemic Brain Injury.” *Nature Medicine* 15 (8): 946–50. https://doi.org/10.1038/nm.1999.

Shikata, Yasushi, Konstantin G. Birukov, and Joe G. N. Garcia. 2003. “S1P Induces FA Remodeling in Human Pulmonary Endothelial Cells: Role of Rac, GIT1, FAK, and Paxillin.” *Journal of Applied Physiology (Bethesda, Md.: 1985)* 94 (3): 1193–1203. https://doi.org/10.1152/japplphysiol.00690.2002.

Shima, T., K. A. Hossmann, and H. Date. 1983. “Pial Arterial Pressure in Cats Following Middle Cerebral Artery Occlusion. 1. Relationship to Blood Flow, Regulation of Blood Flow and Electrophysiological Function.” *Stroke* 14 (5): 713–19. https://doi.org/10.1161/01.str.14.5.713.

Shimizu, Hisashi, Masafumi Takahashi, Takashi Kaneko, Takashi Murakami, Yoji Hakamata, Shinji Kudou, Tetsuya Kishi, et al. 2005. “KRP-203, a Novel Synthetic Immunosuppressant, Prolongs Graft Survival and Attenuates Chronic Rejection in Rat Skin and Heart Allografts.” *Circulation* 111 (2): 222–29. https://doi.org/10.1161/01.CIR.0000152101.41037.AB.

Shimokawa, H., N. A. Flavahan, R. R. Lorenz, and P. M. Vanhoutte. 1988. “Prostacyclin Releases Endothelium-Derived Relaxing Factor and Potentiates Its Action in Coronary Arteries of the Pig.” *British Journal of Pharmacology* 95 (4): 1197–1203. https://doi.org/10.1111/j.1476-5381.1988.tb11756.x.

Shuaib, Ashfaq, Ken Butcher, Askar A. Mohammad, Maher Saqqur, and David S. Liebeskind. 2011. “Collateral Blood Vessels in Acute Ischaemic Stroke: A Potential Therapeutic Target.” *The Lancet. Neurology* 10 (10): 909–21. https://doi.org/10.1016/S1474-4422(11)70195-8.

Siedlinski, Mateusz, Ryszard Nosalski, Piotr Szczepaniak, Agnieszka H. Ludwig-Gałęzowska, Tomasz Mikołajczyk, Magdalena Filip, Grzegorz

Osmenda, et al. 2017. “Vascular Transcriptome Profiling Identifies Sphingosine Kinase 1 as a Modulator of Angiotensin II-Induced Vascular Dysfunction.” *Scientific Reports* 7 (March): 44131. https://doi.org/10.1038/srep44131.

Siegel, George J., ed. 1999. *Basic Neurochemistry: Molecular, Cellular and Medical Aspects*. 6. ed. Philadelphia, Pa.: Lippincott Williams & Wilkins.

Singer, Barry A. 2013. “Fingolimod for the Treatment of Relapsing Multiple Sclerosis.” *Expert Review of Neurotherapeutics* 13 (6): 589–602. https://doi.org/10.1586/ern.13.52.

Singleton, Patrick A., Steven M. Dudek, Shwu-Fan Ma, and Joe G. N. Garcia. 2006. “Transactivation of Sphingosine 1-Phosphate Receptors Is Essential for Vascular Barrier Regulation. Novel Role for Hyaluronan and CD44 Receptor Family.” *The Journal of Biological Chemistry* 281 (45): 34381–93. https://doi.org/10.1074/jbc.M603680200.

Skoura, Athanasia, and Timothy Hla. 2009. “Lysophospholipid Receptors in Vertebrate Development, Physiology, and Pathology.” *Journal of Lipid Research* 50 Suppl (April): S293-298. https://doi.org/10.1194/jlr.R800047-JLR200.

Skoura, Athanasia, Teresa Sanchez, Kevin Claffey, Suzanne M. Mandala, Richard L. Proia, and Timothy Hla. 2007. “Essential Role of Sphingosine 1-Phosphate Receptor 2 in Pathological Angiogenesis of the Mouse Retina.” *The Journal of Clinical Investigation* 117 (9): 2506–16. https://doi.org/10.1172/JCI31123.

Smith, Helen K., Janice M. Russell, D. Neil Granger, and Felicity N. E. Gavins. 2015. “Critical Differences between Two Classical Surgical Approaches for Middle Cerebral Artery Occlusion-Induced Stroke in Mice.” *Journal of Neuroscience Methods* 249 (July): 99–105. https://doi.org/10.1016/j.jneumeth.2015.04.008.

Smyth, Emer M., Tilo Grosser, Miao Wang, Ying Yu, and Garret A. FitzGerald. 2009. “Prostanoids in Health and Disease.” *Journal of Lipid Research* 50 Suppl (April): S423-428. https://doi.org/10.1194/jlr.R800094-JLR200.

Sofroniew, Michael V., and Harry V. Vinters. 2010. “Astrocytes: Biology and Pathology.” *Acta Neuropathologica* 119 (1): 7–35. https://doi.org/10.1007/s00401-009-0619-8.

Sommer, Clemens J. 2017. “Ischemic Stroke: Experimental Models and Reality.” *Acta Neuropathologica* 133 (2): 245–61. https://doi.org/10.1007/s00401-017-1667-0.

Starosolski, Zbigniew, Carlos A. Villamizar, David Rendon, Michael J. Paldino, Dianna M. Milewicz, Ketan B. Ghaghada, and Ananth V. Annapragada. 2015. “Ultra High-Resolution In Vivo Computed Tomography Imaging of Mouse Cerebrovasculature Using a Long Circulating Blood Pool Contrast Agent.” *Scientific Reports* 5 (1): 10178. https://doi.org/10.1038/srep10178.

Sternlicht, M. D., and Z. Werb. 2001. “How Matrix Metalloproteinases Regulate Cell Behavior.” *Annual Review of Cell and Developmental Biology* 17: 463–516.

https://doi.org/10.1146/annurev.cellbio.17.1.463.

Stewart, P. A., and M. J. Wiley. 1981. "Developing Nervous Tissue Induces Formation of Blood-Brain Barrier Characteristics in Invading Endothelial Cells: A Study Using Quail--Chick Transplantation Chimeras." *Developmental Biology* 84 (1): 183–92. https://doi.org/10.1016/0012-1606(81)90382-1.

Stöcker, W., F. Grams, U. Baumann, P. Reinemer, F. X. Gomis-Rüth, D. B. McKay, and W. Bode. 1995. "The Metzincins--Topological and Sequential Relations between the Astacins, Adamalysins, Serralysins, and Matrixins (Collagenases) Define a Superfamily of Zinc-Peptidases." *Protein Science: A Publication of the Protein Society* 4 (5): 823–40. https://doi.org/10.1002/pro.5560040502.

Stoffel, W., G. Sticht, and D. LeKim. 1968. "Metabolism of Sphingosine Bases. IX. Degradation in Vitro of Dihydrospingosine and Dihydrospingosine Phosphate to Palmitaldehyde and Ethanolamine Phosphate." *Hoppe-Seyler's Zeitschrift Fur Physiologische Chemie* 349 (12): 1745–48. https://doi.org/10.1515/bchm2.1968.349.2.1745.

Stroke Therapy Academic Industry Roundtable (STAIR). 1999. "Recommendations for Standards Regarding Preclinical Neuroprotective and Restorative Drug Development." *Stroke* 30 (12): 2752–58. https://doi.org/10.1161/01.str.30.12.2752.

Strub, Graham M., Melanie Paillard, Jie Liang, Ludovic Gomez, Jeremy C. Allegood, Nitai C. Hait, Michael Maceyka, et al. 2011. "Sphingosine-1-Phosphate Produced by Sphingosine Kinase 2 in Mitochondria Interacts with Prohibitin 2 to Regulate Complex IV Assembly and Respiration." *FASEB Journal: Official Publication of the Federation of American Societies for Experimental Biology* 25 (2): 600–612. https://doi.org/10.1096/fj.10-167502.

Struijs, Jeroen N., Marianne L. L. van Genugten, Silvia M. A. A. Evers, André J. H. Ament, Caroline A. Baan, and Geertrudis A. M. van den Bos. 2006. "Future Costs of Stroke in the Netherlands: The Impact of Stroke Services." *International Journal of Technology Assessment in Health Care* 22 (4): 518–24. https://doi.org/10.1017/S0266462306051464.

Sugimori, Hiroshi, Hiroshi Yao, Hiroaki Ooboshi, Setsuro Ibayashi, and Mitsuo Iida. 2004. "Krypton Laser-Induced Photothrombotic Distal Middle Cerebral Artery Occlusion without Craniectomy in Mice." *Brain Research. Brain Research Protocols* 13 (3): 189–96. https://doi.org/10.1016/j.brainresprot.2004.06.001.

Swendeman, Steven L., Yuquan Xiong, Anna Cantalupo, Hui Yuan, Nathalie Burg, Yu Hisano, Andreane Cartier, et al. 2017. "An Engineered S1P Chaperone Attenuates Hypertension and Ischemic Injury." *Science Signaling* 10 (492). https://doi.org/10.1126/scisignal.aal2722.

Szerafin, Tamás, Nóra Erdei, Tibor Fülöp, Eniko T. Pasztor, István Edes, Akos Koller, and Zsolt Bagi. 2006. "Increased Cyclooxygenase-2 Expression and Prostaglandin-Mediated Dilation in Coronary

Arterioles of Patients with Diabetes Mellitus." *Circulation Research* 99 (5): e12-17. https://doi.org/10.1161/01.RES.0000241051.83067.62.

Takabe, Wakako, Eiji Warabi, and Noriko Noguchi. 2011. "Anti-Atherogenic Effect of Laminar Shear Stress via Nrf2 Activation." *Antioxidants & Redox Signaling* 15 (5): 1415–26. https://doi.org/10.1089/ars.2010.3433.

Takada, Y., F. Shinkai, S. Kondo, S. Yamamoto, H. Tsuboi, R. Korenaga, and J. Ando. 1994. "Fluid Shear Stress Increases the Expression of Thrombomodulin by Cultured Human Endothelial Cells." *Biochemical and Biophysical Research Communications* 205 (2): 1345–52. https://doi.org/10.1006/bbrc.1994.2813.

Tamura, A., D. I. Graham, J. McCulloch, and G. M. Teasdale. 1981. "Focal Cerebral Ischaemia in the Rat: 1. Description of Technique and Early Neuropathological Consequences Following Middle Cerebral Artery Occlusion." *Journal of Cerebral Blood Flow and Metabolism: Official Journal of the International Society of Cerebral Blood Flow and Metabolism* 1 (1): 53–60. https://doi.org/10.1038/jcbfm.1981.6.

Tanaka, Kenichi A., Nigel S. Key, and Jerrold H. Levy. 2009. "Blood Coagulation: Hemostasis and Thrombin Regulation." *Anesthesia and Analgesia* 108 (5): 1433–46. https://doi.org/10.1213/ane.0b013e31819bcc9c.

Tarbell, John M. 2010. "Shear Stress and the Endothelial Transport Barrier." *Cardiovascular Research* 87 (2): 320–30. https://doi.org/10.1093/cvr/cvq146.

Thompson, Christopher R., Shankar S. Iyer, Natalie Melrose, Rebecca VanOosten, Korey Johnson, Stuart M. Pitson, Lina M. Obeid, and David J. Kusner. 2005. "Sphingosine Kinase 1 (SK1) Is Recruited to Nascent Phagosomes in Human Macrophages: Inhibition of SK1 Translocation by Mycobacterium Tuberculosis." *Journal of Immunology (Baltimore, Md.: 1950)* 174 (6): 3551–61. https://doi.org/10.4049/jimmunol.174.6.3551.

Thorin, Eric, and David J. Webb. 2010. "Endothelium-Derived Endothelin-1." *Pflugers Archiv: European Journal of Physiology* 459 (6): 951–58. https://doi.org/10.1007/s00424-009-0763-y.

Tian, De-Cai, Kaibin Shi, Zilong Zhu, Jia Yao, Xiaoxia Yang, Lei Su, Sheng Zhang, et al. 2018. "Fingolimod Enhances the Efficacy of Delayed Alteplase Administration in Acute Ischemic Stroke by Promoting Anterograde Reperfusion and Retrograde Collateral Flow." *Annals of Neurology* 84 (5): 717–28. https://doi.org/10.1002/ana.25352.

Tilton, R. G., K. C. Chang, W. S. LeJeune, C. C. Stephan, T. A. Brock, and J. R. Williamson. 1999. "Role for Nitric Oxide in the Hyperpermeability and Hemodynamic Changes Induced by Intravenous VEGF." *Investigative Ophthalmology & Visual Science* 40 (3): 689–96.

Turner-Stokes, Lynne, Heather Williams, Alan Bill, Paul Bassett, and Keith Sephton. 2016. "Cost-Efficiency of Specialist Inpatient Rehabilitation for Working-Aged Adults with Complex Neurological Disabilities: A Multicentre Cohort Analysis of a

National Clinical Data Set." *BMJ Open* 6 (2): e010238. https://doi.org/10.1136/bmjopen-2015-010238.

Ungerer, Martin, Zhongmin Li, Christine Baumgartner, Silvia Goebel, Jasmin Vogelmann, Hans-Peter Holthoff, Meinrad Gawaz, and Götz Münch. 2013. "The GPVI-Fc Fusion Protein Revacept Reduces Thrombus Formation and Improves Vascular Dysfunction in Atherosclerosis without Any Impact on Bleeding Times." *PloS One* 8 (8): e71193. https://doi.org/10.1371/journal.pone.0071193.

Vanlandewijck, Michael, Liqun He, Maarja Andaloussi Mäe, Johanna Andrae, Koji Ando, Francesca Del Gaudio, Khayrun Nahar, et al. 2018. "A Molecular Atlas of Cell Types and Zonation in the Brain Vasculature." *Nature* 554 (7693): 475–80. https://doi.org/10.1038/nature25739.

Vemuganti, Raghu, Robert J. Dempsey, and Kellie K. Bowen. 2004. "Inhibition of Intercellular Adhesion Molecule-1 Protein Expression by Antisense Oligonucleotides Is Neuroprotective after Transient Middle Cerebral Artery Occlusion in Rat." *Stroke* 35 (1): 179–84. https://doi.org/10.1161/01.STR.0000106479.53235.3E.

Venkataraman, Krishnan, Yong-Moon Lee, Jason Michaud, Shobha Thangada, Youxi Ai, Herbert L. Bonkovsky, Nehal S. Parikh, Cheryl Habrukowich, and Timothy Hla. 2008. "Vascular Endothelium as a Contributor of Plasma Sphingosine 1-Phosphate." *Circulation Research* 102 (6): 669–76. https://doi.org/10.1161/CIRCRESAHA.107.165845.

Versari, Daniele, Elena Daghini, Agostino Virdis, Lorenzo Ghiadoni, and Stefano Taddei. 2009. "Endothelial Dysfunction as a Target for Prevention of Cardiovascular Disease." *Diabetes Care* 32 Suppl 2 (November): S314-321. https://doi.org/10.2337/dc09-S330.

Vessey, Donald A., Luyi Li, Zhu-Qiu Jin, Michael Kelley, Norman Honbo, Jianqing Zhang, and Joel S. Karliner. 2011. "A Sphingosine Kinase Form 2 Knockout Sensitizes Mouse Myocardium to Ischemia/Reoxygenation Injury and Diminishes Responsiveness to Ischemic Preconditioning." *Oxidative Medicine and Cellular Longevity* 2011: 961059. https://doi.org/10.1155/2011/961059.

Victor, Victor M., Milagros Rocha, Eva Solá, Celia Bañuls, Katherine Garcia-Malpartida, and Antonio Hernández-Mijares. 2009. "Oxidative Stress, Endothelial Dysfunction and Atherosclerosis." *Current Pharmaceutical Design* 15 (26): 2988–3002. https://doi.org/10.2174/138161209789058093.

Vion, Anne-Clémence, Tijana Perovic, Charlie Petit, Irene Hollfinger, Eireen Bartels-Klein, Emmanuelle Frampton, Emma Gordon, Lena Claesson-Welsh, and Holger Gerhardt. 2020. "Endothelial Cell Orientation and Polarity Are Controlled by Shear Stress and VEGF Through Distinct Signaling Pathways." *Frontiers in Physiology* 11: 623769. https://doi.org/10.3389/fphys.2020.623769.

Virani, Salim S., Alvaro Alonso, Hugo J. Aparicio, Emelia J. Benjamin, Marcio S. Bittencourt, Clifton W. Callaway,

April P. Carson, et al. 2021. “Heart Disease and Stroke Statistics-2021 Update: A Report From the American Heart Association.” *Circulation* 143 (8): e254–743. https://doi.org/10.1161/CIR.0000000000000950.

Vitali, C., C. L. Wellington, and L. Calabresi. 2014. “HDL and Cholesterol Handling in the Brain.” *Cardiovascular Research* 103 (3): 405–13. https://doi.org/10.1093/cvr/cvu148.

Vogelgesang, Antje, Grazyna Domanska, Johanna Ruhnau, Alexander Dressel, Michael Kirsch, and Juliane Schulze. 2019. “Siponimod (BAF312) Treatment Reduces Brain Infiltration but Not Lesion Volume in Middle-Aged Mice in Experimental Stroke.” *Stroke* 50 (5): 1224–31. https://doi.org/10.1161/STROKEAHA.118.023667.

Vu, Thiet M., Ayako-Nakamura Ishizu, Juat Chin Foo, Xiu Ru Toh, Fangyu Zhang, Ding Ming Whee, Federico Torta, et al. 2017. “Mfsd2b Is Essential for the Sphingosine-1-Phosphate Export in Erythrocytes and Platelets.” *Nature* 550 (7677): 524–28. https://doi.org/10.1038/nature24053.

Wacker, Bradley K., Tae Sung Park, and Jeffrey M. Gidday. 2009. “Hypoxic Preconditioning-Induced Cerebral Ischemic Tolerance: Role of Microvascular Sphingosine Kinase 2.” *Stroke* 40 (10): 3342–48. https://doi.org/10.1161/STROKEAHA.109.560714.

Wang, Jinsong, Xinzhi Peng, Roberta M. Lassance-Soares, Amir H. Najafi, Lee O. Alderman, Subeena Sood, Zhenyi Xue, et al. 2011. “Aging-Induced Collateral Dysfunction: Impaired Responsiveness of Collaterals and Susceptibility to Apoptosis via Dysfunctional ENOS Signaling.” *Journal of Cardiovascular Translational Research* 4 (6): 779–89. https://doi.org/10.1007/s12265-011-9280-4.

Wang, Shaobin, Brandi Reeves, Erica M. Sparkenbaugh, Janice Russell, Zbigniew Soltys, Hua Zhang, James E. Faber, et al. 2016. “Protective and Detrimental Effects of Neuroectodermal Cell-Derived Tissue Factor in Mouse Models of Stroke.” *JCI Insight* 1 (11): e86663. https://doi.org/10.1172/jci.insight.86663.

Ward, R., R. L. Collins, G. Tanguay, and D. Miceli. 1990. “A Quantitative Study of Cerebrovascular Variation in Inbred Mice.” *Journal of Anatomy* 173 (December): 87–95.

Wei, Ying, Muge Yemisci, Hyung-Hwan Kim, Lai Ming Yung, Hwa Kyoung Shin, Seo-Kyoung Hwang, Shuzhen Guo, et al. 2011. “Fingolimod Provides Long-Term Protection in Rodent Models of Cerebral Ischemia.” *Annals of Neurology* 69 (1): 119–29. https://doi.org/10.1002/ana.22186.

Wilson, Parker C., Wayne R. Fitzgibbon, Sara M. Garrett, Ayad A. Jaffa, Louis M. Luttrell, Michael W. Brands, and Hesham M. El-Shewy. 2015. “Inhibition of Sphingosine Kinase 1 Ameliorates Angiotensin II-Induced Hypertension and Inhibits Transmembrane Calcium Entry via Store-Operated Calcium Channel.” *Molecular Endocrinology (Baltimore, Md.)* 29 (6): 896–908. https://doi.org/10.1210/me.2014-1388.

Winkler, Ethan A., Robert D. Bell, and Berislav V. Zlokovic. 2011. “Central Nervous System Pericytes in Health and Disease.” *Nature Neuroscience*

14 (11): 1398–1405. https://doi.org/10.1038/nn.2946.

Winship, Ian R. 2015. “Cerebral Collaterals and Collateral Therapeutics for Acute Ischemic Stroke.” *Microcirculation (New York, N.Y.: 1994)* 22 (3): 228–36. https://doi.org/10.1111/micc.12177.

Wolburg, Hartwig, and Andrea Lippoldt. 2002. “Tight Junctions of the Blood-Brain Barrier: Development, Composition and Regulation.” *Vascular Pharmacology* 38 (6): 323–37. https://doi.org/10.1016/s1537-1891(02)00200-8.

Xie, Lulu, Hongyi Kang, and Maiken Nedergaard. 2016. “A Novel Model of Transient Occlusion of the Middle Cerebral Artery in Awake Mice.” *Journal of Nature and Science* 2 (2): e176.

Xiong, Yuquan, and Timothy Hla. 2014. “S1P Control of Endothelial Integrity.” *Current Topics in Microbiology and Immunology* 378: 85–105. https://doi.org/10.1007/978-3-319-05879-5_4.

Xiong, Yuquan, Hyuek Jong Lee, Boubacar Mariko, Yi-Chien Lu, Andrew J. Dannenberg, Abigail S. Haka, Frederick R. Maxfield, Eric Camerer, Richard L. Proia, and Timothy Hla. 2016. “Sphingosine Kinases Are Not Required for Inflammatory Responses in Macrophages.” *The Journal of Biological Chemistry* 291 (21): 11465. https://doi.org/10.1074/jbc.A113.483750.

Xiong, Yuquan, Peiying Yang, Richard L. Proia, and Timothy Hla. 2014. “Erythrocyte-Derived Sphingosine 1-Phosphate Is Essential for Vascular Development.” *The Journal of Clinical Investigation* 124 (11): 4823–28. https://doi.org/10.1172/JCI77685.

Yamori, Y., R. Horie, H. Handa, M. Sato, and M. Fukase. 1976. “Pathogenetic Similarity of Strokes in Stroke-Prone Spontaneously Hypertensive Rats and Humans.” *Stroke* 7 (1): 46–53. https://doi.org/10.1161/01.str.7.1.46.

Yanagida, Keisuke, Catherine H. Liu, Giuseppe Faraco, Sylvain Galvani, Helen K. Smith, Nathalie Burg, Josef Anrather, Teresa Sanchez, Costantino Iadecola, and Timothy Hla. 2017. “Size-Selective Opening of the Blood-Brain Barrier by Targeting Endothelial Sphingosine 1-Phosphate Receptor 1.” *Proceedings of the National Academy of Sciences of the United States of America* 114 (17): 4531–36. https://doi.org/10.1073/pnas.1618659114.

Yanagisawa, M., A. Inoue, T. Ishikawa, Y. Kasuya, S. Kimura, S. Kumagaye, K. Nakajima, T. X. Watanabe, S. Sakakibara, and K. Goto. 1988. “Primary Structure, Synthesis, and Biological Activity of Rat Endothelin, an Endothelium-Derived Vasoconstrictor Peptide.” *Proceedings of the National Academy of Sciences of the United States of America* 85 (18): 6964–67. https://doi.org/10.1073/pnas.85.18.6964.

Yanagisawa, M., H. Kurihara, S. Kimura, K. Goto, and T. Masaki. 1988. “A Novel Peptide Vasoconstrictor, Endothelin, Is Produced by Vascular Endothelium and Modulates Smooth Muscle Ca2+ Channels.” *Journal of Hypertension. Supplement: Official Journal of the International Society of Hypertension* 6 (4): S188-191.

https://doi.org/10.1097/00004872-198812040-00056.

Yang, Yi, Eduardo Y. Estrada, Jeffrey F. Thompson, Wenlan Liu, and Gary A. Rosenberg. 2007. "Matrix Metalloproteinase-Mediated Disruption of Tight Junction Proteins in Cerebral Vessels Is Reversed by Synthetic Matrix Metalloproteinase Inhibitor in Focal Ischemia in Rat." *Journal of Cerebral Blood Flow and Metabolism: Official Journal of the International Society of Cerebral Blood Flow and Metabolism* 27 (4): 697–709. https://doi.org/10.1038/sj.jcbfm.9600375.

Yenari, M. A., G. H. Sun, D. M. Kunis, D. Onley, and V. Vexler. 2001. "L-Selectin Inhibition Does Not Reduce Injury in a Rabbit Model of Transient Focal Cerebral Ischemia." *Neurological Research* 23 (1): 72–78. https://doi.org/10.1179/016164101101198154.

Yetik-Anacak, Gunay, and John D. Catravas. 2006. "Nitric Oxide and the Endothelium: History and Impact on Cardiovascular Disease." *Vascular Pharmacology* 45 (5): 268–76. https://doi.org/10.1016/j.vph.2006.08.002.

Yilmaz, Gokhan, Thiruma V. Arumugam, Karen Y. Stokes, and D. Neil Granger. 2006. "Role of T Lymphocytes and Interferon-Gamma in Ischemic Stroke." *Circulation* 113 (17): 2105–12. https://doi.org/10.1161/CIRCULATIONAHA.105.593046.

Yilmaz, Gokhan, and D. Neil Granger. 2008. "Cell Adhesion Molecules and Ischemic Stroke." *Neurological Research* 30 (8): 783–93. https://doi.org/10.1179/174313208X341085.

Yoshimura, Akihiko, and Minako Ito. 2020. "Resolution of Inflammation and Repair after Ischemic Brain Injury." *Neuroimmunology and Neuroinflammation* 2020 (July). https://doi.org/10.20517/2347-8659.2020.22.

Ysebaert, Dirk K., Kathleen E. De Greef, Annelies De Beuf, An R. Van Rompay, Sven Vercauteren, Veerle P. Persy, and Marc E. De Broe. 2004. "T Cells as Mediators in Renal Ischemia/Reperfusion Injury." *Kidney International* 66 (2): 491–96. https://doi.org/10.1111/j.1523-1755.2004.761_4.x.

Yung, Lai Ming, Ying Wei, Tao Qin, Yumei Wang, Charles D. Smith, and Christian Waeber. 2012. "Sphingosine Kinase 2 Mediates Cerebral Preconditioning and Protects the Mouse Brain against Ischemic Injury." *Stroke* 43 (1): 199–204. https://doi.org/10.1161/STROKEAHA.111.626911.

Zeng, Ye, Roger H. Adamson, Fitz-Roy E. Curry, and John M. Tarbell. 2014. "Sphingosine-1-Phosphate Protects Endothelial Glycocalyx by Inhibiting Syndecan-1 Shedding." *American Journal of Physiology. Heart and Circulatory Physiology* 306 (3): H363-372. https://doi.org/10.1152/ajpheart.00687.2013.

Zhang, Guoqi, Li Yang, Gab Seok Kim, Kieran Ryan, Shulin Lu, Rebekah K. O'Donnell, Katherine Spokes, et al. 2013. "Critical Role of Sphingosine-1-Phosphate Receptor 2 (S1PR2) in Acute Vascular Inflammation." *Blood* 122 (3): 443–55. https://doi.org/10.1182/blood-2012-11-467191.

Zhang, H., N. N. Desai, A. Olivera, T. Seki, G. Brooker, and S. Spiegel. 1991.

"Sphingosine-1-Phosphate, a Novel Lipid, Involved in Cellular Proliferation." *The Journal of Cell Biology* 114 (1): 155–67. https://doi.org/10.1083/jcb.114.1.155.

Zhang, Hua, Pranay Prabhakar, Robert Sealock, and James E. Faber. 2010. "Wide Genetic Variation in the Native Pial Collateral Circulation Is a Major Determinant of Variation in Severity of Stroke." *Journal of Cerebral Blood Flow and Metabolism: Official Journal of the International Society of Cerebral Blood Flow and Metabolism* 30 (5): 923–34. https://doi.org/10.1038/jcbfm.2010.10.

Zhang, Ji, and Morton H. Friedman. 2012. "Adaptive Response of Vascular Endothelial Cells to an Acute Increase in Shear Stress Magnitude." *American Journal of Physiology. Heart and Circulatory Physiology* 302 (4): H983-991. https://doi.org/10.1152/ajpheart.00168.2011.

Zhang, Xun E., Shaquria P. Adderley, and Jerome W. Breslin. 2016. "Activation of RhoA, but Not Rac1, Mediates Early Stages of S1P-Induced Endothelial Barrier Enhancement." *PloS One* 11 (5): e0155490. https://doi.org/10.1371/journal.pone.0155490.

Zhang, Yi, Yan Huang, Anna Cantalupo, Paula S. Azevedo, Mauro Siragusa, Jacek Bielawski, Frank J. Giordano, and Annarita Di Lorenzo. 2016. "Endothelial Nogo-B Regulates Sphingolipid Biosynthesis to Promote Pathological Cardiac Hypertrophy during Chronic Pressure Overload." *JCI Insight* 1 (5): e85484. https://doi.org/10.1172/jci.insight.85484.

Zhang, Zhi-Yuan, Zhiren Zhang, Caroline Zug, Barbara Nuesslein-Hildesheim, David Leppert, and Hermann J. Schluesener. 2009. "AUY954, a Selective S1P(1) Modulator, Prevents Experimental Autoimmune Neuritis." *Journal of Neuroimmunology* 216 (1–2): 59–65. https://doi.org/10.1016/j.jneuroim.2009.09.010.

Zhao, Bing-Qiao, Sophia Wang, Hahn-Young Kim, Hannah Storrie, Bruce R. Rosen, David J. Mooney, Xiaoying Wang, and Eng H. Lo. 2006. "Role of Matrix Metalloproteinases in Delayed Cortical Responses after Stroke." *Nature Medicine* 12 (4): 441–45. https://doi.org/10.1038/nm1387.

Zhong, Chongke, Jingyuan Yang, Tan Xu, Tian Xu, Yanbo Peng, Aili Wang, Jinchao Wang, et al. 2017. "Serum Matrix Metalloproteinase-9 Levels and Prognosis of Acute Ischemic Stroke." *Neurology* 89 (8): 805–12. https://doi.org/10.1212/WNL.0000000000004257.

Zhu, Donghui, Yaoming Wang, Itender Singh, Robert D. Bell, Rashid Deane, Zhihui Zhong, Abhay Sagare, Ethan A. Winkler, and Berislav V. Zlokovic. 2010. "Protein S Controls Hypoxic/Ischemic Blood-Brain Barrier Disruption through the TAM Receptor Tyro3 and Sphingosine 1-Phosphate Receptor." *Blood* 115 (23): 4963–72. https://doi.org/10.1182/blood-2010-01-262386.

Zhu, Qing, Min Xia, Zhengchao Wang, Pin-Lan Li, and Ningjun Li. 2011. "A Novel Lipid Natriuretic Factor in the Renal Medulla: Sphingosine-1-Phosphate." *American Journal of*

Physiology. Renal Physiology 301 (1): F35-41. https://doi.org/10.1152/ajprenal.00014.2011.

Zhu, Zilong, Ying Fu, Decai Tian, Na Sun, Wei Han, Guoqiang Chang, Yinhua Dong, et al. 2015. "Combination of the Immune Modulator Fingolimod With Alteplase in Acute Ischemic Stroke: A Pilot Trial." *Circulation* 132 (12): 1104–12. https://doi.org/10.1161/CIRCULATIONAHA.115.016371.

Zlokovic, Berislav V. 2008. "The Blood-Brain Barrier in Health and Chronic Neurodegenerative Disorders." *Neuron* 57 (2): 178–201. https://doi.org/10.1016/j.neuron.2008.01.003.

Zonta, Micaela, María Cecilia Angulo, Sara Gobbo, Bernhard Rosengarten, Konstantin-A. Hossmann, Tullio Pozzan, and Giorgio Carmignoto. 2003. "Neuron-to-Astrocyte Signaling Is Central to the Dynamic Control of Brain Microcirculation." *Nature Neuroscience* 6 (1): 43–50. https://doi.org/10.1038/nn980.

Zoppo, G. J. del. 2010. "The Neurovascular Unit in the Setting of Stroke." *Journal of Internal Medicine* 267 (2): 156–71. https://doi.org/10.1111/j.1365-2796.2009.02199.x.

Zoppo, G. J. del, G. W. Schmid-Schönbein, E. Mori, B. R. Copeland, and C. M. Chang. 1991. "Polymorphonuclear Leukocytes Occlude Capillaries Following Middle Cerebral Artery Occlusion and Reperfusion in Baboons." *Stroke* 22 (10): 1276–83. https://doi.org/10.1161/01.str.22.10.1276.

Zoppo, Gregory J. del, and Takuma Mabuchi. 2003. "Cerebral Microvessel Responses to Focal Ischemia." *Journal of Cerebral Blood Flow and Metabolism: Official Journal of the International Society of Cerebral Blood Flow and Metabolism* 23 (8): 879–94. https://doi.org/10.1097/01.WCB.0000078322.96027.78.

Zwacka, R. M., Y. Zhang, J. Halldorson, H. Schlossberg, L. Dudus, and J. F. Engelhardt. 1997. "CD4(+) T-Lymphocytes Mediate Ischemia/Reperfusion-Induced Inflammatory Responses in Mouse Liver." *The Journal of Clinical Investigation* 100 (2): 279–89. https://doi.org/10.1172/JCI119533.

Appendix. Paper 1

Endothelial $S1P_1$ Signaling Counteracts Infarct Expansion in Ischemic Stroke

Anja Nitzsche*, Marine Poittevin*, **Ammar Benarab***, Philippe Bonnin*, Giuseppe Faraco, Hiroki Uchida, Julie Favre, Lidia Garcia-Bonilla, Manuela C.L. Garcia, Pierre-Louis Léger, Patrice Thérond, Thomas Mathivet, Gwennhael Autret, Véronique Baudrie, Ludovic Couty, Mari Kono, Aline Chevallier, Hira Niazi, Pierre-Louis Tharaux, Jerold Chun, Susan R. Schwab, Anne Eichmann, Bertrand Tavitian, Richard L. Proia, Christiane Charriaut-Marlangue, Teresa Sanchez, Nathalie Kubis, Daniel Henrion, Costantino Iadecola, Timothy Hla and Eric Camerer

* A.N., M.P., A.B., and P.B. contributed equally to this article

Circulation Research Volume 128, Issue 3, 5 February 2021; Pages 363-382

https://doi.org/10.1161/CIRCRESAHA.120.316711

Appendix. Paper 2

Endothelial sphingosine 1-phosphate signaling maintains perfusion of the cerebral cortex in ischemic stroke.

Nitzsche Anja, Poittevin Marine, **Benarab Ammar**, Bonnin Phillipe, Camerer Eric.

https://doi.org/10.1051/medsci/2021103

Med Sci (Paris). 2021 Aug-Sep;37(8-9):709-711. Epub 2021 Sep 7.

Circulation Research

ORIGINAL RESEARCH

Endothelial S1P$_1$ Signaling Counteracts Infarct Expansion in Ischemic Stroke

Anja Nitzsche,* Marine Poittevin,* Ammar Benarab,* Philippe Bonnin,* Giuseppe Faraco, Hiroki Uchida, Julie Favre, Lidia Garcia-Bonilla, Manuela C.L. Garcia, Pierre-Louis Léger, Patrice Thérond, Thomas Mathivet, Gwennhael Autret, Véronique Baudrie, Ludovic Couty, Mari Kono, Aline Chevallier, Hira Niazi, Pierre-Louis Tharaux, Jerold Chun, Susan R. Schwab, Anne Eichmann, Bertrand Tavitian, Richard L. Proia, Christiane Charriaut-Marlangue, Teresa Sanchez, Nathalie Kubis, Daniel Henrion, Costantino Iadecola, Timothy Hla, Eric Camerer

RATIONALE: Cerebrovascular function is critical for brain health, and endogenous vascular protective pathways may provide therapeutic targets for neurological disorders. S1P (Sphingosine 1-phosphate) signaling coordinates vascular functions in other organs, and S1P$_1$ (S1P receptor-1) modulators including fingolimod show promise for the treatment of ischemic and hemorrhagic stroke. However, S1P$_1$ also coordinates lymphocyte trafficking, and lymphocytes are currently viewed as the principal therapeutic target for S1P$_1$ modulation in stroke.

OBJECTIVE: To address roles and mechanisms of engagement of endothelial cell S1P$_1$ in the naive and ischemic brain and its potential as a target for cerebrovascular therapy.

METHODS AND RESULTS: Using spatial modulation of S1P provision and signaling, we demonstrate a critical vascular protective role for endothelial S1P$_1$ in the mouse brain. With an S1P$_1$ signaling reporter, we reveal that abluminal polarization shields S1P$_1$ from circulating endogenous and synthetic ligands after maturation of the blood-neural barrier, restricting homeostatic signaling to a subset of arteriolar endothelial cells. S1P$_1$ signaling sustains hallmark endothelial functions in the naive brain and expands during ischemia by engagement of cell-autonomous S1P provision. Disrupting this pathway by endothelial cell-selective deficiency in S1P production, export, or the S1P$_1$ receptor substantially exacerbates brain injury in permanent and transient models of ischemic stroke. By contrast, profound lymphopenia induced by loss of lymphocyte S1P$_1$ provides modest protection only in the context of reperfusion. In the ischemic brain, endothelial cell S1P$_1$ supports blood-brain barrier function, microvascular patency, and the rerouting of blood to hypoperfused brain tissue through collateral anastomoses. Boosting these functions by supplemental pharmacological engagement of the endothelial receptor pool with a blood-brain barrier penetrating S1P$_1$-selective agonist can further reduce cortical infarct expansion in a therapeutically relevant time frame and independent of reperfusion.

CONCLUSIONS: This study provides genetic evidence to support a pivotal role for the endothelium in maintaining perfusion and microvascular patency in the ischemic penumbra that is coordinated by S1P signaling and can be harnessed for neuroprotection with blood-brain barrier-penetrating S1P$_1$ agonists.

GRAPHIC ABSTRACT: A graphic abstract is available for this article.

Key Words: blood-brain barrier ■ collateral circulation ■ endothelium ■ fingolimod hydrochloride ■ neuroprotective agents ■ stroke

Editorial, see p 383 | Meet the First Author, see p 307

Ischemic stroke is one of the most prevalent causes of death and morbidity worldwide and represents a major societal and economic burden (https://www.who.int).[1] Despite several clinical trials with neuroprotective therapeutics, treatment options remain limited to thrombolysis and mechanical recanalization.[2] Novel

Correspondence to: Eric Camerer, Université de Paris, PARCC, INSERM U970, 56 Rue Leblanc, F-75015 Paris, France. Email eric.camerer@inserm.fr
*A.N., M.P., A.B., and P.B. contributed equally to this article.
The Data Supplement is available with this article at https://www.ahajournals.org/doi/suppl/10.1161/CIRCRESAHA.120.316711.
For Sources of Funding and Disclosures, see page 380.

Circulation Research is available at www.ahajournals.org/journal/res

ORIGINAL RESEARCH

Novelty and Significance

What Is Known?

- Immune suppression and stimulation of vascular function have been investigated as adjunct therapies for the treatment of ischemic stroke.
- S1P (Sphingosine 1-phosphate) signaling through $S1P_1$ (S1P receptor-1) plays important roles in immune cell trafficking and vascular homeostasis.
- S1P receptor modulators including fingolimod have shown promise for the treatment of ischemic and hemorrhagic stroke in both experimental models and small-scale clinical trials.
- Mechanistically, these modulators have been considered to act principally by inhibiting $S1P_1$-mediated sensing of circulating S1P, thus blocking lymphocyte trafficking and immunothrombosis.

What New Information Does This Article Contribute?

- Disruption of homeostatic $S1P_1$ signaling in the vascular endothelium, but not in lymphocytes, profoundly impacts outcome in mouse models of ischemic stroke.
- Receptor polarization shields endothelial $S1P_1$ from circulating endogenous and synthetic ligands and imposes a need for cell-autonomous S1P provision in the ischemic brain.
- A blood-brain penetrating $S1P_1$-selective agonist prevents infarct expansion in permanent and transient models of ischemic stroke when administered during a therapeutically relevant period of time after stroke onset.

Therapies for stroke are currently limited to mechanical and thrombolytic recanalization of the occluded artery. Immune suppression and stimulation of vascular function have both been explored as adjunct therapies to limit the expansion of the infarct core and reduce hemorrhagic transformation. $S1P_1$ has emerged as a potential therapeutic target for both ischemic and hemorrhagic stroke, yet immunosuppression induced by $S1P_1$ modulation could potentially increase the risk of poststroke infection. By revealing that the main protective action of $S1P_1$ modulation depends on the endothelial receptor, we demonstrate that it is possible to obtain protection without the prolonged immunosuppression induced by some $S1P_1$ modulators currently being explored for stroke therapy. Coupled with the need for blood-brain barrier penetration, this finding has implications as to the choice of $S1P_1$ modulators for stroke therapy. Our study also highlights the potential of targeting endothelial function as a therapeutic approach for the treatment of ischemic stroke.

Nonstandard Abbreviations and Acronyms

ACA	anterior cerebral artery
BBB	blood-brain barrier
EC	endothelial cell
eNOS	endothelial nitric oxide synthase
GPCR	G protein-coupled receptor
ICA	internal carotid artery
ICAM	intercellular adhesion molecule
MCA	middle cerebral artery
pMCAO	permanent middle cerebral artery occlusion
S1P	sphingosine 1-phosphate
$S1P_1$	sphingosine 1-phosphate receptor-1
S1P1GS	S1P1 GFP signaling
tMCAO	transient middle cerebral artery occlusion
Spns2	spinster homolog 2

safe and affordable adjunct treatment strategies are, therefore, needed.

Ischemic stroke is caused by thrombotic or embolic occlusion of a large cerebral artery. This produces a core of necrotic tissue immediately downstream of the occlusion site surrounded by an ischemic penumbra that can be rescued if adequate perfusion is sustained.[1,3] The speed by which the core encroaches upon the penumbra depends on the efficiency of retrograde blood supply through cortical collateral anastomoses extended across the borders with neighboring cerebral arterial territories. Although governed primarily by the number and size of existing anastomoses, blood rerouting also depends on the dilatory capacity, integrity, and patency of the regional vasculature.[4] Improving microvascular function to counteract the expansion of the infarct core and improve the efficacy and safety of anterograde reperfusion may, therefore, provide a therapeutic opportunity.[5] Strategies explored to this end include the inhibition of lymphocyte-driven inflammatory thrombosis and the stimulation of endothelial cell (EC) function to promote local redistribution of blood flow, reinforce the blood-brain barrier (BBB), and suppress inflammation and coagulation in affected territories.[5,6]

S1P is a signaling lipid with critical roles in both immune and vascular function exerted by 5 cognate GPCRs (G protein-coupled receptors), $S1P_{1\text{-}5}$.[7] Lymphocytes depend on $S1P_1$-mediated S1P sensing to egress from lymphoid organs, and both inhibition and activation of lymphocyte

$S1P_1$ induce profound lymphopenia.[8] $S1P_1$ is also among the most abundant EC GPCRs, and selective constitutive or temporal deletion of *S1pr1* (encoding $S1P_1$) in mouse ECs impairs embryonic and postnatal angiogenesis, vascular integrity, and flow-mediated vasodilation.[7,9,10] Loss of $S1P_1$ signaling in ECs destabilizes adherens junctions, reduces eNOS (endothelial nitric oxide synthase) activity, and increases the expression of leukocyte adhesion molecules.[10–12] $S1P_1$ thus plays a critical role in sustaining hallmark endothelial functions. S1P is abundant in circulation, where it associates primarily with HDL (high-density lipoprotein) and albumin.[7] Erythrocytes and ECs are the main sources of blood and lymph S1P under homeostasis, whereas platelets store large amounts of S1P that is only released upon activation.[7,9,13] S1P is exported from ECs by Spns2 (spinster homolog 2) and from platelets and erythrocytes by Mfsd2b (major facilitator superfamily domain containing 2B).[7,14]

The multiple sclerosis drug fingolimod (FTY720) is a functional antagonist of $S1P_1$ that also activates $S1P_{3,4,5}$ and has shown promise for the treatment of ischemic and hemorrhagic stroke in both experimental models and small-scale clinical trials.[15–24] Similar efficacy of $S1P_1$-selective agonists argues that FTY720 protection is mediated by $S1P_1$.[6,19,21] Loss of efficacy in lymphocyte-deficient mice and correlation between efficacy on lymphocyte depletion and infarct reduction has indicated that $S1P_1$ modulators provide protection by impairing lymphocyte trafficking and, thereby, lymphocyte-driven thromboinflammation.[19,20] Yet the endothelial receptor pool is also engaged after systemic drug treatment, and the risks and benefits of targeting EC $S1P_1$ have not been specifically evaluated.

In this study, we have addressed the impact of tissue-specific deficiency of $S1P_1$ and sources of its activating ligand on the development, anatomy, and function of the naive brain vasculature and on the outcome of transient and permanent middle cerebral artery occlusion (tMCAO and pMCAO, respectively) in mice. This revealed an important role for EC $S1P_1$ in cerebrovascular homeostasis and a critical protective role for EC-autonomous engagement of $S1P_1$ signaling during cerebral ischemia. When we addressed the capacity of pharmacological agonists to access $S1P_1$ on the brain endothelium, we found that BBB penetration is required for engagement of EC $S1P_1$ and that this receptor pool is an important target for the protective effects of S1P receptor modulation in ischemic stroke.

METHODS

Detailed Methods are available in the Data Supplement.

Data Availability

The authors declare that all supporting data are available within the article and its Data Supplement.

RESULTS

Endothelial $S1P_1$ Plays a Critical Protective Role During Cerebral Ischemia

To define endogenous roles of EC and leukocyte $S1P_1$ in ischemic stroke, we generated EC *S1pr1* knockout mice with *Cdh5*-iCreERT2 or *Pdgfb*-iCreERT2 ($S1pr1^{ECKO}$) and pan-hematopoietic *S1pr1* knockout mice with *Mx1-Cre* or *Vav1-Cre* ($S1pr1^{HCKO}$).[9,11,25] The *Pdgfb*-iCreERT2 allele induced near-complete recombination of an mTmG (membrane targeted tandem dimer Tomato/membrane targeted green fluorescent protein) reporter in ECs in the cerebral cortex after neonatal tamoxifen administration (Figure IA in the Data Supplement). We have previously reported efficient *S1pr1* excision in target tissues with the other Cre drivers.[25,26] In a pMCAO model, in which thermocoagulation and subsequent dissection of a section of the MCA distal to the lenticulostriate arteries yields small and cortically confined infarcts but no overt neurological deficits,[27,28] mean 24-hour infarct volumes were on average 71% larger in neonatally induced $S1pr1^{ECKO}$ males and 65% larger in $S1pr1^{ECKO}$ females than in littermate controls (Figure 1A). The relative increase was greater 3 days after pMCAO with 148% larger infarcts in $S1pr1^{ECKO}$ males (Figure 1B). Although the *Pdgfb*-iCreERT2 allele used for EC-selective gene deletion has off-target effects in megakaryocytes,[25,29] the phenotype could be attributed to ECs as it was reproduced in $S1pr1^{ECKO}$ males generated with the EC-selective *Cdh5*-iCreERT2 (Figure 1C), but not with $S1pr1^{MKKO}$ males generated with the megakaryocyte-selective *Pf4-Cre* (Figure IB in the Data Supplement).[25] In the same experimental model, hematopoietic $S1P_1$ deficiency induced profound lymphopenia but had no impact on infarct size (Figure 1D, Figure IC in the Data Supplement). Similar results were obtained in a filament-based proximal transient MCAO model, in which infarct volumes measured 24 hours after 60 minutes occlusion were on average more than twice as large and neurological deficits exacerbated in $S1pr1^{ECKO}$ mice (Figure 1E). Induction of gene deletion 10 days before surgery in this experiment argued that sensitization to MCAO did not reflect upon developmental consequences of EC *S1pr1* deletion. Yet as control infarcts were smaller than typically observed with proximal MCAO—an observation that may be attributed to protective effects of tamoxifen[30,31]—neonatal deletion was used in all subsequent experiments. When neonatally induced $S1pr1^{ECKO}$ males were subjected to a severe tMCAO model in which reperfusion was delayed to 90 minutes, infarcts covered a substantial portion of the MCA territory in controls, and $S1pr1^{ECKO}$ mice exhibited considerable postreperfusion mortality (68% versus 32%, respectively, P=0.022; Figure ID in the Data Supplement) that manifested >8 hours after occlusion. Postmortem analysis did not reveal bleeding, and hemorrhagic transformation was not increased in $S1pr1^{ECKO}$ survivors (minor bleeds were observed in 1/6 $S1pr1^{ECKO}$ versus 5/14 control infarcts). Loss of the most affected animals may explain

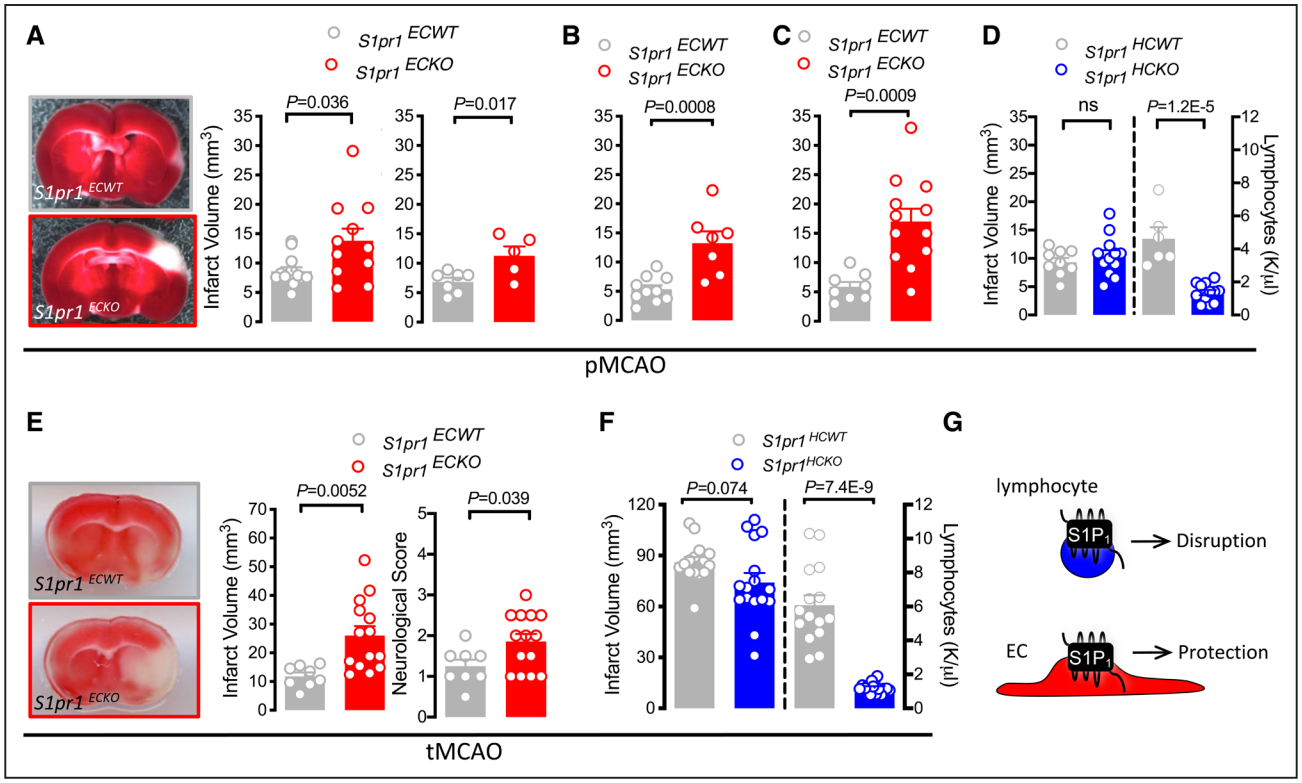

Figure 1. Endothelial S1P$_1$ (sphingosine 1-phosphate receptor-1) signaling limits brain injury after permanent and transient middle cerebral artery occlusion (pMCAO and tMCAO, respectively).
A–**C**, Infarct volumes 24 (**A** and **C**) or 72 (**B**) hours after pMCAO in *S1pr1*^{ECKO} and littermate males (**A**, **middle**, **B**) and females (**A**, **right**) generated by neonatal *S1pr1* deletion with *Pdgfb*-iCreERT2 (**A** and **B**) or *Cdh5*-iCreERT2 (**C**). **Left** of **A**, Representative images. **D**, Basal peripheral blood lymphocyte counts and infarct volumes 24 h after pMCAO in male mice lacking S1P$_1$ in hematopoietic cells (*S1pr1*^{HCKO}; *Vav1*-Cre). **E**, Infarct volumes and neurological deficits 24 h after 60 min tMCAO in male mice lacking S1P$_1$ in endothelial cells (*S1pr1*^{ECKO}; *Cdh5*-iCreERT2; adult deletion). **Left**, Representative images. **F**, Infarct volumes 24 h after 60 min tMCAO in males lacking S1P$_1$ in hematopoietic cells (*S1pr1*^{HCKO}; *Mx1-Cre*). Lymphocyte counts pre-MCAO in **right**. **G**, Schematic representation of the net cell type-specific contribution of S1P$_1$ signaling to stroke outcome. Bar graphs show mean±SEM. Statistical significance assessed by Mann-Whitney test (**A**, males) or unpaired *t* test (all other).

a lack of significant difference in infarct volumes observed in survivors (Figure ID in the Data Supplement) and is further addressed below. Unlike the pMCAO model, hematopoietic S1P$_1$ deficiency afforded some neuroprotection 24 hours after 60 minutes tMCAO (Figure 1F; *P*=0.074). These observations reveal a critical role for endothelial S1P$_1$ in limiting neuronal injury in ischemic stroke irrespective of whether or not the occluded artery is reperfused (Figure 1G). They also support the notion that S1P$_1$ plays a disruptive role in ischemic stroke by supporting lymphocyte egress,[20] yet the effect of specifically impairing this pathway was modest and observed only in the context of reperfusion (Figure 1G).

Ischemia Mobilizes EC-Autonomous S1P Provision for S1P$_1$ Signaling and Stroke Protection

S1P$_1$ drives lymphocyte egress and sustains lung vascular integrity in response to circulating ligand.[13,32] Surprisingly, however, postnatal deletion of *Sphk1&2* in *Mx1*-Cre sensitive cells did not significantly impact infarct volumes after pMCAO or tMCAO (Figure 2A), even if the same deletion strategy nearly abolishes S1P provision to plasma, resulting in lymphopenia and constitutive vascular leak in the lung.[9,13,32] This could reflect compound effects of loss of S1P production also in tissue-resident cells or of loss of circulating S1P on the activation of S1P$_1$ and other S1PRs, notably S1P$_2$,[33] in several cellular compartments.[34] However, lymphocyte S1P$_1$ was dispensable in the pMCAO model (Figure 1D), and deletion of *S1pr2* or *S1pr3* did not impact outcome in the pMCAO model (Figure IIA in the Data Supplement). Selective impairment of S1P release from platelets, which could potentially increase local S1P levels in stroke and change signaling bias,[9,35] did not impact infarct size in the tMCAO model (Figure 2B). Single-cell RNA sequencing analysis suggests that brain ECs express the necessary machinery for de novo S1P synthesis and export and may thus constitute a local source of S1P in the neurovascular unit.[36] Accordingly, impairment of the production (*Sphk1&2*^{ECKO}) or the export (*Spns2*^{ECKO}) of S1P in ECs both exacerbated outcome to a similar degree as EC S1P$_1$ deficiency in the pMCAO and the tMCAO model, pointing to a critical role for cell-autonomous S1P provision for EC S1P$_1$ activation (Figure 2C and 2D and Figure IIB and IIC

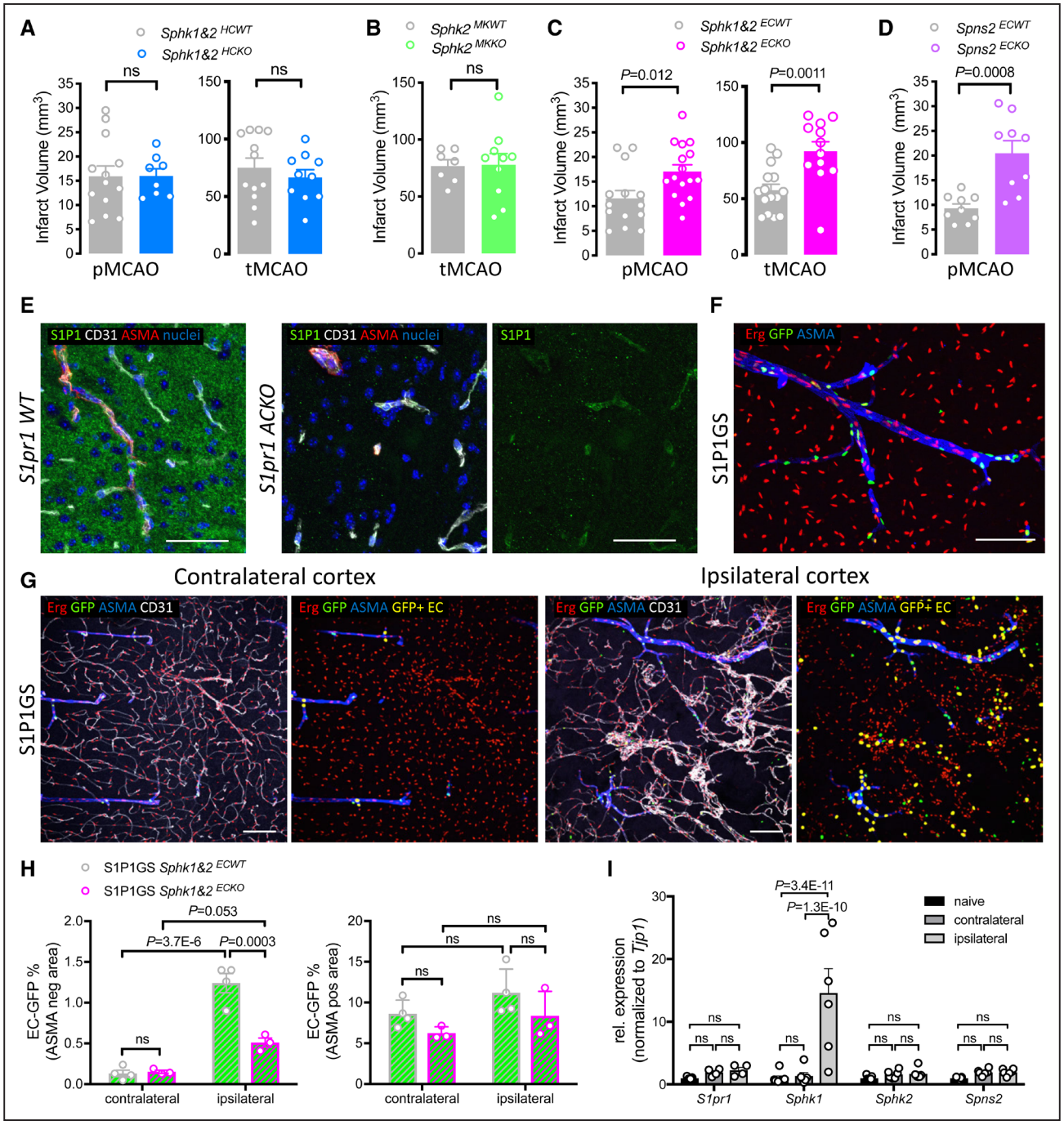

Figure 2. Endothelial cell (EC) autonomous S1P (sphingosine 1-phosphate) provision sustains S1P$_1$ (S1P receptor-1) activation during cerebral ischemia.

A–**D**, Infarct volumes 24 h after permanent middle cerebral artery occlusion (pMCAO) or 60 min transient middle cerebral artery occlusion (tMCAO) in male mice lacking S1P production in hematopoietic cells (*Sphk1&2*^{HCKO}; **A**), platelets (*Sphk2*^{MKKO}; **B**), or endothelial cells (*Sphk1&2*^{ECKO}; **C**), or deficient in S1P export from blood endothelial cells (*Spns2*^{ECKO}; **D**) and respective littermate controls. **E**, S1P$_1$ expression in the naive cerebral cortex of wild-type mice (**left**) and mice lacking S1P$_1$ in astrocytes (*S1pr1*^{ACKO}, *Gfap-Cre*, **right**). Note expression of S1P$_1$ in all vessels. Green, S1P$_1$; white, ECs (CD31); red, vascular smooth muscle cells (ASMA); blue, all cell nuclei (Hoechst). Scale bar: 50 µm. **F** and **G**, S1P$_1$ signaling visualized in S1P$_1$ signaling mice (S1P1GS) in a naive cerebral cortex (**F**) and 48 h after pMCAO (**G**) assessed in the contralateral (**left**) and ipsilateral (**right**) cerebral cortex. Note that S1P$_1$ signaling is highly restricted to arteries in the naive and contralateral cerebral cortex and more widespread but still predominantly endothelial in the ipsilateral cortex. Red, EC nuclei (Erg); green, S1P$_1$ signaling cells (GFP); yellow, S1P$_1$ signaling ECs (GFP/Erg double-positive nuclei); white, ECs (CD31); blue, vascular smooth muscle cells (ASMA). Scale bar: 100 µm. **H**, Quantification of GFP positive ECs as a fraction of total arterial and nonarterial ECs in the ipsilateral and contralateral hemisphere of S1P1GS mice with (*Sphk1&2*^{ECWT}) and without (*Sphk1&2*^{ECKO}) the capacity for EC S1P production 48 h after pMCAO. **I**, Relative expression of *S1pr1*, *Sphk1*, *Sphk2,* and *Spns2* in cerebral microvessels isolated from naive cerebral cortex or 6 h after tMCAO, normalized to *Tjp1* transcript. Bar graphs show mean±SEM. Statistical significance assessed by ANOVA with Tukey multiple comparisons test (**H** and **I**), Mann-Whitney test (**C**, pMCAo), or unpaired *t* test (all other).

in the Data Supplement). Excision efficiency was confirmed to be >85% for *Sphk1* and *Sphk2* in isolated brain ECs from *Sphk1&2*^{ECKO} (Figure IID in the Data Supplement). To address where cell-autonomous $S1P_1$ signaling is engaged after MCAO, we first asked where $S1P_1$ is expressed. Single-cell RNA sequencing of brain microvascular fragments shows enrichment of *S1pr1* transcripts in ECs as well as in astrocytes (Figure IIE in the Data Supplement).[36] Accordingly, protein expression, which initially appeared widespread and diffuse in the cerebral cortex (Figure 2E), could be resolved by selective deletion of *S1pr1* in ECs (*S1pr1*^{ECKO}) or astrocytes (*S1pr1*^{ACKO}; Figure 2E, Figure IIF and IIG in the Data Supplement). The level of EC $S1P_1$ expression is maintained in old mice (Figure IIG and IIH in the Data Supplement).[37] We then generated S1P1GS ($S1P_1$ green fluorescent protein [GFP] signaling) mice—which leave a nuclear GFP signal after $S1P_1$-β-arrestin coupling[38]—with or without the capacity for EC S1P production (*S1pr1*$^{Ki/+}$*:H2B-Gfp*$^{Tg/+}$*:Sphk1&2*$^{ECWT/KO}$). Despite widespread receptor expression in astrocytes and ECs throughout the vascular tree, $S1P_1$ signaling was highly restricted to a subset of arteriolar ECs in both young and old mice (Figure 2F, Figure III and IIJ in the Data Supplement). $S1P_1$-independent H2B-GFP activity was also observed in perivascular cells of arterioles and venules but not in ECs (Figure IIK in the Data Supplement). After pMCAO, $S1P_1$ signaling in the infarct region expanded to capillary and venous ECs, but not to astrocytes (Figure 2G and 2H). While redundant ligand sources[9] or ligand-independent activation[11] sustained homeostatic signaling in arterioles (Figure 2H), the expansion of $S1P_1$ signaling after MCAO was driven principally by EC-autonomous S1P production (Figure 2H). To address the mechanistic basis for this expansion, we evaluated the expression of Sphks, Spns2, and $S1P_1$ in brain microvessels 6 hours after tMCAO. Consistent with single-cell RNA sequencing data,[36] *Sphk2*, *Spns2*, and *S1pr1* and to a lesser degree *Sphk1* were all expressed in cerebral microvessels of naive mice. Ischemia triggered robust induction of *Sphk1* expression in the ipsilateral hemisphere but had little impact on the expression of the other transcripts (Figure 2I, Figure IIL in the Data Supplement). Thus, while circulating S1P sustains lymphocyte trafficking and may contribute to homeostatic signaling in cerebral arterioles, $S1P_1$-dependent neuroprotection in ischemic stroke is driven primarily by engagement of EC-autonomous S1P provision, possibly by transcriptional activation of *Sphk1*.

Postnatal Impairment of EC-Autonomous S1P Signaling Does Not Impact Cerebrovascular Anatomy

Although recombination of loxP-flanked alleles in ECs in neonatal mice in most experiments in this study overcame confounding effects of tamoxifen protection, it also introduced potential confounding effects of deregulated vascular development on stroke outcome. As previously reported for *Cdh5*-iCreERT2-mediated neonatal deletion of *S1pr1*,[11] *Pdgfb*-iCreERT2-mediated deletion induced vascular hypersprouting and delayed outgrowth of the retinal vasculature (Figure 3A and 3B). However, this phenotype was not replicated with *Pdgfb*-iCreERT2-mediated deletion of *Sphk1&2* (Figure 3A and 3B). This suggests that postnatal angiogenesis, like embryonic angiogenesis,[9] is sustained by redundant S1P sources and that abnormal vascular patterning is unlikely to explain sensitivity to MCAO in *Sphk1&2*^{ECKO} mice. Consistent with prenatal development of the cerebral vasculature, we also did not observe significant differences in the number of collateral connections between the MCA and branches of anterior cerebral artery (ACA) extending laterally from the midline between *S1pr1*^{ECKO} and littermate controls (Figure 3C and 3D). Vascular density in the cerebral cortex was also unaltered by *Pdgfb*-iCreERT2-mediated *S1pr1* excision, as has previously been reported for *Cdh5*-iCreERT2-mediated deletion (Figure 3E).[26] Thus, the increased impact of MCAO in mice deficient in EC-autonomous $S1P_1$ signaling cannot be explained by underlying differences in vascular anatomy.

Endothelial $S1P_1$ Maintains BBB Function

Both genetic strategies for EC *S1pr1* deletion employed in this study result in constitutive vascular leak in the lung that can be replicated by plasma but not by EC S1P deficiency.[9,39] *Cdh5*-iCreERT2-mediated *S1pr1* deletion results in subtler and size-selective permeability of the brain endothelium,[26] which was also observed with *Pdgfb*-iCreERT2-mediated *S1pr1* deletion (Figure 4A). Endotoxin challenge (10 mg/kg, 8 hours) increased 4 kD dextran accumulation to the same degree in *S1pr1*^{ECKO} and littermate controls (Figure 4B). Thus, $S1P_1$ deficiency does not critically impair the stability of EC junctions at the BBB. Intriguingly, even if *S1pr1*^{ECKO} mice do not show increased paracellular permeability to dextrans ≥10 kD,[26] naive *S1pr1*^{ECKO} mice did show increased permeability to Evans Blue/albumin, which crosses the BBB primarily by transcellular transport (Figure 4C).[40] Neither basal phenotype was replicated in mice lacking EC S1P production nor was Evans Blue/albumin extravasation affected by lack of plasma S1P (Figure 4A and 4C), again suggesting source redundancy or ligand-independence of homeostatic EC $S1P_1$ signaling at the BBB. Twenty-four hours after pMCAO, Evans Blue/albumin accumulation in the ipsilateral hemisphere exceeded the relative increase in infarct size in *S1pr1*^{ECKO} mice with a more diffuse and widespread appearance and was also significantly higher in the contralateral hemisphere, consistent with results in naive mice (Figure 4D). In the acute phase after 90 minutes tMCAO—which is associated with high mortality of *S1pr1*^{ECKO} mice (Figure ID in the Data Supplement)—full T2 weighted magnetic resonance imaging revealed

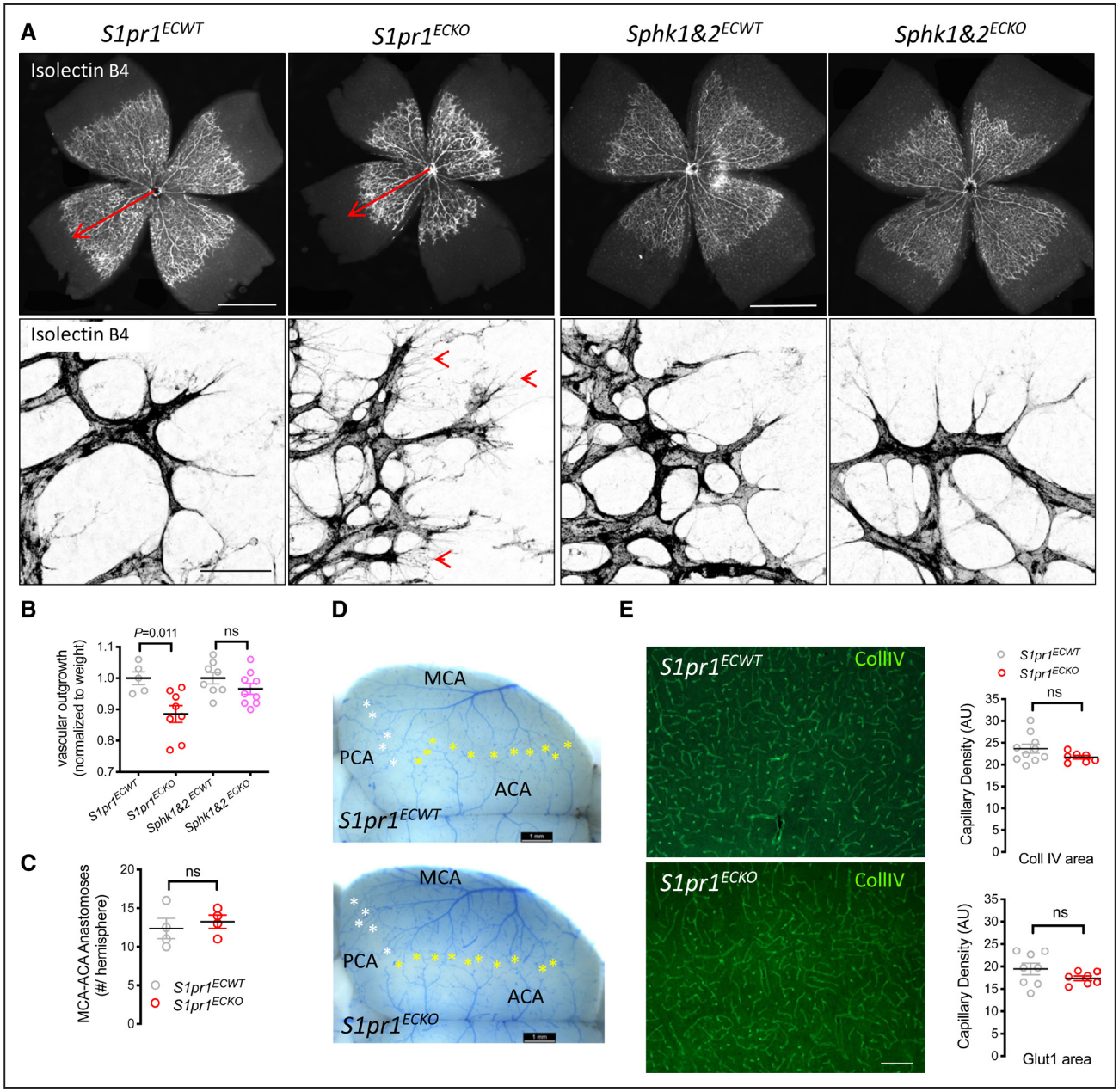

Figure 3. Loss of endothelial cell (EC)-autonomous S1P$_1$ (sphingosine 1-phosphate receptor-1) signaling does not impact cerebrovascular patterning.

A, Isolectin B4 staining shows vascularization of the mouse retina at postnatal day (P)5 after neonatal *Pdgfb* iCreERT2-driven *S1pr1* or *Sphk1&2* deletion. Note delayed expansion of the vascular network (**top**, arrow) and abundant filopodia at the vascular front (**bottom**, arrowheads) of *S1pr1*^{ECKO} but not *Sphk1&2*^{ECKO} retinas. Scale bar: 1 mm (**top**), 50 µm (**bottom**) **B**, Quantification of outgrowth of the retinal vasculature at P5, normalized to weight of pups. **C** and **D**, Collateral connections between the middle cerebral artery (MCA) and branches of the posterior CA (PCA, white asterisk) and of the anterior CA (ACA, yellow asterisk) extending laterally from the midline between *S1pr1*^{ECKO} and littermate controls. **C**, Quantification of ACA-MCA connections. **D**, Representative images. **E**, Vascular density in the cortex of *S1pr1*^{ECKO} and littermate controls assessed by collagen IV (Coll IV) or Glut (Glucose transporter type)-1 staining. Representative images of Coll IV staining (**left**) and quantification of both (**right**), scale bar: 100 µm. Bar graphs show mean±SEM. Statistical significance assessed by 1-way ANOVA with Tukey multiple comparisons test (**B**) and unpaired *t* test (all other).

severe edema in *S1pr1*^{ECKO} mice as early as 2.5 hours after reperfusion with a clear shift in the midline 2 hours later (Figure 4E). Image analysis confirmed significantly larger T2 lesions, demonstrating a clear impact of EC S1P$_1$ deficiency also after 90 minutes of tMCAO despite no significant increase in infarct volumes in the few *S1pr1*^{ECKO} mice that survived for 24 hours (Figure ID in the Data Supplement). Transtentorial herniation may be followed by cerebellar tonsil herniation and could explain increased mortality in *S1pr1*^{ECKO} mice in this model (Figure ID in the Data Supplement). Thus, S1P$_1$ preserves BBB integrity in ischemic stroke most likely by restricting

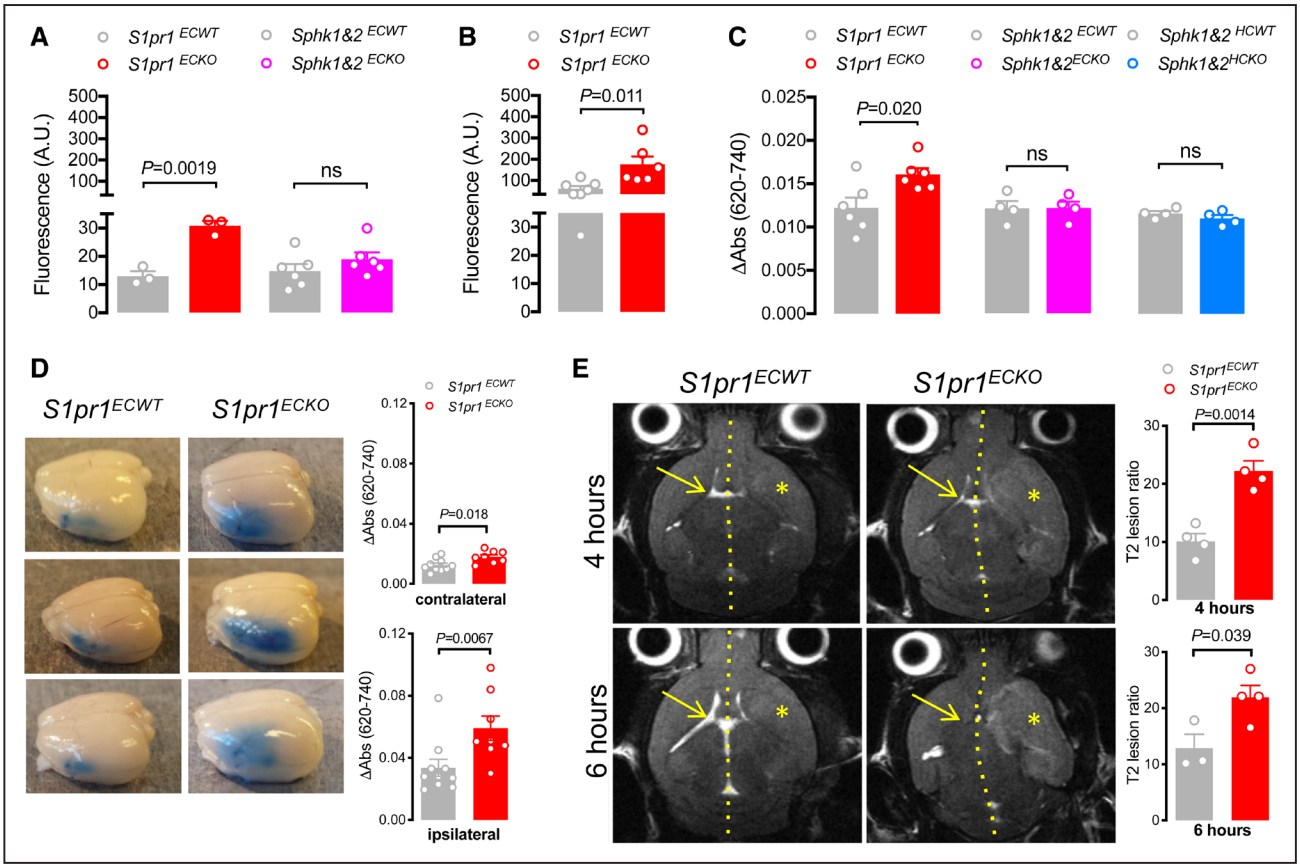

Figure 4. Endothelial S1P$_1$ (sphingosine 1-phosphate receptor-1) sustains blood-brain barrier (BBB) function. **A**, Effect of *Pdgfb*-iCreERT2-mediated deletion of *S1pr1* and *Sphk1&2* on the accumulation of 4 kD TRITC-Dextran in the cerebral cortex of naive mice. **B**, Effect of *Pdgfb*-iCreERT2-mediated deletion of *S1pr1* on the accumulation of 4 kD TRITC-Dextran in the cerebral cortex 8 h after challenge with 10 mg/kg lipopolysaccharide (LPS) intraperitoneal. **C**, Effect of *Pdgfb*-iCreERT2-mediated deletion (endothelial cell-selective knockout [ECKO]) of *S1pr1* and *Sphk1&2* as well as *Mx1*-Cre-mediated deletion (hematopoietic cell-selective knockout [HCKO]) of *Sphk1&2* on the accumulation of Evans Blue/albumin in the cerebral cortex of naive mice. **D**, Effect of *Pdgfb*-iCreERT2-mediated deletion of *S1pr1* on Evans Blue/albumin leak 24 h after permanent middle cerebral artery occlusion (pMCAO) in ipsilateral and contralateral hemispheres. **Left**, Representative brains. **Right**, Corrected absorbance of full hemisphere extracts. **E**, Full T2-weighted magnetic resonance imaging (MRI) 4 and 6 h after 90 min transient middle cerebral artery occlusion (tMCAO) in *S1pr1*^{ECKO} and littermate controls. **Left**, Representative axial sections from level of the mid-olfactory bulb from the same animal at the 2 time points. Hatched line indicates midline, asterisk affected MCA territory, and arrow contralateral ventricle. **Right**, T2 lesion ratios calculated from MRI images based on axial plane images at the mid-olfactory bulb. Bar graphs show mean ± SEM. Statistical significance assessed by Mann-Whitney test (**D**) and unpaired *t* test (all other).

vesicular transport, which underlies BBB dysfunction in the acute phase.[40]

S1P$_1$ Supports Cerebral Vasoreactivity and Promotes Tissue Perfusion After MCAO

We next addressed if EC S1P signaling regulates vessel diameter and thereby the redistribution of blood to the ischemic penumbra through existing cortical collateral anastomoses. Significantly reduced blood flow responses assessed by Doppler ultrasonography in the somatosensory cortex in response to acetylcholine superfusion (Figure 5A) and in the basilar trunk in response to CO_2 inhalation (Figure 5B) both argued a critical role for EC S1P$_1$ in cerebral blood flow regulation. Blood flow responses in the somatosensory cortex in response to whisker stimulation were nevertheless unaltered, suggesting normal neurovascular coupling, as was mean arterial pressure observed during these recordings (Figure 5A, Figure IIIA in the Data Supplement). Flow-mediated dilation was also significantly reduced in posterior cerebral artery segments isolated from *S1pr1*^{ECKO} mice (Figure 5C). A similar phenotype in mesenteric arteries from both *S1pr1*^{ECKO} and *Sphk1&2*^{ECKO} mice (Figure IIIB in the Data Supplement) argued that shear forces can engage EC S1P$_1$ through cell-autonomous S1P release. Impairment of vascular reactivity in *S1pr1*^{ECKO} mice did not, however, impact central blood pressure (assessed by telemetry; Figure 5D) or basal brain perfusion (assessed by arterial spin labeling magnetic resonance imaging; Figure 5E).[41] We next monitored mean blood flow velocities in the left and right internal carotid arteries (ICA) and in the basilar trunk before, 50 and 120 minutes after pMCAO in *S1pr1*^{ECKO} and littermate controls (Figure 5F).

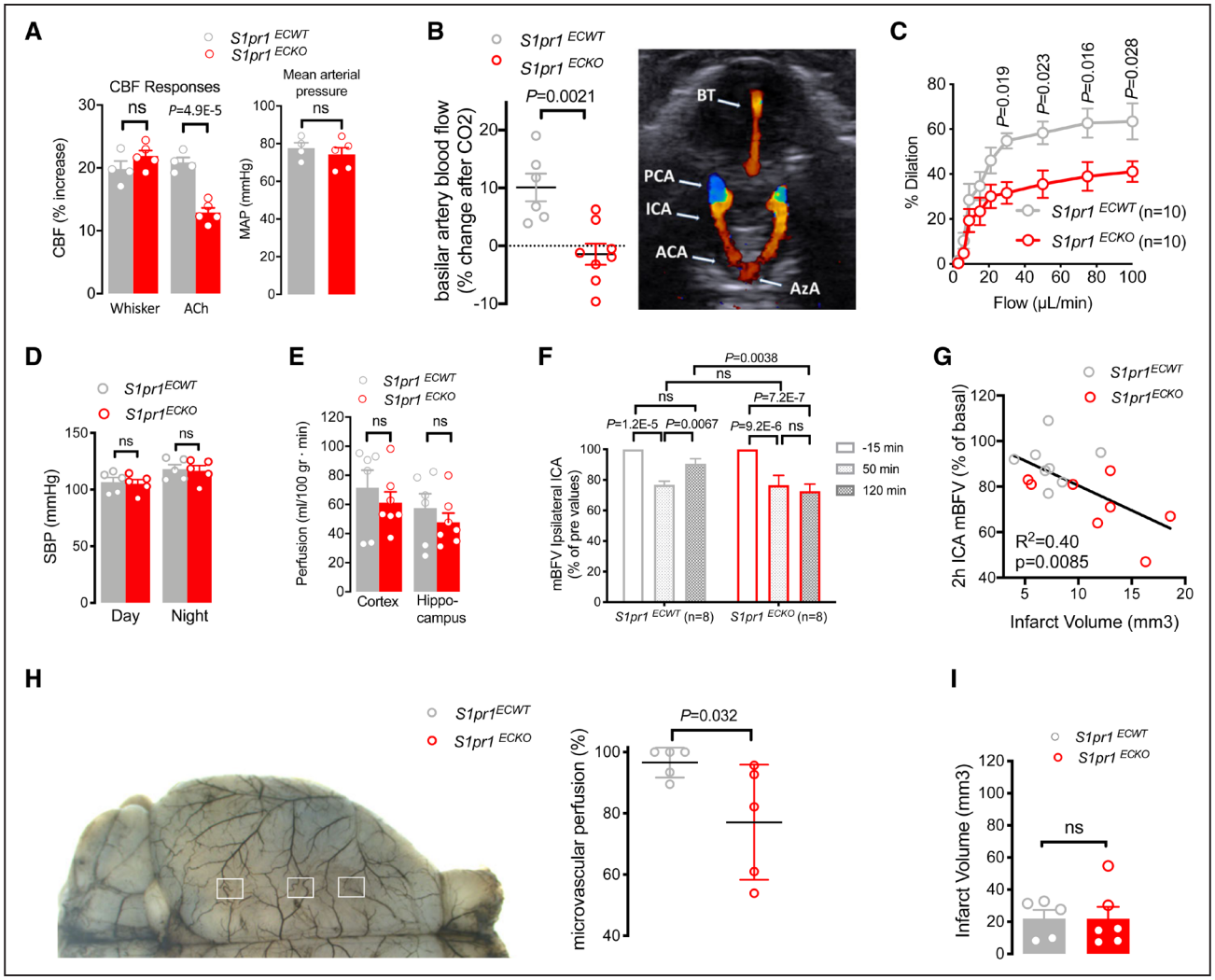

Figure 5. Endothelial S1P$_1$ (sphingosine 1-phosphate receptor-1) regulates cerebral blood flow and supports tissue perfusion in the acute phase of stroke.

A, Somatosensory cortex blood flow (CBF) assessed by laser Doppler flowmetry in mice equipped with a cranial window in response to whisker stimulation or superfusion of the endothelium-dependent vasodilator acetylcholine (ACh; 10 µmol/L) on exposed neocortex (**left**). Mean arterial blood pressures monitored in the femoral arteries during the CBF measurements (**right**). **B**, Mean blood flow velocities (mBFVs) measured by ultrasound in the basilar trunk of *S1pr1*^{ECKO} mice and littermate controls before and 2–5 min after exposure to a gas mixture of 16% O_2, 5% CO_2, 79% N_2 (normoxia-hypercapnia) and the relative change in velocities presented. Doppler image shows vessels analyzed in **B** and **F**. **C**, Flow-mediated dilation in posterior cerebral artery segments of *S1pr1*^{ECKO} and littermate control mice assessed by arteriography. **D**, Blood pressures of nonsedated *S1pr1*^{ECKO} and littermate control mice recorded for 72 h by telemetry. Average day and night systolic blood pressure (SBP) is shown; diastolic blood pressure and heart rates also did not differ between the groups. **E**, Basal perfusion of the cerebral cortex and hippocampus in *S1pr1*^{ECKO} mice assessed by arterial spin labeling magnetic resonance imaging (MRI). **F**, mBFVs measured by ultrasound imaging in left and right intra cranial internal carotid artery (ICA) and basilar trunk (BT) under 0.5% isoflurane anesthesia before, 50 min and 2 h after electrocoagulation-induced permanent middle cerebral artery occlusion (pMCAO). Normalized values in ipsilateral ICA shown, absolute values for all arteries in Figure IIIC in the Data Supplement. **G**, mBFVs in the left ICA 2 h after left MCAO expressed as % of mean preocclusion velocities are plotted against infarct volumes in the same mice determined 24 h after occlusion. **H**, Blood flow in the leptomeningeal vasculature in the ipsilateral hemisphere was imaged by sidestream dark-field imaging through a cranial window 2–2.5 h after pMCAO. **Left** illustrates approximate positions of regions monitored at the MCA/anterior cerebral artery (ACA) border. **Right** shows results of automated analysis of microvascular perfusion in the MCA/ACA and MCA/posterior cerebral artery (PCA) border regions. Representative videos in Data Supplement. **I**, Infarct volumes 3 days after 35 min of transient middle cerebral artery occlusion (tMCAO) in *S1pr1*^{ECKO} males and littermate controls. Graphs show mean±SEM. Statistical significance was assessed by repeated measures (**C**, **D**, and **F**) 2-way ANOVA with Bonferroni (**C** and **F**) or Sidak (**D**) multiple comparisons test, 1-way ANOVA (**A** CBF, **E**), linear regression analysis (**G**), Mann-Whitney test (**H**) or unpaired *t* test (all other). AzA indicates azygos artery.

No significant genotype-dependent difference was observed in baseline mean blood flow velocities (Figure IIIC in the Data Supplement). Permanent left MCAO decreased mean blood flow velocities in the left ICA to 77% of preocclusion values 50 minutes after occlusion in both *S1pr1*^{ECKO} and control mice (Figure 5F). Consistent with this decrease reflecting upon the reduction in MCA territory downstream of the left ICA, we observed

no significant change in mean blood flow velocities in the right ICA or the basilar trunk (Figure IIIC in the Data Supplement). A subsequent recovery to near 90% of preocclusion values at 120 minutes after occlusion in controls was interpreted to reflect upon a downstream increase in peri-infarct reflow through branches of the MCA originating upstream from the occlusion and through the distal branches of the ACA and posterior cerebral artery (Figure 5F, Figure IIIC in the Data Supplement). This recovery at 120 minutes after occlusion was absent in *S1pr1*^{ECKO} mice (Figure 5F, Figure IIID in the Data Supplement), and a significant inverse correlation was observed between relative ICA blood flow at 120 minutes and infarct volumes at 24 hours (Figure 5G). To address perfusion directly in the affected cortex after pMCAO, we next visualized red blood cell flux in the area of collateral anastomoses in the leptomeningeal arteries between the MCA and ACA by sidestream dark-field imaging (Figure 5H, Movies I through III in the Data Supplement). Two hours after pMCAO, unidirectional flow towards the MCA territory was observed in all ACA-MCA collaterals, allowing perfusion of the territory normally supplied by branches of the MCA downstream of, but distal to the occlusion site (Movies I and II in the Data Supplement). Blood moving retrograde switched anterograde up other MCA branches when encountering coagulated blood in the ischemic core (Movie III in the Data Supplement). While the same general pattern was observed in mice of both genotypes, microvascular perfusion in MCA territory proximal to the ACA border was significantly reduced in *S1pr1 ECKO* mice (Figure 5H, Movie II in the Data Supplement). No significant genotype-dependent difference in ICA blood flow reduction at 50 minutes argued that protective effects of S1P$_1$ signaling take time to establish, possibly because of the need to engage EC-autonomous S1P production through *Sphk1* induction (Figure 2I). Accordingly, when occlusion time was reduced to 35 minutes in the tMCAO model, EC S1P$_1$ deficiency no longer influenced infarct size (Figure 5I). These observations are consistent with the notion that EC S1P$_1$ limits the expansion of the necrotic core in the acute phase of ischemic stroke by supporting local vasodilation so as to promote retrograde perfusion of affected MCA territories.

Endothelial S1P$_1$ Signaling Maintains Microvascular Patency in the Ischemic Penumbra

In addition to the active redistribution of blood from neighboring vascular territories, perfusion of the ischemic penumbra is highly dependent on microvascular patency within the affected zone. The recruitment of leukocytes to an activated endothelium in the ischemic penumbra may directly impair capillary blood flow and propagate microvascular thrombosis.[42,43] S1P$_1$ helps sustain the anti-inflammatory status of the aortic endothelium,[12] and we observed a significant increase in ICAM (intercellular adhesion molecule)-1 in brain homogenates and in postcapillary venules in the cerebral cortex of naive *S1pr1*^{ECKO} mice (Figure 6A, Figure IVA in the Data Supplement). This increase was not observed with selective impairment of S1P production in endothelial or hematopoietic cells (Figure 6A, Figure IVA in the Data Supplement). In the acute phase after pMCAO (2.5 hours), however, an increase in ICAM-1 expression in the ipsilateral hemisphere of control but no *S1pr1*^{ECKO} mice overcame the genotype-dependent difference (Figure 6B). MPO (myeloperoxidase) levels were increased in *S1pr1*^{ECKO} mice (Figure 6B), albeit not beyond the increase in infarct size (Figure 1A). We next stained for erythrocytes, neutrophils, platelets, and fibrin(ogen) in sections of brains perfused transcardially with heparinized saline 3 hours after pMCAO. Plasma serotonin was slightly increased at this time independent of genotype, arguing against a significant difference in platelet activation (Figure IVB in the Data Supplement). We nevertheless observed a striking reduction in the penetration of tomato lectin, infused 15 minutes before transcardial perfusion, into the MCA territory superior/distal to the core in *S1pr1*^{ECKO} mice (Figure 6C, Figure IVC in the Data Supplement). This again points to collateral failure. Platelets and fibrin(ogen) were observed within both perfused and nonperfused capillaries only superior to the core and correlated with more intense staining for PECAM (platelet endothelial cell adhesion molecule)-1/CD31 (Figure 6C, Figure IVD and IVE in the Data Supplement). Fibrin deposition was more widespread and significantly more abundant in *S1pr1*^{ECKO} mice (Figure 6C, Figure IVF in the Data Supplement). Occasional neutrophils were observed within capillaries on both sides of the infarct core at similar frequency in both genotypes (Figure IVD, IVF, and IVG in the Data Supplement). These observations confirm that EC S1P$_1$ signaling promotes retrograde perfusion of the ischemic penumbra and suggest that it does so in part by maintaining microvascular patency.

Receptor Polarization Restricts S1P$_1$ Signaling and Ligand Access at the Blood-Neural Barrier

The need for EC-autonomous S1P provision to sustain vascular protective S1P$_1$ signaling in the ischemic brain could be explained by depletion of circulating S1P, as observed in myocardial infarction and during systemic inflammation.[9,44] However, plasma and platelet S1P levels were unchanged in the early acute phase of stroke with or without reperfusion (Figure 7A). An alternative explanation could be that receptor polarization restricts access of S1P$_1$ to circulating ligand at the BBB. To address this possibility, we first used confocal microscopy to evaluate the subcellular localization of EC S1P$_1$. Imaging across one or 2 nuclei allowed us to distinguish

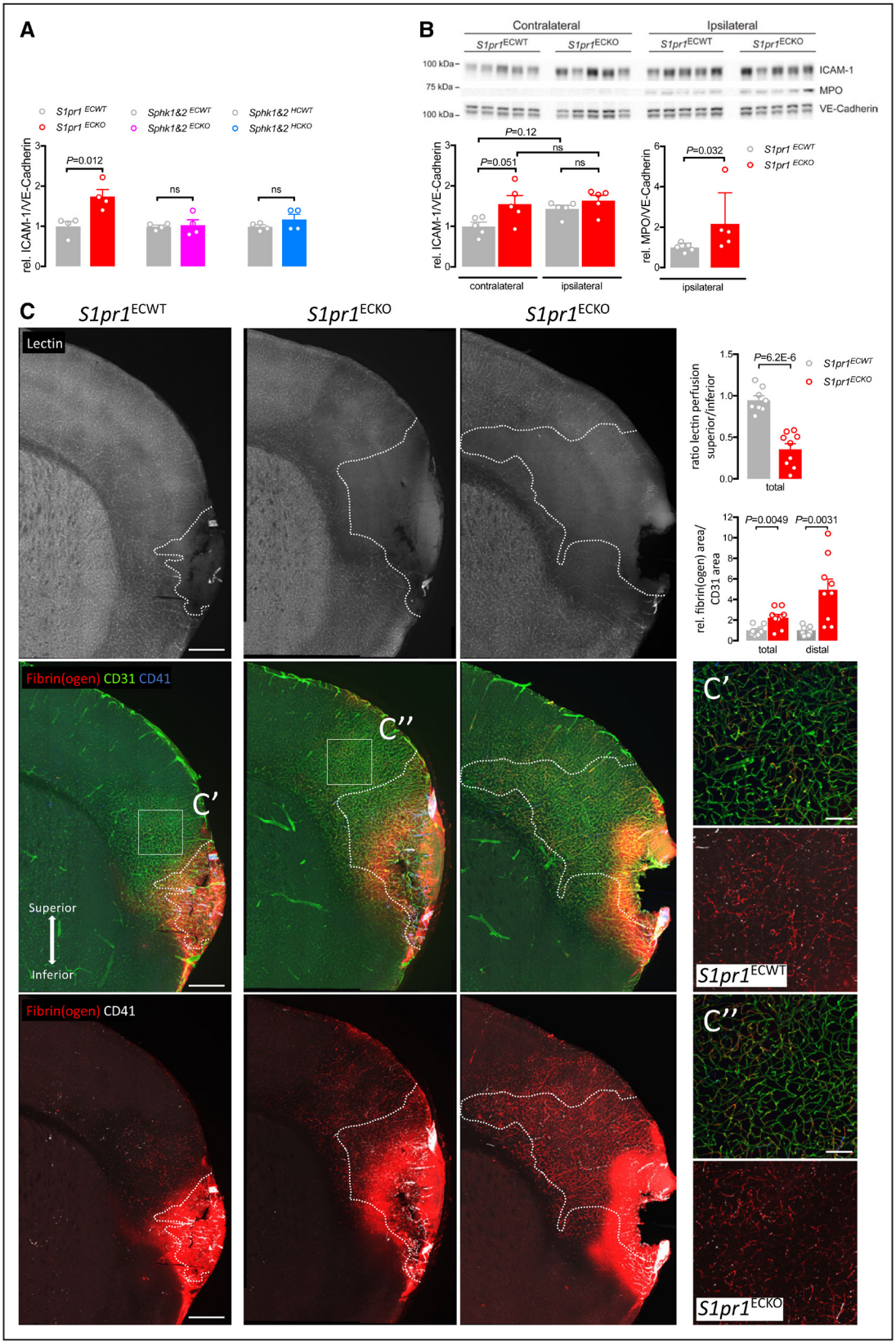

Figure 6. Endothelial S1P$_1$ (sphingosine 1-phosphate receptor-1) suppresses tissue perfusion and fibrin formation in middle cerebral artery (MCA) territories.

A, ICAM (intercellular adhesion molecule)-1 protein in homogenates of cerebral cortex from naive *S1pr1*^{ECKO}, *Sphk1&2*^{ECKO} (*Pdgfb*-Cre) and *Sphk1&2*^{HCKO} (*Mx1*-Cre) mice and littermate controls analyzed by Western blot and normalized to the vascular marker VE-Cadherin. **B**, ICAM-1 and MPO (myeloperoxidase) protein in homogenates of contra- and ipsilateral hemispheres 2.5 h after permanent (*Continued*)

the EC plasma membranes, and *S1pr1*^{ACKO} mice allowed us to discriminate between the abluminal plasma membrane and astrocyte end-feet in the cerebral cortex. In the developing retina, $S1P_1$ was present primarily on the luminal surface of capillary ECs, where it colocalized with ICAM-2 (Figure 7B, Figure VA in the Data Supplement). By contrast, expression was predominantly abluminal on capillary ECs in the adult retina (Figure 7C, Figure VB in the Data Supplement), while a subset of arteriolar ECs retained luminal expression (Figure 7D, Figure VC in the Data Supplement). $S1P_1$ expression was also predominantly abluminal on capillary ECs in the adult brain (Figure 7E, Figure VD in the Data Supplement). Polarization was retained during ischemia (Figure VE in the Data Supplement).

To confirm our impression that $S1P_1$ is surface expressed but luminally excluded in the majority of ECs in the cerebral cortex, we again made use of the $S1P_1$ signaling reporter. In naive S1P1GS mice, hepatocytes show no nuclear GFP although they express $S1P_1$ (Figure VIA in the Data Supplement).[38] Systemic administration of the potent $S1P_1$-selective agonist RP-001 (0.6 mg/kg)[38,45] induced robust $S1P_1$ signaling in hepatocytes as well as ECs of skeletal muscle and lung, but not cerebral cortex (Figure 7F, Figure VI in the Data Supplement). In striking contrast, when injected directly into the brain parenchyma, RP-001 (0.06 mg/kg) substantially increased $S1P_1$ signaling in arteries, capillaries, and veins of the cerebral cortex (Figure 7F). Astrocytes remained GFP negative despite $S1P_1$ expression (Figure VII in the Data Supplement),[36] suggesting together with mostly punctate staining (Figure 7E) that the receptor is not expressed on the astrocyte surface under homeostasis. Further attesting to polarization and a role for $S1P_1$ in blood flow regulation, we observed a significant EC $S1P_1$-dependent increase in cortical blood flow by laser Doppler when RP-001 was administered directly into the cerebrospinal fluid for paravascular access[46] but not systemically (Figure 7G). Surprisingly, induction of $S1P_1$ signaling in brain ECs, although detectable, was also minimal after systemic administration of high dose FTY720 (2×5 mg/kg), despite strong activation of the $S1P_1$ reporter in other organs (Figure 7F, Figure VI in the Data Supplement). It should be noted that although FTY720 is known to cross the BBB and desensitize $S1P_1$ on the brain endothelium, this has been demonstrated with high doses over extended time.[26,47] CYM-5442 is an $S1P_1$-selective agonist reported to distribute rapidly and preferentially to the brain after systemic injection.[48] Accordingly, at a dose required to induce $S1P_1$ signaling equivalent to RP-001 (0.6 mg/kg) and FTY720 (2×5 mg/kg) in hepatocytes, CYM-5442 (10 mg/kg) induced signaling also in brain ECs after systemic administration (Figure 7H, Figure VIA in the Data Supplement).

Collectively, these observations argue that abluminal polarization shields $S1P_1$ from circulating endogenous and synthetic ligands in capillary, venous, and most arterial ECs once the blood-neural barrier is established, and that BBB penetration is required for agonists to harness this receptor pool. Gradual receptor polarization in all but a small subset of arterial ECs with maturation of the blood-neural barrier provides potential explanation for why cell-autonomous S1P provision is required for broader endothelial $S1P_1$ activation during cerebral ischemia (Figure 2A, 2C, 2D, and 2H), although it is dispensable both for $S1P_1$ activation in the developing retina (Figure 3A) and for homeostatic signaling in cerebral arterioles (Figure 2F and 2H).

A BBB-Penetrating $S1P_1$-Selective Agonist Limits Cortical Infarct Expansion After Both pMCAO and tMCAO

Our results so far argue that optimal therapeutic $S1P_1$ targeting for stroke would transiently suppress lymphocyte trafficking and activate but not desensitize EC $S1P_1$, and that CYM-5442 may be better suited than RP-001 and FTY720. CYM-5442 distributes preferential to brain and has a relatively short plasma half-life (3 hours).[48] Accordingly, CYM-5442 induced lymphopenia 3 hours after administration that was evident at 1 mg/kg and as profound as RP-001 (0.6 mg/kg) and FTY720 (1 mg/kg) at 3 mg/kg (Figure 8A). Twenty-four hours later, lymphocyte counts remained low in mice receiving FTY720 but returned to normal in mice receiving CYM-5442 and RP-001 (Figure 8A). In the pMCAO model, CYM-5442 modestly reduced 24-hour infarct volumes at 1 mg/kg (Figure VIIIA in the Data Supplement) and provided substantial benefit when administered both immediately and up to 6 hours after occlusion at 3 mg/kg (Figure 8B). In a modified pMCAO model that included permanent ligation of the ipsilateral CCA, infarct volumes were also reduced at 7 days with daily CYM-5442 (3 mg/kg) administration (Figure VIIIB in the Data Supplement). Consistent

Figure 6 Continued. MCA occlusion (pMCAO) from *S1pr1*^{ECKO} mice and littermate controls. **Top**, Western Blot. **Bottom**, Quantification. **C**, Female *S1pr1*^{ECWT} and *S1pr1*^{ECKO} mice were analyzed 3 hours after pMCAO. Representative images of brain sections from *S1pr1*^{ECWT} (**left**) and *S1pr1*^{ECKO} (**middle** and **right**) mice. Dashed line indicates the perfusion border assessed by tomato lectin infusion 15 min before sacrifice (**top**). Fibrin(ogen) (red); endothelial cells (CD31, green), and platelets (CD41, blue/white). Square indicates area of higher magnification to the **right**. Note the extended area of poor perfusion superior to the infarct core and fibrin deposition both within and beyond the nonperfused regions. Scale bar: 500 µm for low magnification image and 100 µm for high magnification images. Lectin perfusion was assessed superior and inferior to the infarct core in an area of 600 µm×1200 µm (total), and fibrin(ogen) only superior to the infarct core in an area of 800 µm×1200 µm (total) or only within the distal part in an area of 800 µm×600 µm (distal). Bar graphs show mean±SEM. Statistical significance assessed by 1-way ANOVA with Holm-Sidak multiple comparisons test (**B**, **left**), Mann-Whitney (**B**, **right**) or unpaired *t* test (all other).

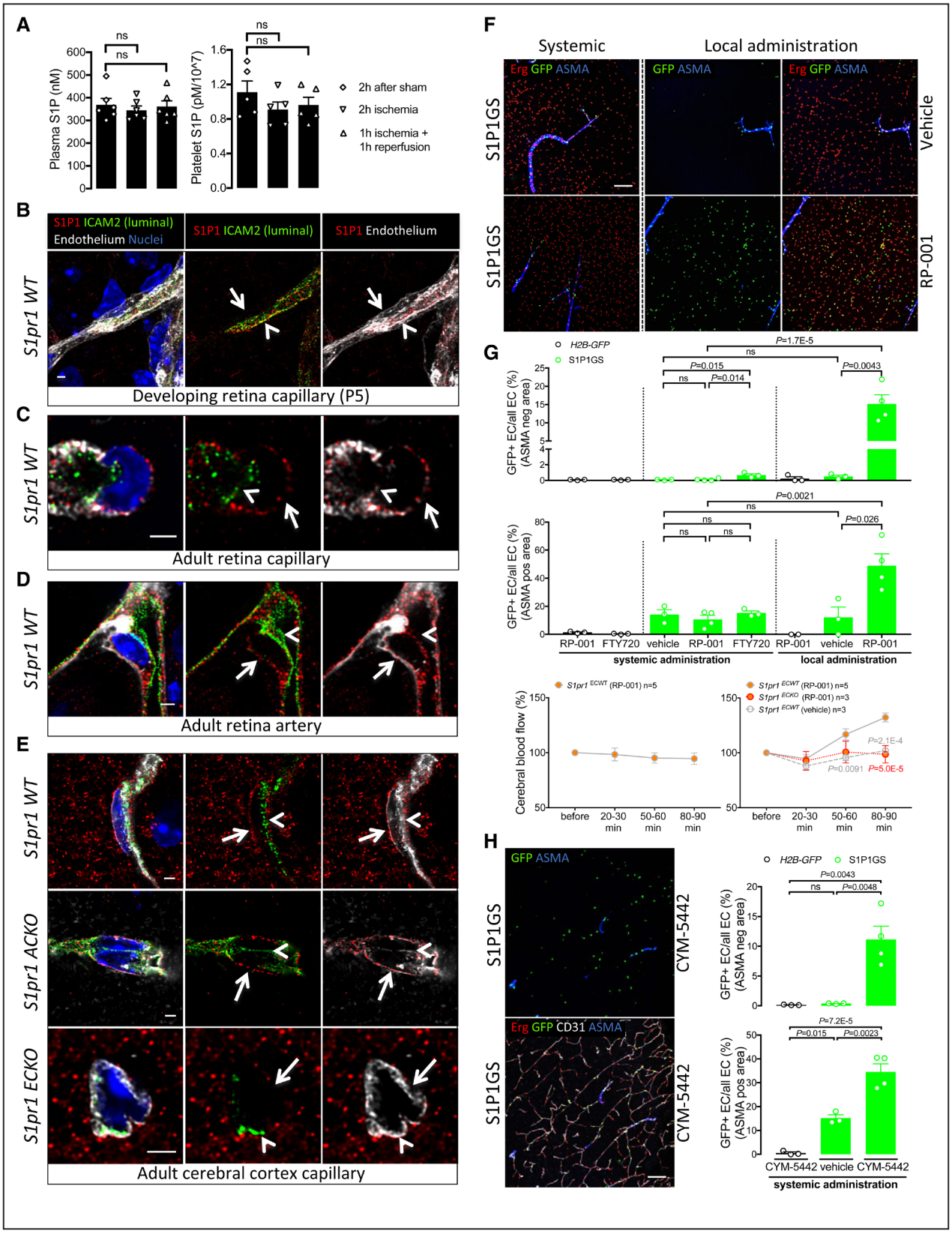

Figure 7. Receptor polarization restricts S1P$_1$ (sphingosine 1-phosphate receptor-1) signaling and ligand access at the blood-neural barrier.

A, S1P levels in plasma (**left**) and platelets (**right**) after permanent and transient filament-induced middle cerebral artery occlusion (MCAO) relative to sham. **B**–**E**, Assessment of S1P$_1$ polarization in capillaries (**B**, **C**, and **E**) and artery (**D**) of the developing retina (**B**), adult retina (**C** and **D**) and adult cerebral cortex (**E**) of wild-type mice (**B**, **C**, **D**, **E upper**) and mice lacking *S1pr1* in astrocytes (*S1pr1*^{ACKO}; (*Continued*)

with the engagement of and dependence on EC $S1P_1$, CYM-5442 (3 mg/kg) reversed sensitivity to pMCAO in *Sphk1&2*^{ECKO} mice (Figure 8C versus Figure IIB in the Data Supplement), but not in *S1pr1*^{ECKO} mice (Figure 8D versus 1A). CYM-5442 (3 mg/kg) also afforded significant protection when administered during reperfusion 60 minutes after MCAO (Figure 8E). Consistent with a mechanism involving collateral blood supply,[28] protection in tMCAO was delimited to the cortex, where an infarct reduction of 70% mirrored protection achieved in the cortically restricted pMCAO model (Figure 8E). RP-001, which did not efficiently cross the BBB (Figure 7F), did not provide protection in the pMCAO model despite inducing equivalent lymphopenia and strong $S1P_1$ signaling in other organs (Figure 8A and 8F, Figure VIA in the Data Supplement). Thus, optimal $S1P_1$ targeting for ischemic stroke requires BBB penetration for engagement of endothelial receptors (Figure 8G) and can provide substantial protection against cortical infarct expansion independent of reperfusion and in a therapeutically relevant time window.

DISCUSSION

$S1P_1$ modulators have shown promise in experimental models and small-scale clinical trials of ischemic and hemorrhagic stroke.[6,22] Yet as their mechanisms of action are not fully elucidated, optimal drug properties and targeting strategies remain to be defined. As protection has been attributed to suppression of lymphocyte-mediated thromboinflammation, most current strategies focus on inhibiting the function of lymphocyte $S1P_1$.[6,19,20,24] Using a variety of genetic and experimental murine models to address endogenous roles of $S1P_1$ signaling in cerebral ischemia, we confirm the potential benefit of targeting lymphocyte receptors but also reveal a critical role for EC $S1P_1$ in cerebrovascular homeostasis and endogenous protection against ischemic brain damage. Compromised BBB function, reduced vasodilatory capacity, and fibrin deposition in the ischemic penumbra provoked collateral failure and rapid expansion of the infarct core in mice with selective deficiency of $S1P_1$ in ECs. This provides genetic evidence to support the critical and multifaceted neuroprotective roles of the endothelium in ischemic stroke and the importance of S1P signaling in coordinating these functions. Addressing mechanisms of $S1P_1$ engagement, we uncover that the receptor is abluminally polarized and insensitive to circulating ligands in most ECs at the blood-neural barrier, imposing a need for cell-autonomous ligand provision for stroke protection and BBB penetration for supplemental therapeutic receptor engagement. This suggested optimal benefit of joint targeting of lymphocyte and, in particular, EC receptor pools with BBB-penetrating $S1P_1$ agonists, a strategy that we demonstrate to limit cortical infarct spreading in mouse models of MCAO independent of reperfusion.

Our findings argue that endothelial $S1P_1$ is dynamically engaged to limit infarct expansion, as neonatal deletion of $S1P_1$ did not visibly alter vascular anatomy in the adult brain and as exacerbation of infarct size was also observed when $S1P_1$ deficiency was induced in adulthood. Moreover, EC-selective deficiency in sphingosine kinases sensitized to MCAO to a similar degree as $S1P_1$ deficiency even if it did not reproduce defects in retinal angiogenesis or in cerebrovascular homeostasis observed in *S1pr1*^{ECKO} mice, and sensitization was overcome by compensating for the lack of endogenous ligand with a pharmacological $S1P_1$ agonist.

$S1P_1$ supports hallmark functions of the endothelium in (1) mediating smooth muscle relaxation, (2) maintaining vascular integrity, and (3) suppressing inflammation.[7] We provide evidence that $S1P_1$ exerts all these functions in the brain as follows:

1. A role for EC $S1P_1$ in control of cerebral blood flow in the naive brain was suggested by impaired acetylcholine- and hypercapnia-induced blood flow responses in *S1pr1*^{ECKO} mice, impaired flow-mediated dilation in *S1pr1*^{ECKO} cerebral arteries ex vivo, and the capacity of an $S1P_1$ agonist to stimulate cerebral blood flow in wild-type but not

Figure 7 Continued. E middle) or in endothelial cells (ECs; *S1pr1*^{ECKO}; **E lower**). Note that $S1P_1$ expression (red) colocalizes with the luminal EC marker ICAM (intercellular adhesion molecule)-2 (green) in capillaries of the developing retina but not in the mature retina and brain. Luminal expression remains in some arterial ECs in the mature retina. The nonpolarized EC marker isolectin B4 (**B** and **C**) or Glut (Glucose transporter type)-1 (**D** and **E**) is shown in white, and the nuclear marker Hoechst in blue. Arrowheads indicate luminal and arrows abluminal side of the endothelium. Scale bars: 2 µm. Plots of fluorescence intensity are provided in Figure V in the Data Supplement. **F**, $S1P_1$ signaling in the cerebral cortex studied in $S1P_1$ GFP signaling reporter mice (S1P1GS) after systemic (0.6 mg/kg i.v.) or local (0.06 mg/kg intraparenchymal) administration of RP-001 or systemic FTY720 (2×5 mg/kg p.o.) or vehicle control by the same route. Note that signaling (GFP positive nuclei, green), usually restricted to ASMA positive arterioles (blue), is widespread in Erg-positive EC (red) after local administration of RP-001. GFP/Erg double-positive EC nuclei were counted in arterial (ASMA positive, **lower**) and other ECs (ASMA negative, **upper**) and expressed as a percentage of all ECs in the same category. **Upper**, Representative images; **lower**, image-based quantification (only statistical analysis for S1P1GS mice is shown and was done within and across treatment groups, respectively). Scale bar: 100 µm. GFP induction in other tissues in Figure VI in the Data Supplement, high-resolution image and quantification of non-EC GFP in Figure VII in the Data Supplement. **G**, Evolution of blood flow velocities in the cerebral cortex after injection of RP-001 i.v. (0.6 mg/kg; **left**) or into the cerebrospinal fluid (0.06 mg/kg; **right**) of *S1pr1*^{ECKO} and littermate control mice. Error bars: SEM. **H**, $S1P_1$ signaling in the cerebral cortex after systemic administration of CYM-5442 (10 mg/kg) or vehicle control. **Left**: Representative images, scale bar: 100 µm; **right**: Image-based quantification of GFP/Erg double-positive ECs as a fraction of total arterial and nonarterial ECs, respectively. Bar graphs show mean ± SEM. Statistical analyses by Mann-Whitney (**F**, local administration) or by 1- or 2-way ANOVA with Dunnett (**A**) or Tukey (all other) multiple comparisons test (all other).

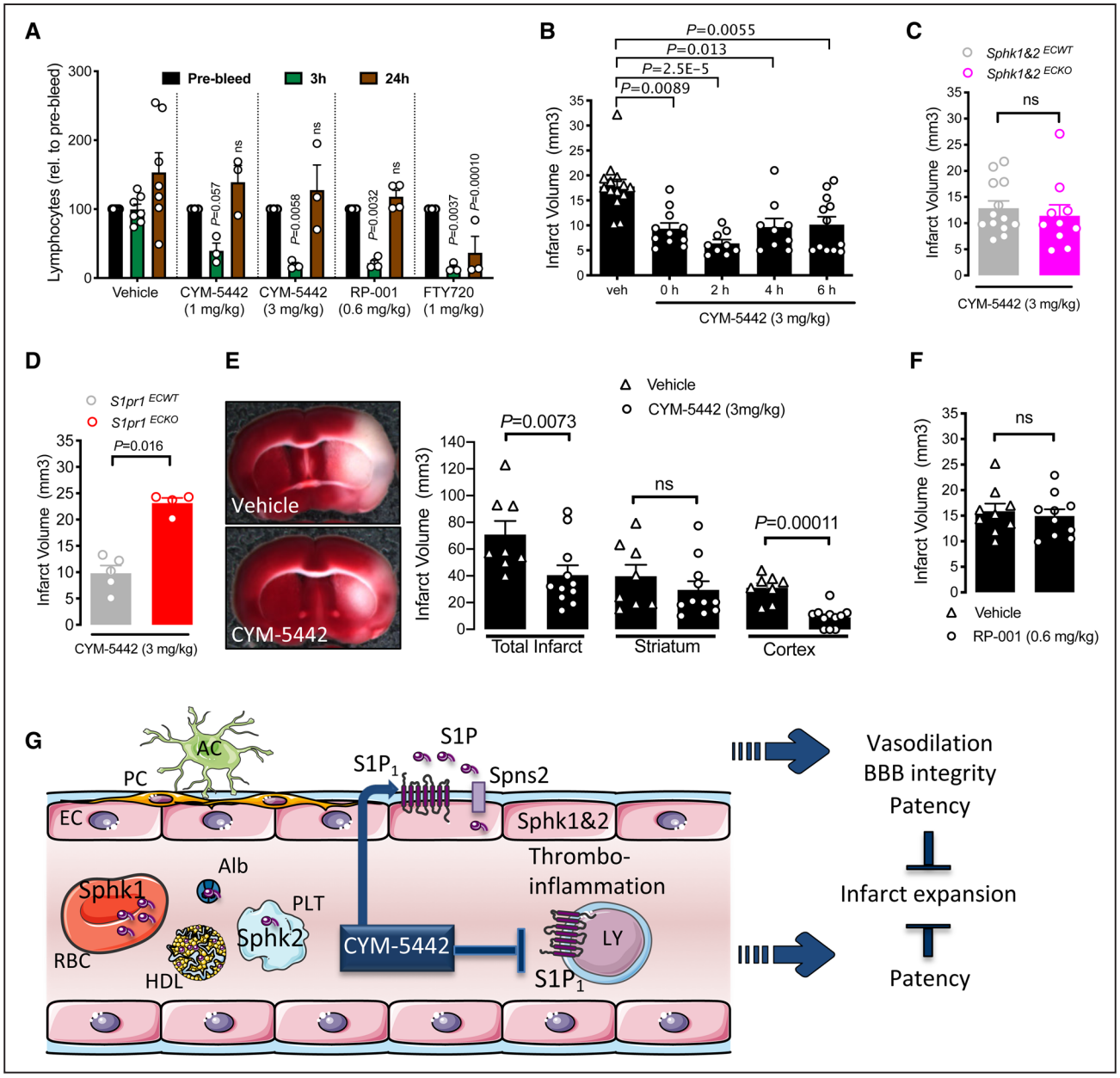

Figure 8. A blood-brain barrier (BBB) penetrating S1P$_1$ (sphingosine 1-phosphate receptor-1) agonist limits cortical infarct expansion in ischemic stroke.

A, Effects of CYM-5442, RP-001, and FTY720 at indicated concentrations on lymphocyte (LY) counts 3 and 24 h after bolus administration. Values normalized to prebleed. Statistical significance assessed in comparison to vehicle control at indicated time points. **B**, Effect of CYM-5442 (3 mg/kg i.p. 0–6 h after occlusion) on infarct size 24 h after permanent middle cerebral artery occlusion (pMCAO) in wild-type males. **C** and **D**, Effect of CYM-5442 (3 mg/kg i.p. immediately after occlusion) on the impact of EC Sphk1&2 (**C**) and S1P$_1$ (**D**) deficiency (*Pdgfb*-iCreERT2) on infarct size 24 h after pMCAO. **E**, Effect of CYM-5442 (3 mg/kg i.p. immediately before reperfusion) on infarct size 24 h after 60 min transient middle cerebral artery occlusion (tMCAO; **left**, representative infarcts; **right**, total and regional infarct size). **F**, Effect of RP-001 (0.6 mg/kg i.p. immediately after occlusion) on infarct size 24 h after pMCAO. **G**, Protective actions of CYM-5442 are accounted for mostly by engagement of endothelial S1P$_1$, which promotes vasodilation and BBB integrity and limits fibrin deposition. By inducing transient lymphopenia through modulation of LY receptors, CYM-5442 may further reduce thromboinflammation, as has been previously described for FTY720. These distinct actions will act in concert to limit inflammation and edema and promote microvascular patency and perfusion of affected brain regions. Bar graphs show mean ± SEM. Statistical significance assessed by repeated measures 2-way ANOVA (**A**), Kruskall-Wallis test with Dunn multiple comparisons test (**B**), unpaired *t* test (**C** and **F**), or Mann-Whitney test (**D** and **E**). AC indicates astrocytes; Alb, albumin; PC, pericytes; PLT, platelet; and RBC, red blood cell.

in *S1pr1*^{ECKO} mice. Impaired blood flow recovery and microvascular perfusion in *S1pr1*^{ECKO} mice in the acute phase after MCAO argued that S1P$_1$ also actively supports endothelial function during cerebral ischemia. This was substantiated by the impact of S1P$_1$ deficiency on injury to the cortex,

in which MCA branches are well connected to contiguous vascular territories, but not the striatum, in which they are not.[28,49,50] $S1P_1$ coordinates developmental angiogenesis by promoting perfusion of the nascent vasculature[11] and supports flow-mediated dilation of mesenteric arteries.[10] eNOS, which is important for the vasoactive functions of $S1P_1$,[10,11] also promotes the early establishment of collateral supply, thus counteracting infarct expansion in ischemic stroke.[51] It is, therefore, likely that $S1P_1$ acts at least in part, through eNOS. Blunted vasodilation in response to acetylcholine, hypercapnia, and flow, but not whisker stimulation, with EC $S1P_1$ deficiency is intriguing and argues against a role for $S1P_1$ in the mechanisms through which the endothelium contributes to retrograde propagation of vasoactive signals generated by neural activity. The dissociation between endothelium-dependent responses and functional hyperemia has also been observed in mice fed a high-salt diet, which display marked suppression of the eNOS-driven response to acetylcholine, but not of functional hyperemia.[52,53] While the role of eNOS and other effectors downstream of $S1P_1$ in this context remains to be specifically addressed, our results suggest that one important mechanism by which EC $S1P_1$ limits infarct expansion is by facilitating retrograde perfusion of the affected MCA territory through collateral anastomoses with contiguous arterial branches.

2. Further attesting to the importance of $S1P_1$ in supporting the functions of the brain endothelium, naive *S1pr1*^{ECKO} mice also displayed impaired BBB integrity. Although subtler in the naive brain than defects in lung vascular integrity observed in the same genetic model,[9,39] dramatic and early onset edema after MCAO nevertheless argues for an important role for $S1P_1$ in supporting BBB function during ischemia. Evans Blue/albumin leak more than doubled in *S1pr1*^{ECKO} 24 hours after pMCAO, and magnetic resonance imaging revealed profound edema within hours after tMCAO. This suggests a possible role for $S1P_1$ in regulating vesicular transport, as edema in ischemic stroke involves transcellular transport in the early phase and tight junction impairment in the late phase.[40] Minimal impact of $S1P_1$ deficiency on 4 kDa dextran leak in a model of septic encephalopathy in this study also argued against a critical role for $S1P_1$ in maintaining tight junctions. This is consistent with a report showing that ApoM-S1P regulates vesicular transport in cerebral arterioles through $S1P_1$ signaling.[54] A second important mechanism by which EC $S1P_1$ limits infarct expansion is, therefore, through the regulation of BBB integrity, suggesting that benefit afforded by $S1P_1$ agonists on edema formation in ischemic and hemorrhagic stroke may involve direct actions on the BBB.[6,21,24]
3. EC $S1P_1$ deficiency was associated with increased ICAM-1 expression in the naive brain, suggestive of a role for $S1P_1$ in suppressing endothelial activation and leukocyte adhesion. However, expression was not further increased in the context of ischemia, and we observed no significant difference in the early recruitment of neutrophils to the ischemic penumbra in *S1pr1*^{ECKO} mice, nor in hemorrhagic transformation, which depends on leukocyte-mediated BBB destruction at later stages. Circulating markers of platelet activation and platelet recruitment to ischemic capillaries were also not substantially affected by EC $S1P_1$ deficiency. However, the deposition of fibrin, which extended well beyond the boundary of no perfusion 3 hours after pMCAO, reached significantly further into distal MCA territories in *S1pr1*^{ECKO} mice than in littermate controls. This suggests that microvascular coagulation contributes to rapid deterioration of collateral supply in *S1pr1*^{ECKO} mice. Whether this reflects the loss of direct actions of $S1P_1$ signaling on the anticoagulant or profibrinolytic status of the endothelium or is a consequence of reduced perfusion remains to be determined. Regardless, it highlights the critical dynamic role of the endothelium in maintaining microvascular patency.

Endothelial $S1P_1$ signaling thus counteracts the expansion of the ischemic core by concerted actions on hallmark endothelial functions in the regulation of blood flow, BBB integrity, and microvascular patency.

Highly restricted $S1P_1$ signaling in the naive cerebral cortex and the need for EC-autonomous S1P provision during cerebral ischemia both argue that S1P signaling is tightly controlled at the BBB. Characterization of $S1P_1$ expression and signaling indicates that $S1P_1$ may remain silent in most ECs after maturation of the blood-neural barrier due to $S1P_1$ polarization away from circulating S1P in all but a subset of arteriolar ECs. As homeostatic functions of $S1P_1$ in the naive brain did not all depend on EC S1P production, this subset of cells may sense circulating or other S1P sources. Although it is possible that the S1P1GS reporter mouse under-represents homeostatic $S1P_1$ signaling, limited GFP accumulation in both ECs and perivascular cells suggests that brain ECs may export S1P only when stressed. In the resting state, most brain ECs express *Sphk2*, *Spns2*, and *S1pr1*, but not *Sphk1*.[36] Induction of *Sphk1* transcription as an acute response to ischemia observed in this study could thus represent a trigger for EC $S1P_1$ activation in stroke and explain the limited effect of $S1P_1$ deficiency observed immediately after MCA occlusion. High expression of lipid phosphate phosphatase-3 in pericytes, smooth muscle cells, and astrocytes of the neurovascular unit suggests that local S1P availability is also regulated by

dephosphorylation.[36,54] Limiting local S1P availability may serve both to maintain EC $S1P_1$ responsiveness and to prevent S1P-mediated activation of astrocytes.[55–57] Restricted EC $S1P_1$ signaling also in peripheral organs suggests that polarization is not unique to the brain, although it has greater impact on the access of synthetic ligands at the BBB. Thus, homeostatic $S1P_1$ signaling in the cerebral cortex appears to be maintained by a small subset of primarily arteriolar ECs that may have access to circulating ligand, while broader receptor engagement in ischemic stroke depends on the activation of EC-autonomous S1P production, possibly through the expression of *Sphk1*.

What are the implications of our study for therapeutic targeting of $S1P_1$ in stroke? While modest protection observed in $S1pr1^{HCKO}$ mice in the tMCAO model supports the previously suggested benefit of targeting lymphocyte receptors,[20] increased stroke severity and loss of efficacy of $S1P_1$ agonists in $S1pr1^{ECKO}$ mice point to the endothelial receptor pool as their principal therapeutic target. This argues against the use of competitive antagonists or strong functional antagonists, which induce prolonged lymphopenia and may disable EC receptors. Most $S1P_1$ agonists also induce lymphopenia, suggesting that these could provide benefit through both cellular targets. Our results argue that BBB penetration is needed to reach the EC receptor pool. FTY720, the $S1P_1$ modulator employed in most experimental and clinical studies thus far, is nonspecific, did not efficiently penetrate the BBB in this study, desensitizes EC $S1P_1$ at high doses, and induces long lasting lymphopenia.[8,26,54] While FTY720 is probably mostly activating on EC $S1P_1$ at therapeutic doses, our study argues that a more specific drug could be not only safer but also more efficacious. CYM-5442, an $S1P_1$-selective agonist used in this study, is also desensitizing at high doses but rapidly distributes to the brain, triggers only transient immunosuppression, and is mostly washed out from plasma and brain 24 hours after administration.[48] The suitability of other second-generation S1PR modulators needs to be defined. It is promising that recently Food and Drug Administration-approved Ozanimod and Siponimod both improve BBB function in models of intracerebral hemorrhage.[21,24] New biased agonists have been developed that are minimally desensitizing on EC receptors and do not induce lymphopenia[59,60]; protection afforded with ApoM-Fc in a tMCAO model is consistent with our findings and suggest that targeting EC $S1P_1$ alone may provide considerable benefit.[59] The S1P1GS mouse used in this study and an analogous firefly split luciferase-based reporter provide valuable tools to assess BBB penetration of $S1P_1$ agonists that elicit β-arrestin recruitment.[38,61]

In conclusion, this study supports a key role for $S1P_1$ signaling in regulating endothelial function and vascular reactivity in the brain that expands with the engagement of EC-autonomous S1P provision to become a critical determinant of neuronal survival during cerebral ischemia. Although EC $S1P_1$ signaling is partially sustained by cell-autonomous S1P provision, it can be boosted with BBB-penetrating pharmacological agonists. Joint targeting of lymphocyte[20] and EC $S1P_1$ with BBB-penetrating agonists is feasible and provides protection in transient and permanent ischemic stroke models in a therapeutically relevant time frame. Mechanistically, $S1P_1$ targeting may promote regional blood flow, microvascular patency, and BBB integrity, independent of the prolonged immunosuppression induced by some $S1P_1$ modulators.[48] This is consistent with observed efficacy of FTY720 on downstream microvascular perfusion even in patients with failed recanalization to altapase[22] and suggests that $S1P_1$ agonists may preserve microvascular function and the recruitment of the collateral circulation even when recanalization is either not possible or not successful. This therapeutic strategy could, therefore, be envisioned in patients as soon as stroke is diagnosed, without waiting for the outcome of thrombolysis, which provides measurable benefit in <1/3 of patients treated.[62] Sustained $S1P_1$ expression during aging in mice (this study) and humans (Figure IX in the Data Supplement),[63] and efficacy of $S1P_1$ agonist on vascular parameters in murine models of diabetes and hypertension suggest that $S1P_1$ remains a viable target in the typical stroke patient.[10,64] This is underscored by efficacy of FTY720 in small-scale human trials for ischemic and hemorrhagic stroke, which also do not report an unexpected increase in bleeding, cardiac adverse events, or poststroke infections.[22,23,65,66] Our findings suggest that this strategy may be refined with focus on minimally desensitizing BBB-penetrating $S1P_1$ agonists. The critical protective roles for EC $S1P_1$ and its mechanisms of engagement observed in this study may also be relevant to hemorrhagic stroke, vascular dementia, and ischemic disease of other organs.

ARTICLE INFORMATION

Received January 24, 2020; revision received November 12, 2020; accepted December 1, 2020.

Affiliations

Université de Paris, Paris Cardiovascular Research Centre, INSERM U970, France (A.N., M.P., A.B., T.M., G.A., V.B., L.C., A.C., H.N., P.-L.T., A.E., B.T., E.C.). Institut des Vaisseaux et du Sang, Hôpital Lariboisière, France (M.P., P.-L.L.). Université de Paris, INSERM U965 and Physiologie Clinique - Explorations-Fonctionnelles, AP-HP, Hôpital Lariboisière, France (P.B., N.K.). Feil Family Brain and Mind Research Institute (G.F., L.G.-B., C.I.) and Center for Vascular Biology (H.U., T.S.), Weill Cornell Medical College, Cornell University, New York. MITOVASC Institute, CARFI Facility, CNRS UMR 6015, INSERM U1083, Angers University, France (J.F., M.C.L.G., D.H.). INSERM U1141, Hôpital Robert Debré (P.-L.L., C.C.-M.). Assistance Publique-Hôpitaux de Paris (AP-HP), Service de Biochimie, Hôpital de Bicêtre, Le Kremlin Bicêtre, France (P.T.). Université Paris-Sud, France (P.T.). UFR de Pharmacie, EA 4529, Châtenay-Malabry, France (P.T.). National Institute of Diabetes and Digestive and Kidney Diseases, National Institutes of Health, Institutes of Health, Bethesda, MD, USA (M.K., R.L.P.). Neuroscience Drug Discovery, Sanford Burnham Prebys Medical Discovery Institute, La Jolla, CA (J.C.). Skirball Institute of Biomolecular Medicine, New York University School of Medicine, NY (S.R.S.). Université de Paris, INSERM U1148, Hôpital Bichat, France (N.K.). Vascular Biology Program, Boston Children's Hospital, MA (T.H.).

Acknowledgments

We are grateful for input from all members of the Leducq SphingoNet network and for support from the technical and administrative platforms at the contributing institutions.

Sources of Funding

This work was supported by Fondation Leducq (SphingoNet; E. Camerer, T. Sanchez, R.L. Proia, C. Iadecola, and T. Hla), Fondation pour la Recherche Medicale (DCP20171138945; E. Camerer, A. Eichmann, and B. Tavitian), the French National Research Agency (ANR-19-CE14-0028; E. Camerer, D. Henrion, and P. Bonnin), Fondation de France (E. Camerer), Marie Curie Actions (PRESTIGE-2016-3-0011; A. Nitzsche), Lefoulon Delalande (A. Chevallier and A. Nitzsche), the Intramural Research Program of the National Institutes of Health, the National Institute of Diabetes and Digestive and Kidney Diseases (R.L. Proia), National Institutes of Health, National Institute of Neurological Disorders and Stroke (NS114561; T. Sanchez) and Fondation Grace de Monaco (P.-L. Léger and C. Charriaut-Marlangue).

Disclosures

None.

Supplemental materials

Methods
Online Figure Legends
Video Legends
References 67–82
Online Table I
Online Figures I–IX

REFERENCES

1. Moskowitz MA, Lo EH, Iadecola C. The science of stroke: mechanisms in search of treatments. *Neuron*. 2010;67:181–198. doi: 10.1016/j.neuron.2010.07.002
2. Powers WJ, Rabinstein AA, Ackerson T, Adeoye OM, Bambakidis NC, Becker K, Biller J, Brown M, Demaerschalk BM, Hoh B, et al; American Heart Association Stroke Council. 2018 guidelines for the early management of patients with acute ischemic stroke: a guideline for healthcare professionals from the American Heart Association/American Stroke Association. *Stroke*. 2018;49:e46–e110. doi: 10.1161/STR.0000000000000158
3. Manning NW, Campbell BC, Oxley TJ, Chapot R. Acute ischemic stroke: time, penumbra, and reperfusion. *Stroke*. 2014;45:640–644. doi: 10.1161/STROKEAHA.113.003798
4. Bonnin P, Mazighi M, Charriaut-Marlangue C, Kubis N. Early collateral recruitment after stroke in infants and adults. *Stroke*. 2019;50:2604–2611. doi: 10.1161/STROKEAHA.119.025353
5. Shuaib A, Butcher K, Mohammad AA, Saqqur M, Liebeskind DS. Collateral blood vessels in acute ischaemic stroke: a potential therapeutic target. *Lancet Neurol*. 2011;10:909–921. doi: 10.1016/S1474-4422(11)70195-8
6. Dreikorn M, Milacic Z, Pavlovic V, Meuth SG, Kleinschnitz C, Kraft P. Immunotherapy of experimental and human stroke with agents approved for multiple sclerosis: a systematic review. *Ther Adv Neurol Disord*. 2018;11:1756286418770626. doi: 10.1177/1756286418770626
7. Proia RL, Hla T. Emerging biology of sphingosine-1-phosphate: its role in pathogenesis and therapy. *J Clin Invest*. 2015;125:1379–1387. doi: 10.1172/JCI76369
8. Cyster JG, Schwab SR. Sphingosine-1-phosphate and lymphocyte egress from lymphoid organs. *Annu Rev Immunol*. 2012;30:69–94. doi: 10.1146/annurev-immunol-020711-075011
9. Gazit SL, Mariko B, Thérond P, Decouture B, Xiong Y, Couty L, Bonnin P, Baudrie V, Le Gall SM, Dizier B, et al. Platelet and erythrocyte sources of S1P are redundant for vascular development and homeostasis, but both rendered essential after plasma S1P depletion in anaphylactic shock. *Circ Res*. 2016;119:e110–e126. doi: 10.1161/CIRCRESAHA.116.308929
10. Cantalupo A, Gargiulo A, Dautaj E, Liu C, Zhang Y, Hla T, Di Lorenzo A. S1PR1 (Sphingosine-1-Phosphate Receptor 1) signaling regulates blood flow and pressure. *Hypertension*. 2017;70:426–434. doi: 10.1161/HYPERTENSIONAHA.117.09088
11. Jung B, Obinata H, Galvani S, Mendelson K, Ding BS, Skoura A, Kinzel B, Brinkmann V, Rafii S, Evans T, et al. Flow-regulated endothelial S1P receptor-1 signaling sustains vascular development. *Dev Cell*. 2012;23:600–610. doi: 10.1016/j.devcel.2012.07.015
12. Galvani S, Sanson M, Blaho VA, Swendeman SL, Obinata H, Conger H, Dahlbäck B, Kono M, Proia RL, Smith JD, et al. HDL-bound sphingosine 1-phosphate acts as a biased agonist for the endothelial cell receptor S1P1 to limit vascular inflammation. *Sci Signal*. 2015;8:ra79. doi: 10.1126/scisignal.aaa2581
13. Pappu R, Schwab SR, Cornelissen I, Pereira JP, Regard JB, Xu Y, Camerer E, Zheng YW, Huang Y, Cyster JG, et al. Promotion of lymphocyte egress into blood and lymph by distinct sources of sphingosine-1-phosphate. *Science*. 2007;316:295–298. doi: 10.1126/science.1139221
14. Vu TM, Ishizu AN, Foo JC, Toh XR, Zhang F, Whee DM, Torta F, Cazenave-Gassiot A, Matsumura T, Kim S, et al. Mfsd2b is essential for the sphingosine-1-phosphate export in erythrocytes and platelets. *Nature*. 2017;550:524–528. doi: 10.1038/nature24053
15. Czech B, Pfeilschifter W, Mazaheri-Omrani N, Strobel MA, Kahles T, Neumann-Haefelin T, Rami A, Huwiler A, Pfeilschifter J. The immunomodulatory sphingosine 1-phosphate analog FTY720 reduces lesion size and improves neurological outcome in a mouse model of cerebral ischemia. *Biochem Biophys Res Commun*. 2009;389:251–256. doi: 10.1016/j.bbrc.2009.08.142
16. Wei Y, Yemisci M, Kim HH, Yung LM, Shin HK, Hwang SK, Guo S, Qin T, Alsharif N, Brinkmann V, et al. Fingolimod provides long-term protection in rodent models of cerebral ischemia. *Ann Neurol*. 2011;69:119–129. doi: 10.1002/ana.22186
17. Hasegawa Y, Suzuki H, Sozen T, Rolland W, Zhang JH. Activation of sphingosine 1-phosphate receptor-1 by FTY720 is neuroprotective after ischemic stroke in rats. *Stroke*. 2010;41:368–374. doi: 10.1161/STROKEAHA.109.568899
18. Ichijo M, Ishibashi S, Li F, Yui D, Miki K, Mizusawa H, Yokota T. Sphingosine-1-phosphate receptor-1 selective agonist enhances collateral growth and protects against subsequent stroke. *PLoS One*. 2015;10:e0138029. doi: 10.1371/journal.pone.0138029
19. Brait VH, Tarrasón G, Gavaldà A, Godessart N, Planas AM. Selective sphingosine 1-phosphate receptor 1 agonist is protective against ischemia/reperfusion in mice. *Stroke*. 2016;47:3053–3056. doi: 10.1161/STROKEAHA.116.015371
20. Kraft P, Göb E, Schuhmann MK, Göbel K, Deppermann C, Thielmann I, Herrmann AM, Lorenz K, Brede M, Stoll G, et al. FTY720 ameliorates acute ischemic stroke in mice by reducing thrombo-inflammation but not by direct neuroprotection. *Stroke*. 2013;44:3202–3210. doi: 10.1161/STROKEAHA.113.002880
21. Sun N, Shen Y, Han W, Shi K, Wood K, Fu Y, Hao J, Liu Q, Sheth KN, Huang D, et al. Selective sphingosine-1-phosphate receptor 1 modulation attenuates experimental intracerebral hemorrhage. *Stroke*. 2016;47:1899–1906. doi: 10.1161/STROKEAHA.115.012236
22. Tian DC, Shi K, Zhu Z, Yao J, Yang X, Su L, Zhang S, Zhang M, Gonzales RJ, Liu Q, et al. Fingolimod enhances the efficacy of delayed alteplase administration in acute ischemic stroke by promoting anterograde reperfusion and retrograde collateral flow. *Ann Neurol*. 2018;84:717–728. doi: 10.1002/ana.25352
23. Zhu Z, Fu Y, Tian D, Sun N, Han W, Chang G, Dong Y, Xu X, Liu Q, Huang D, et al. Combination of the immune modulator fingolimod with alteplase in acute ischemic stroke: a pilot trial. *Circulation*. 2015;132:1104–1112. doi: 10.1161/CIRCULATIONAHA.115.016371
24. Bobinger T, Manaenko A, Burkardt P, Beuscher V, Sprügel MI, Roeder SS, Bäuerle T, Seyler L, Nagel AM, Linker RA, et al. Siponimod (BAF-312) attenuates perihemorrhagic edema and improves survival in experimental intracerebral hemorrhage. *Stroke*. 2019;50:3246–3254.
25. Niazi H, Zoghdani N, Couty L, Leuci A, Nitzsche A, Allende ML, Mariko B, Ishaq R, Aslan Y, Becker PH, et al. Murine platelet production is suppressed by S1P release in the hematopoietic niche, not facilitated by blood S1P sensing. *Blood Adv*. 2019;3:1702–1713. doi: 10.1182/bloodadvances.2019031948
26. Yanagida K, Liu CH, Faraco G, Galvani S, Smith HK, Burg N, Anrather J, Sanchez T, Iadecola C, Hla T. Size-selective opening of the blood-brain barrier by targeting endothelial sphingosine 1-phosphate receptor 1. *Proc Natl Acad Sci USA*. 2017;114:4531–4536. doi: 10.1073/pnas.1618659114
27. Poittevin M, Deroide N, Azibani F, Delcayre C, Giannesini C, Levy BI, Pocard M, Kubis N. Glatiramer acetate administration does not reduce damage after cerebral ischemia in mice. *J Neuroimmunol*. 2013;254:55–62. doi: 10.1016/j.jneuroim.2012.09.009
28. Prinz V, Endres M. Modeling focal cerebral ischemia in rodents: Introduction and overview. In: Dirnagl U, ed. *Rodent models of stroke*. Humana Press: Springer Protocols; 2016:19–30.

29. Claxton S, Kostourou V, Jadeja S, Chambon P, Hodivala-Dilke K, Fruttiger M. Efficient, inducible Cre-recombinase activation in vascular endothelium. *Genesis*. 2008;46:74–80. doi: 10.1002/dvg.20367
30. Zhang Y, Jin Y, Behr MJ, Feustel PJ, Morrison JP, Kimelberg HK. Behavioral and histological neuroprotection by tamoxifen after reversible focal cerebral ischemia. *Exp Neurol*. 2005;196:41–46. doi: 10.1016/j.expneurol.2005.07.002
31. Wakade C, Khan MM, De Sevilla LM, Zhang QG, Mahesh VB, Brann DW. Tamoxifen neuroprotection in cerebral ischemia involves attenuation of kinase activation and superoxide production and potentiation of mitochondrial superoxide dismutase. *Endocrinology*. 2008;149:367–379. doi: 10.1210/en.2007-0899
32. Camerer E, Regard JB, Cornelissen I, Srinivasan Y, Duong DN, Palmer D, Pham TH, Wong JS, Pappu R, Coughlin SR. Sphingosine-1-phosphate in the plasma compartment regulates basal and inflammation-induced vascular leak in mice. *J Clin Invest*. 2009;119:1871–1879. doi: 10.1172/jci38575
33. Kim GS, Yang L, Zhang G, Zhao H, Selim M, McCullough LD, Kluk MJ, Sanchez T. Critical role of sphingosine-1-phosphate receptor-2 in the disruption of cerebrovascular integrity in experimental stroke. *Nat Commun*. 2015;6:7893. doi: 10.1038/ncomms8893
34. Kühn R, Schwenk F, Aguet M, Rajewsky K. Inducible gene targeting in mice. *Science*. 1995;269:1427–1429. doi: 10.1126/science.7660125
35. Frej C, Andersson A, Larsson B, Guo LJ, Norström E, Happonen KE, Dahlbäck B. Quantification of sphingosine 1-phosphate by validated LC-MS/MS method revealing strong correlation with apolipoprotein M in plasma but not in serum due to platelet activation during blood coagulation. *Anal Bioanal Chem*. 2015;407:8533–8542. doi: 10.1007/s00216-015-9008-4
36. Vanlandewijck M, He L, Mäe MA, Andrae J, Ando K, Del Gaudio F, Nahar K, Lebouvier T, Laviña B, Gouveia L, et al. A molecular atlas of cell types and zonation in the brain vasculature. *Nature*. 2018;554:475–480. doi: 10.1038/nature25739
37. Ximerakis M, Lipnick SL, Innes BT, Simmons SK, Adiconis X, Dionne D, Mayweather BA, Nguyen L, Niziolek Z, Ozek C, et al. Single-cell transcriptomic profiling of the aging mouse brain. *Nat Neurosci*. 2019;22:1696–1708. doi: 10.1038/s41593-019-0491-3
38. Kono M, Tucker AE, Tran J, Bergner JB, Turner EM, Proia RL. Sphingosine-1-phosphate receptor 1 reporter mice reveal receptor activation sites in vivo. *J Clin Invest*. 2014;124:2076–2086. doi: 10.1172/JCI71194
39. Blaho VA, Galvani S, Engelbrecht E, Liu C, Swendeman SL, Kono M, Proia RL, Steinman L, Han MH, Hla T. HDL-bound sphingosine-1-phosphate restrains lymphopoiesis and neuroinflammation. *Nature*. 2015;523:342–346. doi: 10.1038/nature14462
40. Knowland D, Arac A, Sekiguchi KJ, Hsu M, Lutz SE, Perrino J, Steinberg GK, Barres BA, Nimmerjahn A, Agalliu D. Stepwise recruitment of transcellular and paracellular pathways underlies blood-brain barrier breakdown in stroke. *Neuron*. 2014;82:603–617. doi: 10.1016/j.neuron.2014.03.003
41. Jackman KA, Zhou P, Faraco G, Peixoto PM, Coleman C, Voss HU, Pickel V, Manfredi G, Iadecola C. Dichotomous effects of chronic intermittent hypoxia on focal cerebral ischemic injury. *Stroke*. 2014;45:1460–1467. doi: 10.1161/STROKEAHA.114.004816
42. Desilles JP, Syvannarath V, Di Meglio L, Ducroux C, Boisseau W, Louedec L, Jandrot-Perrus M, Michel JB, Mazighi M, Ho-Tin-Noe B. Downstream microvascular thrombosis in cortical venules is an early response to proximal cerebral arterial occlusion. *J Am Heart Assoc*. 2018;7:e007804.
43. von Brühl ML, Stark K, Steinhart A, Chandraratne S, Konrad I, Lorenz M, Khandoga A, Tirniceriu A, Coletti R, Köllnberger M, et al. Monocytes, neutrophils, and platelets cooperate to initiate and propagate venous thrombosis in mice in vivo. *J Exp Med*. 2012;209:819–835. doi: 10.1084/jem.20112322
44. Knapp M, Zendzian-Piotrowska M, Błachnio-Zabielska A, Zabielski P, Kurek K, Górski J. Myocardial infarction differentially alters sphingolipid levels in plasma, erythrocytes and platelets of the rat. *Basic Res Cardiol*. 2012;107:294. doi: 10.1007/s00395-012-0294-0
45. Cahalan SM, Gonzalez-Cabrera PJ, Sarkisyan G, Nguyen N, Schaeffer MT, Huang L, Yeager A, Clemons B, Scott F, Rosen H. Actions of a picomolar short-acting S1P$_1$ agonist in S1P$_1$-eGFP knock-in mice. *Nat Chem Biol*. 2011;7:254–256. doi: 10.1038/nchembio.547
46. Rangroo Thrane V, Thrane AS, Plog BA, Thiyagarajan M, Iliff JJ, Deane R, Nagelhus EA, Nedergaard M. Paravascular microcirculation facilitates rapid lipid transport and astrocyte signaling in the brain. *Sci Rep*. 2013;3:2582. doi: 10.1038/srep02582
47. Foster CA, Howard LM, Schweitzer A, Persohn E, Hiestand PC, Balatoni B, Reuschel R, Beerli C, Schwartz M, Billich A. Brain penetration of the oral immunomodulatory drug FTY720 and its phosphorylation in the central nervous system during experimental autoimmune encephalomyelitis: consequences for mode of action in multiple sclerosis. *J Pharmacol Exp Ther*. 2007;323:469–475. doi: 10.1124/jpet.107.127183
48. Gonzalez-Cabrera PJ, Cahalan SM, Nguyen N, Sarkisyan G, Leaf NB, Cameron MD, Kago T, Rosen H. S1P(1) receptor modulation with cyclical recovery from lymphopenia ameliorates mouse model of multiple sclerosis. *Mol Pharmacol*. 2012;81:166–174. doi: 10.1124/mol.111.076109
49. Zhang H, Prabhakar P, Sealock R, Faber JE. Wide genetic variation in the native pial collateral circulation is a major determinant of variation in severity of stroke. *J Cereb Blood Flow Metab*. 2010;30:923–934. doi: 10.1038/jcbfm.2010.10
50. Seyman E, Shaim H, Shenhar-Tsarfaty S, Jonash-Kimchi T, Bornstein NM, Hallevi H. The collateral circulation determines cortical infarct volume in anterior circulation ischemic stroke. *BMC Neurol*. 2016;16:206. doi: 10.1186/s12883-016-0722-0
51. Huang Z, Huang PL, Ma J, Meng W, Ayata C, Fishman MC, Moskowitz MA. Enlarged infarcts in endothelial nitric oxide synthase knockout mice are attenuated by nitro-L-arginine. *J Cereb Blood Flow Metab*. 1996;16:981–987. doi: 10.1097/00004647-199609000-00023
52. Faraco G, Brea D, Garcia-Bonilla L, Wang G, Racchumi G, Chang H, Buendia I, Santisteban MM, Segarra SG, Koizumi K, et al. Dietary salt promotes neurovascular and cognitive dysfunction through a gut-initiated TH17 response. *Nat Neurosci*. 2018;21:240–249. doi: 10.1038/s41593-017-0059-z
53. Faraco G, Hochrainer K, Segarra SG, Schaeffer S, Santisteban MM, Menon A, Jiang H, Holtzman DM, Anrather J, Iadecola C. Dietary salt promotes cognitive impairment through tau phosphorylation. *Nature*. 2019;574:686–690. doi: 10.1038/s41586-019-1688-z
54. Mathiesen Janiurek M, Soylu-Kucharz R, Christoffersen C, Kucharz K, Lauritzen M. Apolipoprotein M-bound sphingosine-1-phosphate regulates blood-brain barrier paracellular permeability and transcytosis. *Elife*. 2019;8:e49405.
55. Gómez-López S, Martínez-Silva AV, Montiel T, Osorio-Gómez D, Bermúdez-Rattoni F, Massieu L, Escalante-Alcalde D. Neural ablation of the PARK10 candidate Plpp3 leads to dopaminergic transmission deficits without neurodegeneration. *Sci Rep*. 2016;6:24028. doi: 10.1038/srep24028
56. Choi JW, Gardell SE, Herr DR, Rivera R, Lee CW, Noguchi K, Teo ST, Yung YC, Lu M, Kennedy G, et al. FTY720 (fingolimod) efficacy in an animal model of multiple sclerosis requires astrocyte sphingosine 1-phosphate receptor 1 (S1P1) modulation. *Proc Natl Acad Sci USA*. 2011;108:751–756. doi: 10.1073/pnas.1014154108
57. Gril B, Paranjape AN, Woditschka S, Hua E, Dolan EL, Hanson J, Wu X, Kloc W, Izycka-Swieszewska E, Duchnowska R, et al. Reactive astrocytic S1P3 signaling modulates the blood-tumor barrier in brain metastases. *Nat Commun*. 2018;9:2705. doi: 10.1038/s41467-018-05030-w
58. Oo ML, Chang SH, Thangada S, Wu MT, Rezaul K, Blaho V, Hwang SI, Han DK, Hla T. Engagement of S1P$_1$-degradative mechanisms leads to vascular leak in mice. *J Clin Invest*. 2011;121:2290–2300. doi: 10.1172/JCI45403
59. Swendeman SL, Xiong Y, Cantalupo A, Yuan H, Burg N, Hisano Y, Cartier A, Liu CH, Engelbrecht E, Blaho V, et al. An engineered S1P chaperone attenuates hypertension and ischemic injury. *Sci Signal*. 2017;10:eaal2722.
60. Poirier B, Briand V, Kadereit D, Schafer M, Wohlfart P, Philippo MC, Caillaud D, Gouraud L, Grailhe P, Bidouard JP, et al. A G protein-biased S1P1 agonist, SAR247799, protects endothelial cells without affecting lymphocyte numbers. *Sci Signal*. 2020;13:eaax8050.
61. Kono M, Conlon EG, Lux SY, Yanagida K, Hla T, Proia RL. Bioluminescence imaging of G protein-coupled receptor activation in living mice. *Nat Commun*. 2017;8:1163. doi: 10.1038/s41467-017-01340-7
62. Saver JL, Gornbein J, Grotta J, Liebeskind D, Lutsep H, Schwamm L, Scott P, Starkman S. Number needed to treat to benefit and to harm for intravenous tissue plasminogen activator therapy in the 3- to 4.5-hour window: joint outcome table analysis of the ECASS 3 trial. *Stroke*. 2009;40:2433–2437. doi: 10.1161/STROKEAHA.108.543561
63. Uhlén M, Fagerberg L, Hallström BM, Lindskog C, Oksvold P, Mardinoglu A, Sivertsson Å, Kampf C, Sjöstedt E, Asplund A, et al. Proteomics. Tissue-based map of the human proteome. *Science*. 2015;347:1260419. doi: 10.1126/science.1260419
64. Whetzel AM, Bolick DT, Srinivasan S, Macdonald TL, Morris MA, Ley K, Hedrick CC. Sphingosine-1 phosphate prevents monocyte/endothelial interactions in type 1 diabetic NOD mice through activation of the S1P1 receptor. *Circ Res*. 2006;99:731–739. doi: 10.1161/01.RES.0000244088.33375.52
65. Fu Y, Zhang N, Ren L, Yan Y, Sun N, Li YJ, Han W, Xue R, Liu Q, Hao J, et al. Impact of an immune modulator fingolimod on acute ischemic stroke. *Proc Natl Acad Sci U S A*. 2014;111:18315–18320.

66. Li YJ, Shi SX, Liu Q, Shi FD, Gonzales RJ. Targeted role for sphingosine-1-phosphate receptor 1 in cerebrovascular integrity and inflammation during acute ischemic stroke. *Neurosci Lett*. 2020;735:135160.
67. Pitulescu ME, Adams RH. Eph/ephrin molecules–a hub for signaling and endocytosis. *Genes Dev*. 2010;24:2480–2492. doi: 10.1101/gad.1973910
68. Muzumdar MD, Tasic B, Miyamichi K, Li L, Luo L. A global double-fluorescent Cre reporter mouse. *Genesis*. 2007;45:593–605. doi: 10.1002/dvg.20335
69. Bonnin P, Leger PL, Deroide N, Fau S, Baud O, Pocard M, Charriaut-Marlangue C, Renolleau S. Impact of intracranial blood-flow redistribution on stroke size during ischemia-reperfusion in 7-day-old rats. *J Neurosci Methods*. 2011;198:103–109. doi: 10.1016/j.jneumeth.2011.02.030
70. Poittevin M, Bonnin P, Pimpie C, Rivière L, Sebrié C, Dohan A, Pocard M, Charriaut-Marlangue C, Kubis N. Diabetic microangiopathy: impact of impaired cerebral vasoreactivity and delayed angiogenesis after permanent middle cerebral artery occlusion on stroke damage and cerebral repair in mice. *Diabetes*. 2015;64:999–1010. doi: 10.2337/db14-0759
71. Faraco G, Moraga A, Moore J, Anrather J, Pickel VM, Iadecola C. Circulating endothelin-1 alters critical mechanisms regulating cerebral microcirculation. *Hypertension*. 2013;62:759–766. doi: 10.1161/HYPERTENSIONAHA.113.01761
72. Garcia-Bonilla L, Racchumi G, Murphy M, Anrather J, Iadecola C. Endothelial CD36 contributes to postischemic brain injury by promoting neutrophil activation via CSF3. *J Neurosci*. 2015;35:14783–14793. doi: 10.1523/JNEUROSCI.2980-15.2015
73. Jackman K, Kunz A, Iadecola C. Modeling focal cerebral ischemia in vivo. *Methods Mol Biol*. 2011;793:195–209. doi: 10.1007/978-1-61779-328-8_13
74. Leger PL, Bonnin P, Moretti R, Tanaka S, Duranteau J, Renolleau S, Baud O, Charriaut-Marlangue C. Early recruitment of cerebral microcirculation by neuronal nitric oxide synthase inhibition in a Juvenile Ischemic Rat Model. *Cerebrovasc Dis*. 2016;41:40–49. doi: 10.1159/000441663
75. Henrion D, Dechaux E, Dowell FJ, Maclour J, Samuel JL, Lévy BI, Michel JB. Alteration of flow-induced dilatation in mesenteric resistance arteries of L-NAME treated rats and its partial association with induction of cyclo-oxygenase-2. *Br J Pharmacol*. 1997;121:83–90. doi: 10.1038/sj.bjp.0701109
76. Franco CA, Jones ML, Bernabeu MO, Geudens I, Mathivet T, Rosa A, Lopes FM, Lima AP, Ragab A, Collins RT, et al. Dynamic endothelial cell rearrangements drive developmental vessel regression. *PLoS Biol*. 2015;13:e1002125. doi: 10.1371/journal.pbio.1002125
77. Lamprecht MR, Sabatini DM, Carpenter AE. CellProfiler: free, versatile software for automated biological image analysis. *Biotechniques*. 2007;42:71–75. doi: 10.2144/000112257
78. Lee YK, Uchida H, Smith H, Ito A, Sanchez T. The isolation and molecular characterization of cerebral microvessels. *Nat Protoc*. 2019;14:3059–3081. doi: 10.1038/s41596-019-0212-0
79. Ruck T, Bittner S, Epping L, Herrmann AM, Meuth SG. Isolation of primary murine brain microvascular endothelial cells. *J Vis Exp*. 2014;93:e52204.
80. Regard JB, Sato IT, Coughlin SR. Anatomical profiling of G protein-coupled receptor expression. *Cell*. 2008;135:561–571. doi: 10.1016/j.cell.2008.08.040
81. Assmann JC, Muller K, Wenzel J, Walther T, Brands J, Thornton P, Allan SM, Schwaninger M. Isolation and cultivation of primary brain endothelial cells from adult mice. *Bio Protoc*. 2017;7:e2294.
82. He L, Vanlandewijck M, Mäe MA, Andrae J, Ando K, Del Gaudio F, Nahar K, Lebouvier T, Laviña B, Gouveia L, et al. Single-cell RNA sequencing of mouse brain and lung vascular and vessel-associated cell types. *Sci Data*. 2018;5:180160. doi: 10.1038/sdata.2018.160

Online Figure I

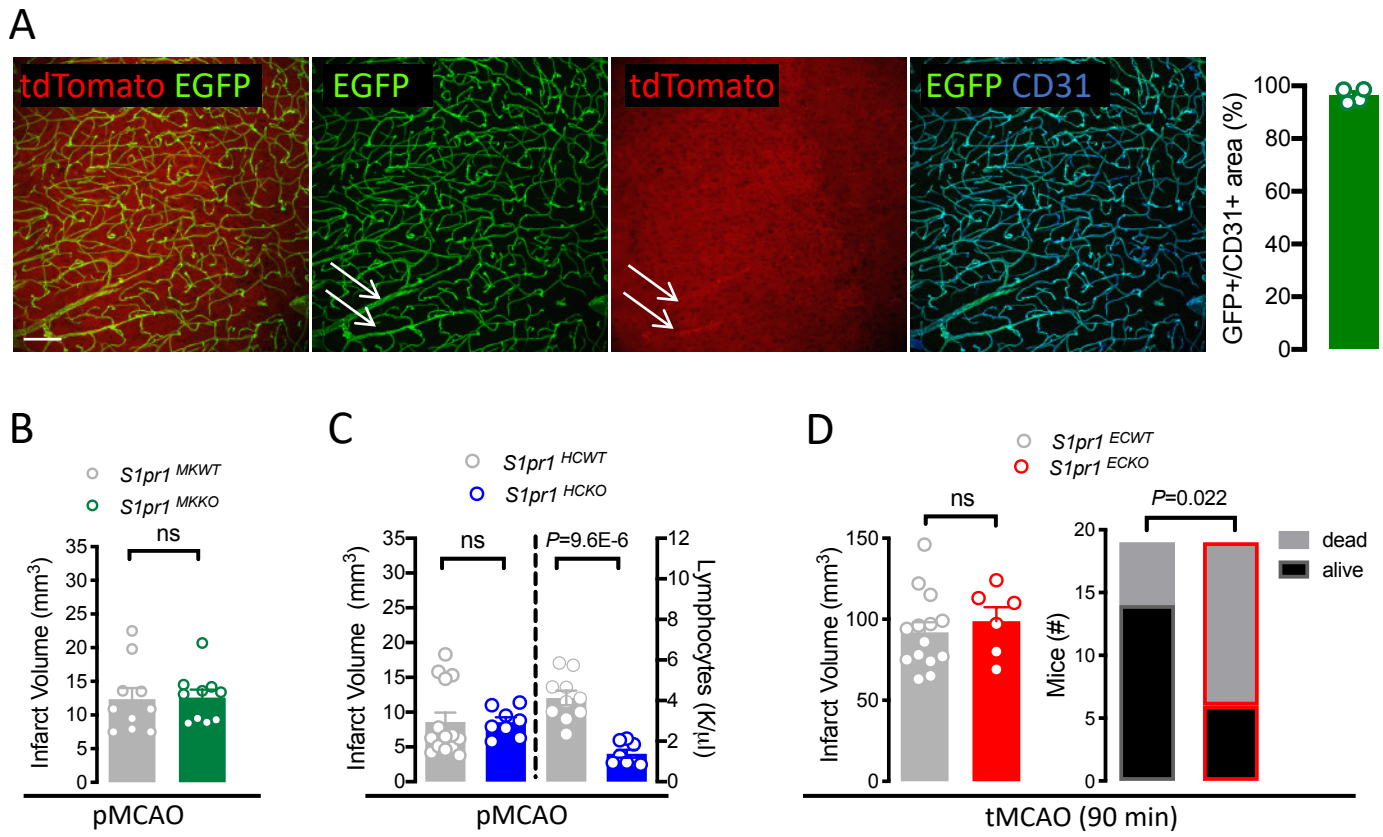

Online Figure II

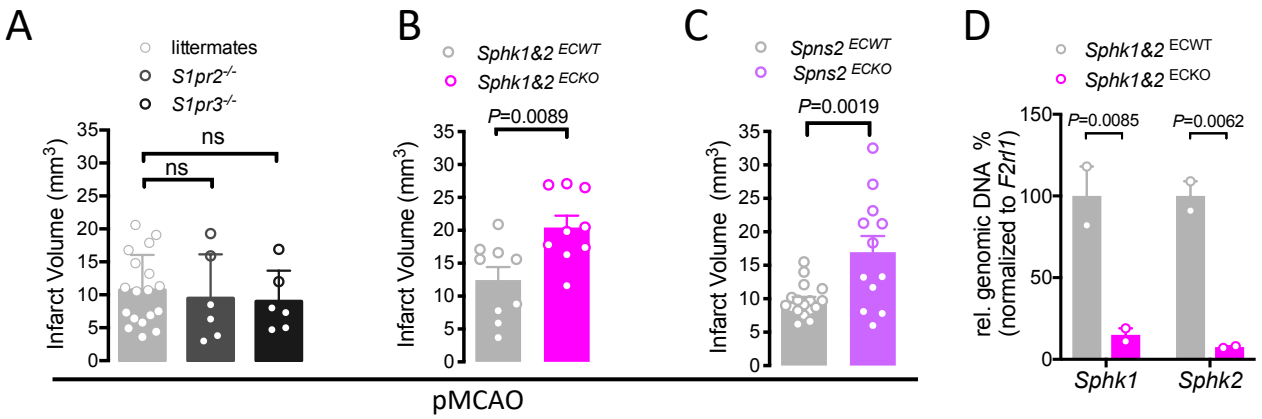

E

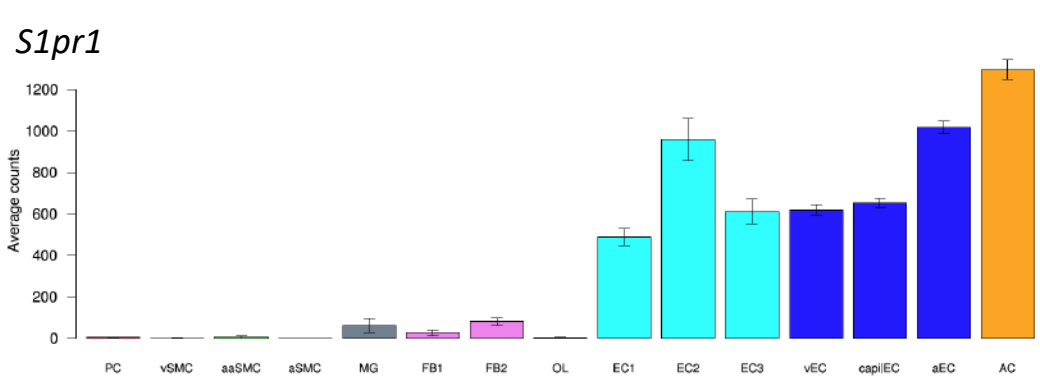

PC - Pericytes; SMC - Smooth muscle cells; MG - Microglia; FB - Vascular fibroblast-like cells; OL - Oligodendrocytes; EC - Endothelial cells; AC - Astrocytes; v - venous; capil - capillary; a - arterial; aa - arteriolar; 1,2,3- subtypes.

F Wild-type mice

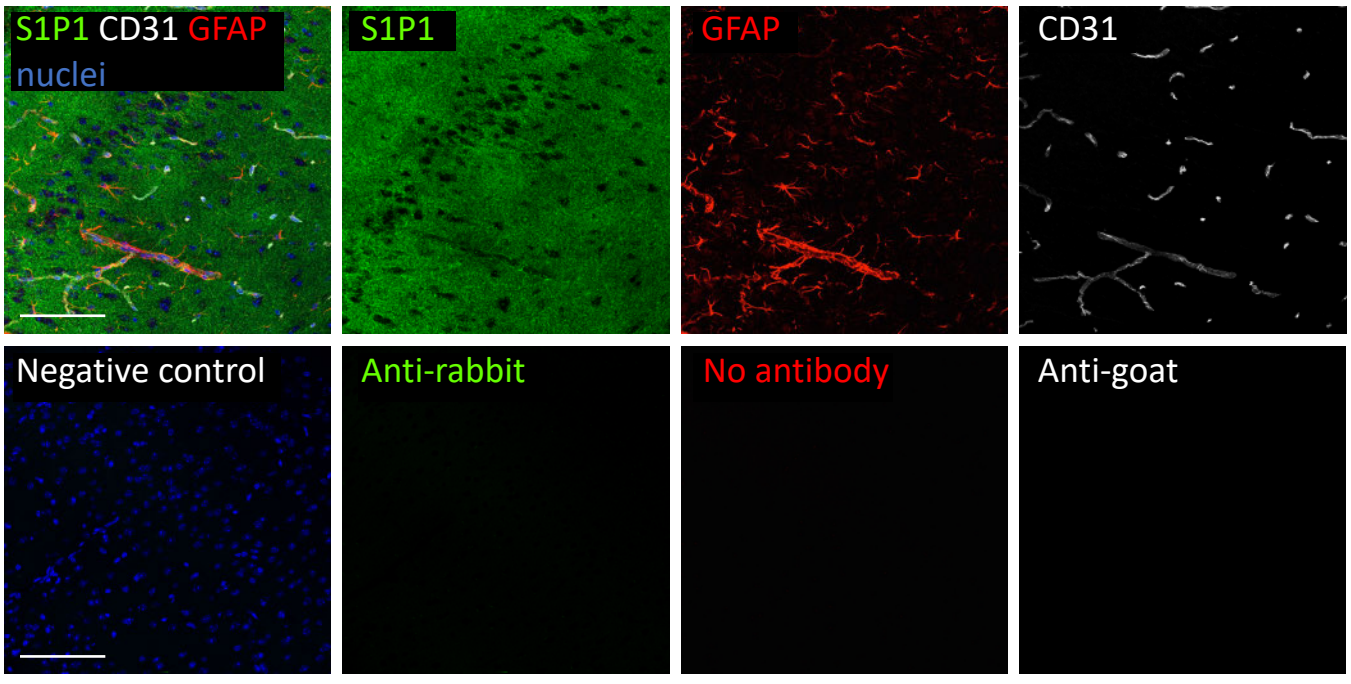

Online Figure II

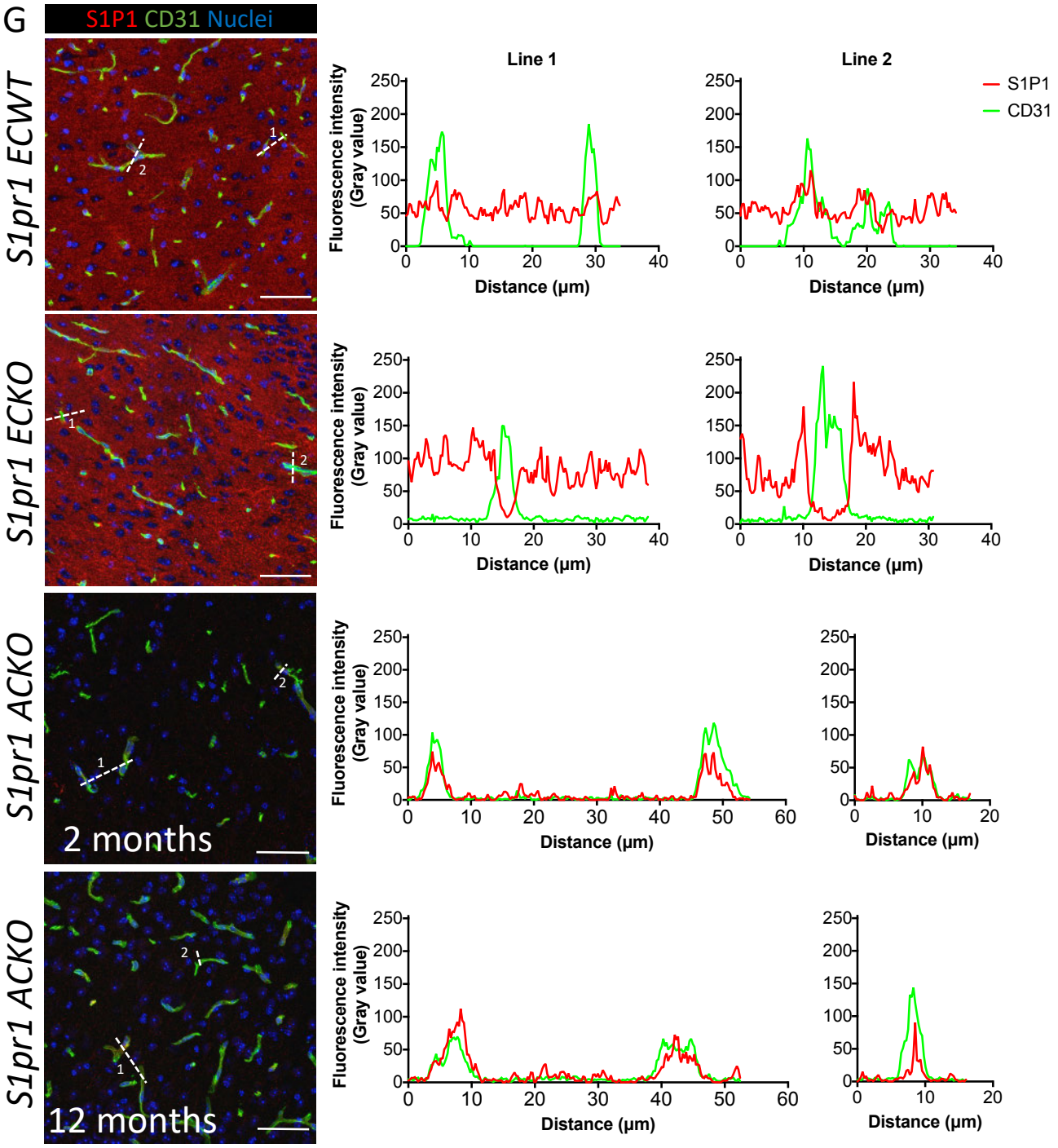

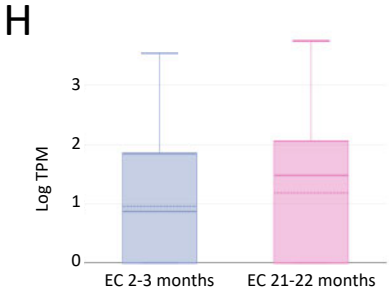

Online Figure II

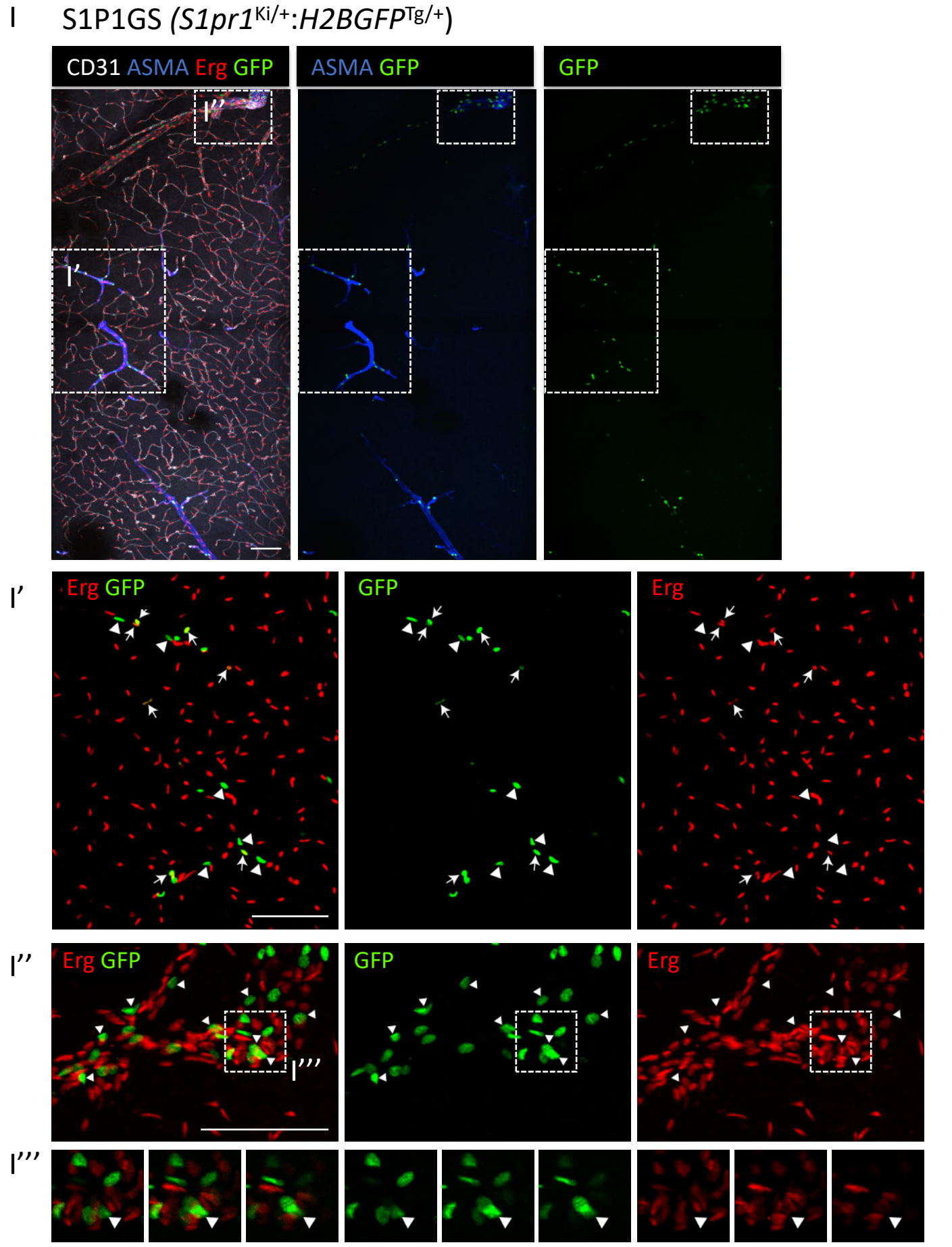

Online Figure II

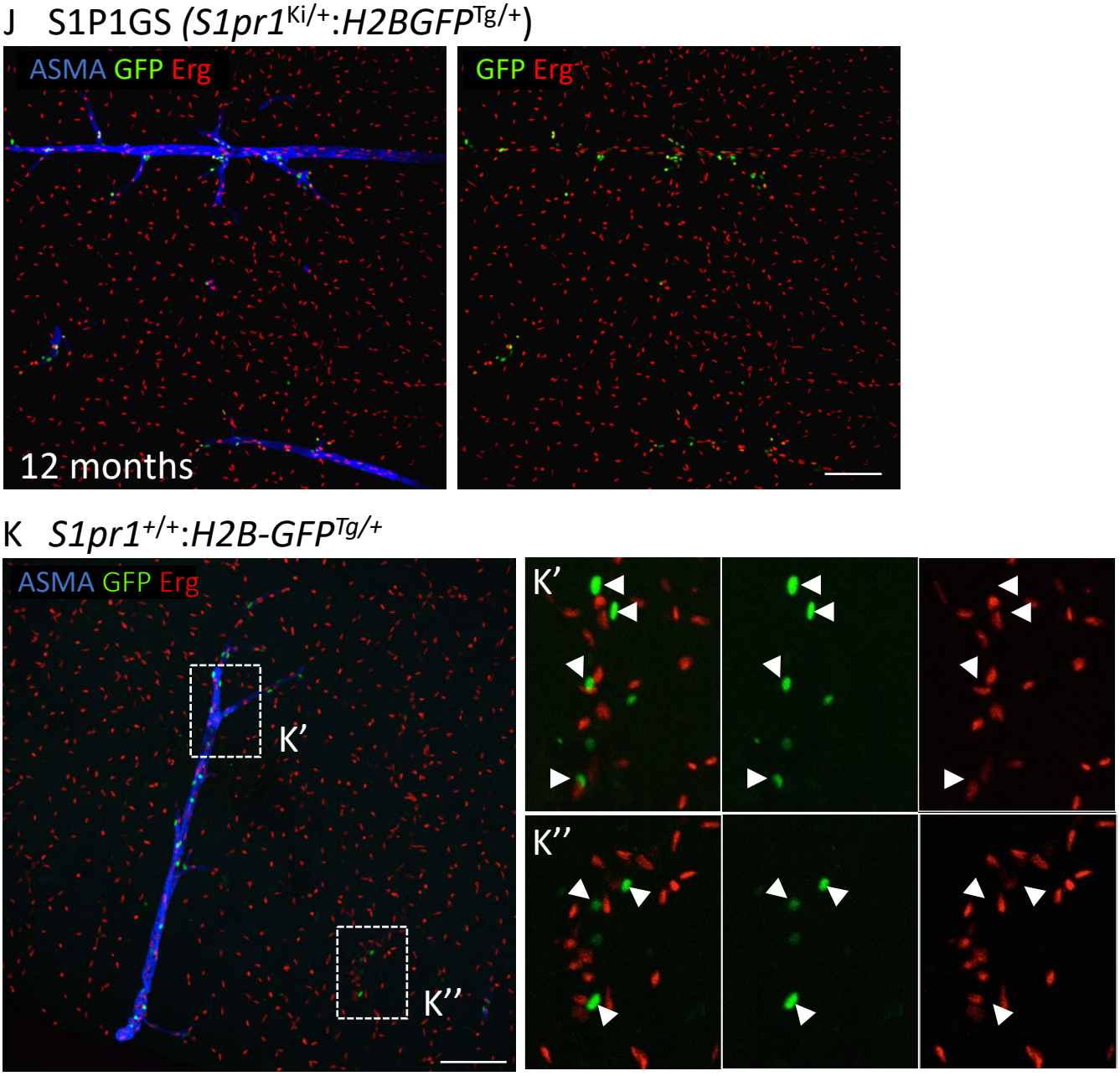

Online Figure III

A

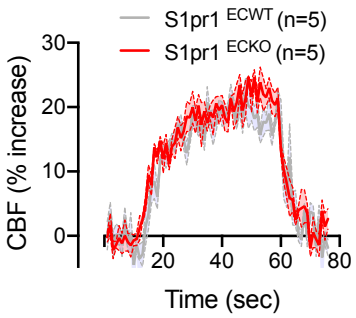

B

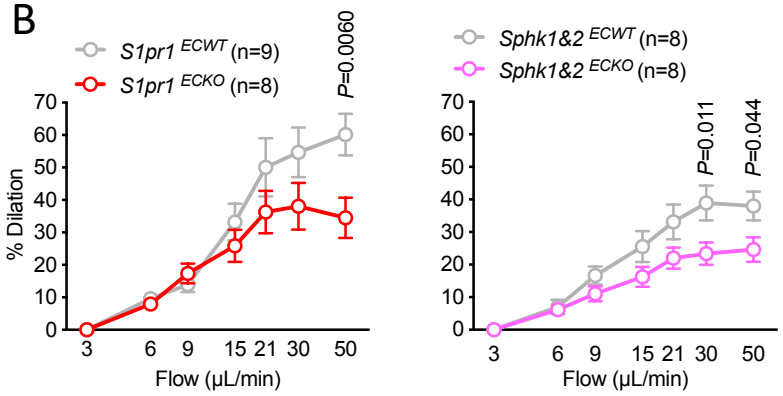

C

vessel	genotype	Mean BFV (cm/second)			n
		basal	50 min	120 min	
Left ICA	*S1pr1 ECWT*	14.1±2.0	10.7±1.3	12.6±1.0	8
	S1pr1 ECKO	14.9±2.0	11.5±3.3	10.7±2.2	8
Right ICA	*S1pr1 WT*	15.1±2.6	14.9±2.7	15.8±1.6	8
	S1pr1 ECKO	15.3±2.5	15.1±2.7	16.3±2.0	8
BT	*S1pr1 WT*	9.9±3.1	10.2±2.9	9.4±3.7	8
	S1pr1 ECKO	11.1±3.4	11.1±3.3	10.0±2.4	8

D

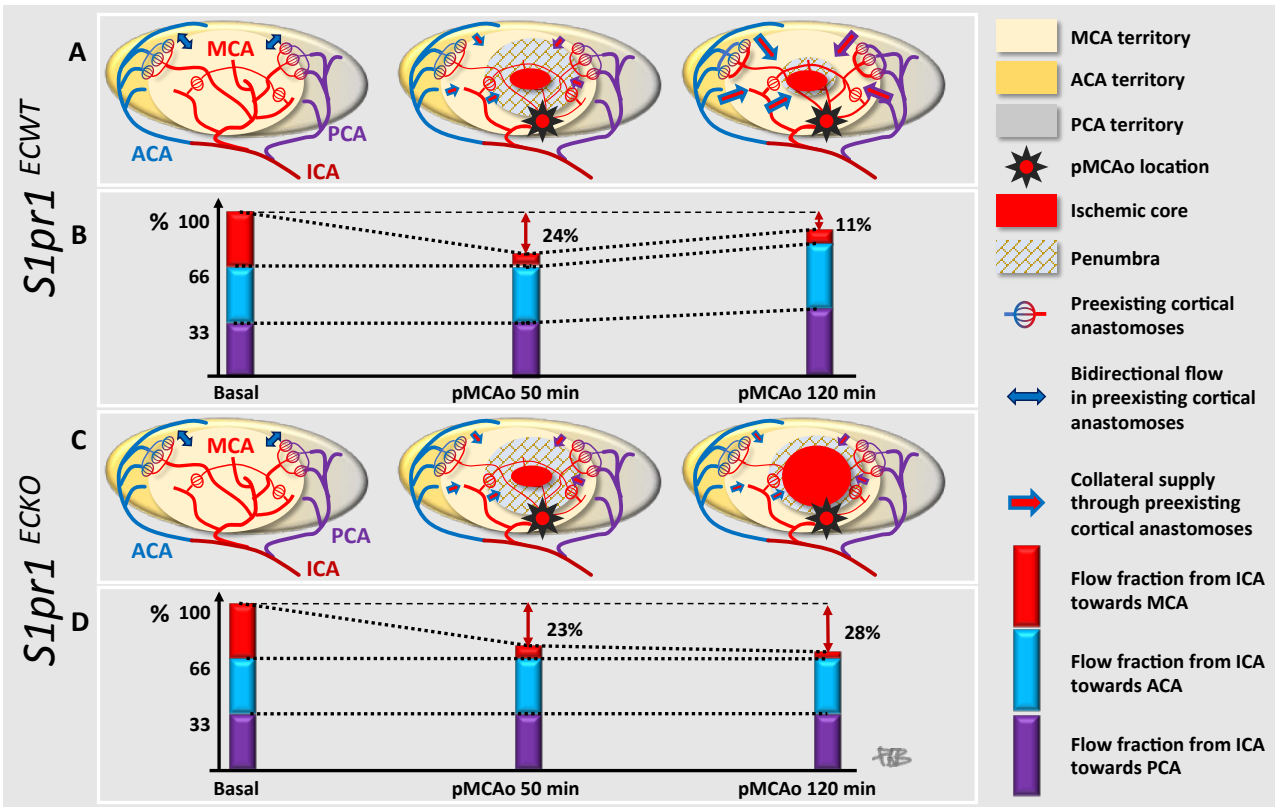

Online Figure IV

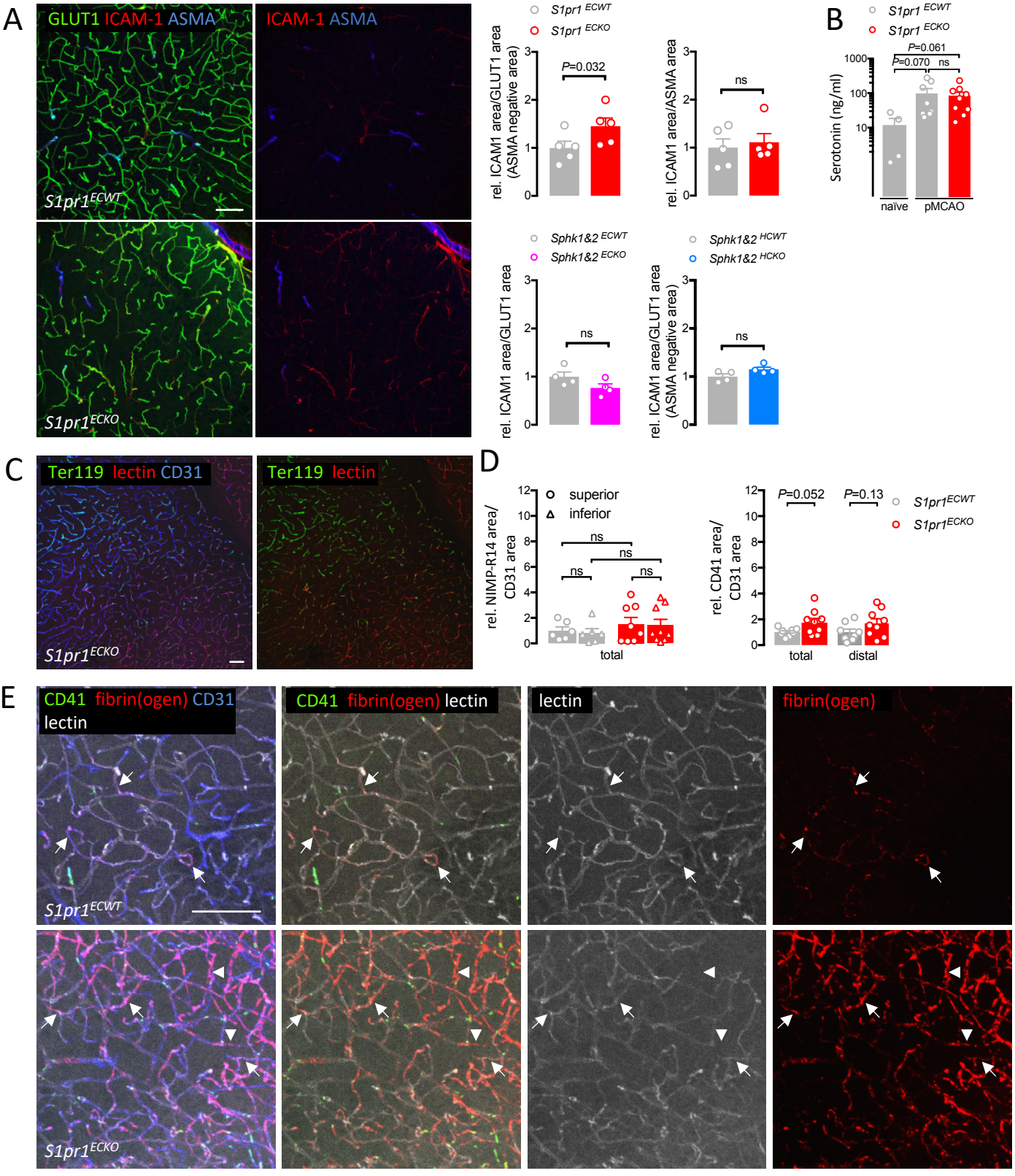

Online Figure IV

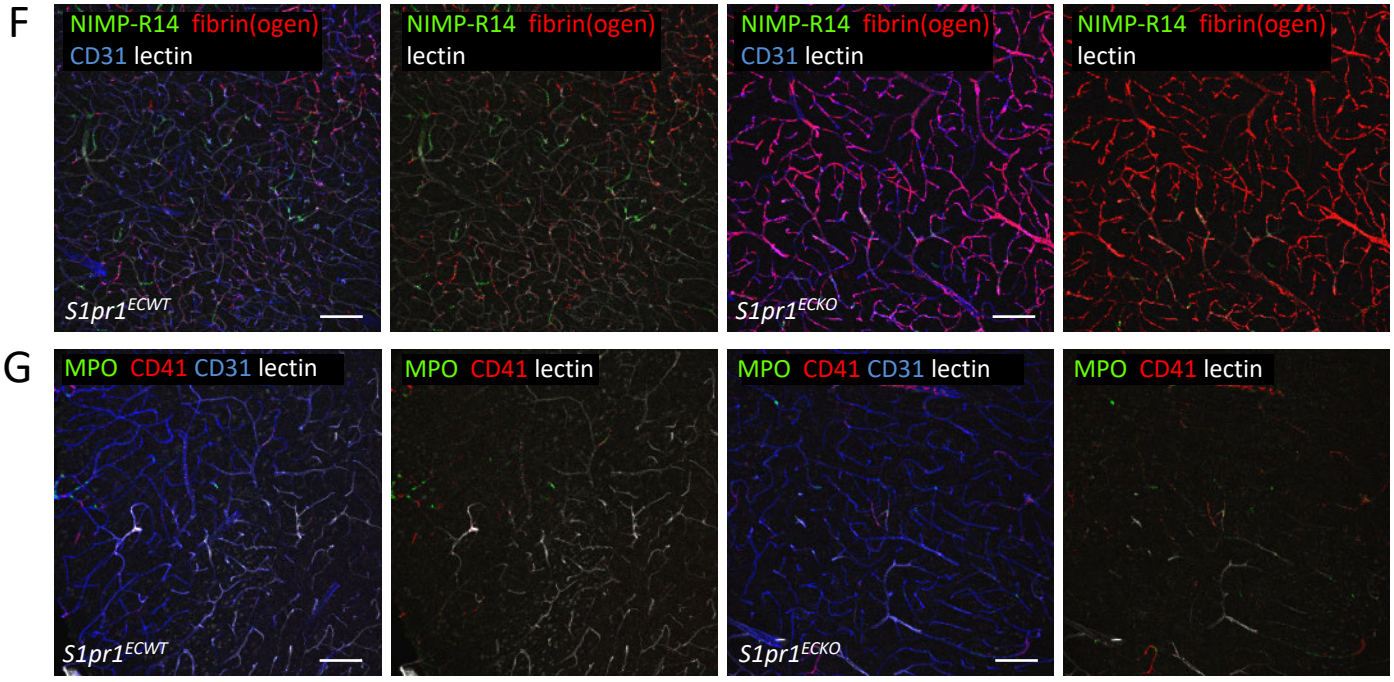

Online Figure V

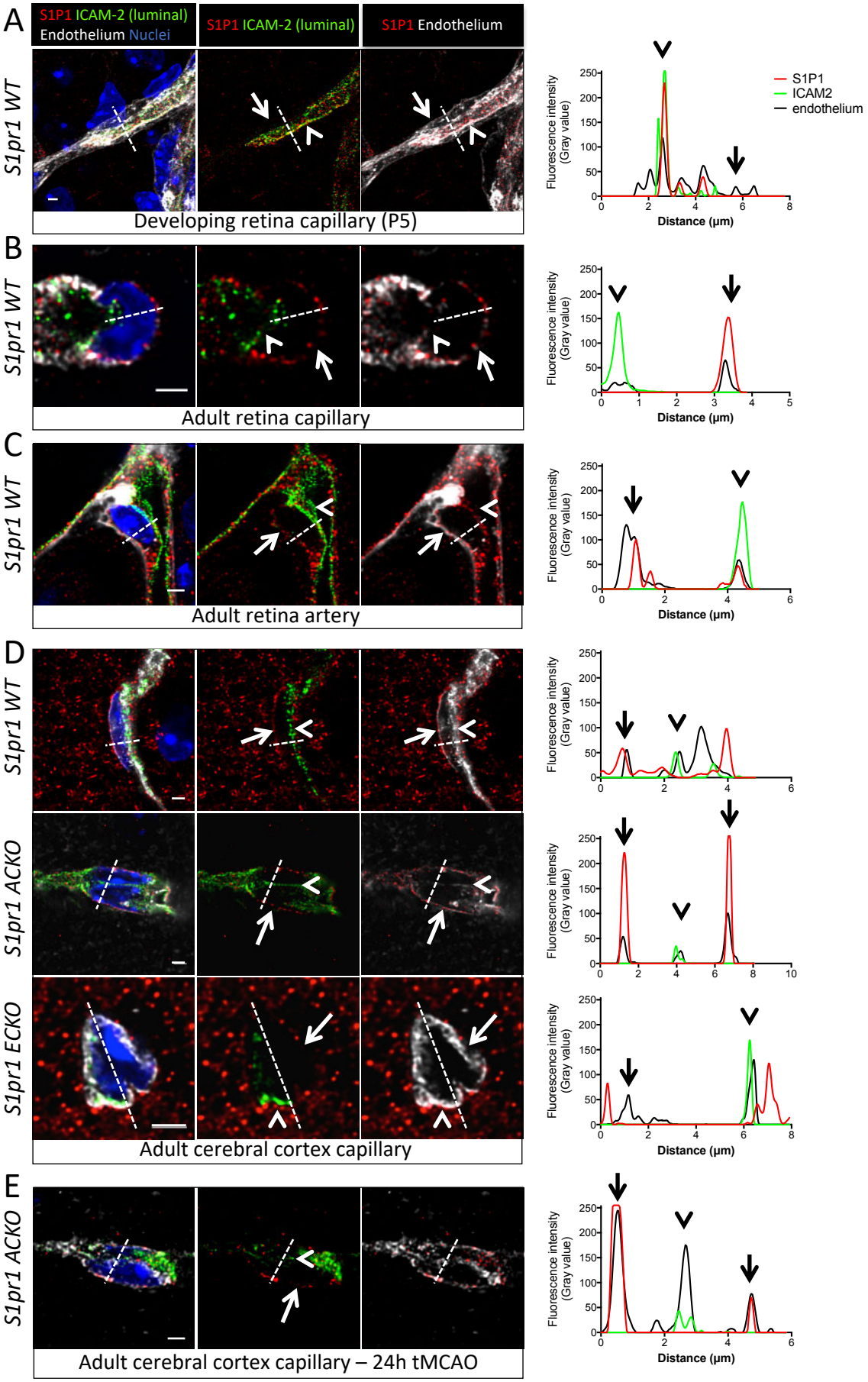

Online Figure VI

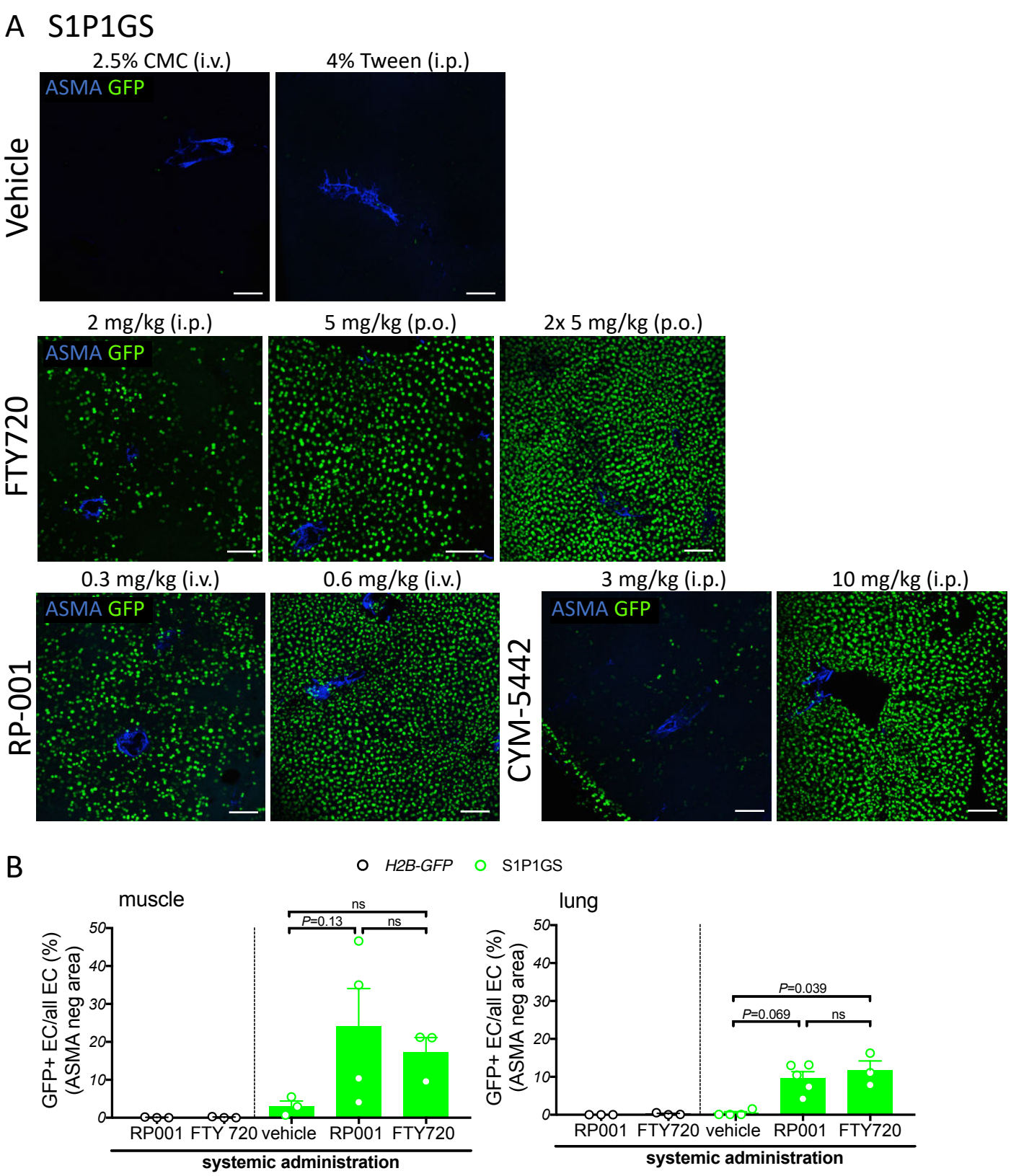

Online Figure VII

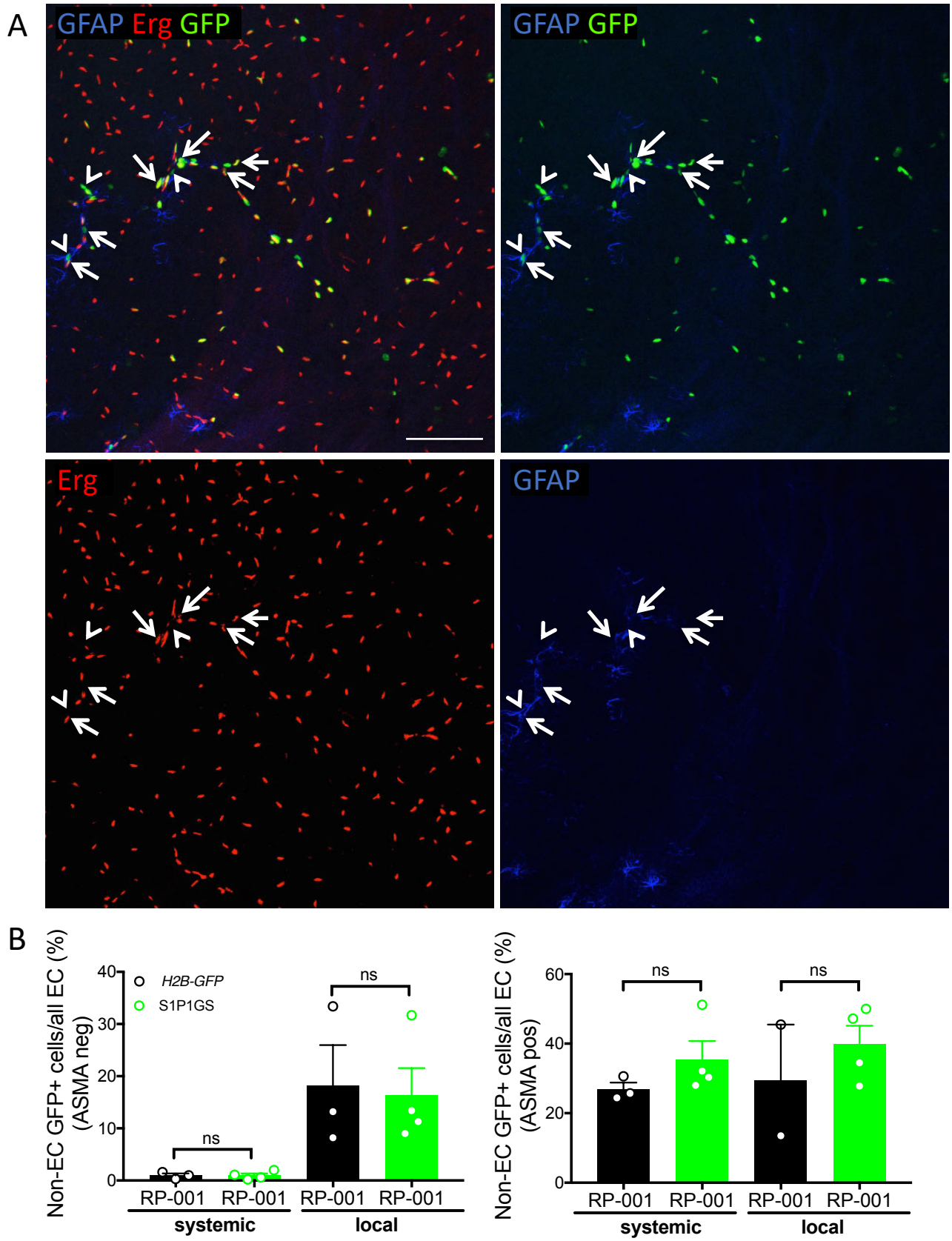

Online Figure VIII

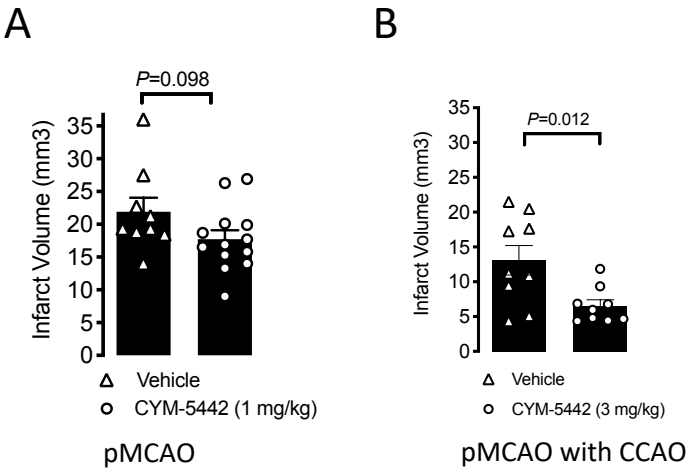

Online Figure IX

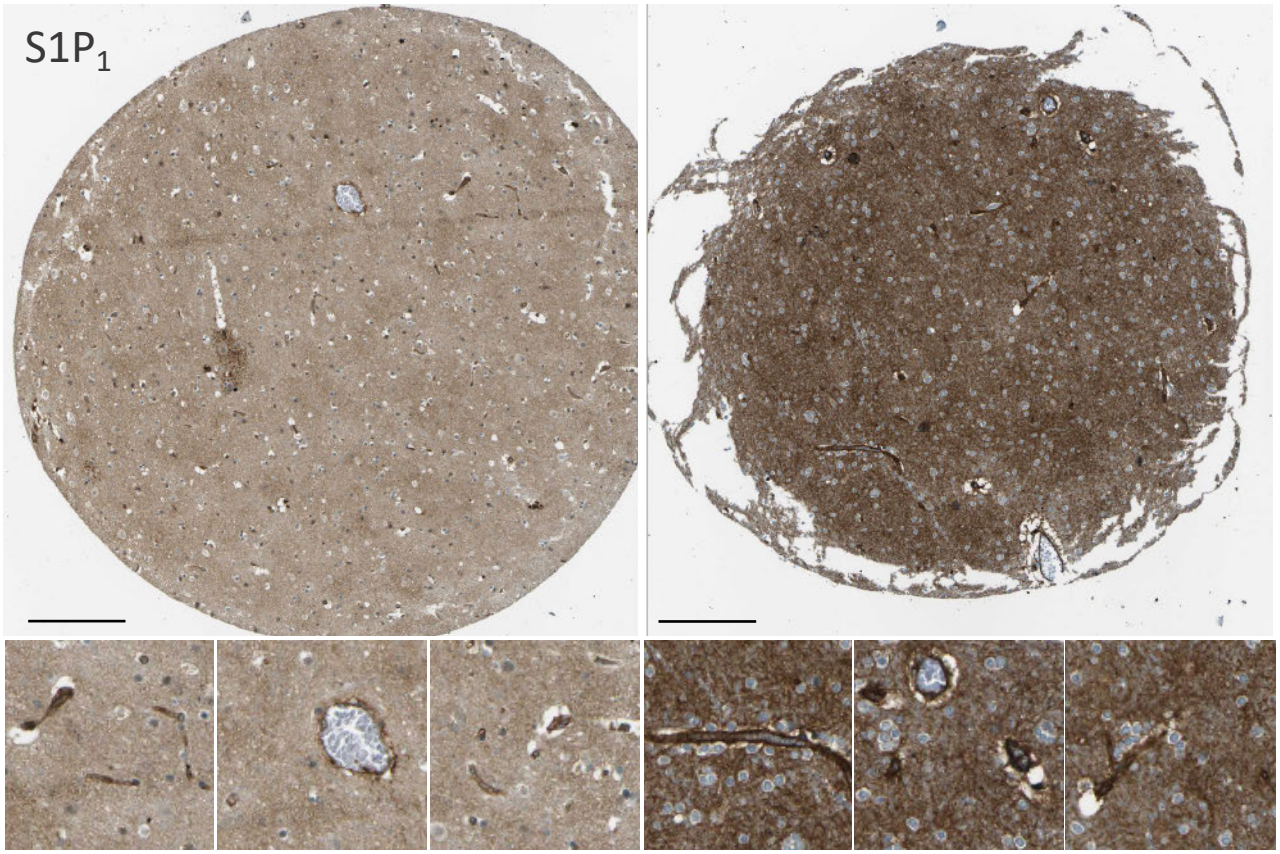

1

SUPPLEMENTAL MATERIAL

Endothelial $S1P_1$ signaling counteracts infarct expansion in ischemic stroke.

Authors: Anja Nitzsche, Marine Poittevin, Ammar Benarab, Philippe Bonnin, Giuseppe Faraco, Hiroki Uchida, Julie Favre, Lidia Garcia-Bonilla, Manuela C. L. Garcia, Pierre-Louis Léger, Patrice Thérond, Thomas Mathivet, Gwennhael Autret, Véronique Baudrie, Ludovic Couty, Mari Kono, Aline Chevallier, Hira Niazi, Pierre-Louis Tharaux, Jerold Chun, Susan R. Schwab, Anne Eichmann, Bertrand Tavitian, Richard L. Proia, Christiane Charriaut-Marlangue, Teresa Sanchez, Nathalie Kubis, Daniel Henrion, Costantino Iadecola, Timothy Hla, and Eric Camerer

Methods
Online Figure Legends
Video Legends
References 67-82
Online Table I
Online Figures I-IX

Methods

Data Availability. The authors declare that all supporting data are available within the article and its online supplementary files.

Study design. This study was carried out between 2014 and 2020 as part of a joint collaborative effort of the SphingoNet Transatlantic Network of Excellence to study roles of S1P signaling in the Neurovascular Unit (https://www.fondationleducq.org/network/sphingosine-1-phosphate-in-neurovascular-biology-and-disease-sphingonet/). Experimental stroke was performed in 4 different laboratories by 5 different experimenters, with some variation in experimental protocols and exclusion criteria (see below). Absolute values therefore should not be compared across experiments. Animals were assigned randomly to treatment groups by alternate allocation. Sample size was based on expected variation in published studies using similar models as well as on genotype distribution of littermates in genetic studies. Surgery and/or data analysis were performed blinded to genotype/treatment by blinding genotypes, drugs and/or images.

Study approval. The study was approved by the institutional animal care and use committees of Paris Descartes and Paris Diderot Universities and Weill Cornell Medical College as well as by the French Department of Education.

Mice. Mouse lines were either in mixed C57BL/6J:129SVJ or in inbred C57BL/6J background. Mice were housed in specific-pathogen free facilities in cages with wood chip bedding and fed a normal mouse breeding diet (A03-10, Scientific Animal Food and Engineering, Augy, France). Adult (>8 weeks of age) mice were used in stroke experiments and compared to age- and sex-matched littermate controls or vehicle controls as appropriate. Two independently generated models were used for endothelial-specific deletion of *S1pr1* (*S1pr1*^{ECKO}). In the first and most used model, recombination of a loxP flanked *S1pr1* knockout allele[56] was induced with *Pdgfb-iCreERT2* (*S1pr1*$^{f/f}$*:PdgfbCre*$^{+}$).[29] The second model, which was used for experiments shown in Figure 1E, 5A, 5E and 5I, used *Cdh5-Cre-ERT2* [67] to excise a different loxP flanked *S1pr1* knockout allele (*S1pr1*$^{f/f}$*:Cdh5Cre*$^{+}$).[11] Activation of ERT2 was achieved by administration of 20 µg tamoxifen *per os* (p.o.) or by intraperitoneal (i.p.) injections thrice between P1 and P5, with the exception of mice used for experiment in Figure 1E, where activation was induced by administration of 75 mg/kg tamoxifen p.o. on three consecutive days 2 weeks prior to experimentation in adult mice. Efficiency of adult deletion of *S1pr1* with *Cdh5Cre* was confirmed to be ~95 % by qRT-PCR of isolated brain endothelial cells[26]. Mice deficient in S1P production (*Sphk1*$^{f/-}$*:Sphk2*$^{f/-}$*:PdgfbCre*$^{+}$*;Sphk1&2*^{ECKO}*)* and export (*Spns2*$^{f/f}$*:PdgfbCre*$^{+}$*;Spns2*^{ECKO}*)* in endothelial cells were generated by neonatal deletion of LoxP flanked alleles for *Sphk1*, *Sphk2* and *Spns2* with *Pdgfb-iCreERT2*.[29] Efficiency of neonatal deletion with *PdgfbCre* is addressed in this study and elsewhere.[9, 25] The mTmG double fluorescent reporter mouse was used to evaluate excision efficiency in the mature brain.[68] It should be noted that *PdgfbCre* is reported not to be efficient with adult induction and to target megakaryocytes in addition to ECs.[25, 29] Moreover, since *Pdgfb-iCreERT2* is less efficient in lymphatic than in blood ECs, *Spns2* deletion was not associated with lymphopenia (not shown). Mice deficient in S1P production in plasma (*Sphk1&2*^{HCKO}; *Sphk1*$^{f/-}$*:Sphk2*$^{f/-}$*:Mx1Cre*$^{+}$) and platelets (*Sphk1&2*^{MKKO}; *Sphk2*$^{f/f}$*:Pf4Cre*$^{+}$; note that platelets only use Sphk2 for S1P production [9]) and in $S1P_1$ expression in platelets (*S1pr1*^{MKKO}; *S1pr1*$^{f/f}$*:Pf4Cre*$^{+}$) or hematopoietic cells (*S1pr1*^{HCKO}; *S1pr1*$^{f/f}$*:Mx1Cre*$^{+}$ or *S1pr1*$^{f/f}$*:Vav1Cre*$^{+}$) have been previously

described and characterized with regard to gene excision, S1P production, and peripheral blood lymphocyte counts.[9, 25] Generation and use of S1P signaling reporter mice (S1PGS; *S1pr1*$^{ki/+}$*:H2B-GFP*$^{Tg/+}$) has been previously described.[12, 25, 38] The effects of tissue specific S1P, Spns2, and S1PR1 deficiency were first tested separately in males and females (as indicated in results and figure legends) in a permanent middle cerebral artery occlusion (pMCAO) model. Once we had established that the same genotype-dependent effects were observed in both sexes, sex-matched groups of either males or females were used to address mechanistic questions in the pMCAO model. Only males were used in the transient (t) MCAO model and in experiments with purchased C57BL/6J animals. Experiments performed in naïve mice were either same-sex or sex-matched as detailed below.

Drug treatment. The following drugs were administrated to either naïve mice or mice submitted to pMCAO or tMCAO: FTY720 (1 mg/kg, 2 mg/kg, 5 mg/kg, in saline; Sigma-Aldrich #SML0700) *per os* or intraperitoneally; CYM-5442 (1 mg/kg, 3 mg/kg, 10 mg/kg in 5 mg/ml DMSO, 4% Tween20, saline; Cayman Chemicals, MI, USA #169625) applied intraperitoneally; CYM-5442 hydrochloride (3mg/kg in saline; Tocris, UK #3601) applied intraperitoneally; RP-001 (Tocris, UK #4289; 10 mM DMSO diluted in 2.5% carboxymethylcellulose sodium salt, Sigma-Aldrich #21902) administrated intraperitoneally at 0.6 mg/kg or locally at a concentration of 0.06 mg/kg into the brain parenchyma (injection volume 1.5 µl) or into the cisterna magna (injection volume 3 µl).

Angiography. Mice were anesthetized with ketamine/xylazine and transcardially perfused with phosphate buffered saline supplemented with heparin (2 U/mL), papaverine (40 mg/mL) and adenosine (1 mg/mL) for 2 minutes followed by a blue polymer (PU4ii, vasQtec, Switzerland) for 30 seconds at 4 mL/min and 110 mmHg. Both solutions were kept at 37°C before use. Brains were removed immediately after, collateral anastamoses between the MCA and branches of the ACA counted thrice in each hemisphere under a Leica M165FC stereo microscope by an investigator blinded to mouse genotype, and images acquired. A sex-matched group of males and females was used for this study.

Telemetry-based blood pressure measurements. Mice were anesthetized with isoflurane (2 %) and a blood pressure probe connected to a telemeter (TA11PA-C10; Data Sciences International) implanted in the left femoral artery. Amoxicillin (20 mg/kg i.p., Clamoxyl; SmithKlineBeecham) and ketoprofen (5 mg/kg i.p., Profenid; Aventis) were administered each in a single dose after surgery. After two weeks of adaptation, blood pressures and physical activity were recorded for 72 hours and daytime and nighttime values averaged to determine systolic, diastolic and pulse pressures, heart rates, and activity levels. Only female mice were used in this study.

CO_2-induced cerebral vasoreactivity monitored in the basilar trunk. Thermoregulated mice were submitted to ultrasound measurements under 0.5% isoflurane anesthesia using an echocardiograph (Acuson S3000, Erlangen, Germany) equipped with a 14-MHz linear transducer (14L5 SP) as previously reported.[69] Heart rates, peak systolic, end-diastolic and time-average mean blood flow velocities (mBFVs) were measured on basilar trunk (BT) before cerebral ischemia 1) under air and 2) 5 min after starting breathing a gas mixture of 16% O_2, 5% CO_2, 79% N_2 (normoxia-hypercapnia). Vasoreactivity was estimated for each mouse as the percentage changes

in mBFV recorded under gas mixture compared to mBFV recorded under air.[70] A sex-matched group of males and females was used for this study.

Surgical procedures for cranial window CBF studies. Mice were anesthetized with isoflurane in a mixture of N_2 and O_2 (Induction, 5%; Maintenance, 2%). The trachea was intubated and mice were artificially ventilated with an oxygen-nitrogen mixture. The O_2 concentration in the mixture was adjusted to provide an arterial pO_2 (PaO_2) of 120–130 mmHg [71]. One of the femoral arteries was cannulated for recording mean arterial pressure (MAP) and collecting blood samples. Rectal temperature was maintained at 37°C using a thermostatically controlled rectal probe connected to a heating pad. End tidal CO_2, monitored by a CO_2 analyzer (Capstar-100, CWE Inc.), was maintained at 2.6–2.7% to provide a pCO_2 of 33–36 mmHg.[71] After surgery, isoflurane was discontinued and anesthesia was maintained with urethane (750 mg/kg, i.p.) and chloralose (50 mg/kg, i.p.). Throughout the experiment, the level of anesthesia was monitored by testing corneal reflexes and motor responses to tail pinch.

Cranial window CBF experiments. A small craniotomy (2x2 mm) was performed to expose the parietal cortex, the dura was removed, and the site was superfused with Ringer's solution (37°C; pH 7.3–7.4; composition in mmol/L: 137 NaCl, 5 KCl, 1 $MgCl_2$, 1.95 Na_2HPO_3, 15 $NaHCO_3$, 2 $CaCl_2$). CBF was continuously monitored at the site of superfusion with a laser-Doppler probe (Perimed) positioned stereotaxically on the cortical surface. The outputs of the flowmeter and blood pressure transducer were connected to a data acquisition system (PowerLab) and saved on a computer for off-line analysis. CBF values were expressed as percentage increases relative to the resting level. After MAP and blood gases were stable (pCO_2: 33-36 mmHg; pO_2: 120-130mmHg; pH: 7.3-7.4), the cranial window was superfused with Ringer's solution, and CBF responses were recorded. To minimize the confounding effects of anesthesia on vascular reactivity, the time interval between the administration of urethane-chloralose and the testing of CBF responses was kept consistent among the different groups of mice studied. Activation of the whisker-barrel cortex (functional hyperemia) was induced by stroking the contralateral vibrissae for 60 seconds, and the evoked changes in CBF were recorded. The endothelium-dependent vasodilator acetylcholine (ACh; 10µM; Sigma) was superfused on the exposed neocortex for 5 min. A sex-matched group of mice was used for this study.

Arterial spin labeling MRI. Resting CBF was assessed using arterial spin labeling magnetic resonance imaging (ASL-MRI) on a 7.0-tesla 70/30 Bruker Biospec small-animal MRI system with 450 mT/m gradient amplitude and a 4,500 $T \cdot m^{-1} \cdot s^{-1}$ slew rate22 as previously described.[52] A sex-matched group of mice was used for this study.

Electrocoagulation-induced pMCAO. Mice were anesthetized by isoflurane (initially 2%, followed by 1.5 to 1.8%). Body temperature was maintained with a heating blanket. Under low-power magnification, the left temporal-parietal region of the head was shaved and an incision was made between the orbit and the ear. A second incision was made on the temporal muscle, and the lateral aspect of the skull was exposed after reflecting the muscle forward permitting visualization of the MCA through the semi-translucent skull. A small hole (1-2 mm) was drilled into the outer surface of the skull just over the MCA (Technobox 810, Bien Air Dental SA, Bienne, Switzerland). The dura mater was removed with fine forceps and the left MCA occluded by electrocoagulation with bipolar forceps and dissected with fine scissors. After surgery, the wound was sutured and

the mice placed under a heating lamp until recovery from anesthesia. In one experiment in which animals were followed for 7 days, the ipsilateral common carotid artery was exposed and ligated under isoflurane (2%) anesthesia immediately prior to pMCAO in order to increase the impact of MCA occlusion. Exclusion criteria included surgery-related injury (focal bleeding, drilling-induced brain damage, and thermal injury), tissue loss, and death. Of 479 mice enrolled in pMCAO experiments, 27 (5%) were excluded due to surgery-related injury (24), tissue loss (1) and death (2). Groups of either males or females were used as detailed in Figure Legends to determine infarct size or as described for individual methods to address mechanism.

Transient focal cerebral ischemia (tMCAO). Transient MCAO was induced using the intraluminal filament model of middle cerebral artery occlusion, as described previously but with slight variations according to practice in the laboratory in which the experiment was conducted.[70, 72, 73] Under isoflurane anesthesia (maintenance 1.5-2%), a heat-blunted nylon suture was inserted into the right external (Fig 1E, Fig 5I, Fig 2I, Online Fig II L) or the common (all other experiments) carotid artery of anesthetized mice and advanced until it obstructed the MCA. In some experiments occlusion was confirmed by cerebral blood flow (CBF) measured using transcranial laser Doppler flowmetry (Periflux System 5010, Perimed, King Park, NY or Moor Instruments, MOORVMS-LDF2, Devon, UK) in the territory irrigated by the right MCA (2 mm posterior, 5 mm lateral to bregma) (Fig 5I, Fig 2I, Online Fig II L) or using a laser-Specle imager (PeriCam PSI system, Perimed, King Park, NY) placed over the entire right hemisphere (Fig 1E). The filament was left in place for 35-90 min as indicated and then withdrawn. Rectal temperature was monitored and kept constant (37.0 ± 0.5°C) during the surgical procedure and in the recovery period until the animals regained full consciousness. Only male mice were used for tMCAO studies. In experiments in which blood flow monitoring was conducted with laser Doppler flowmetry (Fig 5I, Fig 2I, Online Fig II L), only animals that exhibited a reduction in CBF of >85% during MCA occlusion and in which CBF recovered by >80% after 10 minutes of reperfusion, were included in the study.[73] In experiments in which blood flow was monitored with laser Specle (Fig 1E), only animals that exhibited a reduction in CBF of >65% during MCA occlusion and in which CBF recovered by >65% after 10 minutes of reperfusion, were included in the study.[33] In all experiments animals that died prior to the pre-determined endpoint (24 or 72 hours), for which tissue processing-induced damage precluded analysis, or that displayed evidence of subarachnoid hemorrhage or no visible infarct or were excluded from analysis. Of 276 mice enrolled in tMCAO experiments, 85 (31 %) were excluded due to insufficient occlusion (2), insufficient reperfusion (4), death (36), tissue loss/damage (9), no visible infarct (25/experiments where blood flow was not monitored), or SAH (9). In a line that showed extensive death after 90 minutes tMCAO prior to the pre-determined endpoint (24 hours), death was reported (Online Figure I D) and cause of death subsequently explored (Figure 4E).

Neurological evaluation. Where indicated, neurologic examinations were carried out as previously described [33, 59] with slight modifications, as follows: 0: no deficit, 0.5: when held by tail, good extension of affected forelimb but weakness when grabbing the wires of the cage, 1: walking straight or ability to turn in both directions but when held by tail, unable to extend affected forelimb and torso turning to the ipsilateral side, 1.5: preference to walk in one direction, 2: unable to walk straight or to turn in both directions, circling to affected side when held by tail on the bench, 2.5: circling on the spot and walking circling, 3: spontaneous circling to the affected side

(without going anywhere), 3.5: no movement, upon stimulation circling on the spot, 4: no spontaneous locomotor activity or barrel rolling.

Measurement of infarct volume. Infarct volume was assessed on day 3 by cresyl violet (Fig 1C, 5I) or on day 1 by triphenyltetrazolium chloride (TTC; all other) staining. For the first procedure, 30-µm-thick coronal brain sections were stained with cresyl violet and infarct volumes, corrected for swelling, quantified by image analysis software (MCID, Imaging Research, UK or Cartograph v6.3.1, Microvision Instruments, France) as described.[70, 73] For the second procedure, 1 or 1.5 mm coronal brain sections were stained with 2% TTC, imaged, and the area of infarct, ipsilateral hemisphere and contralateral hemisphere measured for each section using ImageJ analysis software (National Institutes of Health, Bethesda, MD) and infarct area on each slice corrected for swelling determined as previously described.[33, 59, 70]

Ultrasound imaging after pMCAO. Before mice were submitted to pMCAO, blood-flow velocities (mBFVs) were measured by ultrasound imaging in both intra cranial internal carotid arteries (ICA) and BT under 0.5% isoflurane anesthesia. Sample volume of the pulsed Doppler was placed in the ICAs downstream from the posterior cerebral artery and upstream from the middle and anterior cerebral arteries; in the BT, sample volume was placed 1 to 2 mm downstream from the confluence of both vertebral arteries. The procedure was repeated 50 and 120 minutes after pMCAO in all the three arteries.

Blood and plasma collection and cell counting. Blood was collected from the retro-orbital venous plexus with EDTA-coated capillaries under isoflurane anesthesia and blood cells enumerated with a Hemavet 950 cell counter (Drew Scientific). Plasma was prepared by centrifugation of blood at 500g for 10 min at room temperature and a subsequent second centrifugation of the supernatant at the same settings. Plasma was stored at -80°C.

Serotonin ELISA. Blood from naïve mice or mice subjected to pMCAO was collected 2.75h post-occlusion as described above. Plasma was diluted 1:4 in assay buffer and analyzed for serotonin levels by ELISA according to manufacturer's instructions (#ADI-900-175, Enzo). Only female mice were used for this analysis.

Evaluation of BBB integrity. BBB integrity was addressed by intravascular infusion of Evans Blue dye or TRITC-conjugated low molecular weight dextran (4 kDa) and by T2 weighted MRI. Whereas accumulation of low molecular weight dextran mostly reflects on the integrity if intercellular tight junctions, Evans Blue binds to albumin, which is transported across the BBB endothelium by caveolin-dependent transcellular transport.[40] Hyper-intensity in T2W MRI reflects on water movement and vasogenic edema. Evans Blue dye (2 %; Sigma-Aldrich Inc., St Louis, MO, USA) in PBS was administered in the tail vein or retro-orbitally (4 ml/kg) of mice 24 hours after stroke (n=8-10) or naïve mice. After two hours of circulation time, animals were transcardially perfused with at least 20 mL of heparinized saline under isoflurane or ketamine/xylazine (100 mg/kg/10 mg/kg) anesthesia and brains removed. Each hemisphere after pMCAO or only the cortex of naïve mice was placed separately in 2 ml and 500-600 µl (200mg cortex/500 µl) of formamide, respectively, and Evans Blue dye extracted for either 24h at 55°C or 72h at room temperature. The absorbance of the supernatant was then measured against a formamide standard at 620 and 740 nm. Similarly, TRITC-conjugated 4kDa Dextran (TdB

Consultancy AB, Uppsala, Sweden) diluted in PBS was administrated retro-orbitally at a concentration 0.2mg/g mouse. Two hours later, animals were perfused transcardially as described above, brains removed, and the cortex lysed in 50% TCA (w/v), 1% Triton-X, 5 mM EDTA, PBS and homogenized with a TissueRuptor (Qiagen). Fluorescence was measured in clear supernatants at 571 nm (excitation: 550 nm, cut off: 570 nm) using a plate reader (FlexStation3, Molecular Devices, San Jose, CA, USA). T2 weighted MRI was performed with a. 4.7 Tesla (T) Bruker small animal MR scanner (Biospec 47/40 USR Bruker, Ettlingen, Germany) under isoflurane anesthesia. T2 weighted brain images were acquired in two imaging planes (axial and coronal) and with a Turbo RARE sequence (TR/TE=500/80ms, slice thickness of 0.7 mm, plan resolution 100 mm) using a volume coil for excitation combined with a brain surface coil for the reception. Only male mice were used for Evans Blue dye extraction after pMCAO and for MRI studies. Other studies were performed on sex-matched groups of mice.

Sidestream Dark Field imaging. 100 minutes after pMCAO, mice were anesthetized with isoflurane (3 %) and a left parietal craniotomy performed with a dental drill to expose a cranial window over the distal region of the left MCA territory. The ischemic and non-ischemic animals were then placed in the lateral position, and cerebral microcirculation of the MCA and at regions of anastomoses between the MCA and ACA or PCA visualized by using sidestream dark field videomicroscopy (MicroScan, MicroVision Medical, Amsterdam, Netherlands) with a 5x imaging objective giving x326 magnification. For visualization of leptomeningeal microcirculation, the probe was attached to a stereotaxic clamp and adjusted to maintain brain contact without compression. Two hours after pMCAO, as many fields as possible of 940 µm x 750 µm were identified along the ACA/MCA border and each recorded during 30 seconds. Automated calculation of vascular perfusion was carried out with dedicated software (Automated Vascular Analysis [AVA] version 4.1; Academic Medical Center, University of Amsterdam, Amsterdam, The Netherlands); fields where superficial bleeding interfered with the identification of vessels were excluded.[74] Only male mice were used for these studies.

Flow-mediated dilation (FMD). Arterial segments isolated from posterior cerebral arteries and mesenteric arteries were cannulated at both ends on glass micro-cannulae and mounted in a perfusion system (Living System; LSI, Burlington, VT) in physiological saline solution (37°C, pH 7.4; partial pressure of O2, 160 mm Hg; and partial pressure of CO2, 37 mm Hg). The arteries were pressurized (diameter ≈220 µm at 75 mmHg) and changes in internal arterial diameter were monitored by video microscopy (Living System, LSI, Burlington, VT) as previously described.[75] After a resting period, endothelial function was tested on precontracted arteries (phenylephrine 10^{-6}M) by assessing the vasodilating response to acetylcholine 10^{-6}M. Arteries were then washed and allowed to recover for 20 minutes. After an equilibration period of low-flow (3µl/min for 10 minutes), FMD was assessed on precontracted arteries submitted to stepwise increases in intraluminal flow (2-minute steps from 3 to 50 µl/min). Only male mice were used for these studies.

Immunostaining, confocal microscopy, and image analysis. Mice were anesthetized with ketamine/xylazine (100 mg/kg/10 mg/kg) and perfused with DPBS (Gibco) containing 2U heparin (Sanofi Aventis France) via left ventricle, followed by perfusion with 1% PFA diluted in 1x DPBS with 2U heparin. Brains, skeletal muscle and lungs were collected and either directly post-fixed in PFA (for S1P1 staining 4% PFA for 30 min or 1% PFA for 1h at RT) or for staining of thick

sections, fresh brains and livers were immediately cut after tissue harvest into 0.8 mm sections using a tissue chopper (The Mickle Laboratory Engineering Co. Ltd, Surrey, UK) and post-fixed in 4% PFA for 1h at RT, and washed at least three times in PBS. For frozen sections the fixed tissue was placed in 30% sucrose overnight, embedded in Cryomatrix (#6769006, Thermofisher) and frozen in dry ice and isopentane, 10 µm sections were prepared. For $S1P_1$ staining frozen brain sections were post-fixed in methanol for 10 min at -20ºC, rehydrated with PBS and blocked at RT for at least 1h in Claudio's blocking buffer (1% FBS (Gibco), 3% BSA (Sigma), 0.5% triton X100 (Biosolve), 0.01% Na deoxycholate (Sigma), 0,02% Na Azide (VWR) in PBS.[76] For all other staining on frozen sections, samples were blocked directly in 3% BSA (Sigma), 5% Normal Donkey Serum (Sigma, #D9663), 0.2% Triton-X100 (Biosolve) in PBS. Thick 0.8 mm sections were blocked and permeabilized in TNBT buffer (0.1 M Tris pH 7.4; NaCl 150 mM; 0.5% blocking reagent from Perkin Elmer, 0.5% Triton X-100) overnight at 4ºC and subsequent washes were done in TNT (0.1 M Tris pH 7.4; NaCl 150 mM; 0.5% Triton X-100). For frozen sections primary antibodies were incubated overnight at 4ºC and secondary antibodies for 2 h at room temperature. For thick sections primary and secondary antibodies were incubated overnight at 4ºC. For detection of biotinylated secondary antibodies, fluorophore-conjugated streptavidin was applied overnight at 4ºC. Frozen sections were mounted in Fluoromount-G (#0100-01, Southern Biotech) or in the case of S1P1 staining in ProLong™ Gold Antifade Mountant (#P36934, ThermoFisher). Thick sections were mounted in Dako Fluorescence Mounting medium (#S3023, Dako). Sex-matched groups of male and/or female mice were used for these studies.

For analysis of brains three hours after pMCAO, biotinylated tomato-lectin (5 µg/g; #B-1175, Vector Laboratories) was injected retro-orbitally under isoflurane (2 %) anesthesia 15 min prior to fixed pressure transcardial perfusion with 10 mL of heparinized DPBS and subsequently with 10 ml of 1% PFA diluted in heparinized DPBS under ketamine/xylazine (100 mg/kg/10 mg/kg) anesthesia and brains removed. Brains were fixed in 4% PFA overnight at 4°C and washed three times in PBS. One hundred fifty µm vibratome sections were blocked and permeabilized in TNBT buffer overnight at 4ºC. Tissue sections were then incubated with primary antibodies diluted in TNBT for 48-72 h at 4ºC, washed in TNT buffer at least 7 times and incubated with appropriate fluorophore-conjugated secondary antibody and fluorophore-conjugated streptavidin to detect biotinylated tomato-lectin diluted in TNBT for 48-72h at 4ºC. Samples were then washed at least 7 times in TNT and mounted on microscopy slides in fluorescent mounting medium (#S3023, Dako). For fibrin(ogen) and platelet staining two 150 µm vibratome sections 450-600 µm apart were stained, for neutrophil staining, one section per brain was stained. Only female mice were used for this study.

Eyes were fixed in 4% PFA for 10 min at RT, retinas dissected and subsequently post-fixed in methanol at -20ºC (in a flat position; stored at -20ºC till further processing) step-wise rehydrated in 50%PBS/50%methanol followed by 100% PBS and blocked in Claudio's blocking buffer. Primary antibodies were diluted in blocking buffer and incubated overnight at 4ºC, followed by several washes in PBS or PBS with 0.2% Tween for S1P1 staining. Appropriate secondary antibodies were added for 1-2 hours at room temperature and retinas were post-fixed with 4% PFA for 10 min at RT and further incubated in PBlec for at least 1h at RT and subsequently incubated with biotinylated isolectinB4 (1:200, B-1205, Vector Labs) overnight at 4ºC, followed by several washes with PBS 0.2% Tween and incubated with streptavidin conjugated to different fluorophores for 2 hours at RT, if required retinas were incubated in Hoechst 33258 (1:10,000,

#94403, Sigma) for 30 minutes. The retinas were flat mounted in either FluromountG (#0100-01, SouthernBiotech) or in the case of S1P1 staining in ProLong™ Gold Antifade Mountant (#P36934, ThermoFisher). Sex-matched groups of male and/or female mice were used for analysis of adult retinas. Sex was not determined in neonatal studies.

The following primary antibodies were used: rabbit anti-$S1P_1$ (1:100, #sc-25489, Santa Cruz EDG-1 Antibody (H-60)), mouse anti-ASMA-Cy3 (1:250, #C6198, Sigma), chicken anti-GFP (1:500, #A10262, ThermoFisher), goat anti-GLUT1 (1:200, sc-1605, Santa Cruz), rabbit anti-GLUT1 (1:300, #07-1401, Millipore), goat anti-CD31 (1:300, #AF3628, R&D Systems), rat anti-ICAM-2 (1:300, #553326, BD Pharmingen), goat anti-ICAM-1 (1:100, #AF796, R&D Systems), rabbit anti-Erg (1:300, #ab92513, Abcam), mouse anti-GFAP-Cy3 (1:250, #MAB3402C3, Millipore), rat anti-CD41 (1:200, #133902, biolegend), rabbit anti-MPO (1:100; #ab9535, abcam), rat anti-NIMP-R14 (1:100, #ab2557, abcam), rat anti-Ter119 (1:100, #553671, BD Pharmingen), rabbit anti-fibrinogen (1:200; #A0080, Dako). The following fluorophore-conjugated streptavidin was used: Alexa405-conjugated (1:100; #S32351, ThermoFisher), Cy3-conjugated (1:100, #43-4315, Invitrogen).

Images were acquired using an inverted Leica SP8 confocal laser scanner microscope equipped with the following objectives: HC PL APO 40x/NA 1.30 Oil CS2, HC PL APO 63x/NA 1.40 OIL CS2; HC PL APO 20x/NA 0.75 IMM CORR CS2. Images acquired with the 20x objective were sampled at a pixel size of 0.568-0.758 µm for XY and 1.041 µm for Z. Bigger tile scans were acquired using the resonant scanner and the 20x objective and were sampled with a pixel size of 0.454 µm for XY and 1.151 µm for Z. Settings for high magnification images (40x and 60x objectives) used for subsequent deconvolution were set according to the Nyquist rate as calculated by the Nyquist Calculator App (https://svi.nl/NyquistCalculator). Images were processed with LAS-X software (Leica, Germany) and ImageJ/Fiji (National Institue of Health, USA). Samples from different genotypes were imaged under constant microscope settings. A minimum of three images was taken per sample. For quantification of fibrin(ogen) and platelets in brains three hours post-pMCAO, tile scans at a size of about 2000 µm x 2900 µm were taken and the region of interest (ROI) was set 1200 x 800 µm superior to the infarct core (outlined as non-perfused, highly fluorescent area, which was partly due to high levels of fibrin(ogen) and partly due to nonspecific background signal at 552 nm excitation), both a rectangle of 1200 x 800 µm and a rectangle of 600 x 800 µm extending 600 µm superior form the core was quantified. For neutrophil quantification the ROI was set next to the infarct core on both the superior and inferior sides and a square of 600 µm x 1200 µm was quantified. The same ROI was chosen to evaluate the level of lectin perfusion. Deconvolution of images for $S1P_1$ high magnification images was performed with Huygens Essential (Scientific Volume Imaging, Hilversum, The Netherlands). Image analysis was performed with ImageJ/Fiji (National Institue of Health, USA) or CellProfiler (version 2.2.0, Broad Institute, Boston, MA, USA).[77]

Cerebral microvessel isolation, RNA extraction, cDNA synthesis and quantitative real time PCR. Microvessels from the cortices of each hemisphere of male naïve mice or mice that had been subjected to tMCAO (1h of occlusion) for 6 hours (between 5h40min and 6h20min) were isolated as previously described [78] using a BSA gradient to remove myelin.[79] Two mice, i.e. four cortices were processed at a time. Isolated microvessels were lysed in 350 µl of RLT Plus lysis buffer by Qiagen, vortexed vigorously and stored at -80°C until RNA isolation. The lysate was loaded onto

QIAshredder columns (Qiagen, #79654) and RNA was isolated using the RNeasy Plus Micro kit (Qiagen, #74034). Complementary DNA was prepared with the entire RNA of one microvessel isolation using the iScript™ cDNA synthesis kit (Bio-Rad Laboratories, #1708882) in a 20 µl reaction volume. The cDNA was diluted with 80 µl of water and 5 µl were used per reaction in duplicates in the subsequent quantitative real-time PCR (qPCR).
The following primers were used in combination with iQ™ SYBR® Green Supermix (Bio-Rad Laboratories, #1708882) in a 2-step amplification cycling mode (95°C for 3 min, 40 cycles of 95°C for 10 sec and 56°C for 30 sec, final melting curve) using a CFX96 C1000 thermocycler (Bio-Rad Laboratories):
Tjp1 (ZO1) FW: CCA AGG TCA CAC TGG TGA AGT C, REV CTT GAA TGT TAC CAT CTC TTG CTG; *Aqp4* FW TGG TTG GAG GAT TGG GAG TCA C, REV CAG TTC GTT TGG AAT CAC AGC TG; *Anpep* (CD13) FW CAA GGG AGC CTC AGT CAT CAG GAT GC; REV GAC AGC TGT CTG TTG GTT CAC G.
The following TaqMan probes were used with the Platinum™ Quantitative PCR SuperMix-UDG with ROX (ThermoFisher, #11730025) in a 2-step amplification cycling mode (50°C for 2 min, 95°C for 10 min and 40 cycles of 95°C for 15 sec and 60°C for 1 min) using a StepOnePlus thermocycler (Applied Biosystems):
Spns2 (Mm01249328_m1; ThermoFisher), *S1pr1* (FW: TTGCACTGAGCCAAAGGTCTAG, REV: CTTGGGACCTTAGTCTTTGAGGAG, probe: TCAAGCTCCCAGAGGGCTCATCTGGT [80], *Sphk1* (FW: GAGAAGTACAGGCGCTTGGG, REV: TGGTAGATGCGCAGGCTTG, probe: TCACAGTGGGCACCTTCTTTCGCCTA, *Sphk2* (FW: GTGGTGCCAATGATCTCTGAAG, REV: GCTCACGGGCATGGTTCT, probe: TGGGCTGTCCTTCAACCTCATACAGACA). The expression levels were normalized to either *Actb*[80] or *Tjp1* (ΔCt) and expression levels were calculated by comparing 2^(-ΔCt) values.

Isolation of cerebral endothelial cells and quantification of gene excision efficiency. Cerebral microvessels from cortices of eight four-week old *Sphk1&2*^{ECWT} and ^{ECKO} mice were isolated as previously described[81] using a BSA gradient for the removal of myelin[79] and puromycin selection was applied for four days. Endothelial cells were further purified by fluorescent activated cell sorting. Briefly, the monolayer of cells was washed three times with PBS and 0.5 mM EDTA and detached by adding a few droplets of 0.05% trypsin (Gibco™ ThermoFisher, #25300096) diluted in PBS/EDTA. Detached cells of two isolations were pooled and resuspended in 800 µl of FACS buffer (2% Fetal Bovine serum (Gibco™ ThermoFisher, #10270098), 1 mM EDTA, PBS), centrifuged at 1500g for 5 min at 4°C and the pellet was resuspended in 5 µg/ml primary antibody (rat anti-mouse CD31, BD Biosciences, #553370; rat anti-mouse ICAM-2, BD Biosciences #553326), incubated for 30 min at 4°C with mild shaking. One ml of FACS buffer was added, the cells were spun down at 1500g for 5 min at 4°C and incubated in donkey anti-rat Alexa647 (10 µg/ml, abcam #ab150155) for 30 min at 4°C with mild shaking. After a final wash with 1 ml FACS buffer, the cells were resuspended in 400 µl FACS buffer and sorted at a BD FACSAria™ II (BD Biosciences) into 1.5ml-tubes. Genomic DNA of 3000-4500 sorted endothelial cells was isolated using the QIAamp DNA Micro Kit (Qiagen, #56304) and excision efficiency was determined by qPCR using the iQ™ SYBR® Green Supermix (Bio-Rad Laboratories, #1708882) and the following primers: *Sphk1*: FW CTGGTGTGTGCAGAGGAGTT, REV AAACCATCCCAAGCCCTCTG; *Sphk2*: FW AGCAGGATGATGAGATGA, REV GGTACGTTGACTACTCCT; *F2rl1* as non-excised input control: ACGTCTACGCCCTCTACCTT, GTTTCTGGCGTGATCCCTGA. QPCR was performed in a 2-

step amplification cycling mode (95°C for 5 min, 40 cycles of 95°C for 10 sec and 55°C (*Sphk2*) or 60°C (*Sphk1*) for 30 sec, final melting curve) with a CFX96 C1000 thermocycler (Bio-Rad Laboratories). The qPCR was run with duplicates and the levels of genomic DNA were normalized to non-excised *F2rl1* (ΔCt) and 2^(-ΔCt) values were compared for determining gene excision efficiency. Sex-matched groups of male and/or female mice were used for these studies.

Western blotting. Anesthetized mice were perfused with DPBS (Gibco) containing 2U heparin (Sanofi Aventis France) as described above. Cerebral cortex was dissected and snap frozen in dry ice and isopentane. Tissue was lysed in RIPA buffer (150 mM NaCl, 1% TritonX-100, 0.5% sodium deoxycholate, 0.1% SDS, 50 mM Tris pH8.0) using a TissueRuptor (Qiagen) and lysate was incubated for 1.5 hours at 4ºC under constant agitation, sonicated (Branson Sonifier 450, Geneva, Switzerland) and subsequently again incubated for 1 h at 4ºC under constant agitation. Samples were centrifuged for 20 min at 4ºC at ~21'000g. Equal protein quantities of the clear supernatant were mixed with NuPAGE™ LDS Sample Buffer (ThermoFisher) and β-mercaptoethanol (0.22 µl/1 µl sample buffer). Proteins were separated on a 26-well 4–12% Criterion™ XT Bis-Tris Protein Gel (BioRad) using a Criterion™ Vertical Electrophoresis Cell (BioRad) and subsequently transferred to a nitrocellulose membrane (0.45 µm, BioRad) using the Criterion™ Blotter system (BioRad). Membranes were cut and blocked in 5% non-fat milk in TBS 0.1% Tween20 (TBS-T) and incubated with primary antibodies overnight at 4ºC under constant agitation, washed three times in TBS-T and incubated with horseradish peroxidase (HRP) conjugated secondary antibodies for 1-2 hours at RT, washed three times in TBS-T and incubated with Clarity Western ECL Substrate (BioRad) or SuperSignal West Femto (ThermoFisher). Chemiluminescence signal was detected by the ChemiDoc MP system (BioRad) and analyzed by Image Lab software (BioRad). Primary antibodies used: goat anti-ICAM-1 (1:1000, #AF796, R&D Systems), goat anti-MPO (1:500, #AF3667, R&D Systems), rabbit anti-VE-Cadherin (1:1000, #ab33168, Abcam). Sex-matched groups of male and/or female mice were used for these studies.

Statistical analysis. Statistical analysis was performed with Prism 5, 7 or 8 software (Prism, GraphPad, San Diego, USA). Specific tests applied are indicated in figure legends and in Online Table I, which includes more detailed information about the number of animmals (n) and statistical tests performed. A value of $P<0.05$ was considered statistically significant, ns indicates not significant. Exact p-values are reported for p-values close to but above 0.05 in order to reduce the probability for type II errors. Experiment-wide multiple corrections were not applied. Parametric tests were used only if normal distribution could be confirmed. In some cases, assumptions about the normality of data were made when those assumptions could not be supported through a well-powered test of normality (indicated in Online Table I). Two mice were excluded based on Rout's outlier tests (one each in Fig 2H, Fig 7G). When multiple comparisons were performed, adjusted *P* values are shown. One or more representative images were chosen to reflect the median response in each experimental subgroup. To illustrate the spread of responses three hours post pMCAO, two representative images from the mutant group are shown in Fig. 6C.

Online Figure Legends

Online Figure I: Endothelial $S1P_1$ signaling limits brain injury after permanent and transient MCA occlusion. A. Evaluation of the efficiency of Cre recombination in the cerebral cortex after neonatal induction of the *Pdgfb*-iCreERT2 allele with a $ROSA^{mTmG}$ two color reporter.[68] In this reporter, Cre recombination switches the otherwise widespread cellular expression of a cell membrane localized red fluorophore (tdTomato) to a cell membrane localized green fluorophore (EGFP). Brain sections were co-stained with CD31 to label endothelial cells. Images show a representative example of excision efficiency in the cerebral cortex and the graph shows the proportion of endothelial cells (>95%) that have undergone recombination and are thus EGFP positive. Note that recombination is efficient throughout the vascular bed, including in arteries, which have slightly more dtTomato because of the vascular smooth muscle cell coverage (indicated with white arrows). Scale bar: 100 μm. **B.** Infarct volumes 24 hours after pMCAO in male mice lacking $S1P_1$ in platelets (*S1pr1*^{MKKO}; *Pf4*-Cre) **C.** Resting peripheral blood lymphocyte counts and infarct volumes 24 hours after pMCAO in female mice lacking $S1P_1$ in hematopoietic cells (*S1pr1*^{HCKO}; *Vav1*-Cre). **D.** Infarct volumes and survival 24 hours after 90 minutes tMCAO in *S1pr1*^{ECKO} (*Pdgfb*-iCreERT2; neonatal deletion) and littermate control male mice. Bar graphs show mean ± SEM, each symbol represents one mouse. Statistical significance assessed by Fisher's exact test (D survival), Mann-Whitney test (C infarcts) or unpaired t-test (all other).

Online Figure II: Endothelial cell autonomous S1P provision sustains $S1P_1$ activation during cerebral ischemia. A. Infarct volumes 24 hours after pMCAO in male mice lacking $S1P_2$ (*S1pr2*) or $S1P_3$ (*S1pr3*) in all cells compared to pooled littermate controls. **B-C.** Infarct volumes 24 hours after pMCAO in female mice lacking S1P production (*Sphk1&2*^{ECKO}; B) or export capacity (*Spns2*^{ECKO}; C) in blood endothelial cells and respective littermate controls. **D.** Genomic DNA excision of *Sphk1* and *Sphk2* in brain endothelial cells isolated from *Sphk1&2*^{ECKO} and littermate controls assessed by quantitative PCR (n=2, pooled from two mice each). **E.** Average single cell RNA sequencing data from quiescent mouse brain vasculature fragments retrieved from http://betsholtzlab.org/VascularSingleCells/database.html.[36, 82] Note robust *S1pr1* RNA expression in all endothelial cell populations as well as in astrocytes. **F.** Ten μm brain sections from naive wild-type animals were immunostained for $S1P_1$ (green), endothelial cells (CD31; white), and astrocytes (GFAP; red) and imaged by laser-scanning confocal microscopy (top panel). Note widespread $S1P_1$ expression in both endothelial cells and astrocytes. Bottom panel shows no primary antibody control staining for antibodies used above. Scale bar: 50 μm. **G.** Ten μm brain sections from naive *S1pr1*^{ECWT}, ^{ECKO} and ^{ACKO} were immunostained for $S1P_1$ (red), endothelial cells (CD31, green) and nuclei (Hoechst), and profiles of fluorescence intensity were plotted along the dashed white lines in maximum projection images made from 6.5-7 μm Z-stacks. Note the high $S1P_1$ levels in endothelial and non-endothelial cells and the efficient deletion of $S1P_1$ in endothelial cells and astrocytes in the respective *S1pr1* ^{ECKO} and ^{ACKO} mice. $S1P_1$ levels are not altered in cerebral vessels of 12-month-old mice compared to 2-month-old mice. **H**. Single cell RNA sequencing data by Ximerakis *et al.*[37] representing *S1pr1* transcripts (TPM; Transcripts Per Kilobase Million) in cerebral endothelial cells isolated from young (2-3 months) and old (21-22 months) mice. **I-K.** Thick brain slices from naive S1P1GS mice (I, J) or H2B-GFP controls (K) were counterstained for vascular smooth muscle cells (ASMA; blue), endothelial cell nuclei (Erg; red) and endothelial cells (CD31; white) and analyzed by confocal microscopy. Note that GFP is restricted to arteries but that arteries (I') and veins (I'') also show perivascular GFP accumulation

in the S1P1GS as well as H2B-GFP controls. However, endothelial cells were rarely if ever positive in H2B-GFP controls. Thus, most if not all endothelial GFP represented $S1P_1$ signaling, and most if not all $S1P_1$ signaling was restricted to a subset of endothelial cells within arterioles, which is maintained in 12-month-old mice (J). Arrows: GFP positive endothelial cell nuclei, arrowheads: GFP positive and Erg negative nuclei. Scale bar: 100 μm. **L.** Quantitative PCR analysis of mRNA isolated from cerebral microvessels isolated from naive mice or 6 hours after tMCAO. Expression was normalized to *Actb*. Bar graphs show mean ± SEM. Statistical significance assessed by one-way (A) or two-way ANOVA with Sidak (D) or Tukey multiple comparisons test (L) or unpaired t-test (B, C).

Online Figure III. Endothelial $S1P_1$ regulates cerebral blood flow and supports tissue perfusion in the acute phase of stroke. A. Somatosensory cortex blood flow (CBF) in response to whisker stimulation assessed by laser Doppler flowmetry in mice equipped with a cranial window (time resolved view of data presented in Figure 5A). **B**. Flow-mediated dilation in mesenteric artery segments of $S1pr1^{ECKO}$, $Sphk1\&2^{ECKO}$ and their respective littermate control mice assessed by arteriography. **C**. Blood-flow velocities (mBFVs) measured by ultrasound imaging in both intra cranial internal carotid arteries (ICA) and basilar trunk (BT) under 0.5% isoflurane anesthesia before, 50 minutes and 2 hours after electrocoagulation-induced pMCAO (extract of these data are presented in Figure 5F). Sample volume of the pulsed Doppler was placed in the ICAs upstream of the posterior, middle, and anterior cerebral arteries; in the BT, sample volume was placed 1 to 2 mm downstream from the confluence of both vertebral arteries. Average recordings ± SD are shown. Each vessel was recorded 2-4 times at each time point and the mean taken for each animal. N represents the number of animals. **D**. Schematic illustration of how blood flow velocities measured in the ipsilateral ICA may reflect the presence (littermate controls) or absence ($S1pr1^{ECKO}$) of collateral engagement in the middle cerebral artery (MCA) downstream. Note that the maximal observed reduction in ICA blood flow of 28 % is in good correspondence with a distal MCA occlusion as ICA supply of the anterior cerebral artery (ACA), posterior cerebral artery (PCA) and upstream branches of the MCA are all retained even if there is no perfusion of the downstream MCA territory. Graphs show mean ± SEM. Statistical significance assessed by ordinary (A) or repeated measures (B) two-way ANOVA with Bonferroni multiple comparisons test.

Online Figure IV. Endothelial $S1P_1$ promotes microvascular perfusion and suppresses fibrin formation in MCA territories downstream of the infarct core after pMCAO. A. Confocal analysis of ICAM-1 expression in the cerebral cortex of naive $S1pr1^{ECKO}$, $Sphk1\&2^{ECKO}$ and $Sphk1\&2^{HCKO}$ mice and littermate controls. Quantification of ICAM-1 in all blood vessels (GLUT1-positive) or only arteries (ASMA positive) or excluding arteries (ASMA negative). Representative images for $S1pr1^{ECWT}$ *and* $S1pr1^{ECKO}$ in left panel, immunostained for endothelial cells (GLUT1, green), ICAM-1 (red) and arterial smooth muscle cells (ASMA, blue). Scale bar: 100 μm. **B.** Serotonin levels determined by ELISA in plasma from naive mice or 2.75 hours after pMCAO in $S1pr1^{ECWT}$ *and* $S1pr1^{ECKO}$ female mice. **C.** Example of co-staining for endothelial cells (CD31, blue), erythrocytes (Ter119, green) and tomato lectin (red) perfused 15 min prior to transcardial perfusion three hours after pMCAO. Note that erythrocytes remained mostly in non-perfused, lectin negative blood vessels, and the existence of a transition zone where both lectin and some erythrocytes are present. Scale bar: 100 μm. **D.** Quantification of neutrophils (NIMP-R14 positive) and platelets (CD41 positive) three hours after pMCAO. Presence of neutrophils

was assessed superior and inferior to infarct core in an area of 600 µm x 1200 µm ("total"), and platelets only superior to the infarct core in an area of 800 µm x 1200 µm ("total") or only within the distal part in an area of 800 µm x 600 µm ("distal'). **E.** Representative images of brain sections three hours after pMCAO approximately 500 µm superior to the infarct core immunostained for fibrin(ogen) (red), platelets (CD41, green), endothelium (CD31, blue) and tomato lectin perfusion (white). Note the presence of fibrin(ogen) in both perfused (arrow) and non-perfused (arrow head) vessels. Scale bar: 100 µm. **F, G.** Representative images of brain sections three hours after pMCAO, immediately superior to the infarct core, immunostained for neutrophils (NIMP-R14 (F) or MPO (G), green), fibrin(ogen) (F, red), platelets (G, CD41, red), perfused lectin (white) and endothelial cells (CD31, blue). Note the presence of both platelets and neutrophils in capillaries of both *S1pr1*^{ECKO} and control mice. Scale bar: 100 µm. Bar graphs show mean ± SEM. Statistical significance assessed by Kruskal-Wallis test with Dunn's multiple comparisons test (B, D neutrophils), unpaired t-test (D platelets) or Mann-Whitney test (A).

Online Figure V. $S1P_1$ expression becomes polarized with maturation of the blood-neural barrier in mice. Assessment of $S1P_1$ polarization in capillaries (**A**, **B, D, E**) and artery (**C**) of the developing retina (**A**), adult retina (**B, C**) and adult cerebral cortex (**D**, **E**) of naïve wild-type (**A, B, C, D** top panel), *S1pr1*^{ACK0} mice (*Gfap*-Cre; **D** middle panel), *S1pr1*^{ECK0} mice (*Pdgfb*-iCreERT2; **D** bottom panel) and in the ipsilateral side of *S1pr1*^{ACK0} mice 24 hours after tMCAO (**E**). High-resolution images were acquired by confocal microscopy and deconvoluted. Merged images show $S1P_1$ in red, the luminal EC marker ICAM-2 in green, the non-polarized EC marker isolectin B4 (**A, B**) or GLUT1 (**D, E**) in white, and the nuclear marker Hoechst in blue. Fluorescence intensity profiles along the dashed white lines in single plane images are plotted (right), note that in A the profile is from a single plane, but the image shown is a stack of 1.53 µm. Arrowheads indicate luminal and arrows the abluminal side of the endothelium. Note that overlapping staining between $S1P_1$ and ICAM-2, which predominates during developmental angiogenesis and is readily observed in arteries of adult retina, is rarely seen in other vessels in adult retina or brain, where $S1P_1$ is instead observed on the abluminal side of the endothelium. Deletion of *S1pr1* selectively in endothelial cells (*S1pr1*^{ECKO}) or astrocytes (*S1pr1*^{ACKO}) resolves otherwise diffuse S1P1 staining in the adult brain and confirms both the specificity of the antibody and expression in both cell types. Deletion of *S1pr1* in astrocytes also allows for better visualization of $S1P_1$ polarization, which is sustained 24 hours after tMCAO. Compare to Fig 7 B-E. Scale bar: 2 µm.

Online Figure VI: Efficiency of GFP induction by S1P1 agonists in the S1P1GS mouse. A. Images of liver sections taken from S1P1GS mice 24 hours after treatment with the $S1P_1$ agonists FTY720 (2 mg/kg i.p.; 5 mg/kg p.o.; 5 mg/kg p.o. on two consecutive days), RP-001 (0.3 mg/kg i.v.; 0.6 mg/kg i.v.) and CYM-5442 (3 mg/kg i.p.; 10 mg/kg i.p.) or vehicle (2.5% carboxymethylcellulose for RP-001 and 4% Tween for CYM-5442 in the experiments shown). ASMA, blue; GFP, green. Note uniform induction of GFP expression in hepatocytes after treatment with 5 mg/kg FTY720, 0.6 mg/kg RP-001 and 10 mg/kg CYM-5442. Scale bar: 100 µm. **B**. Quantification of GFP+ EC nuclei in ASMA negative blood vessels of skeletal muscle (left) and lung (right) in S1P1GS mice and H2B-GFP controls 24 hours after systemic administration of RP-001 (0.6 mg/kg) or FTY720 (2x 5 mg/kg). Note restricted homeostatic signaling in arteries also in skeletal muscle and lung, and similar S1P1GS-dependent induction with the two agonists. Note also that the level of basal signaling observed depends on sensitivity thresholds, which were

always the same within the group compared but not necessarily between tissues. Bar graphs show mean ± SEM. Statistical significance of S1P1 GS mice assessed by Kruskal-Wallis test with Dunn's multiple comparisons test.

Online Figure VII: $S1P_1$ is not surface expressed in naive astrocytes. A. High magnification image of a S1P1GS cortex after local administration of the $S1P_1$ agonist RP-001 shows GFP expression in endothelial cells (Erg positive nuclei, red; compare with Fig. 7F) and some perivascular cells but not in astrocytes (GFAP positive cells, blue). As both transcript and protein are abundant in astrocytes (Online Fig. II, Fig 2E, 7E), this may suggest that the receptor is not presented on the cell surface in naive astrocytes, consistent with expression in organelle-like structures (Fig 7E). Arrows, GFP positive endothelial cell nuclei; arrow heads, GFP positive and Erg negative nuclei. Scale bar: 100 μm. **B.** Quantification of non-endothelial GFP-positive nuclei in ASMA-negative area (left) and ASMA-positive area (right) in the cerebral cortex of S1P1GS and H2B-GFP control mice after systemic or local administration of RP-001 (compare with Fig. 7F). Note that induction of GFP signal in non-ECs after local administration of RP-001 is equivalent in H2B-GFP controls (and in vehicle treated mice; not shown). All $S1P_1$-dependent signal induction was therefore in ECs, consistent with no observed co-localization with GFAP. Bar graphs show mean ± SEM. Statistical significance assessed by Kruskal-Wallis with Dunn multiple comparisons test.

Online Figure VIII. Effect of CYM-5442 treatment on infarct size after pMCAO. A. Permanent MCAO was performed on wild-type males and CYM-5442 (1 mg/kg i.p.) or vehicle control applied immediately after occlusion. Infarct volumes were determined by TTC staining of brains isolated 24 hours later. **B.** Permanent CCA occlusion followed by ipsilateral permanent distal MCAO was performed on wild-type males and CYM-5442 (3 mg/kg i.p.) or vehicle control applied daily until brain harvest 7 days later. Infarct size was determined by TTC staining. Bar graph show mean ± SEM. Statistical significance assessed by unpaired t-test.

Online Figure IX: $S1P_1$ is expressed in endothelial cells of the ageing human brain. $S1P_1$ staining on paraffin sections of human cerebral cortex samples (left panel: male, 45 years; right panel: female, 54 years) retrieved from (https://www.proteinatlas.org/ENSG00000170989-S1PR1/tissue/cerebral+cortex#imid_3752608)[63]. Note the strong expression of $S1P_1$ in vascular endothelium. Scale bar: 200 μm.

Supplemental videos: The supplemental videos show sample video clips (940 x 750 μm) of sidestream dark field imaging of blood flow in the pial vasculature 2 hours after pMCAO. **Video 1** shows blood flow at the MCA/ACA border of a $S1pr1^{ECWT}$ mouse. Note unidirectional blood flow in the collateral artery at the center of the clip from the ACA to the MCA branch, and reasonable microvascular perfusion. **Video 2** shows blood flow at the MCA/ACA border of a $S1pr1^{ECKO}$ mouse. Note unidirectional blood flow in the collateral artery at the center of the clip from the ACA to the MCA branch, and poor microvascular perfusion. **Video 3** shows blood flow in the MCA in the core region of the infarct, close to the occlusion site. Note stasis and clotting at the trunk of the artery with retrograde and confused flow downstream.

Online Table I: Statistical information

Figure	Sample size	Normality test	Statistical test	Post hoc correction	*P*-values
1A males	11-13	Not passed	Mann Whitney, two-tailed	n/a	raw
1A females	5-7	Shapiro-Wilk	Unpaired t-test, two-tailed	n/a	raw
1B	7-10	Shapiro-Wilk	Unpaired t-test, two-tailed	n/a	raw
1C	8-12	Shapiro-Wilk	Unpaired t-test, two-tailed	n/a	raw
1D infarct	9-12	Shapiro-Wilk	Unpaired t-test, two-tailed	n/a	raw
1D lympho	6-12	Shapiro-Wilk	Unpaired t-test, two-tailed	n/a	raw
1E infarct	8-14	Shapiro-Wilk	Unpaired t-test, two-tailed	n/a	raw
1E neuro	8-14	Shapiro-Wilk	Unpaired t-test, two-tailed	n/a	raw
1F infarct	15-16	Shapiro-Wilk	Unpaired t-test, two-tailed	n/a	raw
1F lympho	15-16	Shapiro-Wilk	Unpaired t-test, two-tailed	n/a	raw
2A pMCAO	8-13	Shapiro-Wilk	Unpaired t-test, two-tailed	n/a	raw
2A tMCAO	10-12	Shapiro-Wilk	Unpaired t-test, two-tailed	n/a	raw
2B	7-10	Shapiro-Wilk	Unpaired t-test, two-tailed	n/a	raw
2C pMCAO	14-16	Not passed	Mann Whitney, two-tailed	n/a	raw
2C tMCAO	12-15	Shapiro-Wilk	Unpaired t-test, two-tailed	n/a	raw
2D	9	Shapiro-Wilk	Unpaired t-test, two-tailed	n/a	raw
2H#	3; 4	Shapiro-Wilk	Ordinary 1way ANOVA	Tukey	adjusted
2I	4-7	Not assessed	2way ANOVA	Tukey	adjusted
3B	5-9	Shapiro-Wilk	Ordinary 1way ANOVA	Tukey	adjusted
3C	4	Shapiro-Wilk	Unpaired t-test, two-tailed	n/a	raw
3E Coll IV	7-10	Shapiro-Wilk	Unpaired t-test, two-tailed	n/a	raw
3E Glut1	7-8	Shapiro-Wilk	Unpaired t-test, two-tailed	n/a	raw
4A	3; 6	Shapiro-Wilk	Unpaired t-test, two-tailed	n/a	raw
4B	6-7	Shapiro-Wilk	Unpaired t-test, two-tailed	n/a	raw
4C	6; 4; 4	Shapiro-Wilk	Unpaired t-test, two-tailed	n/a	raw
4D	8-10	Not passed	Mann Whitney	n/a	raw
4E 4 hours	4	Shapiro-Wilk	Unpaired t-test, two-tailed	n/a	raw
4E 4 hours	3-4	Shapiro-Wilk	Unpaired t-test, two-tailed	n/a	raw
5A CBF	4-5	Shapiro-Wilk	Ordinary 1way ANOVA	Sidak	adjusted
5A MAP	4-5	Shapiro-Wilk	Unpaired t-test, two-tailed	N/a	raw
5B	6-8	Shapiro-Wilk	Unpaired t-test, two-tailed	N/a	raw
5C	20	Not assessed	2way RM ANOVA	Bonferroni	adjusted
5D	5	Not assessed	2way RM ANOVA	Sidak	adjusted
5E	6-7	Shapiro-Wilk	Ordinary 1way ANOVA	Sidak	adjusted
5F	8	Not assessed	2way RM ANOVA	Bonferroni	adjusted
5G	16	Not assessed	Linear Regression	n/a	raw
5H	5	Not passed	Mann Whitney, two-tailed	n/a	raw
5I	5-6	Shapiro-Wilk	Unpaired t-test, two-tailed	n/a	raw
6A	4	Not passed*	Unpaired t-test, two-tailed	n/a	raw
6B ICAM-1	5	Not passed*	Ordinary 1way ANOVA	Holm-Sidak	adjusted
6B MPO	5	Not passed	Mann Whitney, two-tailed	n/a	raw
6C	8-9	Shapiro-Wilk	Unpaired t-test, two-tailed	n/a	raw
7A plasma	6	Shapiro-Wilk	Ordinary 1way ANOVA	Dunnett	adjusted
7A platelet	5	Shapiro-Wilk	Ordinary 1way ANOVA	Dunnett	adjusted
7F	2-4	Shapiro-Wilk, passed for S1P1GS	Ordinary 1way ANOVA and unpaired t-test, two-tailed	Tukey	adjusted/raw
7G#	3-5	Not assessed	2way ANOVA	Tukey	adjusted
7H	3-4	Shapiro-Wilk, passed for S1P1GS	Ordinary 1way ANOVA	Tukey	adjusted
8A	3-4	Not passed	2way repeated measures ANOVA	Tukey	adjusted
8B	9-13	Not passed	Kruskall Wallis	Dunn	adjusted

8C	10-13	Shapiro-Wilk	Unpaired t-test, two-tailed	n/a	raw
8D	4-5	Not passed	Mann Whitney, two-tailed	n/a	raw
8E	8-11	Not passed	Mann Whitney, two-tailed	n/a	raw
8F	9-10	Shapiro-Wilk	Unpaired t-test, two-tailed		
I B	10	Shapiro-Wilk	Unpaired t-test, two-tailed	n/a	raw
I C infarcts	8-14	Not passed	Mann Whitney, two-tailed	n/a	raw
I C lympho	8-10	Shapiro-Wilk	Unpaired t-test, two-tailed	n/a	raw
I D infarcts	6-14	Shapiro-Wilk	Unpaired t-test, two-tailed	n/a	raw
I D survival	19	Not assessed	Fisher's exact test	n/a	raw
II A	6-18	Shapiro-Wilk	Ordinary 1way ANOVA	Tukey	adjusted
II B	9	Shapiro-Wilk	Unpaired t-test, two-tailed	n/a	raw
II C	12-17	Shapiro-Wilk	Unpaired t-test, two-tailed	n/a	raw
II D	2	Not assessed	2way ANOVA	Sidak	adjusted
II L	4-7	Not assessed	2way ANOVA	Tukey	adjusted
III A	5	Not assessed	2way ANOVA	Bonferroni	adjusted
III B S1pr1	8-9	Not assessed	2way RM ANOVA	Bonferroni	adjusted
III B Sphk	8	Not assessed	2way RM ANOVA	Bonferroni	adjusted
IV A	4-5	Shapiro-Wilk, S1P1 ECKO ICAM-1/ASMA area not passed	Mann Whitney, two-tailed	n/a	raw
IV B	4-9	Not passed	Kruskal-Wallis	Dunn	adjusted
IV D NIMP-R14	6-9	Not passed	Kruskall Wallis	Dunn	adjusted
IV D CD41	6-9	Shapiro-Wilk	Unpaired t-test, two-tailed	n/a	raw
VI B muscle	3-5	Not passed	Kruskal-Wallis test	Dunn	adjusted
VI B lung	3-5	Not passed	Kruskal-Wallis test	Dunn	adjusted
VII B	2-4	Not passed	Kruskal-Wallis test	Dunn	adjusted
VIII A	8-13	Shapiro-Wilk	Unpaired t-test, two-tailed	n/a	raw
VIII B	9	Shapiro-Wilk	Unpaired t-test, two-tailed	n/a	raw

[#]Removal of outlier based on Rout test.

[*]In order to increase power to evaluate normality ICAM-1 values were pooled from naïve mice and the contralateral side after pMCAO, which resulted in normal distribution without outliers and a significant difference between genotypes (t-test P=0.0007), therefore we assume normal distribution for statistical analysis of each data set.

Maintien de la perfusion corticale par la sphingosine 1-phosphate lors de la phase aiguë de l'accident vasculaire cérébral ischémique

Anja Nitzsche[1], Marine Poittevin[1,2], Ammar Benarab[1], Philippe Bonnin[3,4], Eric Camerer[1]

[1]Université de Paris, Paris-Centre de recherche cardiovasculaire (PARCC), Inserm U970, 56 rue Leblanc, 75015 Paris, France.
[2]Institut des vaisseaux et du sang, hôpital Lariboisière, 75010 Paris, France.
[3]Université de Paris, Inserm U1148, hôpital Bichat, 75018 Paris, France.
[4]Université de Paris, APHP, Physiologie clinique-explorations fonctionnelles, hôpital Lariboisière, 75010 Paris France.
philippe.bonnin@aphp.fr
eric.camerer@inserm.fr

> L'accident vasculaire cérébral ischémique est une cause majeure de morbidité et de mortalité dans le monde ; il entraîne un coût économique et sociétal important, qui impose la recherche de stratégies thérapeutiques pour limiter sa gravité. Le traitement en urgence demeure principalement la recanalisation artérielle, soit par thrombolyse pharmacologique, soit par thrombectomie mécanique, qui n'apportent un bénéfice significatif que chez un tiers des patients [1]. Les traitements dits neuro-protecteurs n'ont pas encore montré de bénéfice clair, et la recherche de traitements adjuvants à la recanalisation dénués d'effet indésirable est donc nécessaire. L'ischémie cérébrale est provoquée par l'occlusion d'une artère cérébrale principale par un mécanisme d'embolie d'origine artérielle ou cardiaque, ou par un mécanisme de thrombose artérielle *in situ*. L'occlusion provoque la formation d'un corps de nécrose juste en aval de l'occlusion artérielle, entouré d'une couronne de tissu cérébral en souffrance ischémique, ou zone de pénombre *(Figure 1)*. L'extension secondaire de la nécrose cérébrale à la zone de pénombre peut être limitée, grâce à la restauration rapide de la perfusion cérébrale par le truchement de la recanalisation rapide ou par la mise en place précoce d'une circulation collatérale contournant l'obstacle [2]. Cette collatéralité peut s'établir par l'intermédiaire d'anastomoses corticales préexistantes, étendues en surface des hémisphères cérébraux entre les territoires vasculaires cérébraux adjacents ; la rapidité de sa mise en place conditionne la sauvegarde de la zone de pénombre [3]. L'efficacité de la collatéralité corticale dépend de l'intégrité des circuits micro-vasculaires, de leur perméabilité et de leur capacité à se dilater afin d'assurer l'apport sanguin. Les stratégies visant à améliorer la fonction micro-vasculaire consisteraient alors à inhiber la thrombose d'origine inflammatoire induite par les lymphocytes, à stimuler la fonction endothéliale (vasodilatation flux-dépendante), et à renforcer la barrière hémato-encéphalique dans les territoires atteints [4, 5].

La sphingosine 1-phosphate (S1P) est un lipide de signalisation qui joue un rôle majeur dans les systèmes immunitaire et vasculaire. Elle se lie à cinq récepteurs couplés aux protéines G : S1PR1 à S1PR5 [6]. La sortie des lymphocytes des organes lymphoïdes dépend de la détection de la sphingosine-1-phosphate (S1P) par le récepteur S1PR1 ; l'inhibition des récepteurs S1PR1 lymphocytaires entraîne d'ailleurs une lymphopénie profonde. Le récepteur S1PR1 est aussi fortement exprimé sur les cellules endothéliales, et la délétion, restreinte aux seules cellules endothéliales, du gène codant ce récepteur chez la souris perturbe l'angiogenèse embryonnaire et postnatale, l'intégrité vasculaire, et la fonction endothéliale [6]. La perte de la signalisation par les récepteurs S1PR1 endothéliaux déstabilise les jonctions intercellulaires endothéliales, réduit l'activité de l'enzyme de synthèse du monoxyde d'azote (NO) endothéliale, responsable de la vasoréactivité, et augmente l'expression des molécules d'adhérence des leucocytes [6]. S1PR1 joue ainsi un rôle essentiel pour soutenir les fonctions caractéristiques de l'endothélium vasculaire. La S1P est abondante dans le sang circulant, où elle est associée principalement aux lipoprotéines de haute densité et à l'albumine. Les érythrocytes et les cellules endothéliales sont des sources majeures de S1P à l'état stable ; les plaquettes le sont également, mais la libération de la S1P par les plaquettes est subordonnée à leur activation [6]. L'endothélium des vaisseaux capillaires cérébraux présente une particularité, constitutive de la barrière hémato-encéphalique : les cellules endothéliales sont unies par des jonctions intercellulaires serrées ne laissant diffuser que les molécules de petite masse moléculaire. Cette barrière joue donc un rôle protecteur du tissu cérébral, mais empêche l'extravasation de la S1P circulante.

Le fingolimod est un immunomodulateur utilisé dans le traitement de la sclérose en plaques. Phosphorylé par les kinases de sphingosine, le fingolimod peut agir

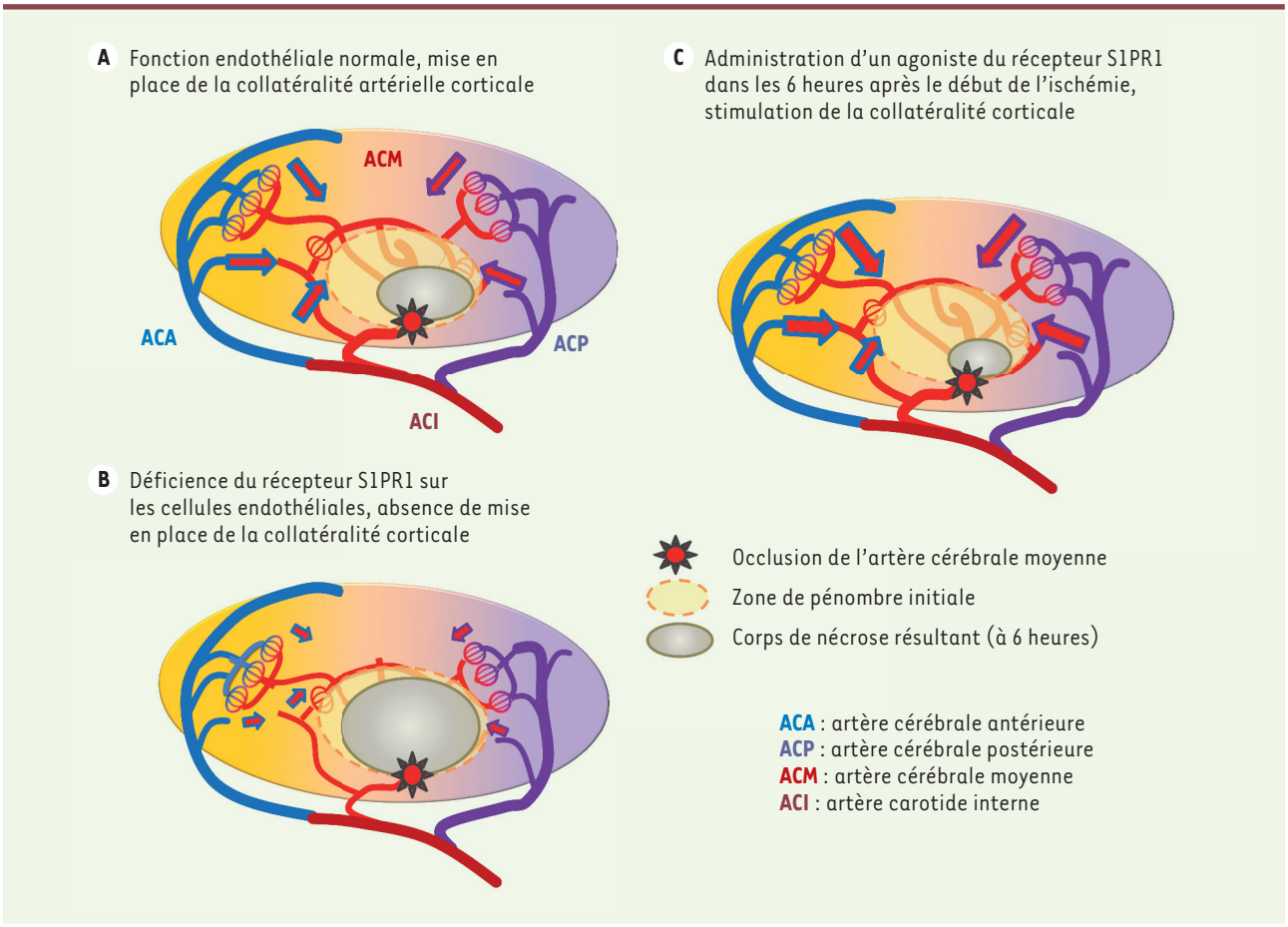

Figure 1. ***Signalisation par sphingosine-1-phosphate (S1P) au cours de l'accident vasculaire cérébral ischémique expérimental chez la souris. A.*** Après occlusion de l'artère cérébrale moyenne, la signalisation par la sphingosine 1-phosphate (S1P) promeut l'intégrité des parois vasculaires, la perméabilité des lumières vasculaires, et la mise en place précoce de la collatéralité corticale avec perfusion rétrograde dans la zone de pénombre vers le corps de nécrose, à partir des anastomoses corticales étendues entre les différents territoires vasculaires de chaque artère cérébrale. Cette signalisation s'effectue essentiellement par l'intermédiaire du récepteur S1PR1 des cellules endothéliales cérébrales, qui est localisé à la face extravasculaire de ces cellules. Comme la S1P ne traverse pas la barrière hémato-encéphalique, la production locale de S1P par les cellules endothéliales est nécessaire à l'obtention des effets vasculaires sus-mentionnés. ***B.*** En l'absence des fonctions protectrices de la signalisation par la S1P, faisant suite, par exemple, à la délétion du gène codant le récepteur S1PR1 dans les cellules endothéliales, le corps de nécrose s'étend rapidement aux dépens de la zone de pénombre, et la lésion cérébrale résultante est étendue. ***C.*** En stimulant la signalisation de la S1P dans les cellules endothéliales cérébrales par des agonistes pharmacologiques ciblant le récepteur S1PR1, l'extension de la nécrose est contrecarrée, à condition toutefois que le passage de la barrière hémato-encéphalique par ces agonistes s'effectue dans un délai court après le début de l'ischémie (figure adaptée de [8]).

comme un agoniste de plusieurs récepteurs S1PR. Dans les lymphocytes, cet effet agoniste induit une internalisation rapide de S1PR1, qui les désensibilise à la S1P. Le fingolimod a donné des résultats prometteurs lorsqu'il a été utilisé pour traiter l'accident vasculaire cérébral d'origine ischémique ou hémorragique dans des modèles expérimentaux et dans des essais cliniques à petits effectifs [4, 7]. D'autres modulateurs spécifiques du récepteur S1PR1 présentent une action bénéfique similaire, suggérant que c'est bien ce récepteur qui est la cible du fingolimod dans ce contexte. Jusqu'à présent, tous ces médicaments étaient considérés comme protecteurs principalement par la modulation de l'immunité pendant l'ischémie cérébrale [4]. Cependant, considérant le rôle majeur du récepteur S1PR1 dans le maintien des fonctions endothéliales dans les autres organes, les mécanismes d'action du récepteur S1PR1 et de ses modulateurs au cours de l'ischémie cérébrale ont été analysés à l'aide de différents outils génétiques et expérimentaux [8].

Chez la souris soumise à une ischémie cérébrale transitoire ou permanente, un déficit en récepteur S1PR1 restreint aux cellules hématopoïétiques n'a entraîné que des effets minimes sur le volume de la lésion cérébrale, alors qu'un déficit de ce récepteur restreint aux cellules endothéliales a provoqué une extension

de l'ischémie, montrant bien l'implication bénéfique de ce récepteur dans le cerveau [8]. Le déficit de signalisation du récepteur S1PR1 restreint aux cellules endothéliales était également associé à une augmentation de l'expression des molécules d'adhérence des leucocytes, à une altération de la mise en place de la collatéralité corticale vers la zone de pénombre, à une réduction de la perfusion des petits vaisseaux, et à l'apparition d'un œdème cérébral *(Figure 1)*. Malgré une disposition vasculaire normale, en particulier des anastomoses corticales, le dysfonctionnement endothélial chez ces souris était accompagné d'une expansion rapide du corps de nécrose dès la phase précoce, avec doublement de la taille de l'infarctus cérébral par rapport aux souris témoins. Étonnamment, l'inactivation des kinases responsables de la synthèse plasmatique de la S1P dans les cellules sanguines circulantes n'a pas eu d'impact sur le volume de lésion cérébrale, alors que leur inactivation dans les cellules endothéliales a reproduit le déficit induit par l'absence de récepteur S1PR1 à la surface des cellules endothéliales. Comme la S1P circulante ne passe pas la barrière hémato-encéphalique, et comme les récepteurs S1PR1 sont principalement situés à la face extravasculaire de la cellule endothéliale cérébrale, l'activation de ces récepteurs par leur ligand, la S1P, nécessite une production de ce ligand par les cellules endothéliales elles-mêmes, une situation contrastant avec celle de l'activation de ces récepteurs au cours du développement du système vasculaire ou dans l'homéostasie circulatoire, qui dépend alors de la liaison de ces récepteurs avec la S1P circulante [6, 9, 10]. À l'appui de ce modèle, seuls les agonistes du récepteur S1PR1 pénétrant la barrière hémato-encéphalique ont eu la capacité de protéger les souris de l'ischémie cérébrale dans les modèles d'accident vasculaire cérébral, capacité perdue chez la souris mutante dont le récepteur S1PR1 est supprimé sélectivement dans les cellules endothéliales [8]. La production de la S1P par la cellule endothéliale cérébrale et sa signalisation par son récepteur S1PR1 sont donc nécessaires à la régulation des fonctions de la cellule endothéliale au cours de l'ischémie cérébrale. Bien que cette signalisation ne soit que partiellement soutenue par l'autoproduction de S1P, elle peut être stimulée par des agonistes pharmacologiques pénétrant la barrière hémato-encéphalique pour favoriser localement le rétablissement de la circulation sanguine de façon indépendante de l'immunosuppression induite par certains modulateurs de S1PR1 *(Figure 1)*. A la lumière de l'utilisation des modulateurs de S1PR1 pour traiter la sclérose en plaques, et compte tenu des résultats des essais cliniques effectués à petite échelle chez des patients victimes d'accidents vasculaires cérébraux, on sait que la modulation de S1PR1 est peu susceptible d'être associée à des complications hémorragiques, même lorsque ces médicaments sont associés à des thrombolytiques [7, 11]. Une stratégie thérapeutique utilisant des agonistes adaptés pour cibler S1PR1 sur les cellules endothéliales pourrait donc être envisagée chez les patients dès le diagnostic d'accident vasculaire cérébral, sans attendre le résultat de la recanalisation. Le rôle protecteur majeur du récepteur S1PR1 endothélial dans l'homéostasie vasculaire et au cours de l'ischémie cérébrale, et les stratégies thérapeutiques visant à son recrutement pourraient également être pertinents pour la prise en charge au cours de l'accident vasculaire cérébral hémorragique, de démence vasculaire, ou d'accidents ischémiques dans d'autres organes. ◊

Endothelial sphingosine 1-phosphate signaling maintains perfusion of the cerebral cortex in ischemic stroke

LIENS D'INTÉRÊT

Les auteurs déclarent n'avoir aucun lien d'intérêt concernant les données publiées dans cet article.

RÉFÉRENCES

1. Jauch EC, Saver JL, Adams HP Jr, *et al.* Guidelines for the early management of patients with acute ischemic stroke: a guideline for healthcare professionals from the American heart association/American stroke association. *Stroke* 2013 ; 44 : 870-947.
2. Manning NW, Campbell BC, Oxley TJ, Chapot R. Acute ischemic stroke: time, penumbra, and reperfusion. *Stroke* 2014 ; 45 : 640-4.
3. Bonnin P, Mazighi M, Charriaut-Marlangue C, Kubis N. Early collateral recruitment after stroke in infants and adults. *Stroke* 2019 ; 50 : 2604-11.
4. Dreikorn M, Milacic Z, Pavlovic V, *et al.* Immunotherapy of experimental and human stroke with agents approved for multiple sclerosis: a systematic review. *Ther Adv Neurol Disord* 2018 ; 11 : 1-14.
5. Shuaib A, Butcher K, Mohammad AA, *et al.* Collateral blood vessels in acute ischaemic stroke: a potential therapeutic target. *Lancet Neurol* 2011 ; 10 : 909-21.
6. Proia RL, Hla T. Emerging biology of sphingosine-1-phosphate: its role in pathogenesis and therapy. *J Clin Invest* 2015 ; 125 : 1379-87.
7. Tian DC, Shi K, Zhu Z, *et al.* Fingolimod enhances the efficacy of delayed alteplase administration in acute ischemic stroke by promoting anterograde reperfusion and retrograde collateral flow. *Ann Neurol* 2018 ; 84 : 717-28.
8. Nitzsche A, Poittevin M, Benarab A, *et al.* Endothelial S1P1 signaling counteracts infarct expansion in ischemic stroke. *Circ Res* 2021 ; 128 : 363-82.
9. Camerer E, Regard JB, Cornelissen I, *et al.* Sphingosine-1-phosphate in the plasma compartment regulates basal and inflammation-induced vascular leak in mice. *J Clin Invest* 2009 ; 119 : 1871-9.
10. Gazit SL, Mariko B, Therond P, *et al.* Platelet and erythrocyte sources of S1P are redundant for vascular development and homeostasis, but both rendered essential after plasma S1P depletion in anaphylactic shock. *Circ Res* 2016 ; 119 : e110-26.
11. Li YJ, Shi SX, Liu Q, *et al.* Targeted role for sphingosine-1-phosphate receptor 1 in cerebrovascular integrity and inflammation during acute ischemic stroke. *Neurosci Lett* 2020 ; 735 : 135160.

Abstract :

Titre : Exploiter la signalisation lipidique endothéliale pour la protection contre les accidents vasculaires cérébraux ischémiques.

Mots-clés : barrière hémato-encéphalique ; Circulation collatérale ; endothélium ; Fingolimod ; sphingosine 1-phosphate ; agents neuroprotecteurs; accident vasculaire cérébral.

Résumé :

L'accident vasculaire cérébral ischémique (AVC) représente la première cause de morbidité et la deuxième cause mortalité dans le monde ; il induit un coût économique très élevé sur le système de santé et un énorme fardeau social à cause de la prise en charge des patients qui souffrent de séquelles physiques invalidantes permanentes. Actuellement le traitement en urgence disponible est principalement basé sur la levée de l'obstacle artérielle, soit par thrombolyse pharmacologique, soit par thrombectomie mécanique. Cependant, le nombre de patients qui reçoivent ces deux traitements est très limité en raison du délai très courts de l'instauration des traitements qui est moins de 6 heures après le début des symptômes et des contre-indications thérapeutiques. De ce fait, cette situation implique une urgence de rechercher et de développer des traitements adjuvants à la revascularisation artérielle. Sur le plan physiopathologique, l'ischémie cérébrale est le résultat d'une occlusion d'une artère cérébrale par suite d'une embolie d'origine artérielle ou cardiaque, ou à la suite d'une thrombose artérielle causée par la rupture d'une plaque athéromateuse. Sur le plan anatomopathologique l'occlusion artérielle induit au niveau du parenchyme cérébral une souffrance aigue et on distingue deux zones distinctes, un noyau de nécrose juste en aval de l'occlusion artérielle ou les lésions sont définitives, entouré d'une couronne de tissu cérébral, ou zone de pénombre qui représente le tissu en souffrance mais qui peut être sauvé. L'extension secondaire de la nécrose cérébrale à la zone de pénombre pourrait potentiellement être limitée, grâce à la restauration rapide de la perfusion cérébrale par la revascularisation artérielle ou par la promotion à un stade très précoce de la circulation cérébrale collatérale dans l'objective est de maintenir un débit de perfusion cérébrale suffisant tout en contournant l'occlusion artérielle.

La Sphingosine 1-phosphate (S1P) est un lipide bioactif avec une contribution majeure à la régulation des systèmes immunitaire et vasculaire. Pour induire la signalisation cellulaire S1P est active en se liant à cinq récepteurs couplés aux protéines G : S1PR1 à S1PR5. Une des principales fonctions de la signalisation S1P est la régulation de la migration des lymphocytes des organes lymphoïdes et ceci se fait via l'activation du récepteur S1P1 exprimé au niveau des lymphocytes. L'inhibition pharmacologique des récepteurs S1P1 lymphocytaires entraîne une altération la migration des lymphocytes et une lymphopénie profonde. Les cellules endothéliales expriment aussi d'une manière significative le récepteur S1P1, et chez les souris déficientes en signalisation endothéliales S1P1 on observe une altération des jonctions intercellulaires endothéliales, une réduction significative de l'activité de l'enzyme de synthèse du monoxyde d'azote (NO) endothéliale, résultant d'une situation de vasoconstriction artériolaire et d'une promotion de l'expression des molécules d'adhérences des leucocytes et l'établissement d'un environnement pro-inflammatoire. Le taux plasmatique de la S1P est

très élevé, elle est principalement associée aux lipoprotéines de haute densité et à l'albumine qui la transportent dans le sang circulant. Les érythrocytes et les cellules endothéliales sont les principales sources de génération de S1P à l'état physiologique ; les plaquettes aussi contribuent à la production de S1P, cependant un contexte d'activation plaquettaire est nécessaire afin de permettre de libérer le contenu plaquettaire en S1P.

Le Fingolimod (FTY720) est prescrit en thérapeutique clinique comme traitement immuno-modulateur oral pour les patients atteint de formes récurrentes de la sclérose en plaques. Le FTY720 phosphorylé (FTY720-P) est la forme pharmacologique active de FTY720, elle exerce un effet agoniste sur 4 des 5 récepteurs S1PRs. Dans les lymphocytes, cet effet agoniste induit une internalisation rapide du récepteur S1P1, puis dégradation du récepteur S1P1 résultant en un état de désensibilisation à la S1P. Le potentiel thérapeutique du FTY720 a été évalué dans plusieurs pathologies du système nerveux central et plus particulièrement lors des AVC, et des résultats prometteurs ont été observé lors de son utilisation comme traitement dans des modèles expérimentaux d'AVC d'origine ischémique ou hémorragique ainsi que dans des essais cliniques initiaux. D'autres modulateurs spécifiques du récepteur S1P1 ont démontré aussi un effet bénéfique similaire, suggèrent ainsi que le récepteur S1P1 est la cible thérapeutique du FTY720. Jusqu'à présent, l'effet protecteur du FTY720 était attribué à la modulation de l'immunité pendant l'ischémie cérébrale. Cependant, le rôle important du récepteur S1P1 et la contribution majeure aux fonctions endothéliales suggèrent que le récepteur S1P1 au niveau des cellules endothéliales contribue aux effets protecteurs observés lors de l'utilisation des modulateurs du récepteurs S1P1 et de FTY720.

Les objectifs de mon projet de thèse étaient d'utiliser des outils génétiques et pharmacologiques chez la souris pour 1) déterminer les rôles endogènes des S1P1 hématopoïétiques et endothéliales dans l'AVC ischémique expérimental ; 2) déterminer comment le récepteur S1P1 endothélial cérébral est engagé par son ligand endogène ; 3) élucider le mécanisme par lequel la signalisation S1P1 endogène fournit une protection dans l'AVC ischémique ; 4) identifier la cible cellulaire des modulateurs pharmacologiques du récepteur S1P1 dans l'AVC ischémique. Mon projet de thèse faisait partie d'une étude en collaboration menée dans le cadre d'un réseau de recherche transatlantique sur la signalisation S1P dans l'unité neuro-vasculaire. Dans cette collaboration, mon rôle principal était de modéliser l'AVC ischémique chez la souris.

Les résultats observés lors de l'utilisation des deux modèles d'ischémies cérébrales à savoir transitoire et permanente chez la souris, objectivent des lésions cérébrales chez les souris déficientes en S1P1 aux niveaux des cellules hématopoïétiques, cependant on retrouve des lésions cérébrales plus conséquentes et des volumes d'extension d'ischémie plus importants chez les souris déficiente en récepteur S1P1 au niveau des cellules endothéliales approximativement le double des lésions observe chez les souris contrôles. Ces résultats démontrent le rôle bénéfique du récepteur S1P1 aux niveaux des cellules endothéliales cérébrales lors du contexte d'ischémie. Chez les souris déficientes en récepteur S1P1 au niveau des cellules endothéliales une surexpression des molécules d'adhérences des leucocytes est retrouvée, avec un déficit de l'engagement de la circulation collatérales an niveau de la zone de pénombre. Les souris déficientes en récepteur S1P1 au niveau des cellules endothéliales présente une limitation de la perfusion des petits vaisseaux, l'évolution

d’un œdème cérébral, tout en notant un arrangement vasculaire normale et un nombre d’anastomoses corticale similaire entre les souris contrôles et les souris mutantes. La suppression de la production de la S1P au niveau des cellules sanguines circulante par un déficit des kinases 1 et 2 de la sphingosine n’a pas eu d’impact sur le volume des lésions cérébrale, tandis que le déficit des kinases 1 et 2 de la sphingosine au niveau des cellules endothéliales cérébrales entraine des lésions ischémique majeurs similaire à celles observe par la déficience en récepteur S1P1 au niveau des cellules endothéliale cérébrales. Ces résultats nous informent sur les mécanismes qui régulent l’activation du récepteur S1P1 lors de l’ischémie cérébrale. En contraste direct avec la signalisation S1P1 au niveau des cellules endothéliales pulmonaire, qui sont activées par la S1P plasmatique produite principalement par les sources sanguines, nous avons objectivé qu’au niveau du récepteur S1P1 des cellules endothéliales cérébrales l’activation est assurée par la S1P autoproduite par les cellules endothéliales cérébrales, et l’absence d’action physiologique du S1P plasmatique malgré sa très grande l’abondance.

Par l’utilisation de techniques d’imagerie d’écho-doppler vasculaire des artères du tronc supra-aortique nous avons observé que les souris déficientes en S1P1 au niveau des cellules endothéliales présentaient également une altération de la récupération du flux sanguin au niveau de l’hémisphère ischémique dans la phase aiguë après ischémie cérébrale permanente, indiquant un rôle du récepteur S1P1 dans la régulation de la fonction endothéliale a la phase aiguë de l’ischémie cérébrale. Le récepteur S1P1 est impliqué dans la régulation de l'angiogenèse développementale en favorisant la perfusion des vaisseaux nouvellement formés et contribuer à la dilatation médiée par le flux des artères mésentériques en soutenant l'activité eNOS. Bien que cela n'ait pas été directement abordé dans notre étude, cela peut suggérer que le récepteur S1P1 est fonctionnel également au niveau du système vasculaire cérébral mature au moins en partie via eNOS.

L’utilisation d’imagerie par IRM cérébrales nous a permis d’observer que les souris déficientes en récepteur S1P1 au niveau des cellules endothéliales naïves présentent également un défaut dans l'intégrité de la barrière hémato- encéphalique. Cette observation suggère un role de la signalisation S1P1 dans le maintien de la fonction de la barrière hémato–encéphalique dans le cerveau ischémique. On observe aussi deux fois plus d'accumulation de bleu d'Evans/albumine 24 heures après ischémie cérébrale permanente chez les souris déficientes en récepteur S1P1 au niveau des cellules endothéliales que chez les souris contrôles On objective aussi la formation d’œdème majeur en quelques heures après 90 minutes d’ischémie transitoire, ce qui peut expliquer la mortalité précoce élevée des souris déficientes en récepteur S1P1 au niveau des cellules endothéliales dans ce modèle.

L’utilisation de technique d’imageries cellulaires a démontée que le récepteur S1P1 au niveau des cellule endothéliales est principalement exprimé à la surface abluminale autrement dit le récepteur est polarisé dans la majorité des cellules endothéliales cérébrales.

Nous avons ensuite étudié le potentiel thérapeutique de CYM-5442 qui est un agoniste sélectif du récepteur S1P1. CYM-5442 est connu pour désensibiliser le récepteur S1P1 à des concentrations élevées, cependant, avec des propriétés de distribution rapide dans le parenchyme cérébral et une induction d’une lymphopénie transitoire.

Nous avons confirmé que CYM-5442 peut traverser la barrière hémato-encéphalique pour activer les récepteurs S1P des cellules endothéliales cérébrales avec l'utilisation de la microscope confocal et d'une souris reportrice S1P1 où l'expression d'une protéine fluorescente verte est induite dans le noyau des cellules dans lesquelles la signalisation S1P1 est active. En effet CYM-5442 induit une signalisation et une expression de fluorescence qui témoigne de l'activation du récepteur S1P1 au niveau des cellules endothéliales cérébrale. Ceci était en contraste avec RP-001, un autre agoniste puissant et sélectif de récepteur S1P1, qui n'activait le récepteur S1P1 sur les capillaires cérébraux que lorsqu'il était injecté directement dans le parenchyme cérébral. Les deux agonistes ont induit une lymphopénie transitoire équivalente, mais seul le CYM-5442 à apporter une protection dans les modèles d'AVC ischémique utilisé dans notre étude. Cette protection est non observée chez les souris déficientes en récepteur S1P1 au niveau des cellules endothéliales, démontrant la nécessité de cibler ce récepteur. Ces résultats ont illustré à la fois l'importance de la modulation du récepteur S1P1 au niveau des cellules endothéliales pour les effets thérapeutiques des modulateurs du récepteur S1P1 et le nécessité de traverser la barrière hémato-encéphalique pour atteindre et activer le récepteur S1P1.

Ces observations suggèrent que la stratégie optimale pour maximiser le bénéfice de l'engagement de la signalisation S1P dans le contexte d'un AVC ischémique impliquerait un double ciblage des lymphocytes et des cellules endothéliales avec des agonistes du récepteur S1P1 qui traverse la barrière-hémato encéphalique.

En résumé, nos résultats démontrent un rôle important pour la signalisation endothéliale endogène du récepteur S1P1 dans la lutte contre l'extension des lésions ischémiques à travers trois fonctions principales, notamment la régulation de la circulation cérébrale collatéral, l'intégrité de la barrière hémato-encéphalique et le maintien de la perméabilité micro vasculaire. Nos résultats suggèrent également que le récepteur S1P1 dans la plupart des cellules endothéliales cérébrales sont activées par la production de S1P autonome des cellules endothéliales cérébrales au cours de l'ischémie cérébrale. Nous observons aussi, que le récepteur S1P1 est polarisé sur les cellules endothéliales capillaires cérébrales et n'est donc pas exposé au ligand circulant. Ces observations ont des implications importantes pour la modulation du récepteur S1P1 pour le traitement de l'accident vasculaire ischémique et nous informe aussi sur la valeur diagnostique du S1P au niveau du plasma à la phase aiguë.